

FINAL REPORT

**North Carolina Department of Transportation
Research Project No. HWY-2002-12**

Evaluation of Bridge Analysis Vis-à-vis Performance

By

Janos Gergely
Principal Investigator

Timothy O. Lawrence
Graduate Research Assistant

Claudia I. Prado
Graduate Research Assistant

Chad T. Ritter
Graduate Research Assistant

William B. Stiller
Graduate Research Assistant

Department of Civil Engineering
University of North Carolina at Charlotte
9201 University City Boulevard
Charlotte, NC 28223

December 15, 2004

Technical Report Documentation Page

1. Report No. FHWA/NC/2003-08		2. Government Accession No.		3. Recipient's Catalog No.	
4. Title and Subtitle Evaluation of Bridge Analysis vis-à-vis Performance				5. Report Date December 15, 2004	
				6. Performing Organization Code	
7. Author(s) Janos Gergely, Timothy O. Lawrence, Claudia I. Prado, Chad T. Ritter, and William B Stiller				8. Performing Organization Report No.	
9. Performing Organization Name and Address University of North Carolina at Charlotte, Civil Engineering Department 9201 University City Blvd, Charlotte, NC 28223				10. Work Unit No. (TRAIS)	
				11. Contract or Grant No.	
12. Sponsoring Agency Name and Address North Carolina Department of Transportation Research and Analysis Group 1 South Wilmington Street Raleigh, North Carolina 27601				13. Type of Report and Period Covered Final Report 7/1/01-6/30/03	
				14. Sponsoring Agency Code 2002-12	
Supplementary Notes:					
16. Abstract The objective of the project was to evaluate the current NCDOT bridge analysis and rating procedures. These procedures include both field inspections and bridge ratings using in-house softwares. First, the NCDOT simple and continuous span bridge analysis softwares were verified through several examples using different methods, including the governing AASHTO bridge rating procedures, AASHTOWare bridge rating softwares, as a well as a spreadsheet program developed by UNC Charlotte. Parallel to this effort, four bridges were also tested during the first phase of the project to compare the test data with the analytical predictions. These bridges are located within Division 10 (including Anson, Cabarrus, Mecklenburg, Stanly, and Union Counties), North Carolina, and included the first glass fiber reinforced polymer (GFRP) deck bridge built in the Carolinas. The variables used in bridge rating procedures include, among other factors, girder end conditions, impact and distribution factors, deck-to-girder composite action, and others. Based on the fact that most of these factors are unique to specific bridges and bridge types, as proved by the preliminary data, it was clear that it is unrealistic to expect that analytical procedures alone (including detailed finite element methods) will capture the true performance of individual bridges. Therefore, the second phase of the project focused on a broader approach, which included: the development of a simple spreadsheet based program to provide a lower and upper bound solution; the use of non-destructive tests (NDT) for materials and construction details; and the development of a simplified bridge test protocol to evaluate the true response of individual bridges.					
17. Key Words Bridge analysis, load rating, load testing, distribution factor, impact factor, GFRP deck			18. Distribution Statement		
19. Security Classif. (of this report) Unclassified		20. Security Classif. (of this page) Unclassified		21. No. of Pages 228	22. Price

DISCLAIMER

The contents of this report reflect the views of the authors and not necessarily the views of the University. The authors are responsible for the facts and the accuracy of the data presented herein. The contents do not necessarily reflect the official views or policies of either the North Carolina Department of Transportation or the Federal Highway Administration at the time of publication. This report does not constitute a standard, specification, or regulation.

ACKNOWLEDGEMENTS

The research documented in this report was sponsored by the North Carolina Department of Transportation (NCDOT) and the Federal Highway Administration's (FHWA) Innovative Bridge Research and Construction (IBRC) program. A Technical Advisory Committee (TAC) composed of representatives of the two agencies provided valuable guidance and technical support for this research project. The project TAC Committee included Lin Wiggins (Chair), Henry Black, Rodger Rochelle, Rick Lakata, Tom Koch, Cecil Jones, and Greg Perfetti of NCDOT, and Paul Simon of FHWA.

The authors would like to thank Garland Haywood, Ronald Lee and the Division 10 Bridge Maintenance Unit for their technical and material assistance throughout the project. Their assistance included bridge identification, site preparation, traffic control, loading truck, access to snooper truck, and other materials and supplies for the seven bridge tests. Concrete Supply of Charlotte, N.C. provided the use of their truck to load two of the bridges, Vulcraft of Florence, S.C. supplied the work platform for one of the bridges, and Zapata Engineering of Charlotte, N.C. provided additional instruments to the last two bridge tests. Their contributions are greatly appreciated.

The authors are also thankful to the UNC Charlotte research team, including Mike Moss and Dan Rowe of the College of Engineering, and the undergraduate research assistants working on the project, including Jennifer Carroll, Peter Foster, Chris Frank, Drew Lyerly, Brad McConnell, Logan Smith, Avery Turner, Jeremy Wallace, and Brian Zapata. Their help is gratefully acknowledged.

EXTENDED SUMMARY

The objective of the project was to evaluate the current NCDOT bridge analysis and rating procedures. These procedures include both field inspections and bridge ratings using in-house softwares. First, the NCDOT simple and continuous span bridge analysis softwares were verified through several examples using different methods, including the governing AASHTO bridge rating procedures, AASHTOWare bridge rating softwares, as well as a spreadsheet program developed by UNC Charlotte. Parallel to this effort, four bridges (one with a GFRP deck) were also tested during the first phase of the project; bridges located within Division 10 (including Anson, Cabarrus, Mecklenburg, Stanly, and Union Counties), North Carolina, to compare the test data with the analytical predictions.

The first phase of the project proved that the NCDOT bridge rating software directly follows the latest AASHTO requirements (with one small exception), providing a safe and conservative approach to assess the existing bridges. Furthermore, the experimental results also showed that the analytical predictions can not, in most cases, provide an accurate estimate of the true behavior of these (especially older concrete) bridges. Significant strength reserves were identified due to several factors, including girder/deck composite action, impact and distribution factors, material strength, contribution of non-structural elements, girder end conditions, etc...

Based on the fact that most of these factors are unique to specific bridges and bridge types, as proved by these preliminary data, it was concluded that it is unrealistic to expect that analytical procedures alone will capture the true performance of individual bridges. Therefore, the second phase of the project focused on a broader approach, which

included: the development of a simple spreadsheet based program to provide a lower and upper bound solution; the use of non-destructive tests (NDT) for materials and construction details; and the development of a simplified bridge test protocol to evaluate the true response of individual bridges.

The spreadsheet program allows the user to input a range of values for most of the above-mentioned influencing factors, and when combined with more realistic material properties from NDT tests, the output provides a lower and upper bound bridge response (i.e. strain, deformation, bridge rating and posting).

During the development of the simplified testing protocol, three additional bridges were tested. Similarly to the previous four bridges, this experimental phase of the project involved the instrumentation (using up to 102 instruments) and the load testing of these bridges using static, slow and dynamic load cases using truck weights close to the operating rating. However, in addition to this large setup, an independent data acquisition system was also used with a small number of additional instruments.

The purpose of this parallel (and much smaller) setup was to investigate whether a scaled down instrumentation will provide realistic information on impact and distribution factors, support conditions, composite actions and non-structural elements. Based on the last three bridges tested, it was concluded, that a relatively simple instrumentation setup can be effective in the load rating of bridges through testing. These diagnostic tests are also included in the “Manual for Bridge Rating Through Load Testing”, a document published by NCHRP.

The specific recommendations that are suggested by the authors based on the seven bridges analyzed and tested can be summarized as:

Ø Reconsider the use of PercEffective in the NCDOT bridge rating software, especially for concrete girder bridges with only minor hairline cracks in tension zone.

It is also recommended to use actual concrete strength values determined by NDT.

Ø Consider reducing or eliminating the impact factor for existing bridges with “healthy” approach slabs and deck joints. This would increase most bridge ratings by 20-30%

Ø Consider the use of UNC Charlotte’s spreadsheet program (properly tested) to allow the analysis to include simple span girder end restraint. This could be as high as 30% for semi-integral and integral end walls.

Ø Consider the composite action (up to a certain horizontal shear level) between steel girders and concrete decks for older bridges with certain construction details.

Ø Expand the bridge files to include non-destructive tests and damage extent and propagation (cracks, spallings, and corrosion signs).

Ø Use bridge load testing (based on fully developed and detailed testing protocols) to verify transverse load distribution, impact factor, and member strain levels.

Ø Revise and expand the current NCDOT analysis software to allow for parametric studies, upgrade inspection field reports to include specific information on materials, and damage/corrosion details, and combine the analysis with selected bridge tests.

In conclusion, the current NCDOT analysis software provides safe and conservative bridge rating in accordance with the latest AASHTO requirements. However, parametric studies in combination with properly planned load tests can provide a more realistic estimate of bridge performance at the load level investigated, and will result (in most cases) in higher load ratings for existing bridges.

TABLE OF CONTENTS

DISCLAIMER	3
ACKNOWLEDGEMENTS	4
EXTENDED SUMMARY	5
1. INTRODUCTION	10
1.1 Background	10
1.2 Literature Review	12
2. PROJECT OVERVIEW	17
2.1 Objectives	17
2.2 Significance of Work	18
3. LOAD RATING	20
3.1 Bridge Condition Evaluation	20
3.2 AASHTO Load Rating Guidelines	22
3.3 NCDOT Bridge Rating Procedures	23
3.4 Sample Analysis	26
3.5 AASHTOWare	33
3.6 UNCC Bridge Analysis Software	36
4. BRIDGE SELECTION	38
4.1 Selection Criteria	38
4.2 GFRP Deck Bridge	39
4.3 Concrete Deck Girder Bridges	39
4.4 Steel Girder Bridges	43
4.5 Crutch Bent Bridge	50
4.6 Summary of Bridge Selection	52
5. EXPERIMENTAL RESULTS	54
5.1 Bridge 89-0022	54
5.2 Bridge 59-0361	63
5.3 Bridge 12-0271	68
5.4 Bridge 59-0038	78
5.5 Bridge 12-0227	86
5.6 Bridge 59-0841	96
5.7 Bridge 89-0219	102

6.	ANALYTICAL STUDIES AND COMPARISONS	108
6.1	Bridge Rating.....	108
6.2	Distribution Factors	110
6.3	Impact Factors.....	112
6.4	Composite Action	114
6.5	Girder End Conditions	117
6.6	Strain Levels	119
6.7	Crutch Bent Retrofit.....	121
7.	NCDOT BRIDGE ANALYSIS SOFTWARES	124
7.1	Simple Span Analysis Software.....	124
7.2	Continuous Span Analysis Software.....	130
7.3	Conclusions.....	134
8.	BRIDGE RATING THROUGH LOAD TESTING	135
8.1	Rating Procedure.....	136
8.2	Personnel and Equipment Needs	138
9.	SUMMARY AND CONCLUSIONS	140
9.1	General Conclusions	140
9.2	Concrete Girder Bridges	142
9.3	Steel Girder Bridges.....	142
9.4	GFRP Deck Bridge	143
9.5	Crutch Bent Repair	143
10.	RECOMMENDATIONS AND IMPLEMENTATION	144
11.	REFERENCES	146
12.	APPENDICES	148
	A – UNC Charlotte Bridge Analysis Software Instruction Manual	148
	B – GFRP Deck Bridge Construction Report	166
	C – Instrumentation and Load Testing.....	196
	D – Load Paths.....	222

1. INTRODUCTION

1.1 Background

Over 50% of the nation's bridges are either structurally deficient or functionally obsolete. So, why don't we see a lot of structural collapses and closed bridges? First, most of the problems are identified during the scheduled bridge inspection. Based on the inspection report, structural analyses and rating are performed. Bridge postings prompt actions, and regular maintenance needs are issued as necessary.

The second reason is the actual bridge capacity and performance may be far superior to the performance shown by current rating procedures. Similarly to engineering practices in other fields, safety factors are included in bridge design and analysis as well. Furthermore, bridges often exhibit inherent strength reserves from various factors, such as higher composite action, girder end restraints, contributions from secondary elements, etc... Therefore, in order to assess the bridge capacity more realistically, for bridge posting or for special permits, the results from actual load tests may improve/supplement the current analytical procedures.

In 1968, the Federal Highway Act created the National Bridge Inspection Program (NBIP) which required state agencies to track and catalogue the conditions of bridges on principal highways. This program was later changed by the Surface Transportation Assistance Act of 1978 to include all bridges on public roads. Each year, State highway agencies are required to comply with the National Bridge Inspections Standards (NBIS), which contains five major provisions: inspection procedures,

frequency of inspections, qualifications for individuals performing inspection, inspection reports, and inventories.

The evaluation of the load carrying capacity of bridges is an important process, and it is essential in alerting motorists of any load carrying deficiencies by posting load restrictions. The inspection information of each bridge in the State is then submitted to the Federal Highway Administration (FHWA), and stored in the National Bridge Inventory (NBI) database. The information stored is used by the FHWA to allocate state funding for the Highway Bridge Replacement Program (HBRP).

It is believed that the current rating process may underestimate the load carrying capacity of some of the bridges, resulting in unwarranted load posting. In 2003, North Carolina DOT reported 2,400 National Highway System (NHS) bridges and 14,422 non-NHS bridges. Of the 2,400 NHS bridges, 18.7% and 28.9% were designated deficient with ADT>50,000 and ADT<50,000, respectively (NBI 2003). The numbers were 32.1% and 33.9% for non-NHS bridges with ADT>10,000 and ADT<10,000, respectively.

Load-restricting postings create difficulties for shipping goods. Routes have to be changed and special permits need to be approved. School bus routes have to be changed (school busses require an SV-16 ton posting, or better), resulting in increased commuting time for the students. Postings reduce the service level of a road, which in turn, has an economic impact on the geographical area served by the particular bridge. In some cases, trucks are not able to deliver products to certain areas due to bridge postings. On the other hand, it is difficult to enforce these postings, especially in rural areas. The reality may be however, that the analysis procedures are overly conservative, and they might unnecessarily result in a bridge posting.

The University of North Carolina at Charlotte (UNC Charlotte), in collaboration with the North Carolina Department of Transportation (NCDOT), developed a research project to evaluate the current analysis procedures used to determine the load rating of North Carolina bridges.

The project was divided into three phases and was projected to take two years to complete. The first phase focused on the testing of a glass fiber reinforced polymer (GFRP) deck, a new type of decking system never used before in the state of North Carolina. The second phase required the evaluation of the current bridge rating procedures used by NCDOT, and the testing of three bridges. In the third and final phase, the findings of phase two are analyzed, and improvements are suggested to the existing procedure to better predict the response of the bridges to service conditions.

1.2 Literature Review

The true strength of existing bridges puzzled DOT officials, engineers and researchers for a long time. It has been observed very early on that standard analytical procedures do not and can not accurately predict all the factors influencing a bridge's load carrying capacity. Among these factors, one must mention the distribution and impact factors, unintended composite actions and girder end fixities, strength increase due to non-structural elements, etc...

NCHRP Report 301 (Moses, 1987) makes recommended revisions concerning steel girder bridges for the AASHTO "Manual for Condition Evaluation of Bridges". These recommendations were included in the 2nd Edition of the AASHTO manual (AASHTO, 2000) which was used for this report. Another important resource in this

field is the “Guide Specifications for the Strength Evaluation of Existing Steel and Concrete Bridges”, (AASHTO, 1988).

NCHRP Report 306 (Burdette and Goodpasture, 1988) discusses several topics concerning unintended composite action between the deck and girders of a bridge designed to have no composite action. Other topics covered in this report were the stiffening affect of railings and the unintended continuity that occurs within simple span bridges.

The effects that railings (especially concrete railings) and curbs have on bridges have been known for some time. Sartwell (1976) analyzes this behavior for a simple-span bridge. His theoretical results based on the interaction of the rail and curb for a concrete deck bridge closely matched what was seen through experimental analysis. He concluded that the parapet and curb increase the strength of the bridge when loads are applied adjacent to the curb.

However, theoretical analyses can only provide a (sometimes too) conservative bridge rating, often resulting in unnecessarily low postings which are nearly impossible to enforce. These analyses can be complemented by sound bridge load tests to evaluate the true capacity of a structure. Currently, the “Manual for Bridge Rating Through Load Testing” (NCHRP Project 12-28(13)A, Lichtenstein and Associates, 1990), provides the most comprehensive load rating available. The authors distinguish between diagnostic and proof load tests.

For the diagnostic test a selected load is positioned on the structure, and its effects are analyzed and compared to analytical predictions. Any discrepancy is rationalized, and the improved model included in future analyses. During proof load testing, the

bridge is incrementally increased, while its members monitored throughout the test. The test is aborted as soon as a predetermined target load is achieved, or the bridge members reached their elastic limit. In this project, diagnostic load tests were performed on seven North Carolina bridges in a two-year period.

Bakht and Jaeger (1990) discuss some of the surprises associated with bridge testing and their affect on the underestimation of the bridge's strength, resulting from enhanced flexural stiffness due to end conditions and the composite action in non-compositely designed bridges.

A study performed by Nowak and Kim (1998) looked into the strain distribution between girders for an existing bridge. They found strain levels less than predicted in the girders at the midspan of the structure. This was partially attributed to a rotational stiffness at the end bents. Strain gages placed near the supports of the bridge yielded some compression in the bottom flange of the girder, which supported the theory that rotational stiffness is present at the support. They also made the conclusion that the AASHTO Standard Specification distribution factors were an overestimate of the distribution measured for single truck loading.

In the field of steel bridges, two publications are highlighted here: one on short span steel bridges (Stallings and Yoo, 1993), and the other on curved steel girder bridges (Galambos et al., 2000). Two papers by Aktan et al. (1997 and 1998) discuss the analytical (modal analysis) and experimental aspects of bridge structural identification. The authors emphasize the as-built bridge information and on finite element analysis.

Gergely et al. (2000), and Pantelides and Gergely (2002) performed detailed analytical studies on several Interstate bridges in the Salt Lake Valley in order to assess

the capacity of these structures for gravity and lateral loads. These analyses included finite element non-linear pushover analyses, a method that studies the behavior of structures well beyond their service load conditions.

Furthermore, to evaluate the increase in bridge capacity by composite retrofit, three bridge bents were tested as well. The composite repair and retrofit significantly improved the bridge's ductility and lateral load capacity (Pantelides and Gergely, 2002). It is important to mention that the bridge retained its gravity load capacity even when its lateral load capacity dropped significantly – an important life safety issue in regions with high seismic demands.

An experimental study is currently under way in South Carolina (Schiff and Philbrick, 1999), with the primary objective to assess and rate highway bridges by load testing. In the first phase, the investigators provided a detailed review of current technologies and practices, followed by the development of a bridge testing protocol, and the field test of this new method.

The present project also includes the analysis and load testing of the first glass fiber reinforced polymer deck bridge in the Carolinas. This new decking material has been extensively researched by the Delaware Center for Composite Materials (2000). The focus of the research was on the connection between the deck panels and the supporting structure, the connection between the deck panels, and the service life of the deck material. It was found that the connection of the deck panel to the girder was best accomplished by grouting three shear studs spaced at 24", with each shear stud being surrounded with a spiral to confine the concrete around the shear stud. With this

arrangement, laboratory testing found composite action to occur between the deck and the girder.

Another study done on a bridge improvement published by Alampalli and Kunin (2001) involved replacement of the concrete deck of a truss bridge with a GFRP deck system. When the GFRP was tested, the system showed no composite action with the supporting floor beams. In addition to the lack of composite action, there was also no transfer of shear between adjacent panels. The panels however, lacked the mechanical connections used in the previous study, and were simply butt connected with epoxy.

In a similar study Bridge Diagnostics, Inc. (2000) field-tested a GFRP deck on a truss bridge in Warrensburg, NY. The GFRP was being used to replace the heavier concrete deck slab. The bridge used a beam and stringer system to support the deck and live load. They found the deck to act compositely with the stringers and beams. Similarly to the Delaware study, the panel to steel connection was made with studs, but the details of the connection were unclear. One noteworthy finding was the localized cupping of the top flange when the axle load passed over a strain gage.

2. PROJECT OVERVIEW

2.1 Objectives

The objective of the project was to evaluate the current NCDOT bridge analysis and rating procedures. These procedures include both field inspections and bridge ratings using in-house softwares. First, the NCDOT simple and continuous span bridge analysis softwares were verified through several examples using different methods, including the governing AASHTO bridge rating procedures, AASHTOWare bridge rating softwares, as well as a spreadsheet program developed by UNC Charlotte.

Parallel to this effort, four bridges (one with a GFRP deck) were also tested during the first phase of the project; bridges located within Division 10 (including Anson, Cabarrus, Mecklenburg, Stanly, and Union Counties), North Carolina, to compare the test data with the analytical predictions.

The second phase of the project focused on a broader approach, which included: the development of a simple spreadsheet based program to provide a lower and upper bound solution; the use of non-destructive tests (NDT) for materials and construction details; and the development of a simplified bridge test protocol to evaluate the true response of individual bridges.

The UNC Charlotte spreadsheet program allows the user to input a range of values for most of the above-mentioned influencing factors, and when combined with more realistic material properties from NDT tests, the output provides a lower and upper bound bridge response (i.e. strain, deformation, bridge rating and posting).

During the development of the simplified testing protocol, three additional bridges were tested. Similarly to the previous four bridges, this experimental phase of the project involved the instrumentation (using up to 102 instruments) and the load testing of these bridges using static, slow and dynamic load cases using truck weights close to the operating rating. However, in addition to this large setup, an independent data acquisition system was also used with a small number of additional instruments.

The purpose of this parallel (and much smaller) setup was to investigate whether a scaled down instrumentation will provide realistic information on impact and distribution factors, support conditions, composite actions and non-structural elements. Based on the last three bridges tested, it was concluded, that a relatively simple instrumentation setup can be effective in the load rating of bridges through testing. These diagnostic tests are also included in the “Manual for Bridge Rating Through Load Testing”, a document published by NCHRP.

The proposed project was performed in close collaboration with NCDOT and FHWA engineers and personnel at both divisional and State level. Both the AASHTO Standard Specifications (1992 and interims) and the North Carolina requirements were considered in the load tests and bridge analyses. The project provided valuable information on the correlation between predicted and actual bridge behavior under a specific truck loading, and under a typical day’s traffic conditions.

2.2 Significance of Work

This project provided a unique opportunity to monitor the construction of the first glass fiber reinforced polymer (GFRP) deck bridge in North Carolina. A construction

report has been prepared, recording every step of the construction process. Once the bridge was completed, using close to a hundred instruments, the behavior of the bridge was monitored while loaded with a moving concrete truck.

Furthermore, five conventional bridges were also analyzed and tested. The results revealed important strength reserves in these bridges (ranging from 1 month to 55 years of age), attributed to girder end restraints, composite action between girders and decks, and contribution from secondary elements, among other factors. To analyze these bridges, analysis procedures developed by NCDOT, as well as commercially available software and in-house spreadsheet programs were used.

Also, the last bridge studied in this project was a bridge with timber deck on steel girder. The bridge was retrofitted using a crutch bent installed in one of the spans. This investigation proved the effectiveness of this relatively simple retrofit method.

And finally, this project provided a great opportunity for UNC Charlotte graduate and undergraduate students to become more familiar with bridge analysis and testing procedures, and to interact with NCDOT personnel at both State and Division 10 level.

Overall, the authors hope that this research will benefit the NCDOT Bridge Maintenance Unit in future bridge analysis and testing procedures.

3. LOAD RATING

3.1 Bridge Condition Evaluation

The Manual for Condition Evaluation of Bridges (AASHTO, 2000) provides detailed procedures on the inspection, material testing, and load rating of bridges. This manual includes specific requirements for bridge records, including the following information: construction, shop, and as-built drawings; specifications, material certification and tests; load test data, maintenance and repair history, accident records, postings, inspection history and requirements. It also requires a detailed inventory data with complete geometric and component descriptions, inspection information, and bridge condition and load rating data.

All public bridges are subject to a biannual bridge inspection program. Routine inspections (the most common inspection type – others are initial, damage, in-depth, and special inspections) closely follow the requirements of the National Bridge Inspection Standards. These inspections are conducted by qualified inspection personnel and the results are recorded in standard inspection forms and bridge records (see Figure 3.1).

```

B80028                BRIDGE MAINTENANCE UNIT                RUN DATE 08/22/02
                      DATA ON EXISTING STRUCTURE
-----
COUNTY:              DIV.:  DIST.:  STRUCTURE NUMBER:      LENGTH:
CABARRUS              10      1      12 0271              135 FEET
-----
ROUTE CARRIED:        FEATURE INTERSECTED:
SR1157                IRISH BUFFALO CREEK
-----
LOCATED:              BRIDGE NAME:
0.3 MI. N.JCT.US601  BYP
-----
FUNC. CLASS:  SYST.ON:  SYST.UNDER:  ADT & YR:  RAIL TYPE:
UC            FA            -----  6400 --  LT 311 RT 311
-----
BUILT:  BY:  PROJ:  FED.AID PROJ:  DESIGN LOAD:
1933  SHPWC  6150  E-323-A  H-15
-----
REHAB:  BY:  PROJ:  ALIGNMENT:  SKEW:  LANES:
-----  -----  TAN  090  ON 02 UNDER 00
-----
NAVIGATION:          HT.CRN.TO BED:  WATER DEPTH:
VC --- FT  HC ---- FT  22 FT  2 FT
-----
SUPERSTRUCTURE:
REINFORCED CONCRETE DECK GIRDERS
-----
SUBSTRUCTURE:
ABUTMENTS:RC SPILL THROUGH ON PILE FOOTINGS,INT.BENTS:RCP&W
-----
SPANS:
1245'2 , 1245'1 , 1245'2
-----
BEAMS OR GIRDERS:
3 LINES OF 18 X30 RC DECK GIRDERS @ 8'0 CENTERS
-----
FLOOR:              ENCROACHMENTS:  DECK (OUT TO OUT):
10 RC,5 AWS        B UTILITY PIPE  023.2
-----
CLEAR ROADWAY:      BETWEEN RAILS:  SIDEWALK OR CURB:
020.0              021 .0  LT 00.5 RT 00.5
-----
VERT.CL.OVER:  VERT.CL.UNDER:  HOR.CL.UNDER:  SPECIAL PERMIT:
99 FT 99 IN  00 FT 00 IN  00.0 FT  ---
-----
INV.RTG.:  OPE.RTG.:  CONTR.MEMBER:  POSTED:
HS- 9  HS- 16  RCDG  SV 23  TTST 27 DATE 03 13 2002
-----
SYSTEM:              GREEN LINE ROUTE:
8 URBAN-SECONDARY  NO
-----
2ND OPENING:  3RD OPENING:  4TH OPENING:  5TH OPENING:
-----
REMARKS:
-----

```

Figure 3.1 Bridge record sheet

In order to learn more about the inspection procedures, the UNC Charlotte research team joined the Division 10 bridge inspection crew to several bridges scheduled for routine inspection. During this process, the two-man crew performed several field measurements on the superstructure, the substructure, and the channel profile (where applicable). The inspectors also noted the condition and the grade of deterioration (where applicable) for all structural and non-structural elements, and took digital pictures of selected bridge details. All of this information was included in the inspection report and sent to the Analysis Team of the Bridge Maintenance Unit.

As a part of the bridge condition evaluation, the AASHTO (2000) manual provides guidelines on material testing, including both field and laboratory tests. These tests are aimed, using destructive and non-destructive methods, at the in-situ or laboratory assessment of strength and condition of concrete, steel, and timber materials.

3.2 AASHTO Load Rating Guidelines

As part of the condition assessment of bridges, the above-mentioned manual (AASHTO, 2000) also provides detailed bridge load rating procedures. These calculations are performed in order to evaluate the safe load carrying capacity of bridges, and are performed or updated following each bridge inspection.

Highway bridges are rated at two levels, inventory and operating levels. The *inventory rating* (IR) represents “a load level which can safely utilize the structure for an indefinite period of time.” This rating uses a large safety factor, since this day-to-day use will imply the largest amount of traffic passing over the bridge. The *operating rating* (OR) represents “the absolute maximum permissible load level to which the structure

may be subjected.” This rating uses a smaller safety factor in order to maximize the capabilities of the bridge for the occasional special case. Therefore, the OR is not intended for everyday use.

The rating can use either the allowable stress (AS) method, or the load factor (LF) method. The selection of the method will change the load factors and the member capacity values used in Equation 3.1:

$$RF = \frac{C - A_1 \times D}{A_2 \times L \times (1 + I)} \quad 3.1$$

where: RF – rating factor for live load; C – capacity of the member; A_1 – factor for dead loads; D – dead load effect; A_2 – factor for live loads; L – live load effect; and I – impact factor.

This rating factor can also be used to determine the bridge rating in tons (using Equation 3.2). The overall bridge rating will be governed by the member with the lowest rating factor.

$$RT = (RF) \times W \quad 3.2$$

where: RT – bridge member rating in tons; and W – weight of nominal truck used to determine live load effects.


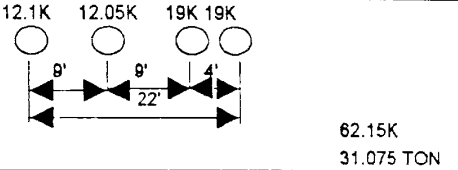

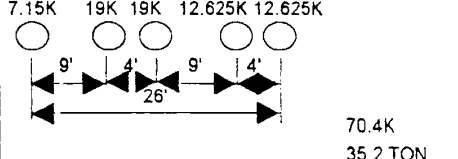
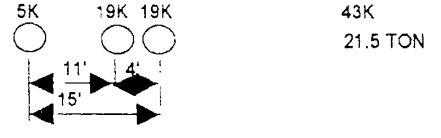
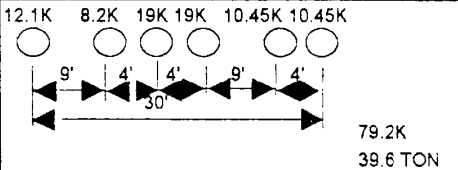
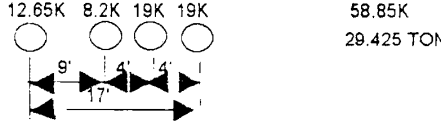
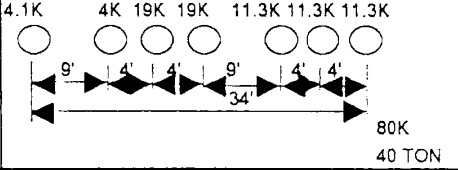
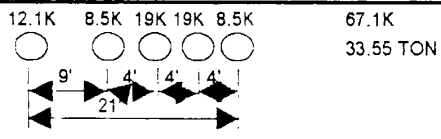
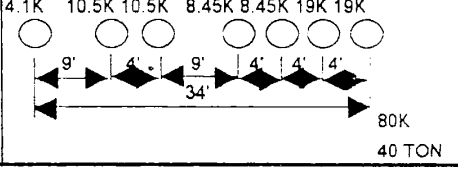
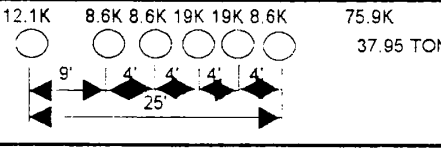
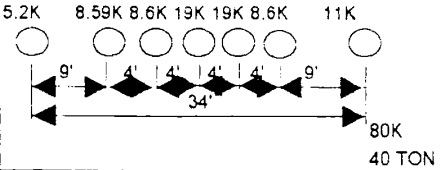
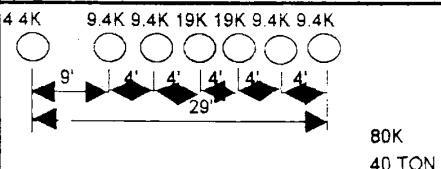
3.3 NCDOT Bridge Rating Procedures

The computer analysis programs currently used by the NCDOT are MS-DOS based programs, and are based on equations recommended by AASHTO (2000) for bridge superstructures.

The input files for these programs are generated using bridge records and the most current inspection reports. These files include general bridge data, such as bridge number, county number, date inspected, and date of analysis; geometric information, including span length, size of members, bridge dead loads; material properties from as-built drawings, or from AASHTO recommended values when no other data is available.

In addition, the programs prompt the user to input the percentage of the girder that is still effective. This is where the inspection process ties in with the computer program. From the notes and photographs of a particular component the bridge inspectors provided in their report, the analyzing engineer estimates the percent effective of the cross-section. Obviously, this is a subjective estimate, and it is intended to result in a conservative load rating.

After all the information is input into the program, the computer calculates the dead load moment, girder capacity, and live load moments. The program computes live load moments by positioning different types of legal truck loads to determine critical elements on the bridge. The schematics shown on Figure 3.2 are used by the programs to model real vehicle axle spacing and axle loads. Each of these trucks are identified by a reference number and is placed into one of two categories: single vehicles (SV), and truck tractor semi-trailer (TTST).

SINGLE VEHICLE(SV)		TRUCK TRACTOR SEMI-TRAILER(TTST)	
REF. #	SCHEMATIC	REF. #	SCHEMATIC
SH		T4A	
S3A		T5B	
S3C		T6A	
S4A		T7A	
S5A		T7B	
S6A			
S7A			
S7B			

7/18/95

Figure 3.2 NCDOT legal loads

Using these live load moments the program calculates two rating factors, inventory and operating. These factors are then multiplied by the weight of the truck, and then divided by the distribution factor to develop a rating for that girder. To calculate the rating factors, the program utilizes Equation 3.3.

$$RF_i = \left(\frac{\left(M_n \times \frac{PercEff}{100} \right) - (A_1 \times MomentDL)}{A_2 \times MomentLL_i \times I} \right) \times 2 \quad 3.3$$

where: M_n – moment capacity of the girder; PercEff – percent of girder resisting loading; MomentDL – moment due to dead load; MomentLL – moment due to live load; I – impact factor; $A_1 = 1.3$ (dead load factor); $A_2 = 1.3$ for operating, 2.17 for inventory (live load factor); and i – indicates this value varies with each truck.

To convert this rating factor into a rating, Equation 3.4 is used:

$$Rating_i = \frac{(TruckWeight_i \times RF_i)}{DistFactor} \quad 3.4$$

where: Truck Weight – weight of vehicle; RF – rating factor; and DistFactor – distribution factor (based on AASHTO or user input).

3.4 Sample Analysis

This section outlines a sample computer analysis first by hand calculations, then by using the NCDOT computer output. For simplicity, the hand calculations will be limited to the S3C truck. The same process can be repeated for all the remaining loading trucks. The structure being analyzed is a simple-span reinforced concrete deck girder (RCDG) bridge. The process is similar for steel girder bridges with a few exceptions, such as, serviceability requirements, compact section requirements, etc.

- Hand Calculations:

Span = 45 ft

PercEff = 95%

Beam spacing = 6 ft

$$\text{Impact} = \left(\frac{50}{\text{Span} + 125} \right) + 1 = 1.294 < 1.3 \quad \text{.....OK}$$

$$\text{Distribution factor} = \left(\frac{\text{Spacing}}{6} \right) = 1$$

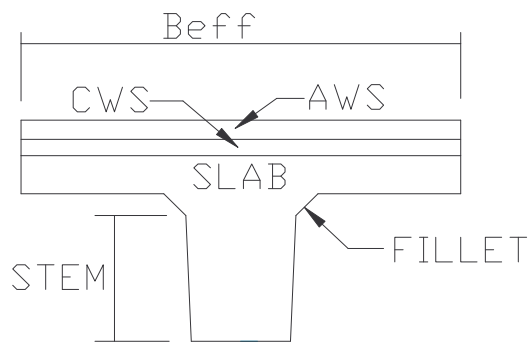


Figure 3.3 Sample girder section

Dead Load

Asphalt Wearing Surface (AWS) = 2 in.

Concrete Wearing Surface (CWS) = 3 in.

Slab = 6.5 in.

Fillet = 4 in.

$B_{eff} = 72$ in.

Stem Depth = 27 in.

Top Stem = 18 in.

Bottom Stem = 18 in.

Diaphragm = 35 lb/ft

Post & Rail = 67 lb/ft

$$DL_{Slab} = \left[AWS \times 12 + CWS \left(\frac{150}{12} \right) \right] \times Spacing + Spacing \times Slab \left(\frac{150}{12} \right)$$

$$DL = \left[StemDepth \times TopStem + Fillet^2 \left(\frac{150}{144} \right) \right] + DL_{Slab} + Post \& Rail + Diaphragm = 1481 \text{ lb/ft}$$

$$MomentDL = DL \left(\frac{Span^2}{8000} \right) = 375 \text{ k-ft}$$

Live Load

Truck = S3C

MomentLL_{S3C} = 418.31 k-ft

Girder Capacity Calculation

$$f'_c = 2500 \text{ psi} \quad f_y = 33000 \text{ psi} \quad \beta_1 = 0.85 \quad \Phi = 0.9$$

$$d = 27.46 \text{ in.} \quad B_{eff} = 72 \text{ in.} \quad A_s = 16.974 \text{ in}^2 \quad t = \text{Slab} - \frac{1}{4} \text{ in.}$$

$$a = \left(\frac{A_s \times f_y}{0.85 \times f'_c \times B_{eff}} \right) = 3.661 \text{ in.} < t = 6.25 \text{ in.} \dots\dots\dots \text{Rectangular Compression Zone}$$

$$M_n = \phi \times \left[A_s \times f_y \left(d - \frac{a}{2} \right) \right] \left(\frac{1}{12000} \right) = 1077 \text{ k-ft}$$

Rating Factor

A1 = 1.3 A2 = 1.3 for operating, 2.17 for inventory

$$RF_{inv} = \left(\frac{M_n \times \left(\frac{PercEff}{100} \right) - A_1 \times MomentDL}{A_{2inv} \times MomentLL_{S3C} \times I} \right) \times 2 = 0.913$$

$$RF_{oper} = \left(\frac{M \times \left(\frac{PercEff}{100} \right) - A_1 \times MomentDL}{A_{2oper} \times MomentLL_{S3C} \times I} \right) \times 2 = 1.524$$

Load Rating

$$Rating_{inv} = \left(\frac{TruckWeight_{S3C} \times RF_{inv}}{DistFactor} \right) = \underline{\underline{19.6 tons}}$$

$$Rating_{oper} = \left(\frac{TruckWeight_{S3C} \times RF_{oper}}{DistFactor} \right) = \underline{\underline{32.8 tons}}$$

- NCDOT Computer Program Output:

The same information as in the hand calculations was input into the NCDOT program. Figure 3.4 shows the output sheet from the NCDOT bridge analysis program. The echo input information is summarized at the bottom of the figure. This sheet shows the calculated operating and inventory ratings for each of the North Carolina trucks. As it can be seen, for the S3C truck the inventory rating is 19.6 tons, and the operating rating is 32.6 tons, values very close to the results of the hand calculations.

To determine if a load restricting postings is needed on an analyzed bridge, the program compares each operating rating with the legal weight of the each truck. If the operating rating for any of the vehicles is less than the weight of that particular truck, then the bridge needs to be posted. If this is true for more than one truck in each category, SV or TTST, then the lowest operating rating that does not pass will be considered the posting for the bridge.

↑

NORTH CAROLINA DEPARTMENT OF TRANSPORTATION - BRIDGE MAINTENANCE
ANALYSIS SECTION

BRIDGE NUMBER	Example 1	DATE OF RATING	6/19/02
COUNTY	0	RATED BY	UNCC
DATE OF INSPECTION	example	CHECKED BY	

Load Factor Method
REINFOR. CONCRETE DECK GIRDER RATING

Truck	Weight	Operating	Inventory	Controls	LLmoment
HS15	15.00	23.7	14.2	Strength	404.01
H15	15.00	32.1	19.2	Strength	296.81
TR2	15.75	34.2	20.5	Strength	293.95
TR3	24.94	34.5	20.7	Strength	458.10
TR4	33.60	34.4	20.6	Strength	619.46
TR5	36.75	39.9	23.9	Strength	584.85
SH	12.50	32.1	19.2	Strength	247.34
S3C	21.50	32.6	19.5	Strength	418.31
S3A	25.02	33.7	20.2	Strength	470.94
S4A	29.42	35.5	21.2	Strength	526.78
S5A	33.55	36.2	21.7	Strength	587.41
S6A	37.95	38.4	23.0	Strength	628.95
S7B	40.00	37.6	22.5	Strength	674.60
S7A	40.00	39.7	23.8	Strength	639.64
T4A	31.08	39.3	23.6	Strength	503.60
T5B	35.20	39.2	23.5	Strength	569.55
T6A	39.60	41.7	25.0	Strength	603.95
T7A	40.00	42.7	25.6	Strength	595.54
T7B	40.00	44.5	26.7	Strength	578.79

Last update 3-26-98-----NON-INTERSTATE TRAFFIC-----Version 4

INPUT:

Rating for Maximum Moment Possible
Interior RCDG Clear Roadway = 22.000 ft. Number of Beams = 4

Slab Full Thick = 6.50 in. Stem Depth = 27.000 in. Fillet Size = 4 in.
Top Stem Width = 18.00 in. Bot Stem Width = 18.00 in.

Number of Bars	Size Number	Distance
4	11	3.000
2	11	6.000
2	10	6.000
4	10	9.000

Weights:

Asphalt Wear. Surf. = 2.00 in. Concrete Wear. Surf. = 3.00 in.
Diaph = 67 lb/ft. Post-Rail = 35 lb/ft.

RCDG Spacing = 6.000 ft.
Percentage Effective = 95.000 % Span = 45.000 ft.
Concrete Compression Stress = 2500 psi Reinfor. Steel Yield Stress = 33000

COMPUTED BY THE PROGRAM:

Dead Load = 1481 lb/ft. Eff. Slab Width = 72.00 in. Impact + 1 = 1.25
Dist. Factor = S/6.0 = 1.000 Modulus Ratio of Elasticity n = 12

Figure 3.4 Output sheet from NCDOT program

This is done for both SV and TTST separately; therefore, if a bridge is posted, it will be posted for both SV and TTST, as needed. TTST are generally longer vehicles with wider axle spacing, so the ratings are generally larger. Figure 3.5 is a summary sheet for the bridge analysis. The three columns near the center of the page, from left to right, are the trucks reference numbers, truck weight in tons, and operating rating for each particular truck.

For the SV, each one of the operating ratings is larger than the legal weights, except for S7B and S7A. The lower of these two ratings is rounded down to the closest whole number and governs the load-restricting posting. In this case, S7B governs the SV category with 37 tons. For the TTST, none of the operating ratings are lower than the legal weights. Therefore, the bridge is not restricted for TTST.

The result of these comparisons is noted on the summary sheet:

SV-37 tons TTST-Legal gross weight

```

=====
NORTH CAROLINA DEPARTMENT OF TRANSPORTATION - BRIDGE MAINTENANCE
ANALYSIS SECTION
=====
RATING SUMMARY SHEET
Non-InterState Highway Bridge
STRUCTURE NUMBER: Example 1    COMPILED BY: UNCC    DATE: 6/19/02
COUNTY: 0                    CHECKED BY:         DATE:
=====
MEMBER:          RCDG
-----
HS inv          14.2
HS opr          23.7
-----
SH   12.50      32.1
S3C  21.50      32.6
S3A  25.02      33.7
S4A  29.42      35.5
S5A  33.55      36.2
S6A  37.95      38.4
S7B  40.00      37.6
S7A  40.00      39.7
-----
T4A  31.08      39.3
T5B  35.20      39.2
T6A  39.60      41.7
T7A  40.00      42.7
T7B  40.00      44.5
-----
CALCULATED POSTING:          | Design Loading:
SV 37 tons - TTST LGW       |                          unknown
-----
CONTROLLING MEMBER:         | INVENTORY RATING:
RCDG                        |                          HS  14.2
-----
EXISTING POSTING:           | OPERATING RATING:
Not Posted                   |                          HS  23.7
-----
RECOMMENDED POSTING:       | Item 70 - Bridge Posting
SV 37 tons - TTST LGW     | CODE:                          4
-----
REASON FOR POSTING CHANGE:
-----
ANALYSIS METHOD  Inventory Rating: LF          Operating Rating: LF
-----
COMMENTS:
=====

```

Figure 3.5 NCDOT program summary sheet for the example bridge

3.5 AASTHOWare

The AASTHOWare software package consists of three programs: Opis, Virtis and Pontis. These three programs allow for the exchange of data between the programs. This enables the user to input data for the structure only once, and then share it between the programs to carry out each program's specific functions. Therefore, a user can design a bridge with Opis, which is design software that was not evaluated during this research. Then export the data to Virtis, a load rating software to determine the Inventory and Operating Ratings, and finally, export that data to Pontis, a bridge management system that generates data for the National Bridge Inventory (NBI).

The Virtis and Pontis programs were developed by AASTHOWare to implement the NCHRP 12-50 methods (*Transportation Research Board, 2003*). This 1998 project concluded in 2002 with the development of a methodology for bridge-design software validation. From this, "Process 12-50", a systematic method of comparing and evaluating bridge design and analysis software, was generated. Process 12-50 provides a standardized report format for presenting and comparing results for a specific bridge design and a powerful method for formally reviewing specification changes.

The demonstration copies of Virtis and Pontis were evaluated for ninety days, during this project. This time limitation only allowed for the analysis of one of the scheduled test bridges. The outputs were compared with the current NCDOT load rating software.

Virtis

The software Virtis Version 4.1 was developed by AAHSTO in 2001. It is a bridge load rating software with the capability of using either LFD or LRFD. The demonstration copy used during this research employed the 1996 AASHTO Standard Specifications for Load Factor Design and the 1998 AASHTO LRFD Specifications. However, full versions of this product allow for code updates (interim revisions) as required.

Virtis allows the user to input all design data for the bridge, or import it from Opis, including shear reinforcement. The user input option allows the user to define different beam shapes, end conditions, and material properties. The program can evaluate steel, timber, or reinforced and prestressed concrete members. The bridge can be defined as a simple beam or continuous, or a combination of both for multiple spans with the end conditions defined as pinned-pinned, fixed-fixed, or a combination.

For steel girder bridges, this program allows the user to detail information concerning the deterioration of the beam. A deterioration profile can be created for the web, top and bottom flanges, and top and bottom cover plates. This profile can be generated based on field inspection notes, and will greatly affect the load rating of the bridge.

The program will also consider percent effective of the bridge member's section. However, adjusting the percent effective from the default 100% created a controlling Ultimate Shear Capacity versus Ultimate Moment Capacity. While this may realistically be the controlling factor, there is a known problem with the software in this regard. The modification of the percent effective does not allow the user to ignore shear.

The program can evaluate the entire bridge, a selected span, or a single girder. It will report the calculated load ratings for the controlling load vehicle. It will also generate graphs and tables for moment, shear, and displacement. This program however, will not generate load postings. It generates inventory and operating ratings that are used in determining the required posting. These ratings were used to compare and evaluate the current NCDOT load rating software.

Pontis

The software Pontis Version 4.1 was developed by AASHTOWare as a bridge management system. It allows the user to either create or import data from Virtis and determine the sufficiency ratings of the bridge. Pontis is currently used by most states. Missouri and Florida Departments of Transportation have utilized the program since 1998.

The sufficiency rating calculations follow the items described by NBI (USDOT, 1995). These rating are based on inspection details, which are entered into the program from the field inspection notes. The program transfers the field inspection ratings into NBI Coding. This is then used to determine the bridge sufficiency rating. The Federal Highway Administration (FHWA) considers a bridge structurally deficient when the sufficiency rating is below 50.

The software's management system also entails the ability of project planning, programming, and preservation of the structure. For the purposes of this research however, only the inspection function was used.

3.6 UNCC Bridge Analysis Software

In order to perform some of the lower and upper bound analyses on several bridges, the researchers developed a simple-span bridge analysis (Excel based) software. For reference, the file is attached to this report, and a detailed instruction manual is provided in Appendix A.

An output example is shown in Figure 3.6, illustrating the ratings for 59-0038. As it can be seen, the software evaluates the bridge rating using both LFD and LRFD methods. Furthermore, it is possible to input pinned, fixed, and partially fixed girder end connections. Even though the software does not have continuous span capabilities, this feature allows the user to investigate the effect partial fixity has on the bridge rating.

The software also allows the engineer to input calculated or user defined distribution factors and impact factors for both concrete and steel girder bridges. For RCDG bridges, cracked section properties are used, as needed. In order to allow a more direct comparison between analytical rating and load test results, an added feature allows for the calculation of strains and stresses in the bridge girders.

Another feature for this software is the capability to save the input and output files electronically. This allows the user to store the bridge data between two inspections, reducing the time needed to re-run the program.

The intent of the development of this program was not to replace the existing NCDOT bridge analysis software, only to complement its capabilities with added features that allow for a lower and upper bound analysis. However, if there is a need expressed by NCDOT, the software can be further developed to include continuous span girders, as well as a variety of other customized features.



NCDOT BRIDGE BEAM ANALYSIS SPREADSHEET

Type of Bridge:	Steel Girders w/ RC Deck	Date:	10/5/04
Bridge Number:	59-0038	Number of Spans:	1
Clear Roadway:	24.833 ft	Controlling Clear Span:	34 ft
		Analyzed Beam:	Interior Beam

Beam Type:	User Defined	Beam Spacing:	4.083 ft	Effective Width:	48.996 in
Depth:	20 in	Ixx:	1172 in^4	Area:	17.4 in^2
Slab Thickness:	7 in	Mu	365.48 k*ft	Sxx:	117 in^3
AWS Thickness:	8 in	Zxx:	132.9 in^3		
CWS Thickness:	0 in	Steel Yield Stress:	33000 psi	Percent Effective:	95.7%
Deck fc:	1500 psi			Skew Angle:	0

One Lane Loading Scheme Only

Load Vehicle:	HS_15	Moment LL:	257.70 k*ft	Beam Connections:	Pinned - Pinned
Design Vehicle:	H_15	Impact Factor:	30.00%		
		User Defined Dead Load:	820 lb/ft		

Distribution Factors:	LFD:	0.742	LRFD:	0.433
Load Rating:	Operating Rating:	HS 15.5	Operating Rating:	HS 26.5
	Inventory Rating:	HS 9.3	Inventory Rating:	HS 15.9

% Difference in Ratings: 171%

<u>Vehicle</u>	<u>Weight (tons)</u>	<u>LLMoment (k*ft)</u>	LFD: <u>Opr Rating</u>	LRFD <u>Opr Rating</u>
SH	12.5	178.94	18.6	31.8
S_3C	21.5	300.08	19.0	32.6
S_3A	25.0	333.35	20.0	34.2
S_4A	29.4	365.42	21.4	36.7
S_5A	33.6	402.70	22.1	37.9
S_6A	38.0	418.30	24.1	41.3
S_7B	40.0	454.20	23.4	40.1
S_7A	40.0	418.26	25.4	43.6
T_4A	31.1	327.15	25.2	43.3
T_5B	35.2	375.05	24.9	42.7
T_6A	39.6	384.60	27.4	46.9
T_7A	40.0	370.80	28.7	49.1

5 0

Recommended Postings:	LFD:	LRFD
	SV: 19.0 tons	SV: No Posting tons
	TTST: 25.2 tons	TTST: No Posting tons

Current Postings:	SV: 19.0 tons	TTST: 25.0 tons
-------------------	---------------	-----------------

Figure 3.6 UNC Charlotte bridge rating software printout

4. BRIDGE SELECTION

4.1 Selection Criteria

The criteria for selecting appropriate bridges for this project were created to ensure a true representation of typical bridges, especially those with higher maintenance needs. The selection and prioritization was coordinated with the NCDOT Bridge Maintenance Unit using the available computer database. Each selection was based on the following criteria (not in order of importance):

- Importance and traffic – to minimize commuter inconvenience the NCDOT suggested that only bridges on the secondary system should be considered, with adequate possibilities for traffic detours.
- Load ratings – the selected bridges had a wide range of load ratings, anywhere from bridges posted for SV-14 tons, to bridges with no postings.
- Bridge condition and estimated remaining life – only bridges with a reasonable life expectancy were considered.
- Bridge superstructure system – both concrete and steel girder bridges were selected, with simply supported and continuous systems.
- Site access – to allow the research team to prepare bridges for testing, only structures with reasonable foot and vehicular access were considered.
- Location of bridges – in order to avoid long travel times for the research team, only bridges within Division 10 were considered.

4.2 GFRP Deck Bridge

This project provided a unique opportunity to the researchers at UNC Charlotte to monitor the construction, instrumentation and field testing of the first glass fiber reinforced polymer (GFRP) deck bridge in North Carolina. The original Bridge 89-022 was built in 1944, and replaced in September 2001.

The original steel girder and concrete deck system superstructure was replaced with 7 – W24x94 steel girders and a composite deck supplied by Martin Marietta Composites. As it was mentioned earlier, this deck replacement project was funded with a discretionary grant from the Federal Highway Administration’s (FHWA) Innovative Bridge Research and Construction (IBRC) program. Table 4.1 at the end of this chapter provides more specific details for Bridge 89-022. In addition, a detailed, phase-by-phase construction report and structural description for this composite deck bridge is included in Appendix B.

4.3 Concrete Deck Girder Bridges

During this project, two reinforced concrete deck girder (RCDG) bridges were analyzed, instrumented and tested. The first RCDG structure was Bridge 59-361, a rural two-lane bridge located in western Mecklenburg County, North Carolina on Bellhaven Blvd. (SR 2373). The bridge consists of three simple spans of approximately 40 ft each. The deck is supported by four reinforced concrete girders spaced at 6 ft-8 in. on center. Construction of bridge 59-361 was completed in 1935; since that time, there have not been any structural modifications made to either the substructure or the superstructure. Figure 4.1 shows an elevation view of bridge 59-361, and Figure 4.2 shows a typical

cross section of the bridge superstructure.



Figure 4.1 Side view of Bridge 59-361

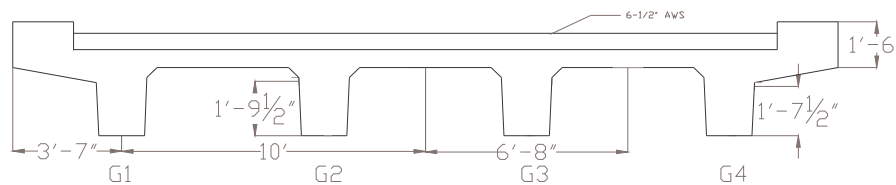


Figure 4.2 Typical cross-section of the superstructure for Bridge 59-361

The steel reinforcement is not shown in Figure 4.2 for clarity. The deck is reinforced with #4 bars at 6 in. o.c. in the bottom of the deck and #4 bars at 16 in. o.c. in the top of the deck longitudinal to the direction of traffic. In the transverse direction, #5 bars at a varying spacing were used. The girders were reinforced with (4) - #11 bars 3 in. from the bottom of the girder, (2) - #11 and (2) - #10 bars 6 in. from the bottom of the

girder, and (4) - #10 bars 9 in. from the bottom of the girder. For shear reinforcing, #4 bars at an unknown spacing were used.

The most recent three bridge inspection reports covering a span of five years have been reviewed. According to these reports, bridge 59-361 has isolated, minor hairline cracks in the girders and the piers. Each of these girders was rated as either good or fair. Furthermore, each report stated the same observed condition of the girders. Therefore, it is fair to assume that the cracks did not widen over this five-year period. In order to monitor changing conditions of concrete girders, it is recommended to mark the extent of these cracks, properly identifying the date of the last inspection and markings.

Although the apparent beam conditions have remained the same, the bridge load-restricting posting has been decreased after each report. Until 1999, the bridge was not posted. At the time of inspection, bridge 59-361 was posted at 35 tons for single vehicles, due to a change in material properties specified by AASHTO. The compressive strength of concrete for bridges constructed before 1959 was increased from 2,500 psi to 2,700 psi and the yield strength of steel for bridges constructed before 1954 was decreased from 33,000 psi to 30,000 psi. Obviously, these changes had an impact on the bridge posting.

Since the load testing in November 2001, the bridge has been reposted at 32 tons for single vehicles (SV) and 38 tons for truck tractor semi-trailers (TTST). This change was due to the resurfacing of SR 2373, resulting in an addition of 2.5 in. of asphalt wearing surface for a total of 9" of asphalt.

The second RCDG structure tested was Bridge 12-0271 (Figure 4.3), a three-span reinforced concrete deck girder bridge with three girders. This two-lane secondary route

bridge carries SR1157, Wilshire Avenue in Concord, NC, over Irish Buffalo Creek, just east of the SR1157 and NC601 intersection. It has an overall structure length of 132 ft – 6 in. A typical cross section of the bridge is shown in Figure 4.4.



Figure 4.3 View of girders in span 1 of bridge 12-0271

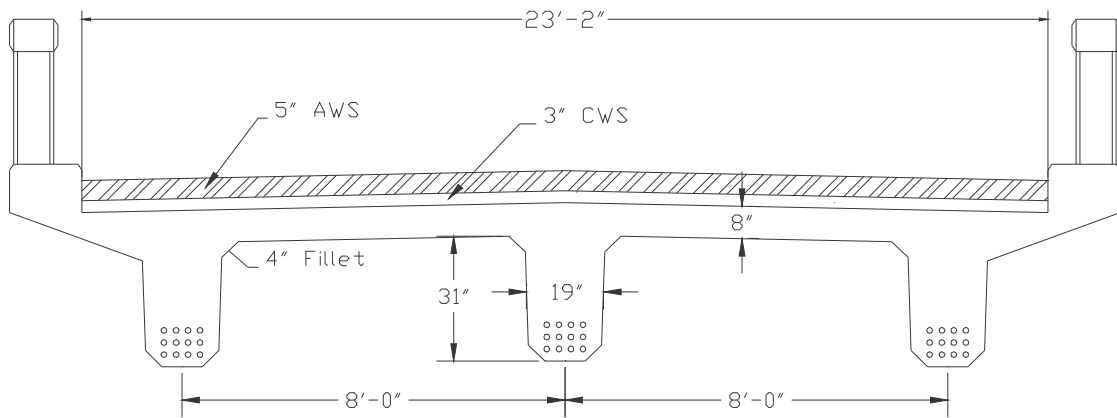


Figure 4.4 Cross section of bridge 12-0271

The bridge was designed for a load vehicle of H-15. It is currently posted for SV at 23 tons and TTST at 27 tons. This posting occurred on March 13, 2002, which represents a reduction from the previous posting of 32 tons. This change in posting occurred due to a change in allowable stresses for concrete and steel. The prior posting was based on unknown material strengths governed by the year of construction.

However, a recent NCDOT memorandum mandates the use of reinforcing steel and concrete allowable stresses from the original plans, whenever the information is available. Based on the original plans, the concrete compressive strength was established as 1,950 psi, and the yield strength of the reinforcing steel was computed as 30 ksi.

The last inspection of this bridge occurred on January 29, 2002. In this report, the bridge inspectors noted that, there were vertical and horizontal cracks on the sides face of the girders at midspan, which led to a decision to use a 95% effectiveness for the girder sections (*PercEff* in Equation 3.3). The current load ratings are Inventory HS-9.9 and Operating HS-16.5, resulting in a sufficiency rating of 48.1%, which gives the bridge an NBI status of structurally deficient.

4.4 Steel Girder Bridges

Three steel girder bridges were analyzed and tested during the two-year period of this project. The first was Bridge 59-0038, a rural two-lane bridge located in southeastern Mecklenburg County, North Carolina on Sam Newell Road (SR 3168). The bridge consists of one simple span of approximately 36 ft. The original superstructure of the bridge consisted of a reinforced concrete deck supported by five steel girders spaced at 4 ft – 1 in. on center. Construction on this bridge was completed in 1945. Since that

time, bridge 59-0038 has been widened using an additional steel girder placed on each side 3 ft – 6 in. from the existing girders in 1988. Another addition to the structure was the asphalt wearing surface added to protect the original deck from excessive wear. Figure 4.5 shows a typical bridge cross section.

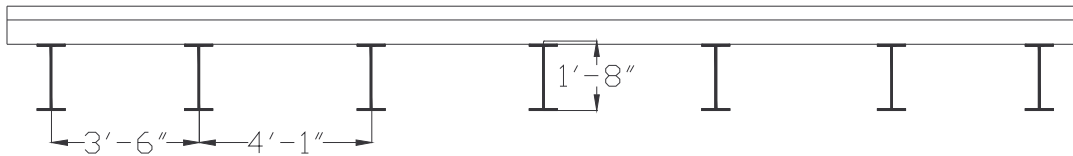


Figure 4.5 Typical cross-section of Bridge 59-0038

Similar to all seven bridges load tested in this project, the most recent three field inspection reports have been reviewed for 59-0038. According to these reports, this bridge has isolated, minor hairline cracks in the deck and concrete substructure. Each of these structural components was rated as *good*. The condition of the steel girders was not documented in these reports. However, it was found that the top flanges of many of the original steel girders had signs of surface corrosion.

Due to unchanging conditions of bridge 59-038, the posting has remained constant at 19 tons SV and 25 tons TTST since 1997. The girders are identified as W20x60 in the inspection reports, but this is not a typical rolled W-shape. Measurements of the girder were taken; however, the dimensions did not match any current rolled shape. Therefore, in calculating the moment of inertia these measurements were used. Information about the reinforcing of the concrete deck was not found either.

The second steel girder bridge tested was Bridge 12-0227 (see Figure 4.6), a structure similar to bridge 59-0038. The bridge has two W24x76 exterior girders and two

W27x94 interior girders. The reinforced concrete deck has an epoxy-wearing surface. It carries state route SR1006 (Mt. Pleasant Road) over Rocky River.

As it can be seen in Figure 4.7, significant debris was present at the time of the bridge instrumentation and testing. Also, it is evident from Figure 4.8 that the add-on timber bent has been repaired in the past. An additional timber post has been installed between the first and second posts, unloading the gravity loads from one of the severely decayed original posts.



Figure 4.6 View of bridge 12-0227



Figure 4.7 View of center spans of bridge 12-0227



Figure 4.8 Repaired timber bent #1 (in the background)

This bridge has a current posting of an SV at 24 tons and TTST at 28 tons, established on July 24, 1995. The bridge provided easy work access on two of the five spans with a ladder, while a snooper truck was required to complete the scheduled tasks only on the third (middle) span.

The as-built plans of the bridge specify the allowable stresses in the structural steel as 18 ksi, and the allowable concrete compression stress as 1,000 psi. The five spans of this bridge are 40 ft – 3 in. for spans 1 and 5, and the three interior spans are 40 ft – 0 in. A typical cross section of the bridge can be seen in Figure 4.9.

For the analysis of the interior girders a 95% effective area was assumed, for the exterior girders 98% was assumed. The bridge plans do not show any shear studs that would result in composite action between the deck and girders, so the bridge was analyzed as a non-composite beam with a concrete deck.

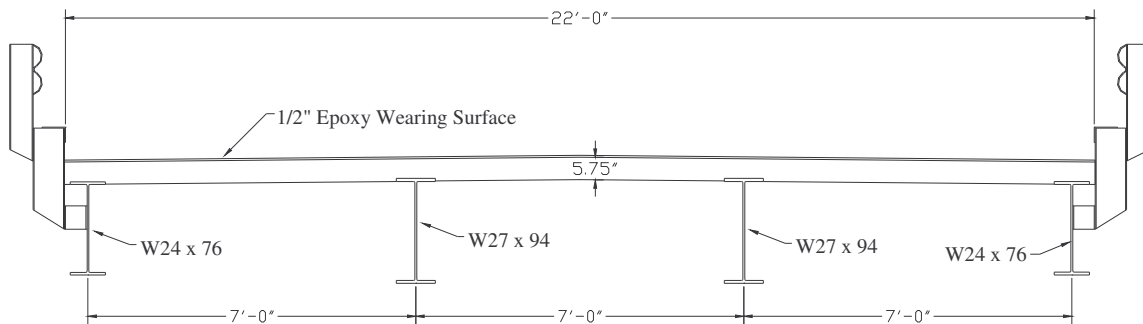


Figure 4.9 Cross section of Bridge 12-0227

The inspection report conducted on October 8, 2001, lists several items of importance. The inspection states that the epoxy wearing surface is missing in certain areas, and may fail to protect the deck. Also, the end diaphragms are cracked and

spalled. The exposed rebars are severely corroded. Figure 4.10 shows a cracked end diaphragm between Girders 1 and 2 of Span 1. Similar damage was present on all end diaphragms of the exterior bays. These defects made the likelihood of effective transverse load distribution questionable.



Figure 4.10 Cracked end diaphragm

The third steel girder bridge analyzed and tested was Bridge 59-0841, a two-lane bridge spanning a portion of Interstate 485 that, at the time of testing, was still under construction. This bridge is located in eastern Mecklenburg County, North Carolina on Caldwell Road (SR 2801). The overall length of this bridge is approximately 290 ft, consisting of two continuous spans of 144 ft and 146 ft, respectively. The reinforced concrete deck is supported by five continuous steel plate girders spaced at 9 ft – 4 in. on center. Figure 4.11 shows the elevation view of the continuous span structure.



Figure 4.11 Elevation view of Bridge 59-0841

Construction on this bridge was completed in early 2002. Older bridges of this size located in Division 10 are used to span wide waterways or heavily traveled interstates. In order to test a continuous bridge over a large waterway, either excessive marine equipment would had to be rented, or the bridge would had to be closed for an extended period of time to allow snooper trucks to park on the bridge and research personnel to gain access to the underside of the structure. Both of these solutions would have been excessively expensive and/or unnecessarily inconvenience commuters. Therefore, it was decided to test this new bridge.

Although construction was progressing on Interstate 485 under bridge 59-0841, no work was planned for the week UNC-Charlotte needed to prepare the bridge for testing. Consequently, commuters were not unnecessarily inconvenienced and construction was not interrupted. Since bridge 59-0841 is a new structure, the bridge maintenance division has not yet scheduled a bridge inspection.

4.5 Crutch Bent Bridge

As it was mentioned earlier, during this project, special interest was expressed from the NCDOT on the effectiveness of a crutch bent retrofit. In order to satisfy this requirement, Bridge 89-0219 was analyzed and tested, a steel bridge with timber decking spanning over a creek. The bridge originally had a load posting for SV loading of 14 tons, and for TTST loading of 18 tons. The load posting prohibited school buses from the legal use of bridge. The intent was to raise the legal posting to at least 16 tons in order to allow school bus traffic.

Bridge 89-0219 is located in Union County, NC carrying route SR1008 across a creek. The bridge was constructed in 1962, and originally consisted of two simple spans, one of them over a creek. The deck consists of $3\frac{3}{4}$ in. x $7\frac{3}{4}$ in. timber boards on ten lines of W14x30 steel beams. The analysis and posting of the bridge was originally done based on an estimated 95% percent effective cross-sectional area. However, this value might be unconservative, considering the significant corrosion of steel girders (see Figure 4.12).

The wooden crutch bent was installed for only one of the spans. This was done in order to avoid lengthy environmental permitting requirements for construction work in a creek bed. Due to the urgency of this project, only the span above dry land was retrofitted, with the second span to be done in the near future, once the environmental permit is secured. The crutch bent was designed by engineers from the NCDOT Bridge Maintenance Unit, and consisted of five (10 in. x 10 in.) timber posts at 6 ft spacing, and 10 in. x $11\frac{3}{4}$ in. cap and sill plate, properly braced (see Figure 4.13).



Figure 4.12 Steel girder corrosion



Figure 4.13 Crutch bent retrofit

4.6 Summary of Bridge Selection

As it can be seen from the previous sections, a large variety of bridges have been analyzed and tested. In order to allow quick referencing of these structures, Table 4.1 shows a summary of all the bridges tested in this project. In this table only the most important details are provided.

Table 4.1 Summary of bridge details

	BRIDGE 89-0022	BRIDGE 59-0361	BRIDGE 12-0271	BRIDGE 59-0038	BRIDGE 12-0227	BRIDGE 59-0841	BRIDGE 89-0219
County	Union	Mecklenburg	Cabarrus	Meckl.	Cabarrus	Meckl.	Union
Road Number	SR 1627	SR 2373	SR 1157	SR 3168	SR 1006	SR 2801	SR 1008
Feature Intersected	dry creek	creek	creek	creek	river	I-485	creek
Year Built	1944	1935	1933	1945	1951	2002	1950
Year Repaired/Retrofitted	2001	n/a	n/a	1988	n/a	n/a	1960, 2003
ADT	2800	6800	6400	13000	1300	n/a	2500
No. Spans	1	3	3	1	5	2 (cont.)	2 (3)
Span Lengths (ft-in)	42 - 0	(2) 38 - 9 (1) 40 - 0	(2) 43 - 9 (1) 45 - 0	36 - 0	(2) 40 - 3 (3) 40 - 0	144 - 0 146 - 0	28 - 4 28 - 1
No. Girders	7	4	3	7	4	5	10
Girder Types	W24x94	RCDG	RCDG	(5) W20x60 (2) W21x...	(2) W24x76 (2) W27x94	steel plate girders	W14x30
Girder Spacing (ft-in)	3 - 11	6 - 8	8 - 0	(2) 3 - 6 (4) 4 - 1	7 - 0	9 - 4	2 - 7
Deck Type	GFRP	concrete	concrete	concrete	concrete	concrete	timber
Original Design Load	unknown	H - 15	H - 15	unknown	H - 15	HS - 25	unknown
Inventory Rating	HS - 14	HS - 13	HS - 9.9	HS - 9	HS - 10	n/a	HS - 7
Operating Rating	HS - 23	HS - 23	HS - 16.5	HS - 15	HS - 17	n/a	HS - 12
SV Posting (tons)	37	32	23	19	24	none	14
TTST Posting (tons)	none	38	27	25	28	none	18
Tested	11/2001	11/2001	09/2002	03/2002	03/2003	04/2002	04/2003

5. EXPERIMENTAL RESULTS

Throughout this project, seven bridges were analyzed, instrumented and tested. Hundreds of experimental data files were generated from recordings of up to a hundred of instruments during static, slow and dynamic loading, focusing on the behavior of structural and non-structural components. The following sections describe the most important findings for each bridge, and their relevance to the project objectives.

5.1 Bridge 89-0022

Strain level and composite action

One method to prove composite or non-composite action in the bridge would be to locate the neutral axis of the girders. With no composite action, the strain in the girders would change from compression to tension at a location near the center of mass of the girder (for this bridge that would be 12.16 in.). The midspan of girders 2 and 4 were instrumented with strain gages on the top and bottom flanges. These instruments were used to help locate the position of the neutral axis. Assuming the strain in the girder remains linear, which should be the case for girder stresses lower than the yield level, the position of the neutral axis (NA) from the bottom of the steel girders can be calculated using Equation 5.1:

$$NA = (d - t_f) \frac{\epsilon_B}{\epsilon_B + \epsilon_T} \quad 5.1$$

where: $d = 24.31$ in. – girder depth; $t_f = 0.875$ in. – flange thickness; ϵ_B – bottom flange strain (in/in); ϵ_T – top flange strain (in/in).

The calculations for the experimental neutral axis location are demonstrated using the readings from the top and bottom flange strain at the midpoint of girder 2 for path 4. Both static (see Figure 5.1) and slow (see Figure 5.2) readings were analyzed. For both cases, the maximum bottom flange tensile strain was measured around $149 \mu\epsilon$, and the maximum top flange strain was approximately $-98 \mu\epsilon$. Using Equation 6.1, the neutral axis was computed as 14.1 in.

When the neutral axis at the midpoint of girder 2 was computed for all five load paths (shown in Table 5.1), the position of the neutral axis was computed to be an average of 14.9 in. above the bottom flange of the girder. Similar result (14.5 in.) was recorder for girder 4 at midspan. With the center of mass of the girder being located at 12.16 in., it is clear that there was some composite action taking place. This result will be further analyzed in Chapter 6.

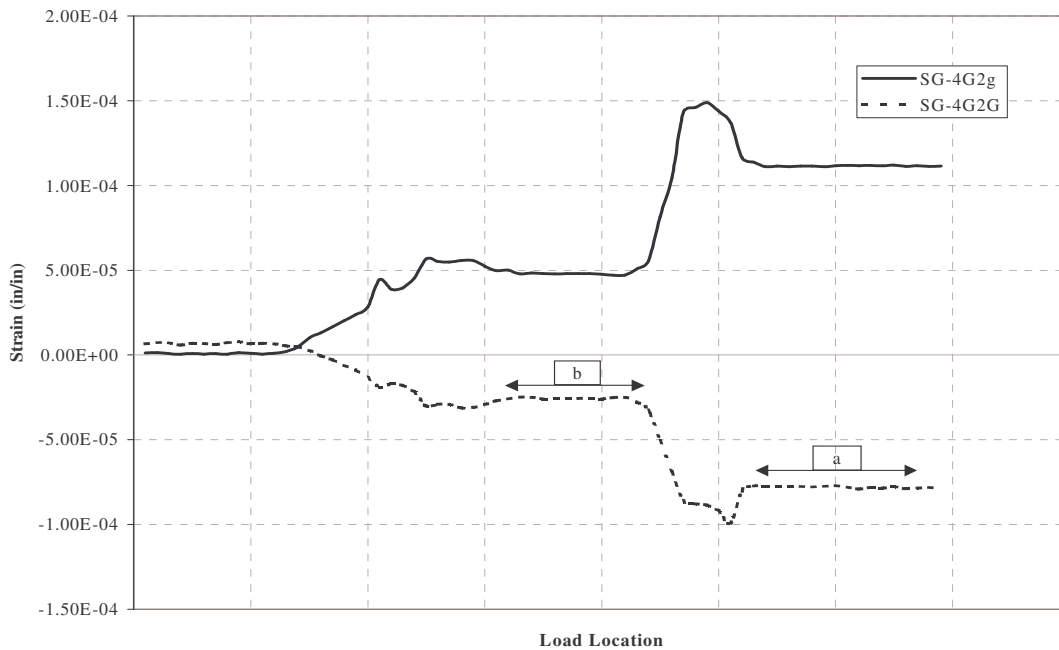


Figure 5.1 Strain at midpoint of girder 2 - static path 4

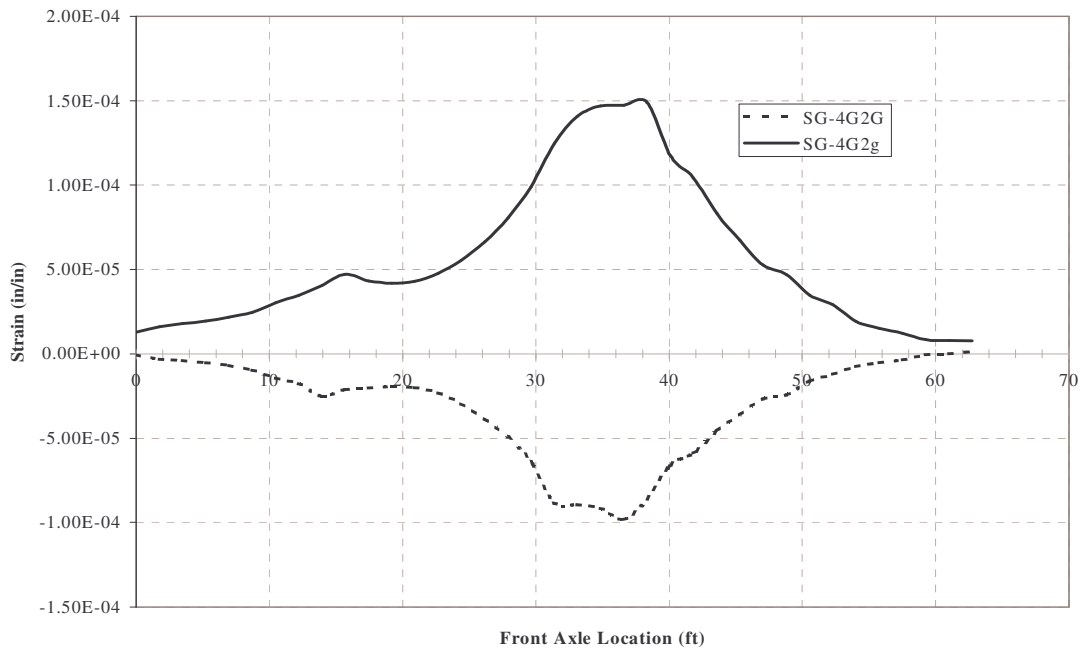


Figure 5.2 Strain at midpoint of girder 2 - slow path 4

TABLE 5.1 Experimental location of neutral axis for girder 2

Path	Gage	Strain (in/in)	Neutral Axis (in.)
1	SG-4G2g	27 E-06	15.4
	SG-4G2G	-14 E-06	
2	SG-4G2g	41 E-06	15.5
	SG-4G2G	-21 E-06	
3	SG-4G2g	72 E-06	15.2
	SG-4G2G	-39 E-06	
4	SG-4G2g	149 E-06	14.1
	SG-4G2G	-98 E-06	
5	SG-4G2g	107 E-06	14.2
	SG-4G2G	-69 E-06	
Average			14.9

Being the first GFRP deck bridge in the Carolinas, special attention was paid to the strain levels in the GFRP deck. Composite materials are linear; therefore, in order to avoid brittle material failure, it is important that at service level, adequate safety factors are used.

Being comprised of glass fiber laminas with various orientations, the strain in the fibers of the panels was not evaluated, and there was no allowable strain given by the panel manufacturer for the laminas themselves. Martin Marietta Composites provided designers only an overall allowable strain on the bottom of the deck panel for compression (-0.26%) and tension (0.26%). The ultimate strain levels should be at least six to eight times higher.

The strain readings in Bays 5 and 6 are plotted for load path 2 in Figure 6.5. The maximum tensile strain was observed in Bay 5, and it was approximately 0.024% (0.00024 in/in, or 240 $\mu\epsilon$). Therefore, the allowable strain in the material is over ten times larger than the strain experienced in the panel.

The maximum negative strain (compression) was recorded in bay 6. The strain at this location reached -0.002%. Once again, the strain induced in the material did not even come close to reaching the strain allowed in the material. In this case the allowable strain in the material was -0.26%, or roughly 130 times the strain present in the deck panel.

Indeed, from these data, one can conclude that the bridge deck is performing well within the manufacturer's specifications. In the future, it will be possible to increase the efficiency of FRP bridge decks significantly.

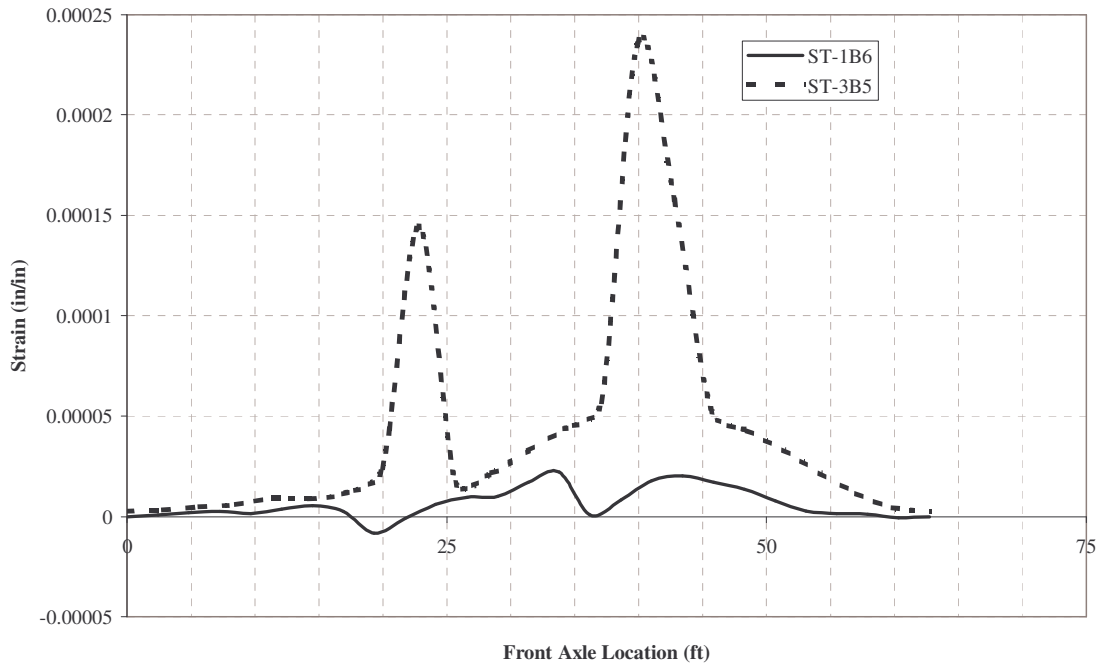


Figure 5.3 GFRP deck strain readings

Deck and girder deformations

In addition to strength requirements (to carry vehicular loads), a bridge also has service performance criteria. Excessive bridge deflections are perceived as a concern to the general public.

Therefore, another focus area for the testing of this bridge was the stiffness of the GFRP panels and steel girders. For the deck information, attention was placed on the data gathered when the loading truck was following path 2. In path 2, one line of wheels was centered between girders 5 and 6. This path placed the load on the side of the bridge where displacement transducers were positioned to record the relative deformation of deck panel 3.

The deflection of the bays is shown in Figure 5.4. From this graph, one can see the maximum deflection of the panel to be 0.017 in. It was also noted that the panel seemed to camber up slightly in bay 6. This camber reached a maximum value of 0.008 in. With the girders spaced at 47 in. o.c., the 0.017 in. deflection, as a ratio to the girder spacing, is $L/2800$. Presently, AASHTO does not have a requirement for the deflection of the composite deck. However, when comparing the deck deflection ratio to the tolerances established for girders, this structure is well within the $L/800$ live load criteria established for bridges (AASHTO Standard Specifications 10.6.2).

Midspan deflections were recorded for girders 1, 4, 5, 6, and 7. These deflections were plotted for all the slow load paths. The deflections for slow path 1 are shown in Figure 5.5. The corresponding maximum deflection for this loading condition occurred at girder 6, and had a magnitude of 0.183 in. This value represents approximately $L/2600$, which is well within the live load limit established by AASHTO.

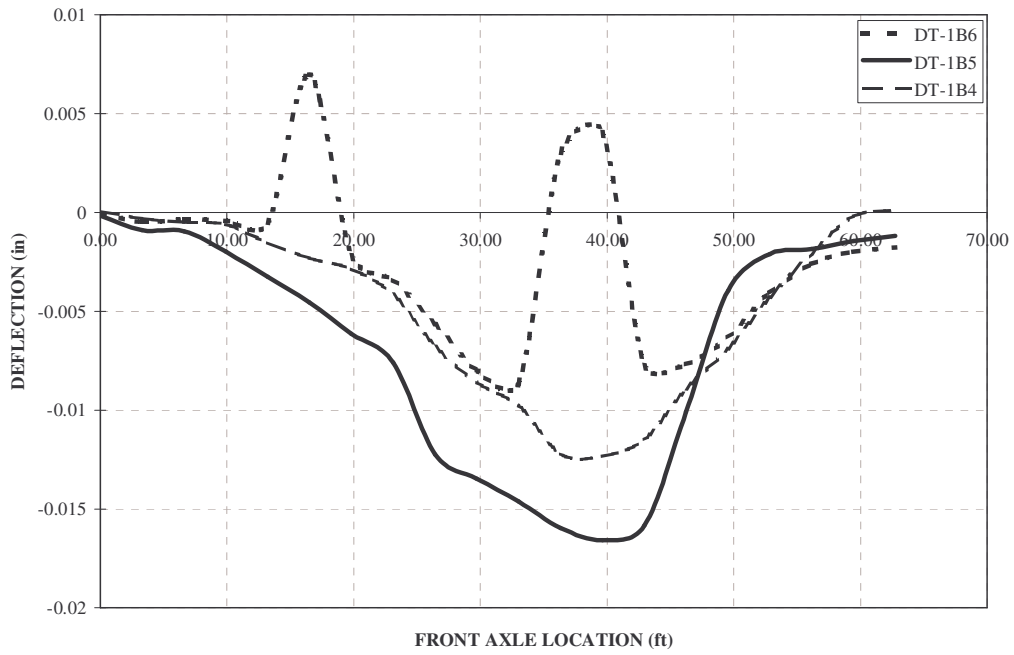


Figure 5.4 GFRP deck panel deflection – path 2

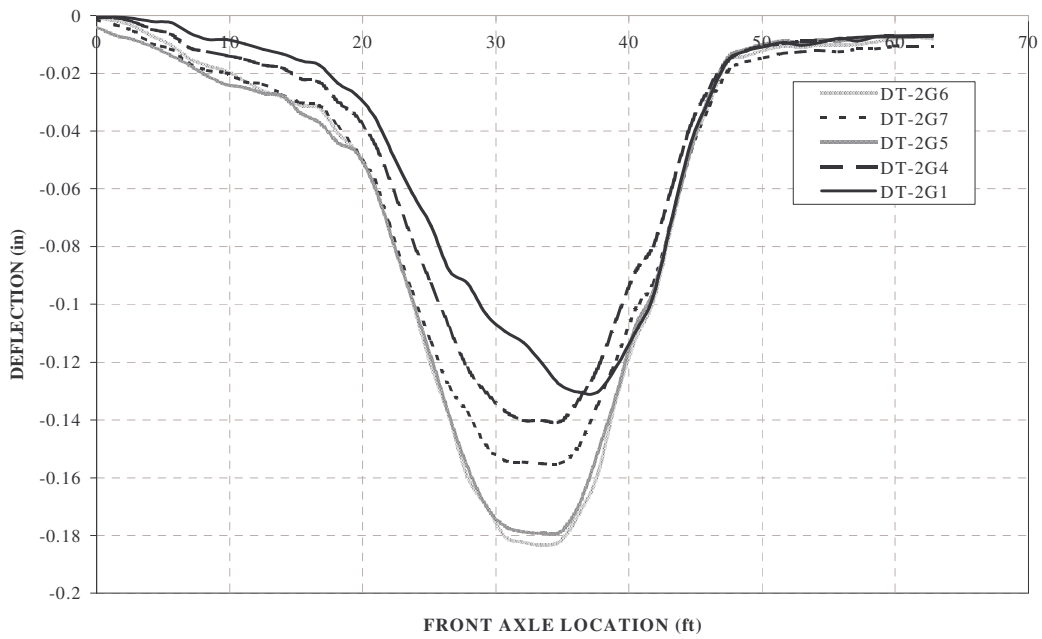


Figure 5.5 Midspan girder deflection – slow path 1

Transverse load distribution

Finally, attention was also given to distribution factors (DF). Present bridge design practice uses DF to estimate what percentage of the load being applied on the top of the deck is being transmitted to the girder being designed. AASHTO specifies a wheel load $DF = S/5.5$ for a span supported by more than 4 steel girders, where S is the span length in feet, and DF is the percentage of the load applied to the girder. Based on recommendations from the GFRP manufacturer, the designers of the superstructure used a conservative value of $DF = S/5$.

In order to experimentally determine the DF for this bridge, the strain readings at the bottom flanges on the girders at midspan (the approximate location of the maximum stresses) were used (see Table 5.2). For this bridge, two load paths were selected, paths 1 and 4 – for path 1 the loading truck is centered in one lane, and for path 4 the loading truck is centered in the opposite lane, moving in the same direction.

It is important to note that the live load distribution factors provided by AASHTO are based on wheel loads (i.e. half the axle load) acting on a specific girder. However, during testing, the full truck load was applied to the entire bridge. Furthermore, the calculations have been made based on both traffic lanes loaded simultaneously. Assuming that the truck positioned in the opposite lane will generate a similar but mirrored strain distribution, the strain values for the opposite lane were simply copied from the original strain profile (e.g. for girder 1 during loading in path 1, $24 \mu\epsilon$ were recorded. For the opposite lane, this value would have corresponded to the strain at the bottom of girder 7). In order to estimate the effect of both lanes loaded simultaneously, a simple superposition was used, which should be valid in the elastic zone.

Table 5.2 Distribution factor at girder midspan

Load Path	Strain at Bottom of Girder ($\mu\epsilon$)	1	2	3	4	5	6	7	Total Strain ($\mu\epsilon$)
Slow 1	one lane	24	27	65	115	146	149	98	624
	opposite lane	98	149	146	115	65	27	24	624
	both lanes	122	176	211	230	211	176	122	1248
	DF	0.39	0.56	0.68	0.74	0.68	0.56	0.39	
Slow 4	one lane	95	149	142	108	63	27	1	584
	opposite lane	1	27	63	108	142	149	95	584
	both lanes	96	176	205	216	205	176	96	1168
	DF	0.33	0.60	0.70	0.74	0.70	0.60	0.33	

Finally, to calculate the truck load distribution factor for both traffic lanes loaded, Equation 5.2, developed by Stallings and Yoo (1993), was used:

$$DF_i = \frac{n\epsilon_i}{\sum_{j=1}^k \epsilon_j w_j} = \frac{4(230)}{1248} = 0.74 \quad 5.2$$

where: n – the number of wheel lines (2 trucks x 2 wheel lines = 4 wheel lines); ϵ_i – strain at the bottom of the i^{th} girder; w_j – the ratio of the section modulus ratio of the i^{th} girder to the section modulus of a typical interior girder; k – the number of girders.

The maximum distribution factor for both paths 1 and 4 occurred at girder 4, with the calculated value of 0.74. It is important to note that, in Equation 5.2 it was assumed that all girders have the same section modulus. For this bridge, this is a reasonable assumption. However, for RCDG bridges, where the sections of the outside concrete girders are increased by curbs and railings, this assumption will generate conservative estimates for interior girders, and slightly unconservative distribution factors for the outside girders.

5.2 Bridge 59-0361

Strain levels

Strain readings were recorded for all seven load paths, for static, slow and dynamic procedures. However, the presence of the LVDTs slowed down the recording speed significantly, to less than 2 readings per second, which made the static versus dynamic comparison obsolete.

The position of the neutral axis was also impossible to determine due to the erroneous readings from the LVDT located on the sides of the girders. As mentioned earlier, the LVDTs used have a high noise range, which made them ineffective for reading very small strain measurements. Since the placement of the LVDTs was close to the presumed neutral axis, where small strains are present anyway, the instruments were unable to record useable data. This was avoided in all the future tests in this project.

Figure 5.7 shows the static strain readings for path 2 – span 1, from the bottom of girders (position 2) 2, 3 and 4. As it can be seen, the maximum reading was close to 30 $\mu\epsilon$. By inspecting all the other static readings, no higher static strain level was observed than 40 $\mu\epsilon$.

Figures 5.7 and 5.8 show the slow strain readings for paths 2 and 5, spans 1 and 2. These readings are comparable with the static readings, except for gage *ST,22gSP2*, bottom of girder 2, span 2. The instrument recorded strain readings close to 70 $\mu\epsilon$. This was also confirmed from other slow readings in span 2. This in turn suggests that, the span 2 (middle span in a three simply supported span concrete bridge) readings were higher due to a smaller degree of girder fixity in the middle span, as compared to the conditions present at the end spans (spans 1 and 3).

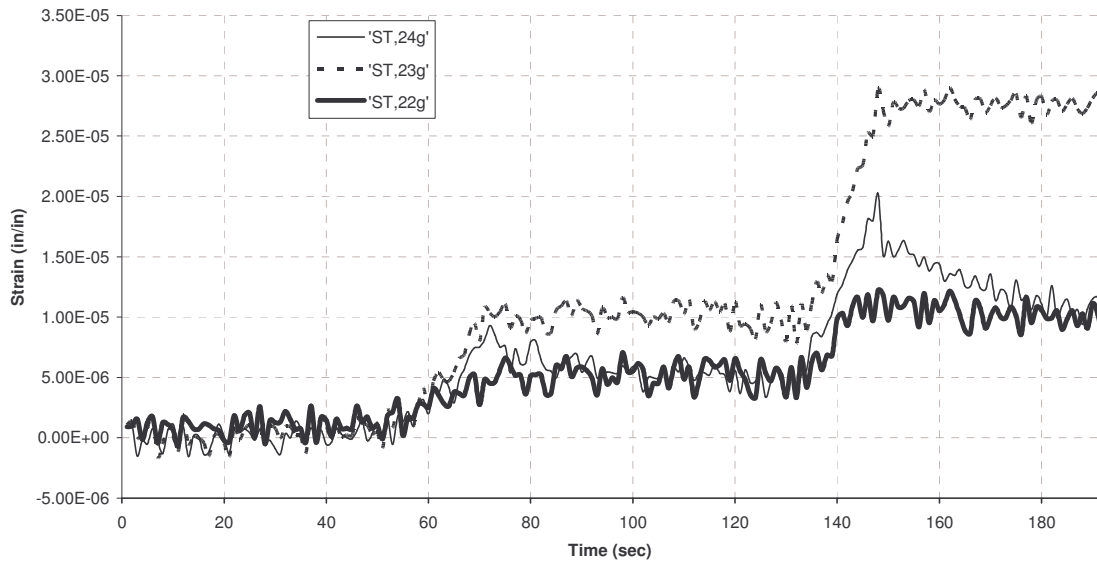


Figure 5.6 Static tensile strain readings – path 2, span 1

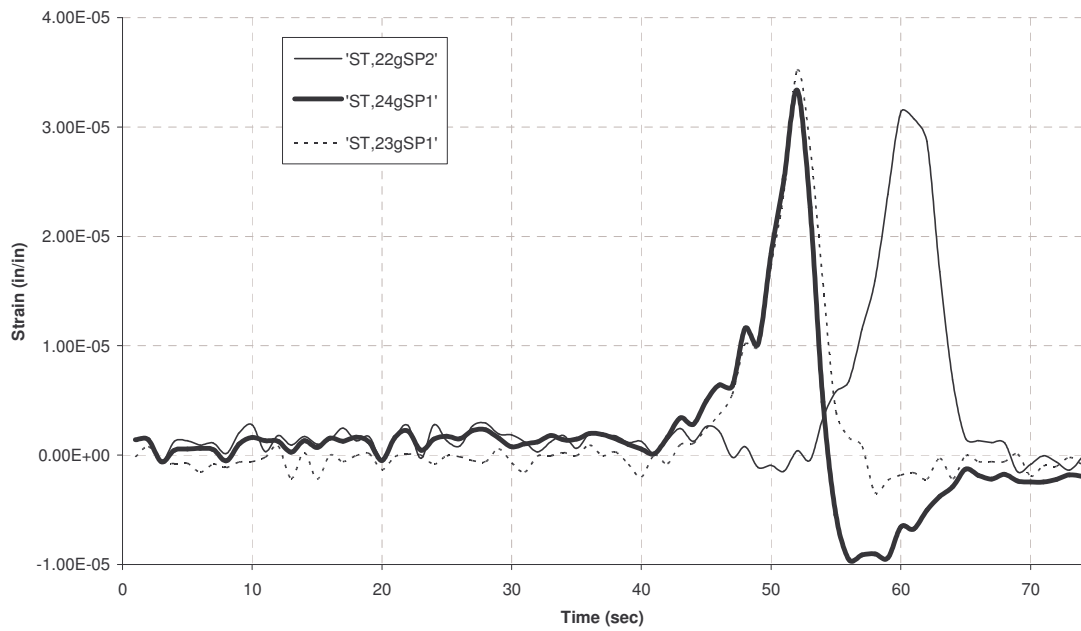


Figure 5.7 Slow tensile strain readings – path 2, spans 1 and 2

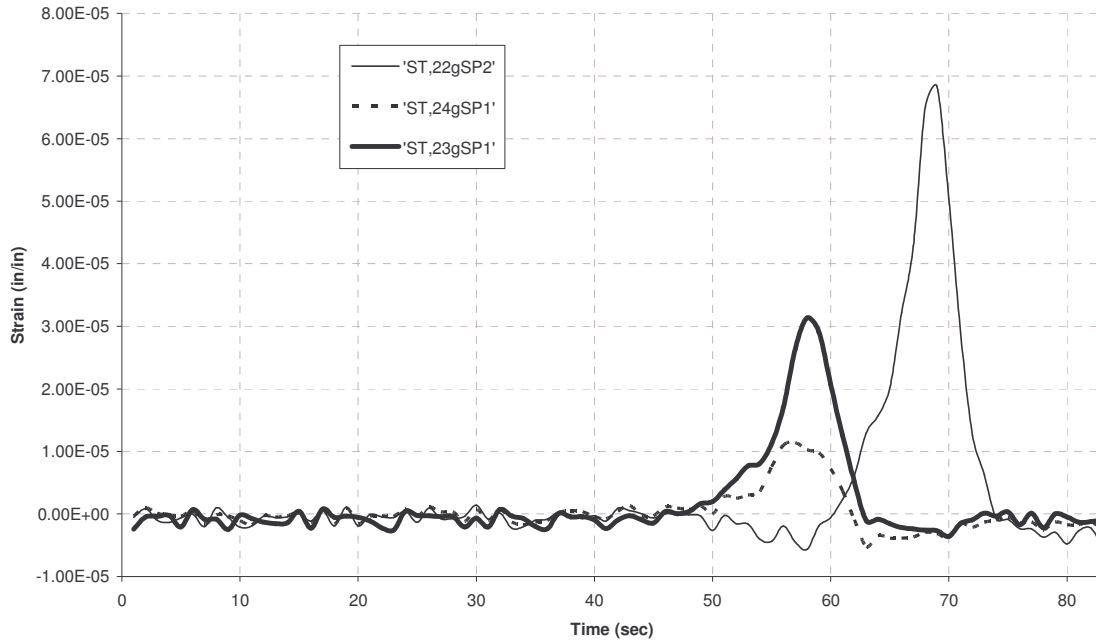


Figure 5.8 Slow tensile strain readings – path 5, spans 1 and 2

Girder deformation

Figure 5.9 shows the deformations for girders 2 and 3 at midspan during slow path 5. As a reminder, path 5 placed the center of the truck on the centerline of the wheel. Therefore, it is not surprising that both girders 2 and 3 have been deforming approximately the same amount in both spans. However, it is interesting to note that the deformations in span 2 were somewhat smaller than the ones measured in span 1. This fact does not fully support the assumption made earlier that span 2 is more flexible due to lower levels of fixity at its support.

It is interesting to note that while the truck was on span 2 (after the timestamp 62 seconds), the displacement transducers in span 1 recorded reasonable deformations. This could support a fact that there might have been continuity between girders. Although one has to remember that the values are overall small, less than 1/25 in.

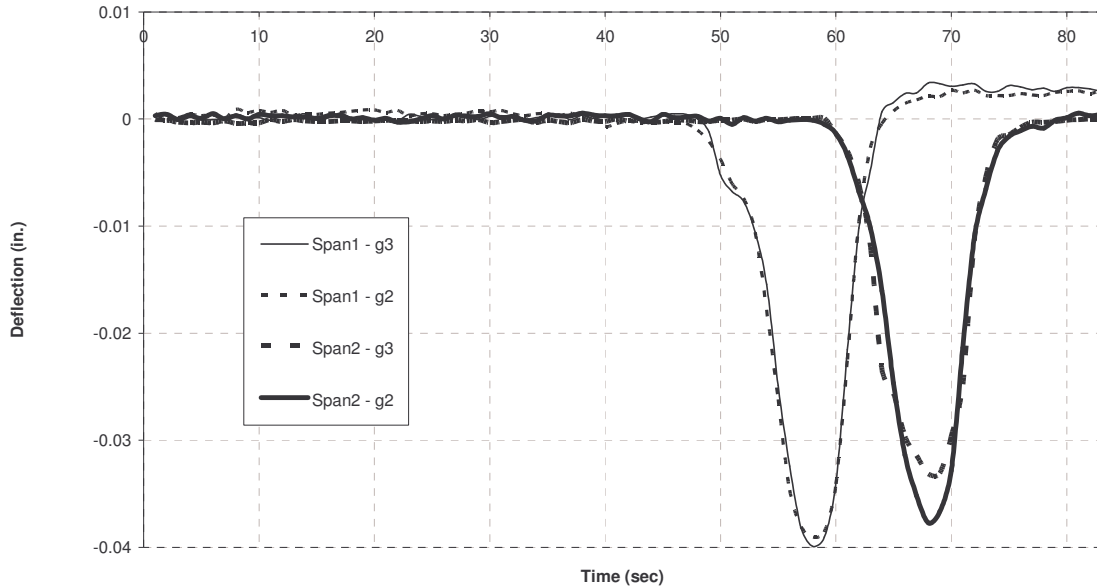


Figure 5.9 Girder midspan deflections – slow path 5

Transverse load distribution

Similarly to the previous bridge, special attention was paid to the transverse distribution of the truck load. Figures 5.10 and 5.11 show the strain distributions to each girder. The points on the graph indicate the girder positions measured from Girder 1. Since there was no strain measurements made for Girder 1, its values had to be estimated based on readings of Girder 4 during a similar test with the loading truck in the opposite lane.

To calculate the distribution factor, a method identical to the one presented for bridge 89-0022 was used. Path 2 and 6 were selected for this analysis. Based on experimental results, the calculated value was $DF = 1.33$ for both paths (see Table 5.3).

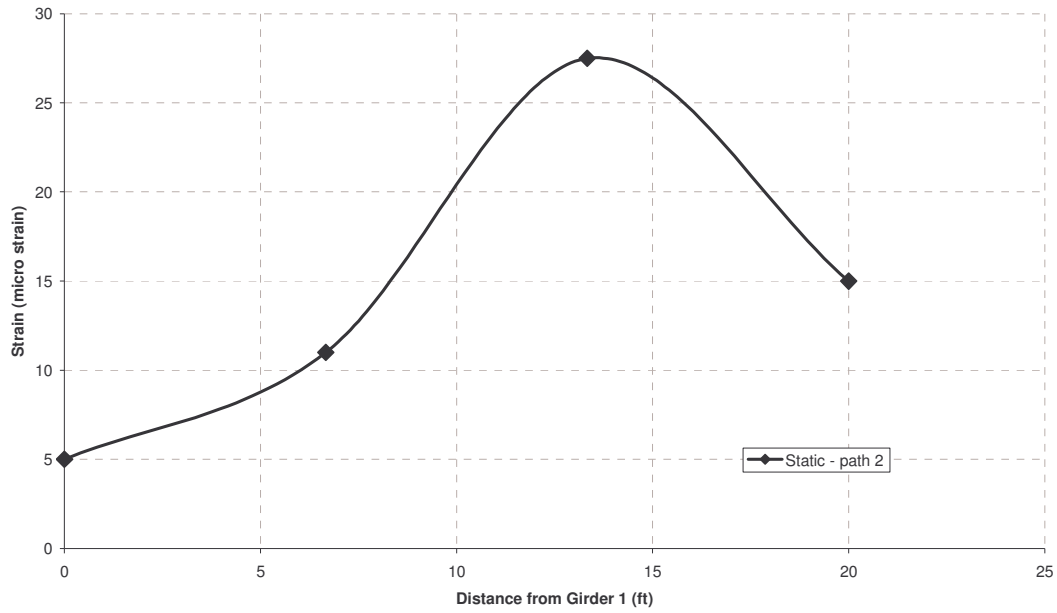


Figure 5.10 Strain distribution - path 2

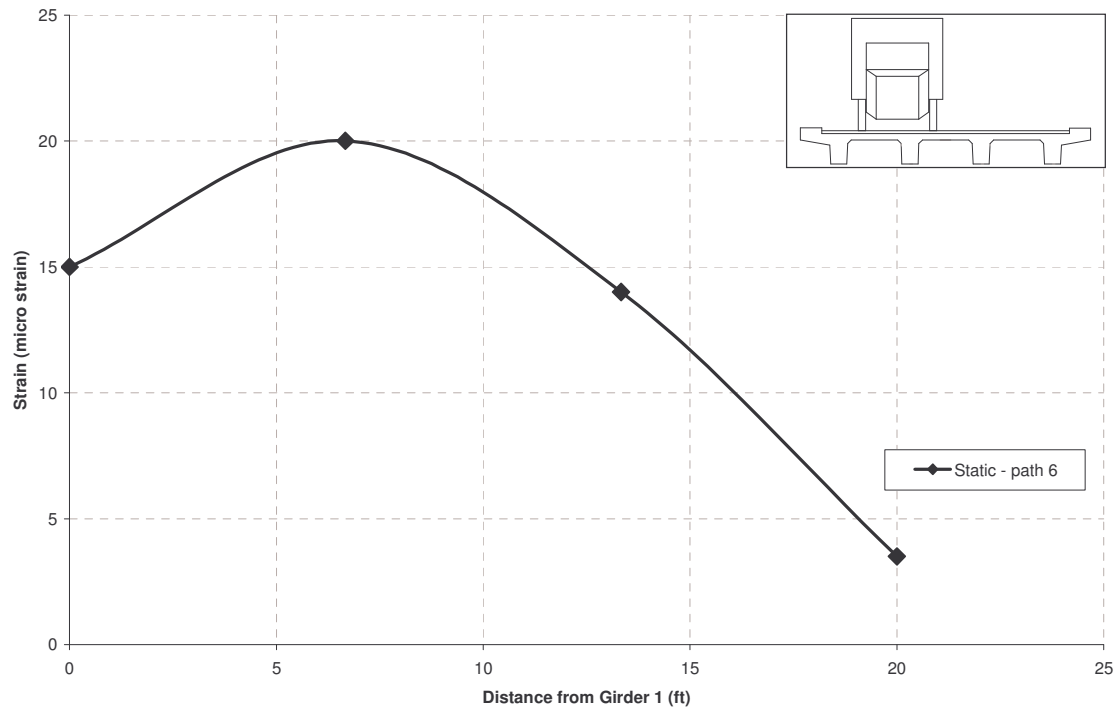


Figure 5.11 Strain distribution - path 6

Table 5.3 Distribution factor at girder midspan

Load Path	Strain at Bottom of Girder ($\mu\epsilon$)	1	2	3	4	Total Strain ($\mu\epsilon$)
Static 2	one lane	5	12	28	15	60
	opposite lane	15	28	12	5	60
	both lanes	20	40	40	20	120
	DF	0.67	1.33	1.33	0.67	
Static 6	one lane	15	20	14	3	52
	opposite lane	3	14	20	15	52
	both lanes	18	34	34	18	102
	DF	0.71	1.33	1.33	0.71	

5.3 Bridge 12-0271

Strain levels

This was the second RCDG bridge tested in this project. Similarly to the first RCDG bridge, low strain levels were measured throughout the bridge. For this bridge, LVDTs were already eliminated and more strain transducers were added to the instrumentation list. Furthermore, in order to investigate the effect of the concrete curbs, these secondary elements were instrumented as well.

The experimental determination of the neutral axis location was important to determine composite interaction of the deck with the beam, and to analyze the strain levels in the concrete girders. In addition to the deck, this bridge has an additional 3 in. of concrete wearing surface (CWS). If the fact that these two surfaces act compositely could be proven, it will greatly affect the depth of the compression zone and the anticipated strain/stress levels in the girders.

In order to experimentally determine the position of the neutral axis, strain transducers were placed at the top and bottom of the girder at midspan locations. The bottom strain transducer was placed along the centerline, while the top strain transducer was placed on the side of the girder at a distance 4 in. down from the deck.

Figure 5.11 shows the strain readings of two of the locations. In Span 1, Girders 2 and 3 were instrumented at top and bottom. Using the similar triangles method, and assuming that the material has not yielded, the neutral axis was determined. The path shown is from Path 4 of the static load sequence.

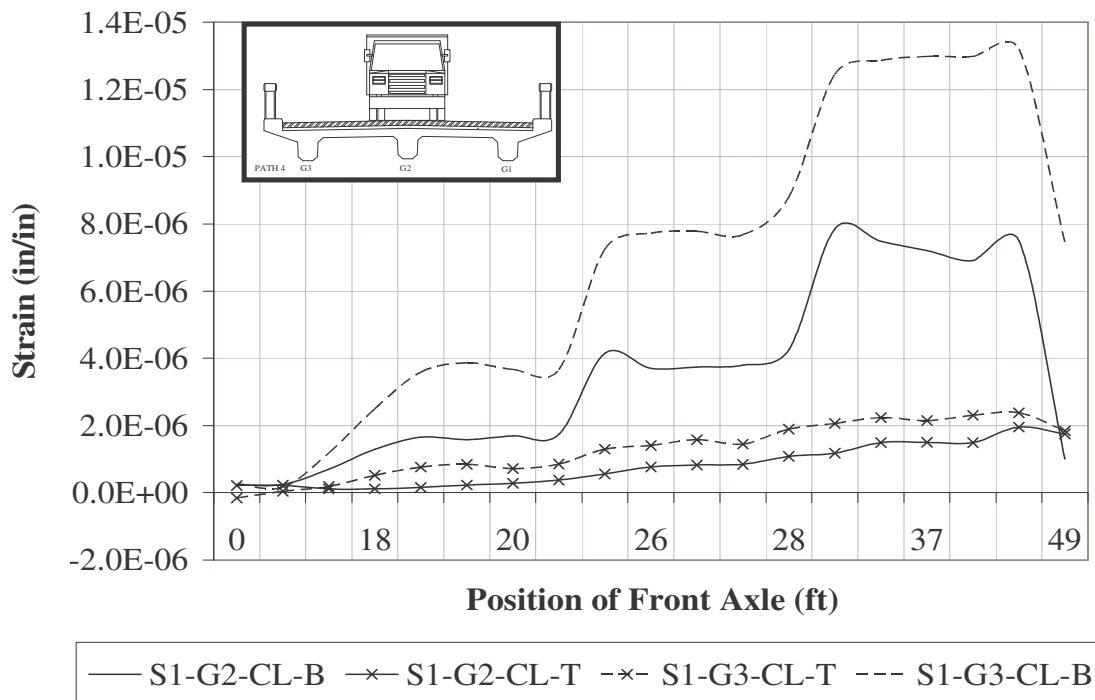


Figure 5.11 Strain levels in girders 2 and 3 – static path 4

The three stopping points are clearly identifiable for the bottom readings. Based on the readings for both girders, the neutral axis was located within the deck. If the strain readings at the top of the beam had been negative, meaning in compression, then the readings would have been above the neutral axis. However, the top strain readings were consistently positive, meaning below the neutral axis and in tension.

The neutral axis was found at 33.0 in. for girder 3 and 34.1 in. for girder 2 measured from the bottom of the girders. Slightly higher NA positions were determined for path 1. Figure 5.12 illustrates the neutral axis of Girders 2 and 3 as a function of the position of the loading vehicle as it moves across the span in static load sequence along path 4.

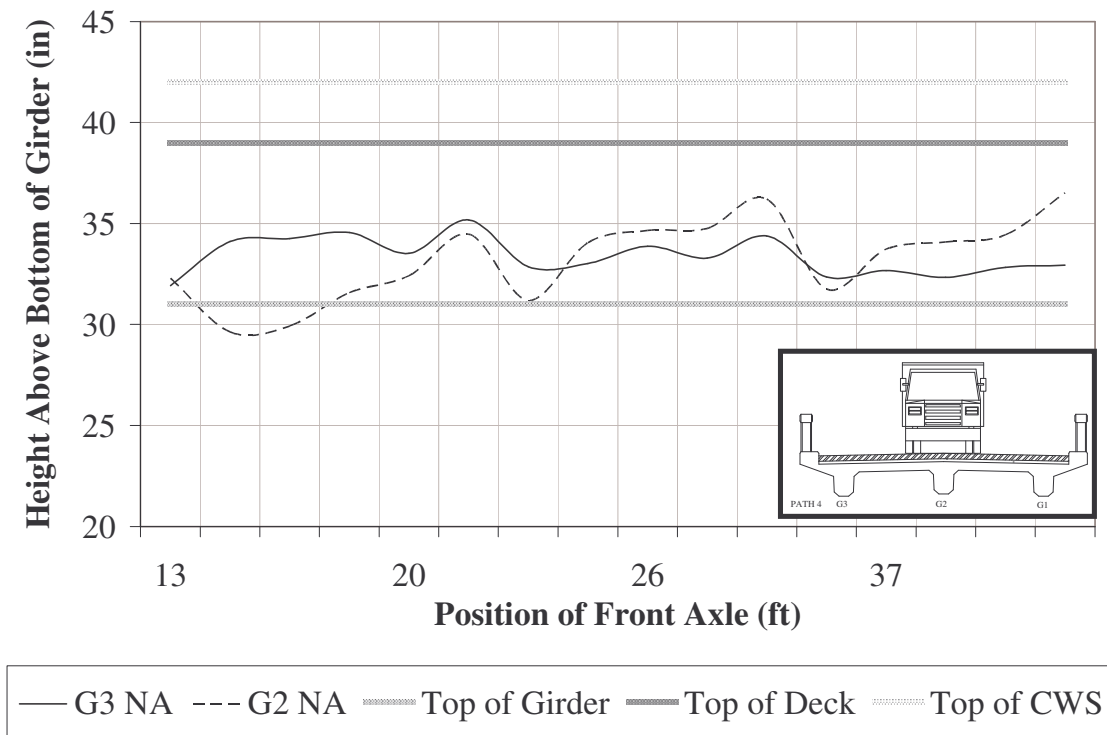


Figure 5.12 Neutral axis for girders 2 and 3 – path 4

The shift of the neutral axis into the deck could also be attributed to the cracked nature of each girder. Girder 2, throughout the length of the bridge, had more cracks in the bottom face of the girder than the others did. There were also more longitudinal cracks within the depth of Girder 2. Figure 5.13 shows some of the longitudinal cracks near the centerline of Girder 2 in Span 1. Photo (a) shows a longitudinal crack (highlighted) that is at an average distance of 14.5” from the bottom of the girder. Photo (b) shows another longitudinal crack (highlighted) running along the bottom of the girder.

Figure 5.14 shows a representative vertical crack. These vertical cracks up to 9 in. are seen throughout the bridge. The image shown was taken at midspan of Girder 2 in Span 1. The crack has been highlighted to aid its clarity. This type of crack is most commonly a flexural crack; although no other sign of distress was visible.

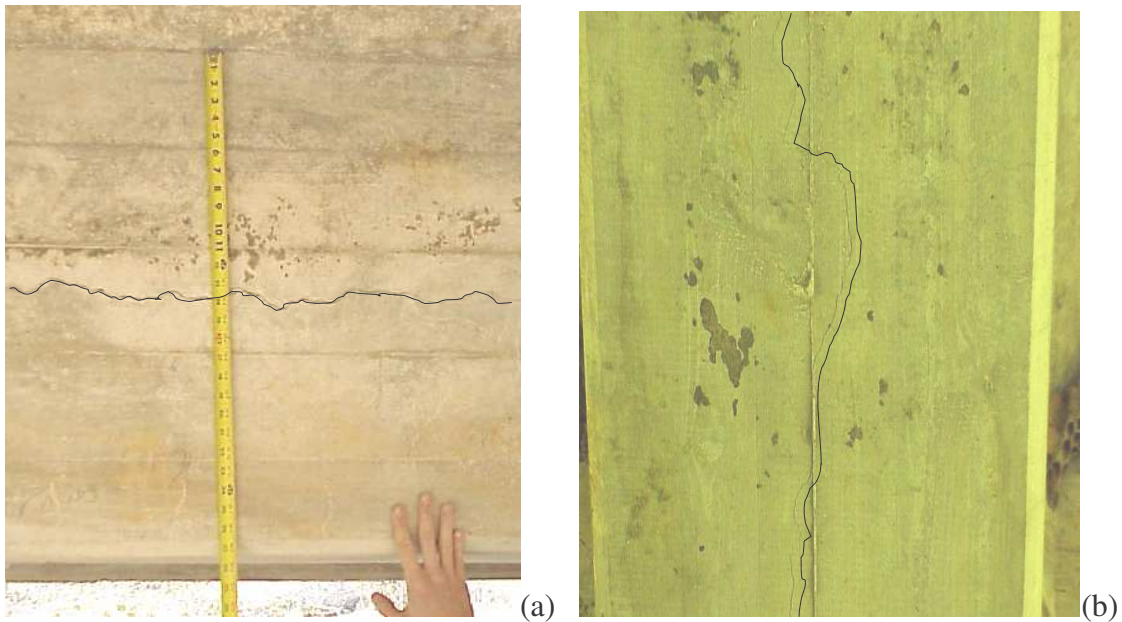


Figure 5.13 Cracked girder sections

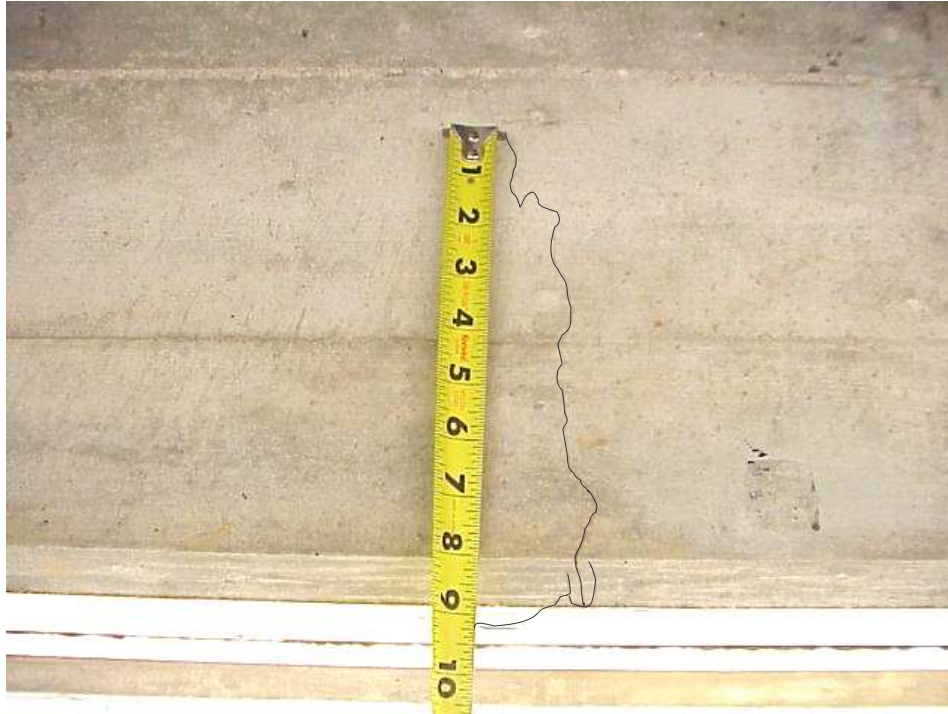


Figure 5.14 Existing vertical crack

Girder deformations

Figure 5.15 illustrates the displacement transducer readings of Path 4 of the static load sequence. The fact that Spans 1 and 3 are the same, should have yielded the same readings as the load vehicle passed through both spans. However, this was not seen and in fact, the highest deflection reading was in the third span, 0.033" not the controlling design span, which was Span 2. Span 2 saw a deflection of 0.031" while Span 1 saw the least amount of deflection at 0.023".

The figure also indicates that some upward movement in Span 2 was recorded as the load vehicle was in both Span 1 and 3. This would indicate some form of continuous span action. This was however, only an average 0.005" movement upward. Therefore, the

continuous span action illustrated here should be ignored since this is out of the accuracy range of the displacement transducers and could be considered noise.

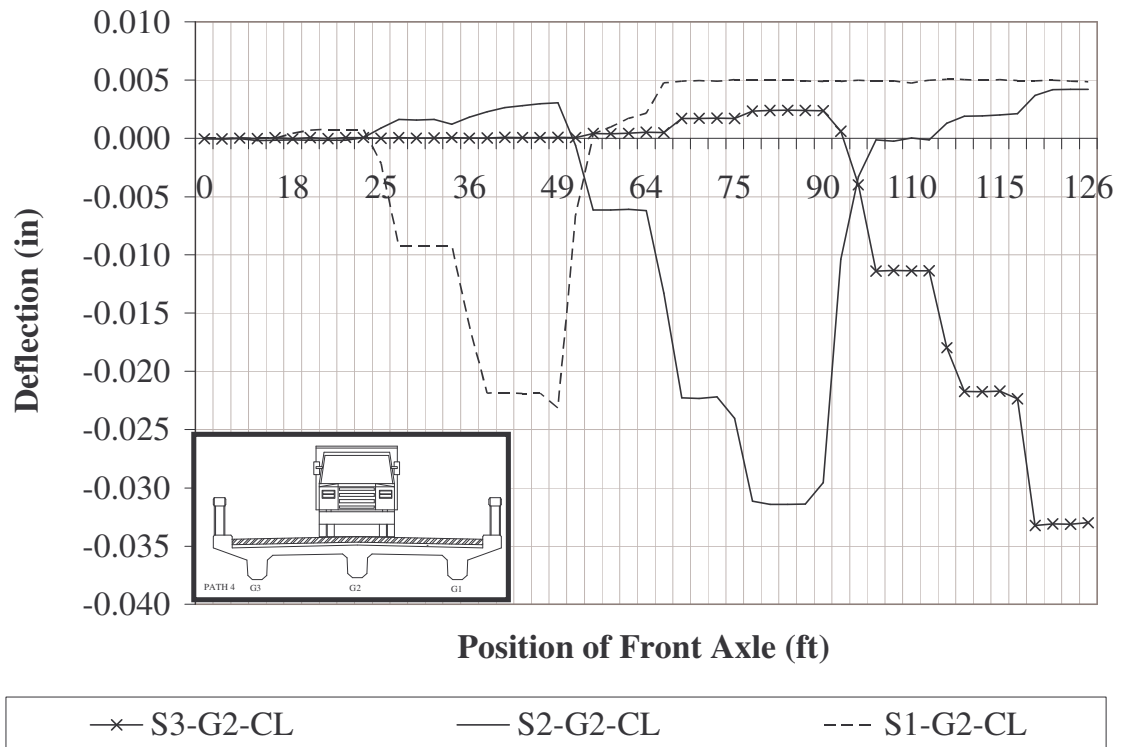


Figure 5.15 Centerline deflections of Girder 2 – static path 4

Having the load vehicle follow a path that places it in the center of one of the lanes will represent the actual loading condition. Figure 5.16 shows the load vehicle following Path 5 of the static load sequence. This places the truck in the center of the opposite lane, facing on-coming traffic. This also places the vehicle almost in the center of two girders. As expected with the load vehicle in Path 5, which places the vehicle

almost between Girders 1 and 2, Girder 3 shows the least deflection at 0.01". Girders 1 and 2 read almost identical deflections at approximately 0.021".

These figures show the deflection readings of the bridge under different load locations. However, in each figure, the measured deflections never reach the predicted deflections for pinned – pinned or fixed – fixed end conditions. This would indicate that the material properties were incorrect or that some interaction from the railings and curb is truly happening and greatly affecting the bridge's load response.

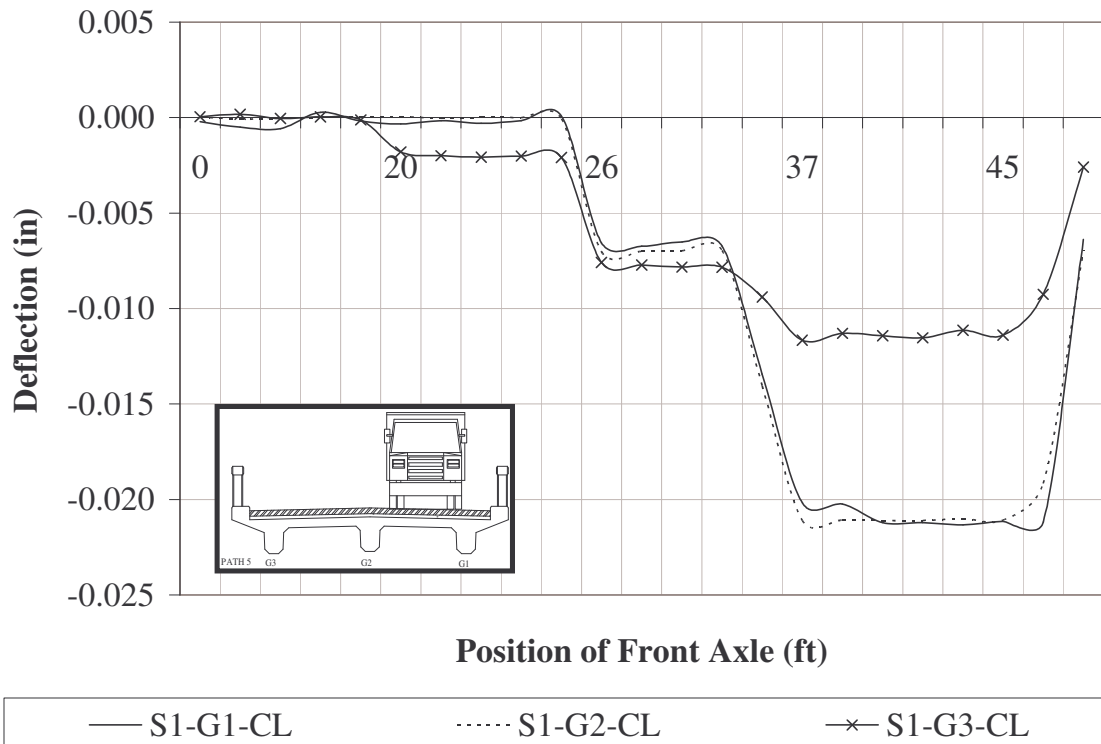


Figure 5.16 Span 1 centerline deflections – static path 5

Transverse load distribution

The determination of the live load distribution to the girders was done using the strain readings at the centerlines of the three girders. Here, two dynamic paths were chosen for analysis. After these readings were compiled in a table format (shown in Table 5.4), the truck load distribution factors were calculated. It is important to note, that the $DF = 1.44$ calculated for this three-girder bridge is significantly higher than the values established for a seven-girder bridge. Obviously, the demand on these three girders to carry the truck load is substantially higher.

Table 5.4 Distribution factor at girder midspan

Load Path	Strain at Bottom of Girder ($\mu\epsilon$)	1	2	3	Total Strain ($\mu\epsilon$)
Dynamic 2	one lane	4	10	14	28
	opposite lane	14	10	4	28
	both lanes	18	20	18	56
	DF	1.29	1.43	1.29	
Dynamic B	one lane	13	9	3	25
	opposite lane	3	9	13	25
	both lanes	16	18	16	50
	DF	1.28	1.44	1.28	

Dynamic effects

The measurement of strains induced by the impact of the load vehicle was monitored during the dynamic load sequences. These dynamic strains were then compared with those seen in the static and slow loading sequences to determine if impact was occurring. These loading sequences only lasted for an approximate duration of 4

seconds, with the DAQ recording five readings every second. The dynamic loadings were all conducted at a vehicle speed of 35 mph, which was the current speed limit.

Figure 5.17 shows the strain readings in all three girders of Span 1 at midspan as the load vehicle was driven through the bridge following path 4. Girder 2 had the highest strain reading of $18 \mu\epsilon$. This value is significantly higher than the $8 \mu\epsilon$ recorded in the static case load sequence seen in Figure 5.11. However, girder 3 read $11 \mu\epsilon$, less than the $14 \mu\epsilon$ seen in static path 4.

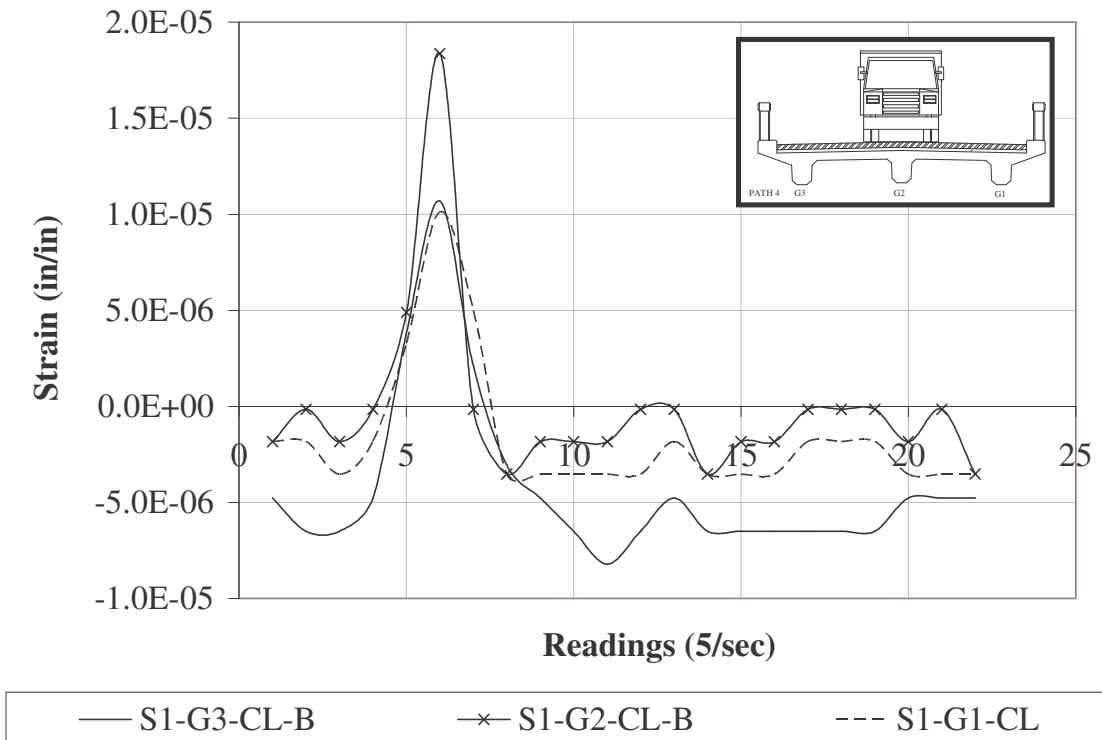


Figure 5.17 Dynamic strain readings in span 1 – path 4

These two readings are at the two extremes measured during dynamic loading. The vast majority of the dynamic readings were approximately equal to the static data. The actual impact is greatly affected by the presence of bumps on the bridge approach (Beal, 1998). It was noticed during the bridge test that some vehicular impact was occurring as vehicles entered the bridge from the approaches. Some differences in the asphalt overlay at the bridge abutments were noticeable at both ends of the bridge. This caused the vehicles to “bounce” on to the bridge. Figure 5.18 shows one of the approaches with the unevenness of the asphalt, which contributes to the bouncing effect.



Figure 5.18 Uneven asphalt at bridge approach

5.4 Bridge 59-0038

Strain levels

Bridge 59-038 is a one span steel girder concrete deck bridge. The seven girders were heavily instrumented with strain gages, strain transducers and displacement transducers. To identify the strain levels recorded during the static loading, the results of two paths will be discussed. For path 1, the loading truck was positioned in the middle of the northbound lane. This positioning also coincided with the left wheel line of the truck halfway between Girders 6 and 7.

Figure 5.19 shows a graph of mid-span strain readings measured on the bottom flange of each girder. As expected, girders 5, 6, and 7 resisted the majority of the load. The highest strain levels recorded on the bottom of the girders reached $113 \mu\epsilon$. The steeply sloped portion indicates the loading truck was moving to the next stopping position, and the flat portion of the graph indicates the truck was stationary at the stopping point.

Figure 5.20 shows the strain readings at mid-span for path 3. For this path, the loading truck was positioned along the center line of the bridge. As it can be seen from this graph, only two stopping points were used for this path. Furthermore, it was expected that the majority of the load would be resisted by girders 3, 4, and 5. The highest readings were recorded at the center line, on girder 4, with values up to $88 \mu\epsilon$. This value is considerably lower than the maximum readings for path 1, which loaded primarily one side of the bridge, as opposed to path 3, for which the load was more evenly distributed.

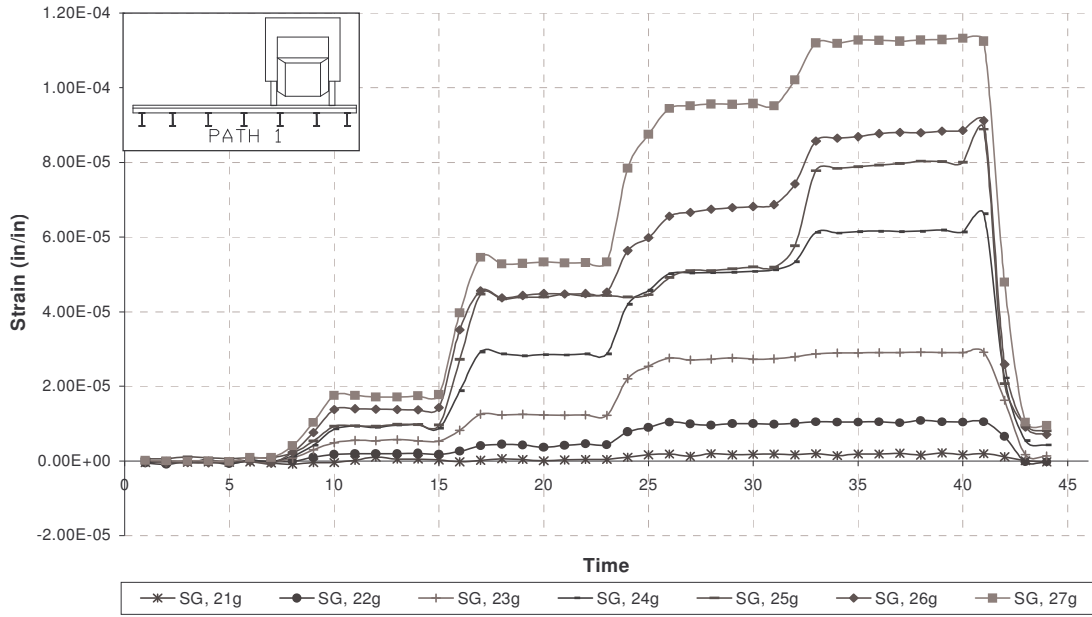


Figure 5.19 Static strain readings at mid-span of girders – path 1

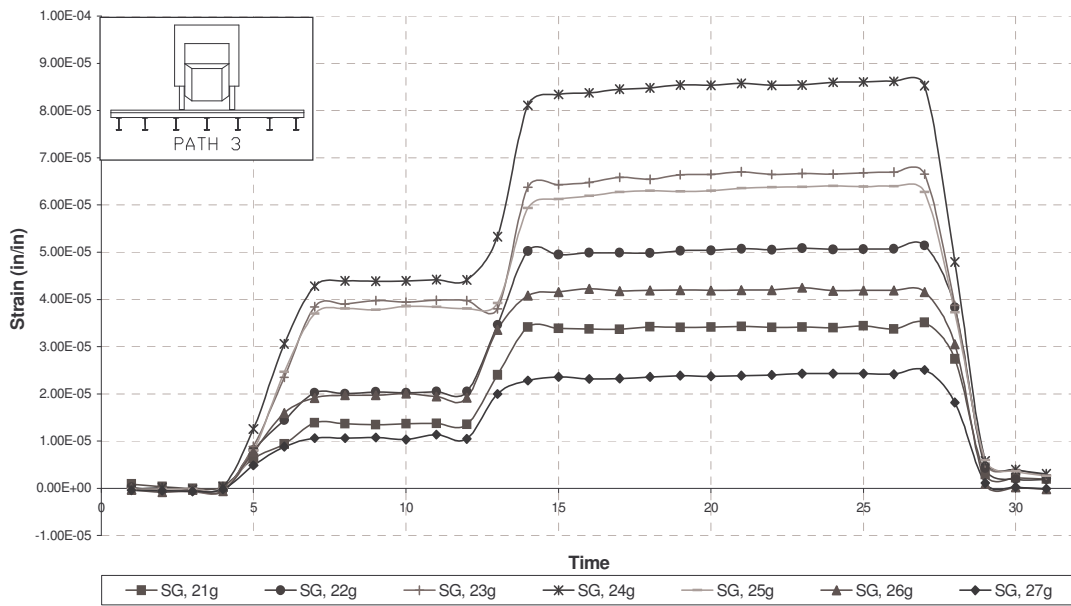


Figure 5.20 Static strain readings at mid-span of girders – path 3

Figure 5.21 shows the mid-span strain readings measured on the top flanges of each girder. This information along with data from Figure 5.19 allows for the determination of the position of the neutral axis, which in turn, provided information as to whether or not the girders and deck are acting compositely. At the time of construction of bridge 59-038, the use of composite members was not a common practice. Although the construction drawings of this bridge are not available, at the beginning of the analysis, it was believed that shear studs were not used; therefore, the bridge should act non-compositely (i.e. the experimental neutral axis should be located at the centroid of the steel girder).

To calculate the neutral axis from test data, the girder was assumed to be in the elastic range, and the strain slope was linear. Considering the small strain levels measured during these tests, this assumption was reasonably accurate. The position of the neutral axis was then determined using similar triangles. Table 5.5 shows the calculated neutral axis for all girders at mid-span.

As it can be seen from this table, all erroneous readings were omitted (shaded information) in this analysis. As shown in Table 5.5, the girders are acting as composite members to some degree, because the position of the neutral axis was not located halfway down the section, in this case 10 in. The average NA position was calculated as 5.28 in., well above the mid-height of the girder web. However, since only three readings were used to come to this conclusion, caution must be used when a scientific trend is sought.

To confirm these findings, the results of path 3 were also analyzed, and summarized in Table 5.6. As it can be seen, the instruments on girders 2, 3, 4, and 5 recorded valid data. The other three girders were either too far away from the loading to

record accurate data, or had malfunctioning strain gages. The average neutral axis for the properly functioning gages was 6.84 in. The other four paths were also analyzed using the same method, and yielded 16 useful neutral axis locations with an average of 6.45 in. from the top of the steel girder; which clearly proves the presence of a load transfer between the girders and concrete deck.

It is important to note that, even though composite action is being discussed, there was no physical evidence of positive connections between girders and deck. Therefore, this apparent composite action could be the result of shear friction, and adhesion between the concrete and steel members.

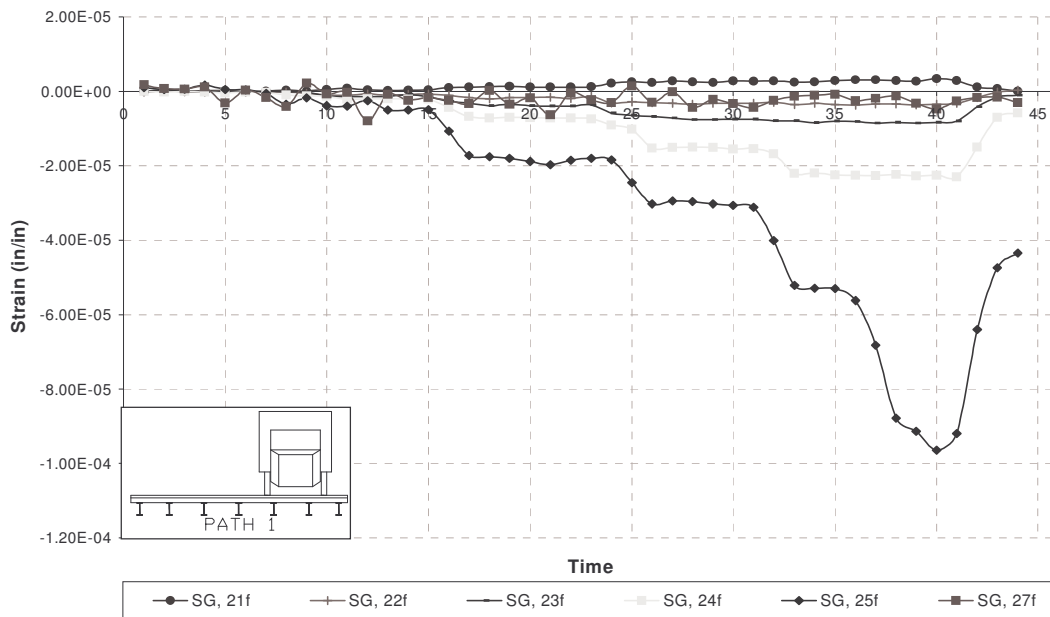


Figure 5.21 Static mid-span strain readings on top flanges – path 1

Table 5.5 Experimental neutral axis locations – static path 1

Girder	Reading on bottom flange ($\mu\epsilon$)	Reading on top flange ($\mu\epsilon$)	N.A below top of girder (in)
7	113	-5	1.45
6	89	Bad gage	n/a
5	80	-96	11.19
4	61	-23	5.93
3	29	-8	4.81
2	10	-3	5.10
1	2	3	12.25

Note: shaded strain values are recorded from malfunctioning gages

Table 5.6 Experimental neutral axis locations – static path 3

Girder	Reading on bottom flange ($\mu\epsilon$)	Reading on top flange ($\mu\epsilon$)	N.A below top of girder (in)
7	24	-4	3.39
6	42	Bad gage	n/a
5	64	-34	7.35
4	86	-42	6.98
3	67	-34	7.15
2	51	-19	5.88
1	34	-2	1.70

Note: shaded strain values are recorded from malfunctioning gages

Transverse load distribution

Figures 5.22 and 5.23 show the strain distribution for paths 1 and 3. Each point on the graph indicates the position of a girder in relation to Girder 1. These graphs allow for the calculation of distribution factors. Table 5.7 summarizes the distribution factor calculations for path 1, resulting in $DF = 0.64$.

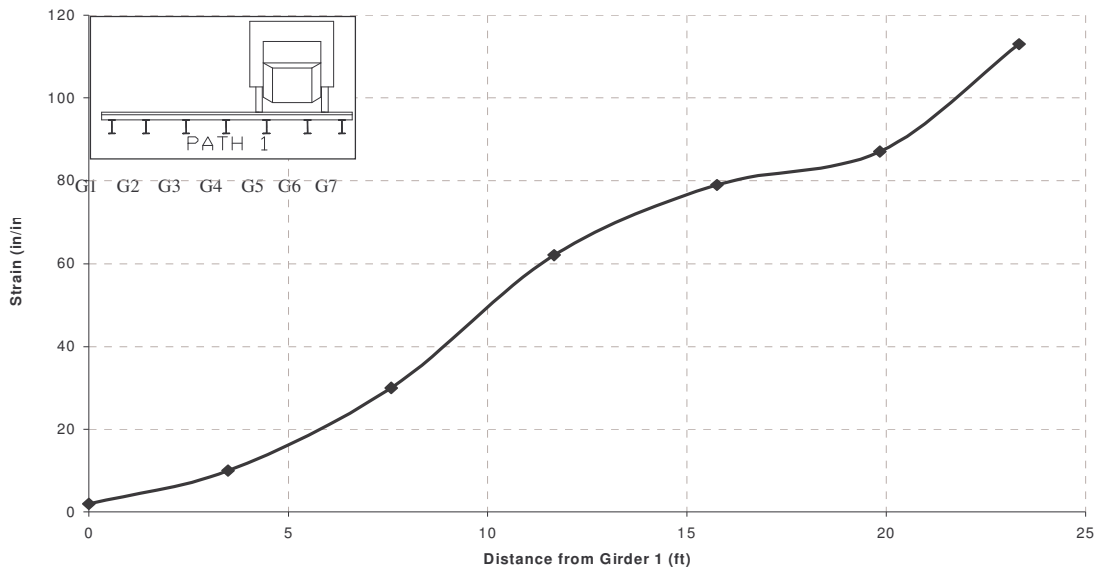


Figure 5.22 Strain distribution at mid-span – static path 1



Figure 5.23 Strain distribution at mid-span – static path 3

Table 5.7 Distribution factor for bridge 59-0038

Load Path	Strain at Bottom of Girder ($\mu\epsilon$)	1	2	3	4	5	6	7	Total Strain ($\mu\epsilon$)
Static 1	one lane	2	10	29	61	80	89	113	384
	opposite lane	113	89	80	61	29	10	2	384
	both lanes	115	99	109	122	109	99	115	786
	DF	0.60	0.52	0.57	0.64	0.57	0.52	0.60	

It is important to note that the graph for path 3 the strain distribution is nearly symmetrical. However, Figure 5.24 shows a discrepancy on the load distribution to girders 2, 3, 5, and 6. The same discrepancy exists in the distribution factors in Table 5.7 – the load is not being transferred to the outside girders as smoothly.

So what is happening at this bridge? As it was outlined in Table 4.1, the bridge built in 1945 was widened in 1988 by the addition of one steel wide flange girder on each side. It is obvious from Figure 5.22 and Table 5.7, a discontinuity has been introduced at the two exterior girders, which affected the transverse distribution of the truck load.

Dynamic effects

Figure 5.24 shows the dynamic strain readings for path 1. As anticipated, girders 6 and 7 recorded the highest levels, and girders 1 and 2 the lowest, respectively. Table 5.8 compares the data between static and dynamic tests for paths 1 and 3. It is clear from this table that there is no significant increase in strain due to impact from the dynamic test. All three dynamic runs have been analyzed for each path, and the results from the highest reading runs were included in Table 5.8. Furthermore, no impact effect was observed for any of the remaining five paths.

So the obvious question could be: why has no impact effect been observed in these tests? There are several possible answers; one could be that the approach slabs leading to the bridge have been paved at the same time as the bridge. Therefore, there is a smooth transition between the road and the bridge. Another would be that bridge 59-038 has an asphalt overlay of 9 in. on a 7 in. concrete deck. This overlay could have dampened the impact effects of the dynamic loads.

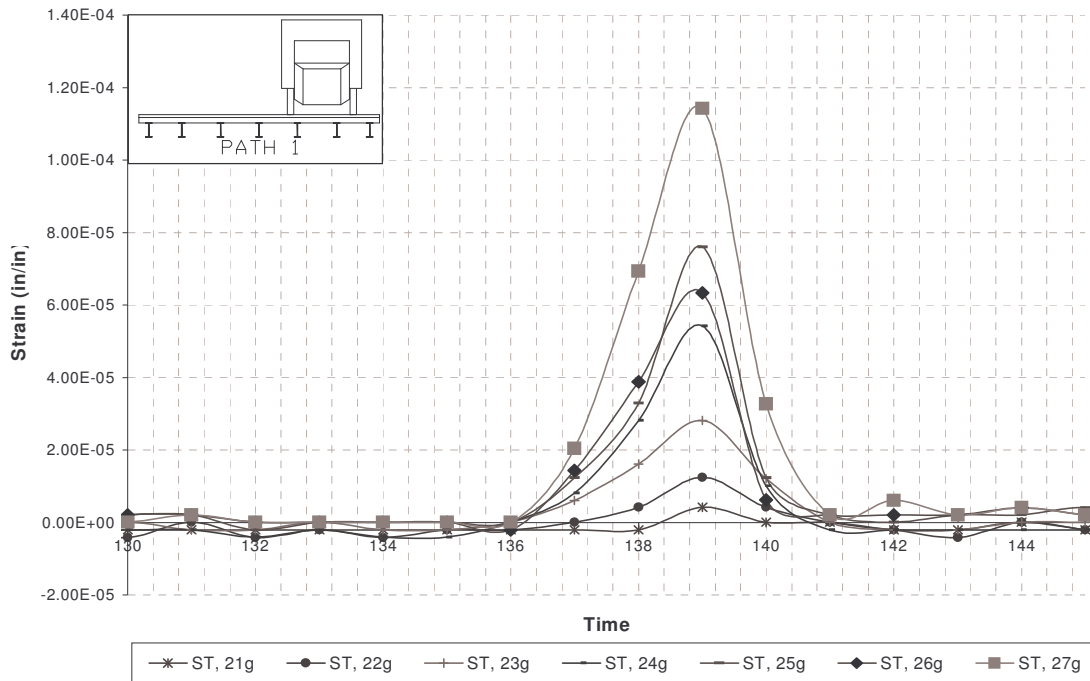


Figure 5.24 Dynamic strain readings at girder mid-span – path 1

Table 5.8 Strain comparisons for static and dynamic cases

Gage Position	Strain Readings – Path 1 ($\mu\epsilon$)		Strain Readings – Path 3 ($\mu\epsilon$)	
	Static	Dynamic	Static	Dynamic
27g	113	114	24	28
26g	89	76	42	31
25g	80	63	64	60
24g	61	54	86	82
23g	29	28	67	62
22g	10	12	51	58
21g	2	4	34	33

5.5 Bridge 12-0227

Strain readings

For the tests conducted on this bridge, the 140 ft displacement transducer was not used. There was an in-field problem with the device the day of testing. Unfortunately, it could not be solved within the tight schedule of the required road closure. Therefore, all the graphs were plotted versus the test time instead of the position of the front axle, as it was done for all the other static tests.

Figure 5.25 shows the strain readings from girder 3 of Span 1. The readings are from the static load sequence following path 2. The data from this path was selected since it generated the highest strain readings in girder 3. The figure shows the readings from both the primary DAQ and the portable DAQ. As it was mentioned earlier, for two bridges a second DAQ system was used with six strain transducers to investigate the possibility of using only a small number of instruments to evaluate a particular bridge. In this figure, each of the instruments from the portable DAQ was designated with a preceding 'Z'.

The figure clearly indicates the loading vehicle's stopping positions on the girder. There was an average of 20% difference in the strain readings between the portable DAQ and the primary DAQ in the centerline and the quarter point instruments. The Z instruments were positioned away from the centerline of the girder, and the difference in the readings can be explained by the girder not being loaded concentrically (there was a noticeable horizontal curvature in most of the girders, a deviation from a straight line up to a few inches); thus inducing some torsion in the beam.

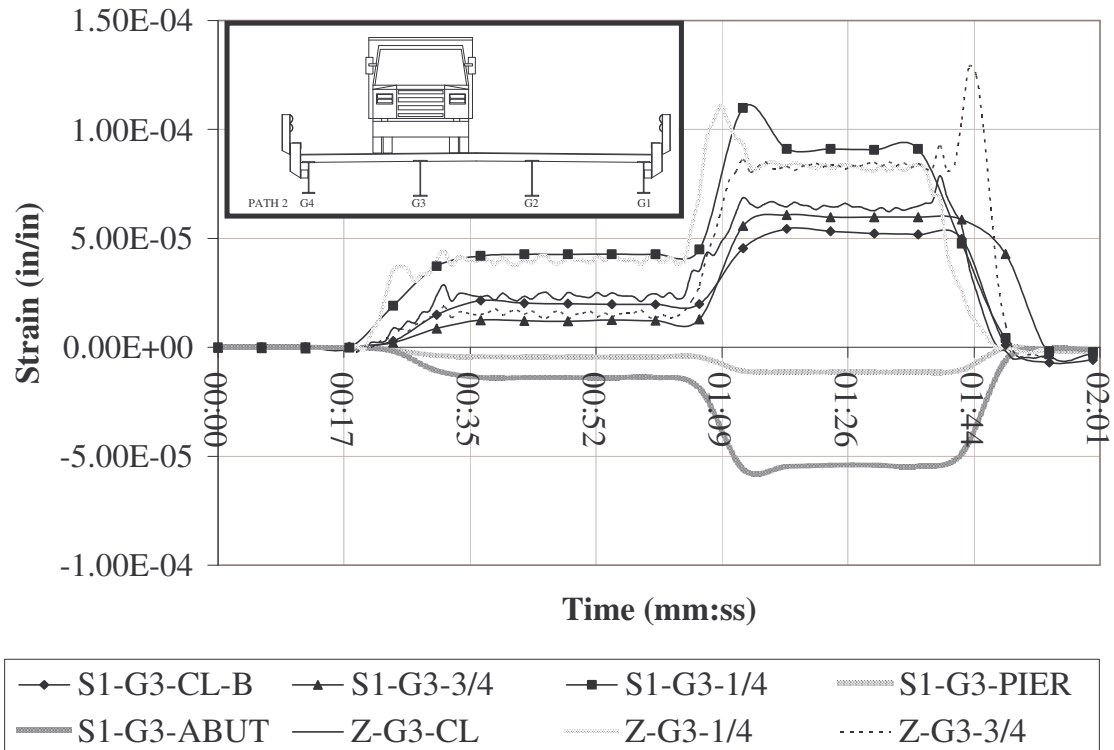


Figure 5.25 Strain readings along girder 3 – static path 2

These readings also indicate that there was some fixity at the supports. The two strain transducers at the abutment and pier recorded negative values up to $-60 \mu\epsilon$, proving that there was a certain degree of fixity present at the ends. According to the report by Bakht (1990), this degree of fixity could be occurring due to bearing restraints. As noted by Bakht, even bridges with elastometric bearings show an increase in stiffness as compared to theoretical analyses.

While some fixity was clearly occurring, the instruments were recording close to zero strain as the load vehicle passed from one span to another, illustrating that there was no continuous action between spans. Figure 5.26 shows the readings from the four girders at the midspan of span 1.

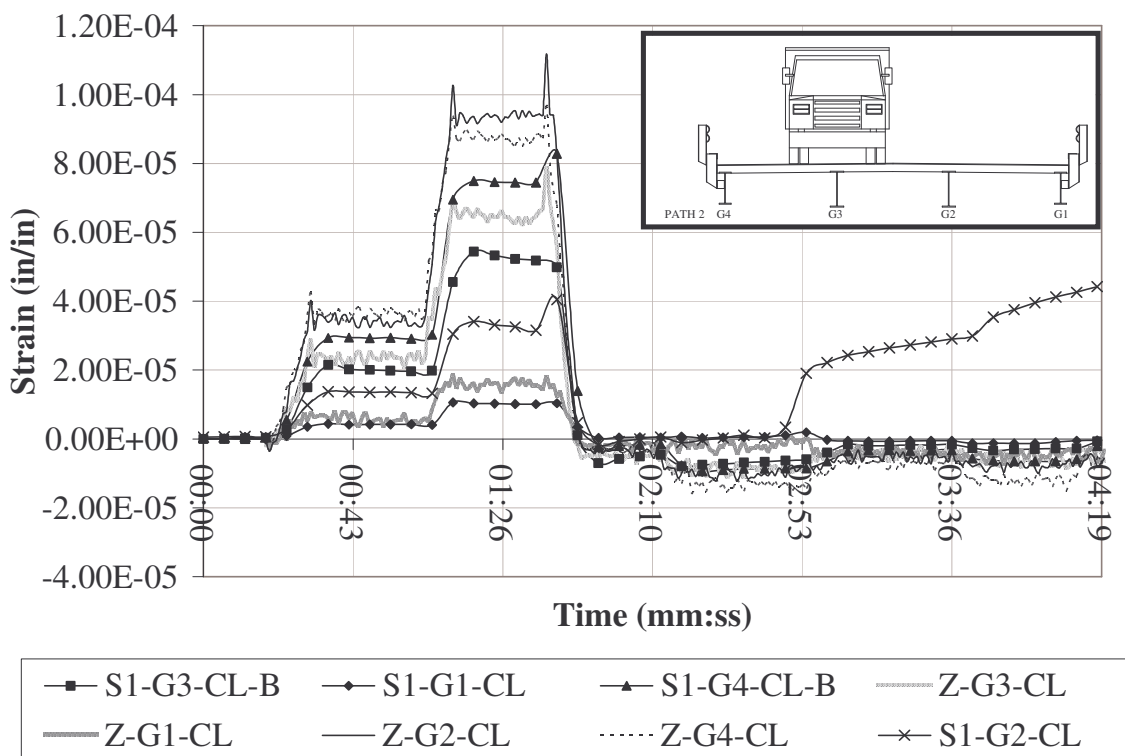


Figure 5.26 Span 1 strain readings at midspan – static path 2

As it can be seen on Figure 5.26, the reading for girder 2 did not follow a logical trend. A new pile was installed at this location at pier 1 (see Figure 5.27) with a noticeable gap between the top of the pile and the bottom of the concrete cap. With this knowledge, and the fact that the deteriorated pile was missing a large portion of its cross-section at ground level, the concrete span had virtually no support under Girder 2. Therefore, two displacement transducers were used to monitor the vertical displacement in the concrete cap. The displacement transducers were placed on either side of the deteriorated pile. Figure 5.28 shows the displacement readings from these two instruments as the load vehicle followed the static path 4.



Figure 5.27 Pier repair

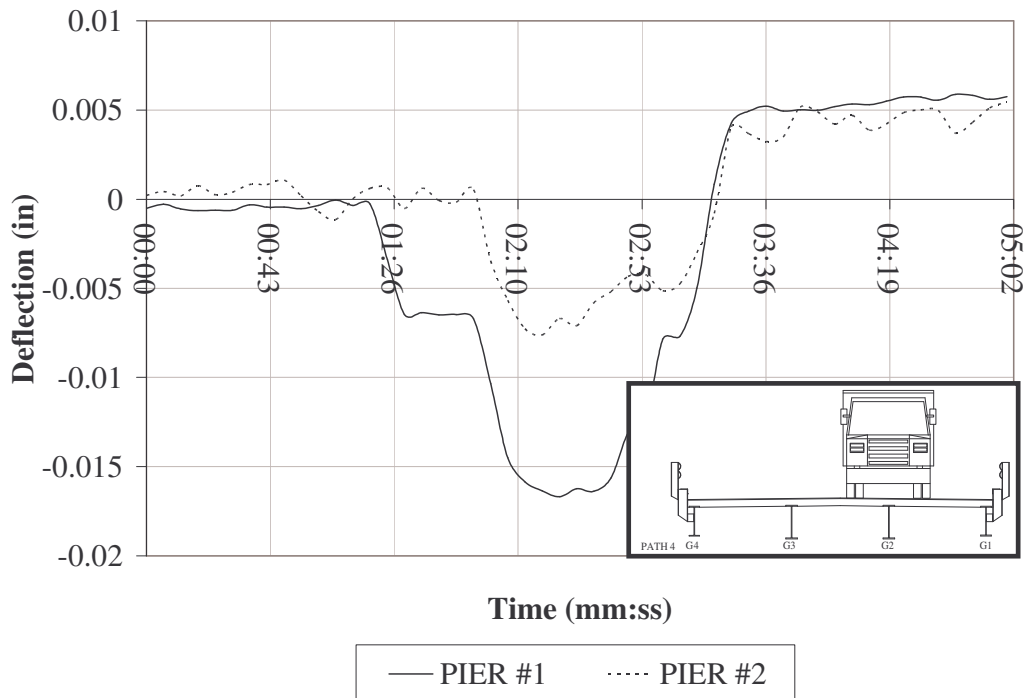


Figure 5.28 Deflection of the concrete cap

The figure clearly illustrates that there is some vertical movement of the concrete cap. The measured maximum deflection in this static load case was 0.017 in. This is a relatively low amount of movement; however, this could easily affect the superstructure's behavior, especially for girder 2, directly above the repaired timber pile.

Similarly to the previous bridges, the composite action between deck and girder was of major interest for bridge 12-0227. As it was done before, in order to establish the experimental location of the neutral axis, strain gages and strain transducers were placed at the bottom and top flanges of the steel girder at several locations.

Figure 5.29 shows the strain readings for the top and bottom of the girder at two locations. These locations are on girder 3 in spans 1 and 2 at midspan. Strain readings were also taken at the midspan of girder 3 in span 3 at the top and bottom of the girder;

however, after reviewing this data, the strain gage at the top position was lost prior to testing and the data recorded was unusable.

Again, using the similar triangles method, and assuming that the steel has not yielded, the neutral axis was determined. In span 1, the average NA was determined to be 18.46 in., while in Span 2, the average NA was 17.40 in. from the bottom flange of the girder. Considering the fact that centroid of the W27x94 interior girders are located at 13.46 in. from the bottom flange, one can conclude that there was a composite action between the steel girders and the concrete deck. However, this composite action relies only on adhesion between the two bridge components. In fact, a similar study was performed for girder 4, and the experimental NA was located at the centroid of the steel girder, dismissing any assumptions of a composite action.

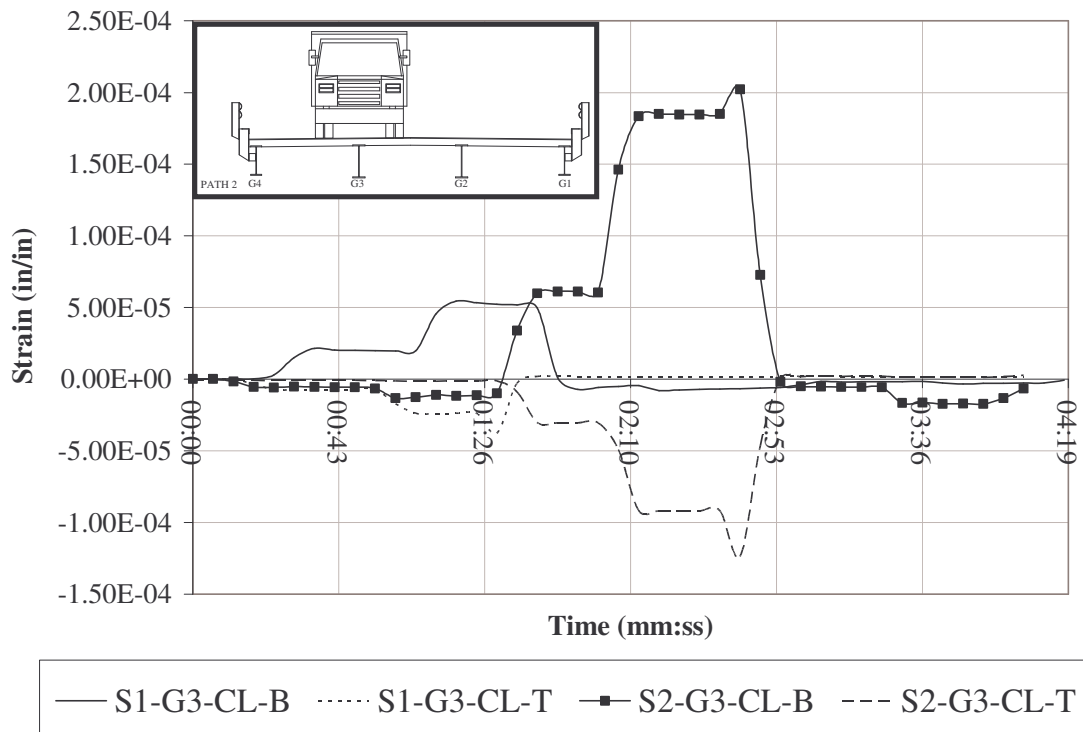


Figure 5.29 Strain readings for girder 3 in spans 1 and 2 – path 2

Girder deformation

Figure 5.30 illustrates the displacement transducer readings for static path 6. The figure shows that in both spans, the instrument on girder 4 measured the highest deflections, with 0.20 in. in span 1, and 0.26 in. in span 2. This fact proves that this girder resisted more load than any other girder. Furthermore, this figure also demonstrates that there was no continuity between spans; i.e. only the instruments in the loaded span recorded meaningful deflections.

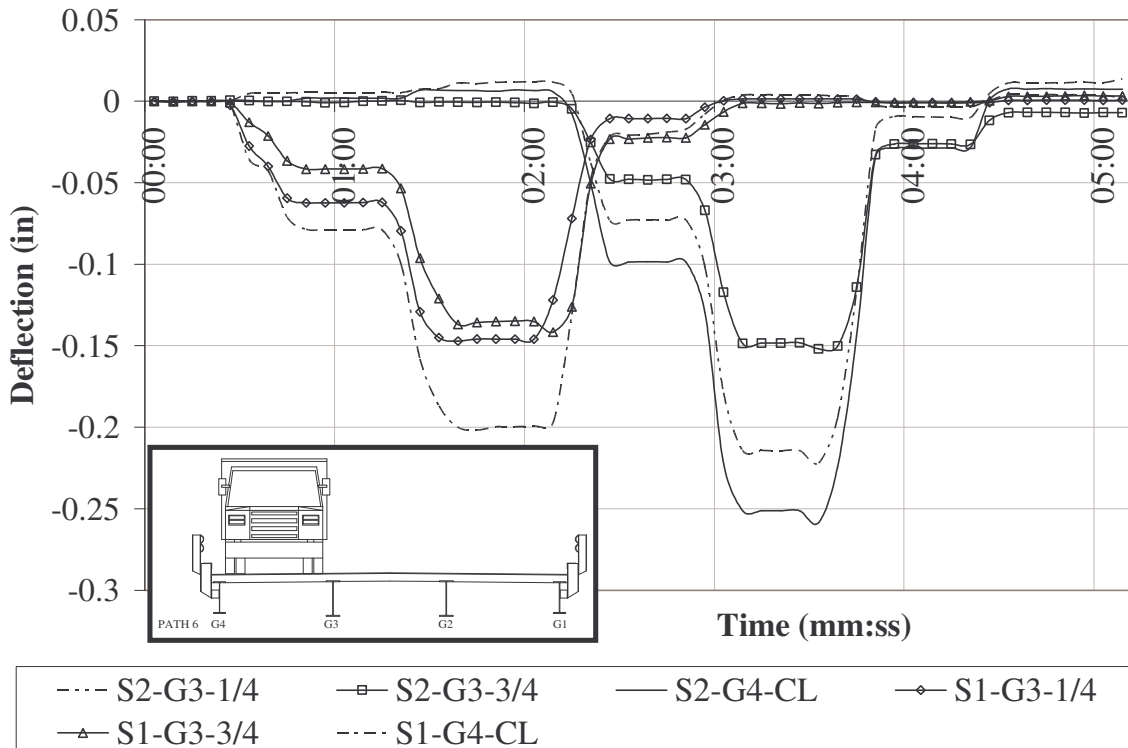


Figure 5.30 Girder deflections – static path 6

Figure 5.31 shows the deformations for static path 3. This path places the loading vehicle on the two interior girders. As expected, girders 2 and 3 showed the most deflection at midspan with girder 2 measuring 0.20 in. in both spans, and girder 3 measuring 0.18 in. in span 1. The displacement transducer at the midspan of girder 3 in span 2 recorded no data.

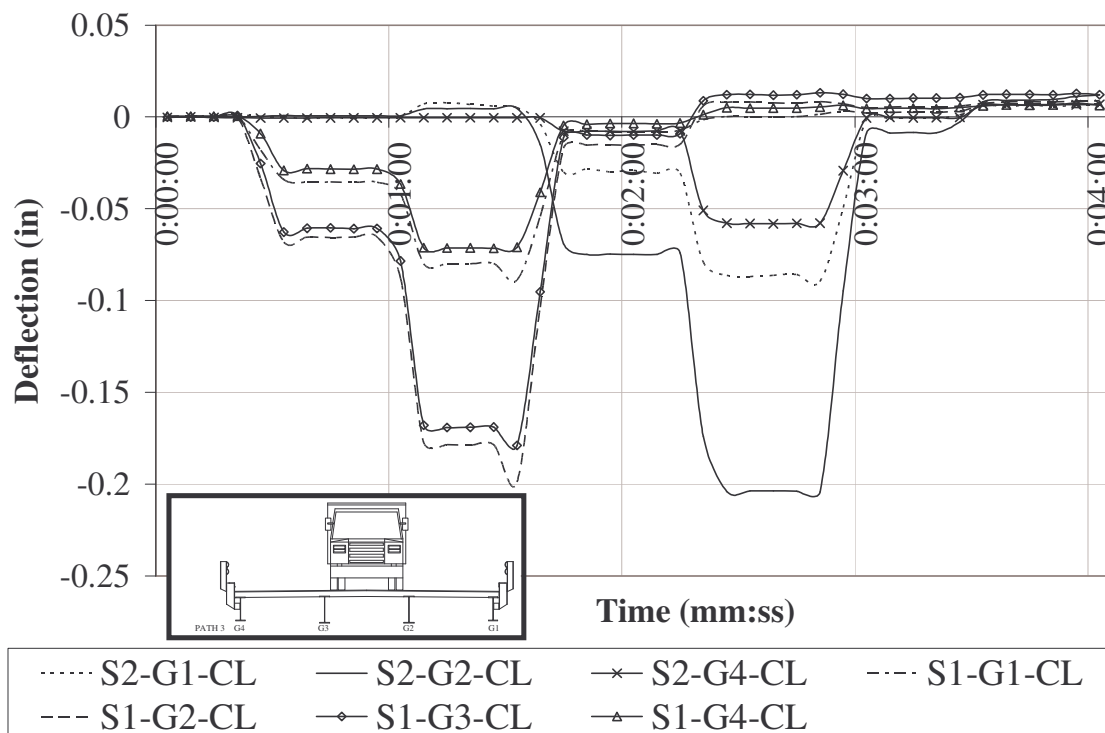


Figure 5.31 Girder deflections – static path 3

Transverse load distribution

The determination of the live load distribution to the girders of the bridge followed the previously described procedure, by using the strain readings at the midspan of the four girders (see Table 5.9).

Table 5.9 Distribution factor for bridge 12-0227

Load Path	Strain at Bottom of Girder ($\mu\epsilon$)	1	2	3	4	Total Strain ($\mu\epsilon$)
Static 5 "Z"	one lane	88	139	39	15	281
	opposite lane	15	39	139	88	281
	both lanes	103	178	178	103	562
	DF	0.73	1.27	1.27	0.73	
Dynamic 5 "Z"	one lane	95	171	51	28	345
	opposite lane	28	51	171	95	345
	both lanes	123	222	222	123	690
	DF	0.71	1.29	1.29	0.71	
Dynamic A "Z"	one lane	81	142	52	26	301
	opposite lane	26	52	142	81	301
	both lanes	107	194	194	107	602
	DF	0.71	1.29	1.29	0.71	

For this analysis, one static and two dynamic paths were selected. As it can be seen, the results clearly suggests a DF = 1.29. Furthermore, the letter "Z" indicates that the strain readings were taken using the six additional strain transducers connected to the standalone data acquisition system. This proves that a handful of instruments attached to carefully selected locations could provide valuable information on transverse load distribution, end restraints and position of neutral axes.

Dynamic effects

Figures 5.32 and 5.33 show the results of the static and dynamic loading of span 1 along path 1. As it can be seen, both of these loadings resulted in maximum strain readings of approximately 120 $\mu\epsilon$ – suggesting no dynamic effects. However, it is clear from Table 5.9 that girder 2 recorded 23 % higher dynamic strains than static strains. This was not a real surprise, considering the condition of the expansion joints, and the uneven approach slab/bridge deck transition.

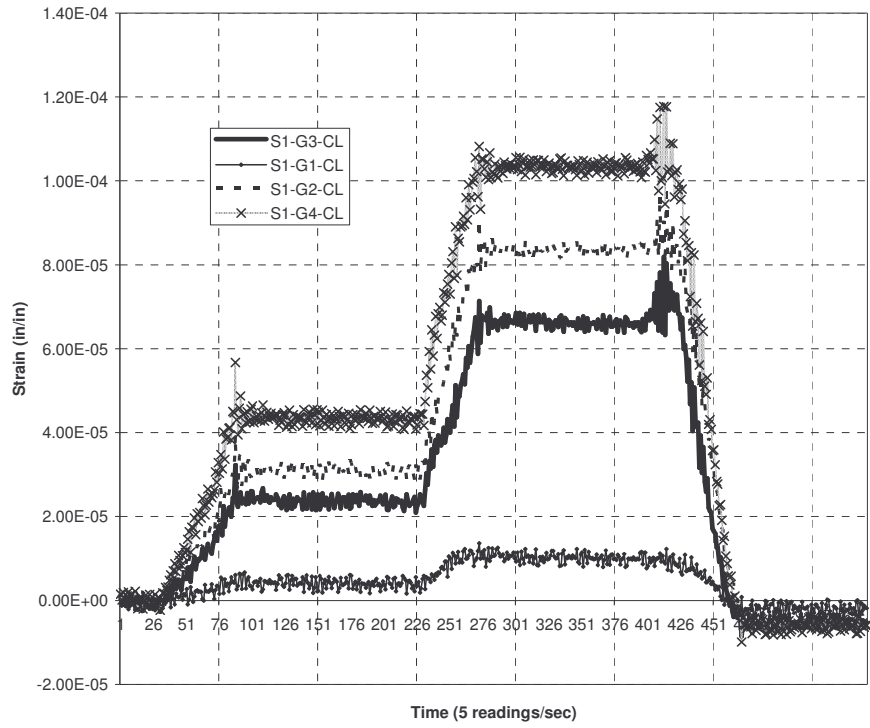


Figure 5.32 Strain readings – static path 1

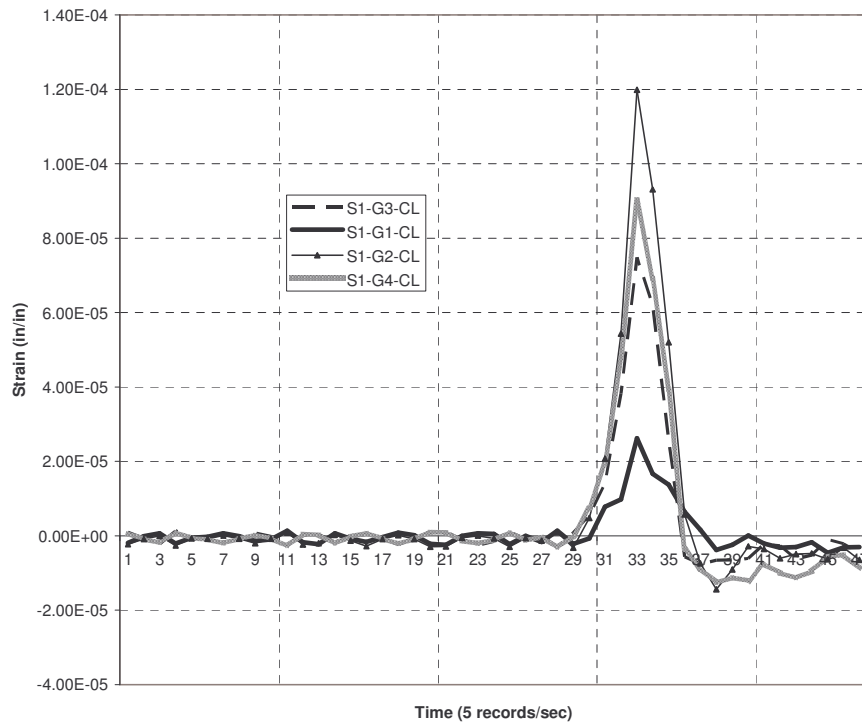


Figure 5.33 Strain readings – dynamic path 1

5.6 Bridge 59-0841

Strain levels

As it was described earlier, bridge 59-0841 is a continuous steel girder bridge. The total length of the two spans is approximately 300 ft over I-485, the outer belt of Charlotte, NC. Only a static loading test was conducted on this bridge. The static tests were performed by positioning two fully loaded NCDOT tandem trucks at various locations on the bridge. Each of these vehicles weighed approximately 25 tons.

Figures 5.34 and 5.35 show the mid-span strain readings on the bottom of each girder on spans 1 and 2 for static path1. During this test, the right wheel of the loading vehicles was positioned directly above girder 1. As it was expected, girders 1 and 2 carried the majority of the loads.

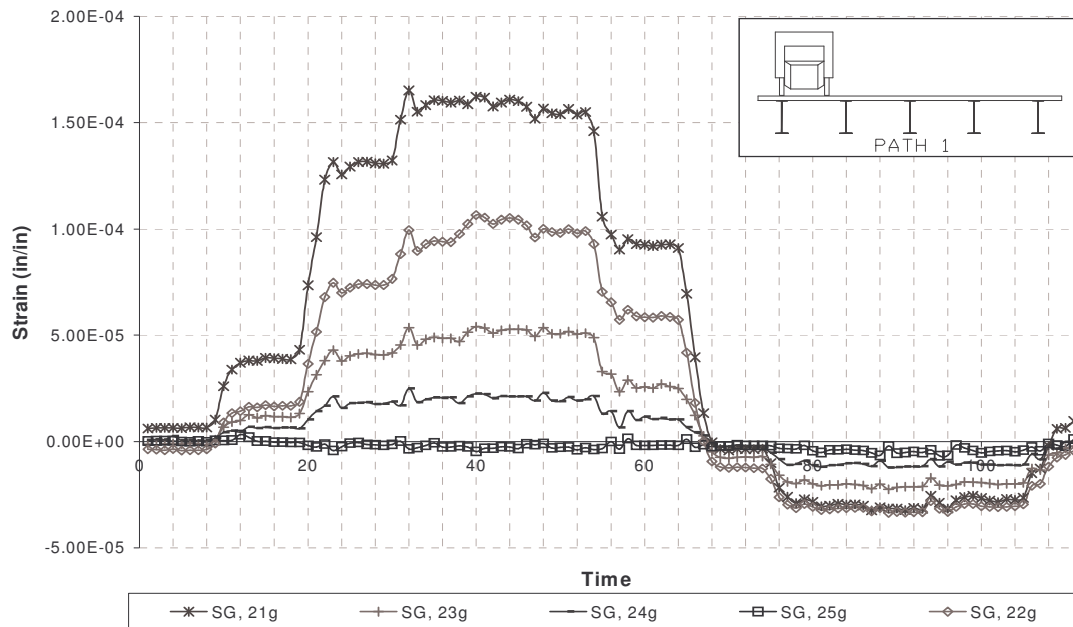


Figure 5.34 Static strain readings for span 1 – path 1

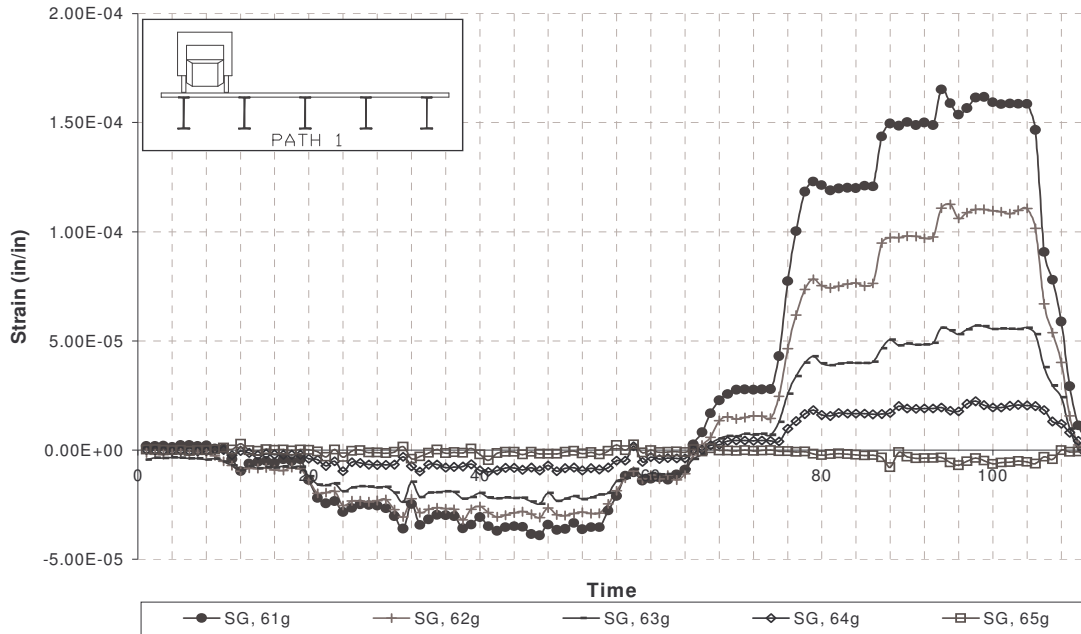


Figure 5.35 Static strain readings for span 2 – path 1

Figures 5.36 and 5.37 show the results of path 3. For this loading case, the trucks were positioned in the center of the eastbound lane. As expected, the girders carry the load more uniformly, and the recorded maximum strains were around $100 \mu\epsilon$. Compared to the $160 \mu\epsilon$ recorded for path 1, this loading condition resulted in smaller girder strains.

Furthermore, as opposed to the previous case, girder 2 was stressed to the same (or higher) levels as compared to girder 1. Finally, these figures clearly identify the moment when the loading trucks move from one span to the other. It is interesting to note, that the stresses completely reverse when the trucks are on the adjacent span. Although the strain levels were in the $30 \mu\epsilon$ range, this reversal must be accounted for in fatigue calculations.

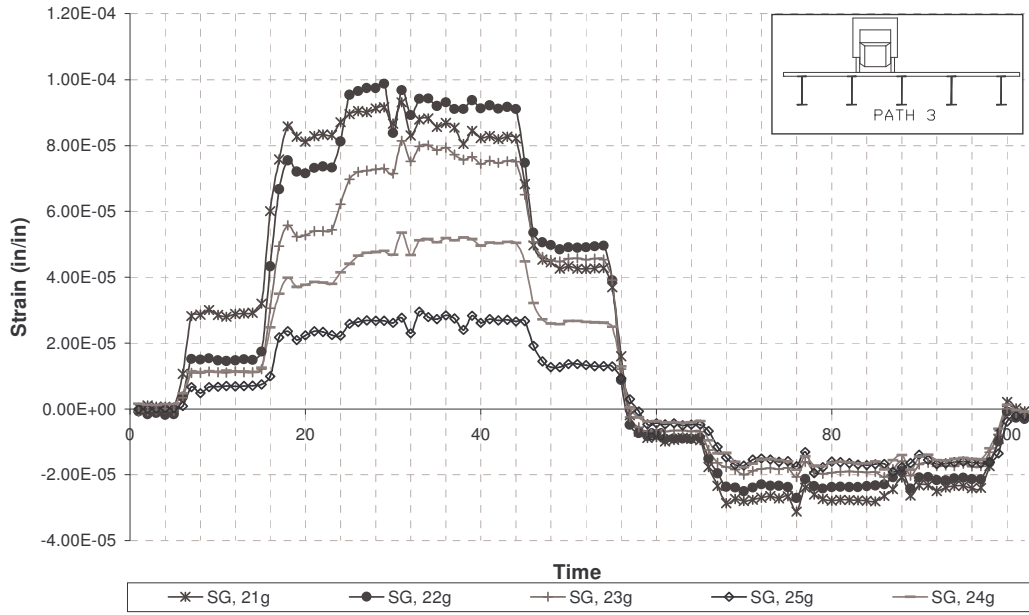


Figure 5.36 Static strain readings for span 1 – path 3

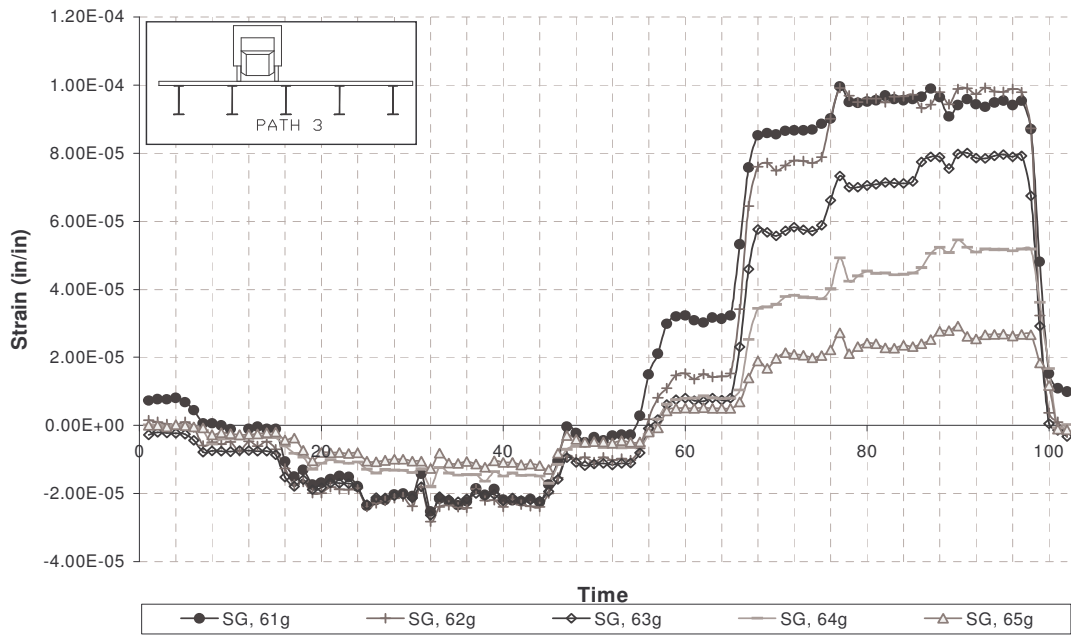


Figure 5.37 Static strain readings for span 2 – path 3

The girders of bridge 59-0841 were designed as composite sections. By using the strain readings from the bottom flanges and readings from the top flanges, the location of the neutral axis for a member was determined. Table 5.10 shows the calculated neutral axis positions for each pair of strain gages at the mid-span of each span. Similar comparisons were made for all pairs on strain gages on the bridge, and an average neutral axis location of 58.25 in. above the bottom flange was calculated.

Considering the fact that these welded plate girders were more than 5 ft deep, these calculations prove that the concrete deck and the steel plate girder were resisting live loads as a composite section.

Table 5.10 Position of neutral axis

Span	Girder	Distance from bottom flange (in.)
1	1	61.46
	2	59.18
	3	56.79
	4	55.86
	5	58.26
2	1	Bad gage
	2	60.04
	3	58.18
	4	55.58
	5	57.71

Girder deformations

Figure 5.38 shows the midspan deformations for girders 1 and 3 in spans 1 and 2. The figure clearly indicates the continuity of the steel girders by reading -0.4 in. (representing an $L/4500$ deformation level) in span 1 when the trucks were positioned in span 1, and by an upward reading of +0.19 in. (instrument DT.21g) when the trucks were moved to span 2. Similar values have been recorded for span 2 displacement transducers (DT.61g and DT.63g).

It is also important to note that girder 1 deformed about 20-30 % more than girder 3 in span 1. However, due to unknown reasons, the difference in deformations between the two girders was smaller in span 2 (i.e. 10-15 %).

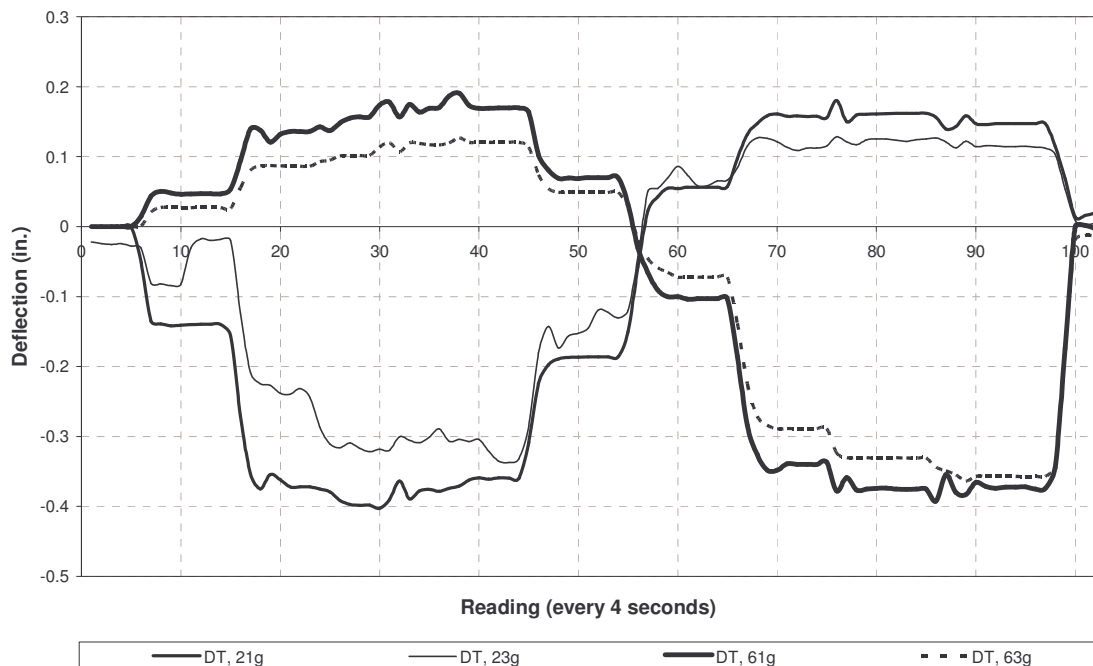


Figure 5.38 Girder deformations for spans 1 and 3 – path 3

Transverse load distribution

To calculate the experimental distribution factor, path 3 was chosen. This path positioned the two trucks on the center of the eastbound lane, producing the most common loading procedure. Figure 5.39 shows the strain distribution at midspan of the five steel girders. Using the previously introduced method, the distribution factors have been calculated for spans 1 and 2, and summarized in Table 5.11. An average DF = 0.90 was calculated for path 3.

Path 3 however, did not generate the highest distribution factor. Bridge 59-0841 has an unusually large space on both sides of the traffic lane, suitable for either a bicycle or for additional traffic lanes to be added in the future. Path 1 for example, positioned the right wheel line of the trucks directly above girder 1, generating a distribution factor of 0.94. However, this factor does not represent the current traffic conditions; therefore, in this report the 0.90 value will be used.

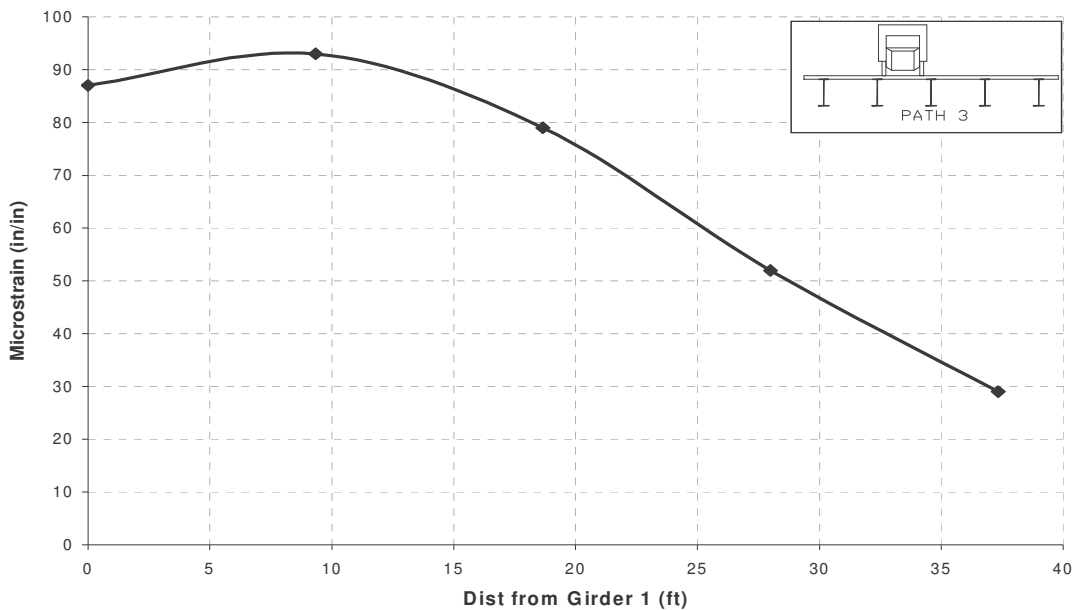


Figure 5.39 Strain distribution at midspan – path 3

Table 5.11 Distribution factor for bridge 59-0841

Load Path	Strain at Bottom of Girder ($\mu\epsilon$)	1	2	3	4	5	Total Strain ($\mu\epsilon$)
Static 3 Span 1	one lane	91	97	73	48	27	337
	opposite lane	27	48	73	97	91	337
	both lanes	118	145	146	145	118	674
	DF	0.70	0.86	0.87	0.86	0.70	
Static 3 Span 2	one lane	87	93	79	52	29	340
	opposite lane	29	52	79	93	87	340
	both lanes	116	145	158	145	116	680
	DF	0.68	0.85	0.93	0.85	0.68	

5.7 Bridge 89-0219

Strain levels

The instrumentation of this bridge consisted of over eighty instruments positioned throughout the two spans of the bridge. Span 1 received the crutch bent retrofit, therefore, the two half spans are designated spans 1A and 1B. Furthermore, girders 2 and 9 were instrumented on the full length, whereas the remainder of the girders received instruments only at midspan, and a few additional locations.

Figure 5.40 shows the readings from selected strain gages and strain transducers. As expected, girders 9 and 10 recorded the highest strain levels in span 2, reaching strain values up to 180 $\mu\epsilon$. These values are significantly lower than the strain recorded in span 1 and at the crutch bent location, at which location the highest strain values were in the 70 $\mu\epsilon$ range – clearly indicating the benefits offered by the crutch bent retrofit. This relatively simple and fast repair method lowered the demand on the girders by 250%, a significant reduction.

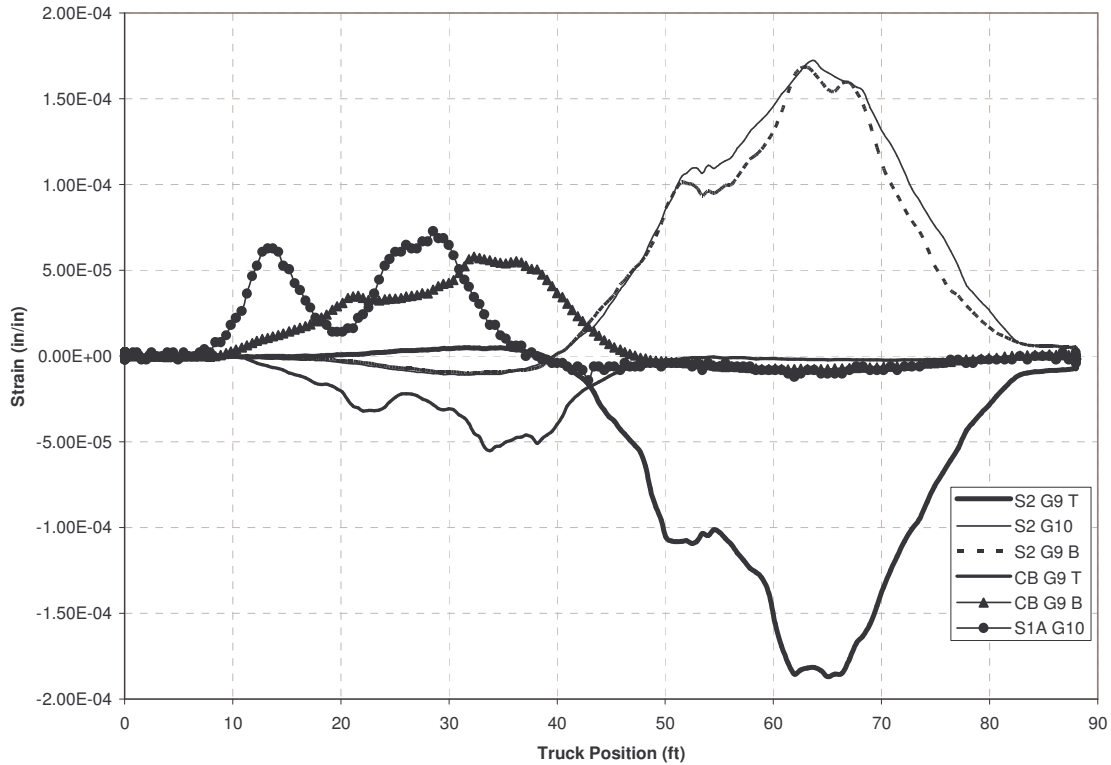


Figure 5.40 Strain readings for girders 9 and 10 – path 1

Figure 5.40 also indicates that there was no composite action between the steel girders and the timber deck. Considering the existing deck-to-girder connections, and the condition of the timber deck, this was no surprise. As it can be seen, girder 9 at the crutch bent and at the midspan of span 2 recorded near identical strain values at the top and bottom flanges, $60 \mu\epsilon$ and $180 \mu\epsilon$, respectively.

Similarly to previous bridges, the condition of the supports was also investigated. Theoretically, the original spans were simply supported. However, as it evident from Figure 5.41, negative strain readings were recorded at the bottom flange of girder 2 in span 2 (the span without retrofit). In fact, at the pier, $59 \mu\epsilon$ were recorded, a third of the peak strain values at midspan, clearly indicating a certain level of end restraint.

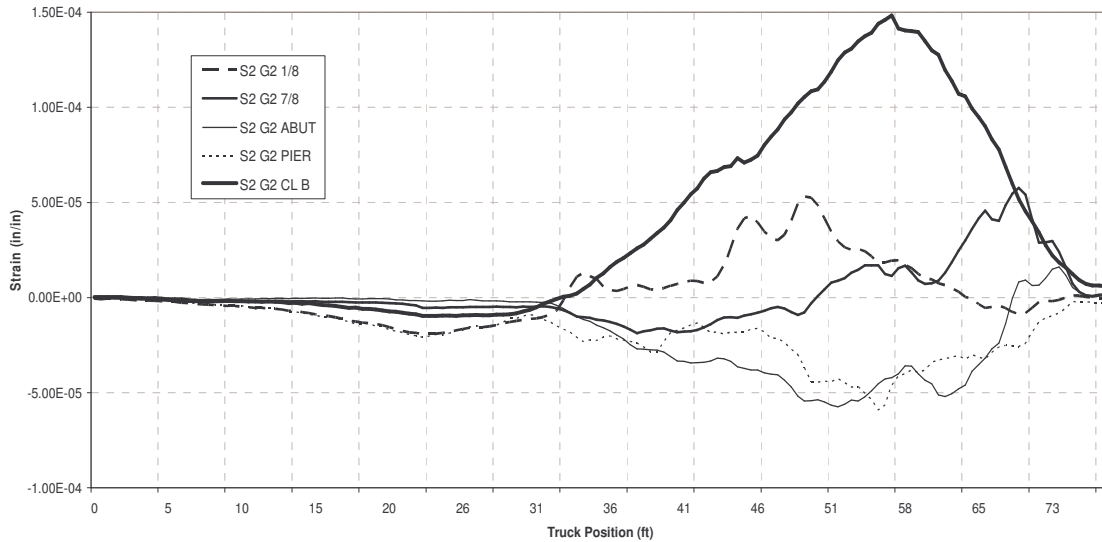


Figure 5.41 Girder 2 strain reading in span 2 – path 3

Girder deformation

Figure 5.42 shows girder 2 deflections throughout the length of the bridge. As it was observed previously, the effect of the crutch bent is significant – it lowered the peak girder deformations from 0.26 in. ($\sim L/1300$) to 0.08 in. ($\sim L/4500$).

From this figure, one could clearly identify the position of the truck, as it travels from span 1A, through span 1B, to span 2. On this figure, two additional readings were included representing two crutch bent (CB) locations, between timber posts 1 and 2, and 2 and 3, respectively. Both of these instruments recorded settlement, one recording deflections up to 0.035 in., the other reached 0.35 in.

This latter value represents a significant settlement, especially if one considers that 0.07 in. was permanent deformation, clearly indicating that the crutch bent was still in the initial settlement phase. After this, the magnitude of the secondary settlement should be minimal in the future, unless a heavier-than-posted truck travels on the bridge.

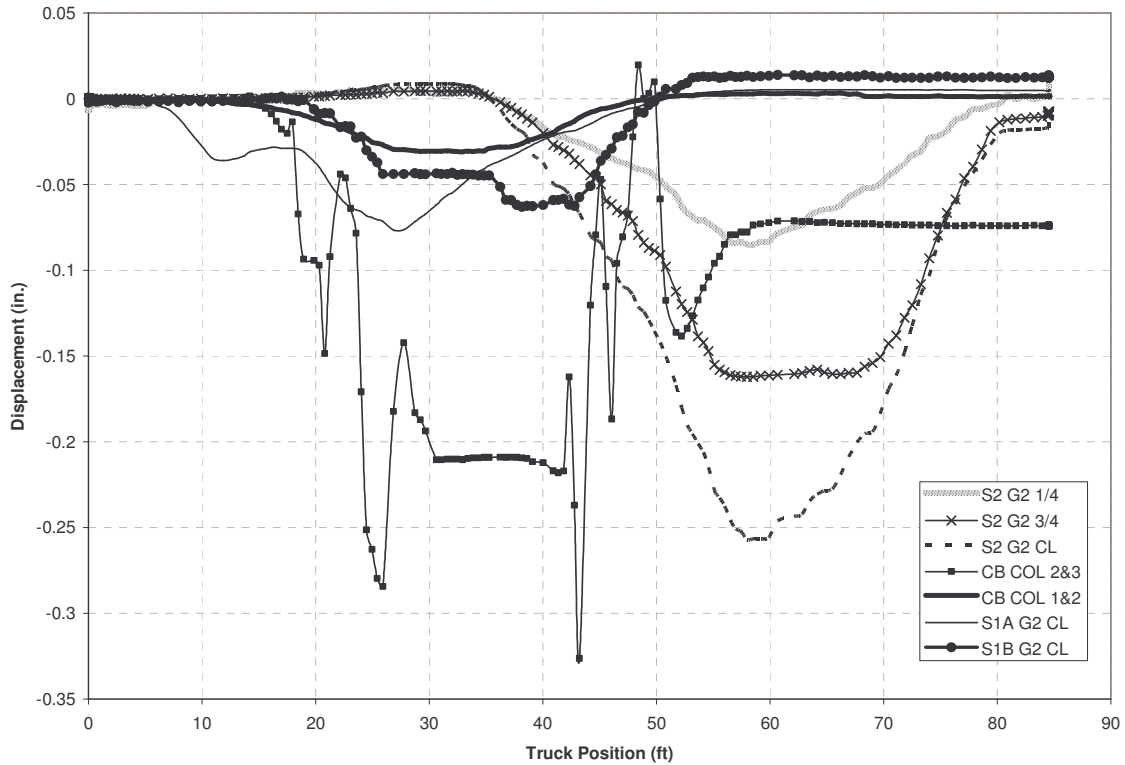


Figure 5.42 Girder 2 deflection readings – path 3

Transverse load distribution

Considering the fact that ten steel girders shared the loads applied to the deck, it was not a surprise to discover that the distribution factors were in the range of 0.54 to 0.64, calculated using two separate load paths for span 1A and 2 (see Table 5.12). The magnitude of the total strains for each load path clearly indicates that the span with the crutch bent significantly reduced the demand on the steel girders.

It is interesting to note that by installing the crutch bent, the girders in the shorter spans (1A and 1B) were resisting the truck load in a different way, concentrating most of the load on girder 2 and 9. However, the girders in original span (2) distributed the load more evenly between girders 1 and 2, and 9 and 10, respectively.

Table 5.12 Distribution factor for bridge 89-0219

Load Path	Strain at Bottom of Girder ($\mu\epsilon$)	1	2	3	4	5	6	7	8	9	10	Total Strain ($\mu\epsilon$)
Slow 3 Span 1A	one lane	64	109	56	40	39	12	12	10	4	6	352
	opposite lane	6	4	10	12	12	39	40	56	109	64	352
	both lanes	68	113	66	52	41	41	52	66	113	68	704
	DF	0.39	0.64	0.38	0.30	0.23	0.23	0.30	0.38	0.64	0.39	
Slow C Span 2	one lane	18	13	8	12	42	49	120	139	168	188	757
	opposite lane	188	168	139	120	49	42	12	8	13	18	757
	both lanes	206	181	147	132	91	91	132	147	181	206	1514
	DF	0.54	0.49	0.39	0.35	0.24	0.24	0.35	0.39	0.49	0.54	

Dynamic effects

Similarly to the previous six bridges, dynamic tests have also been performed on this bridge. The dynamic paths followed the same wheel alignment as the slow loading conditions, except the truck was traveling with the speed limit (35 mph) across the bridge. Each dynamic path was driven twice, following the protocol developed for the slow paths.

Figure 5.43 shows the readings for the span 2 girders (except girder 4, for which the instrument delivered unreliable data – therefore, those readings have been eliminated). The 194 $\mu\epsilon$ strain reading for girder 10 was the highest of all the dynamic tests performed for this bridge. As compared to the slow test results for the same path and girder (shown in Table 5.12), this dynamic value is barely larger (~3 %) than the 188 $\mu\epsilon$ recorded for the path slow C. Therefore, for this bridge, there was no real impact factor determined experimentally.

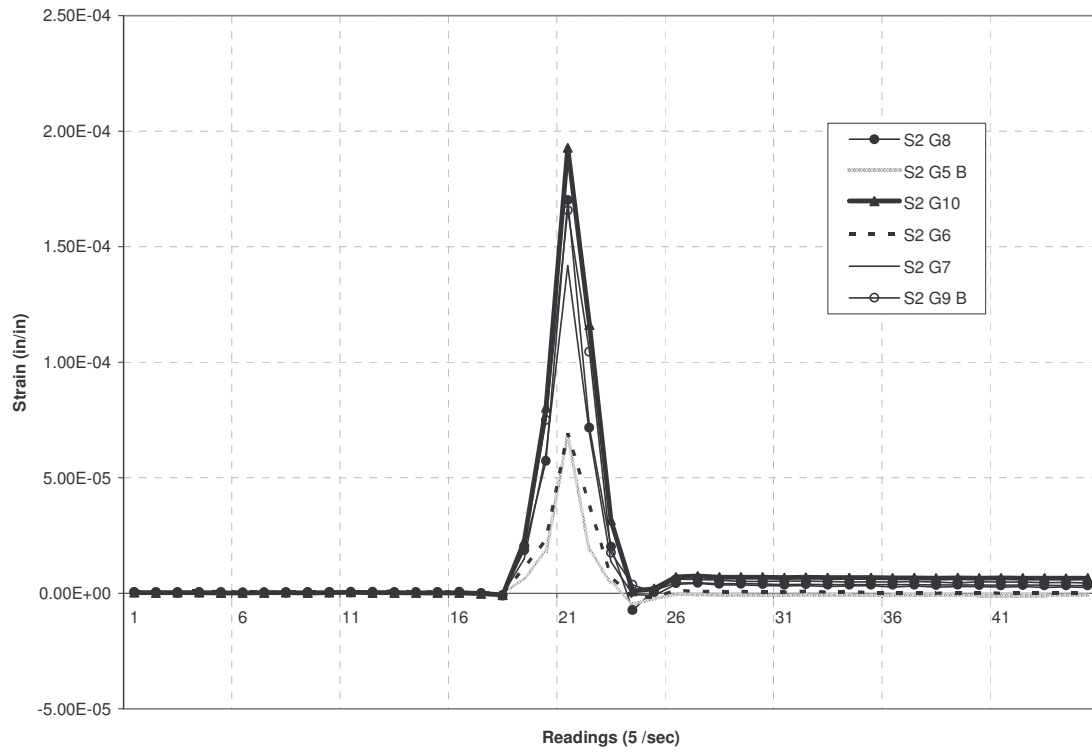


Figure 5.43 Dynamic strain readings in span 2 – path C

6. ANALYTICAL STUDIES AND COMPARISONS

During the first phase of the project, four bridges were tested and analyzed. Based on these preliminary analyses, the loading truck and the instrumentation details were determined. After the actual experiments, the test data was analyzed, and then the results compared with the bridge ratings.

In the second phase, bridge testing was preceded by extensive analyses, including a parametric study with variables, such as material property, girder end fixity, degree of composite action, etc.... These analyses provided a bridge response envelope, considering the combined effects of the above-mentioned factors. This phase was followed by the bridge tests, and then a comparison was performed between the analytical and experimental results.

In this section, nearly all variables involving bridge rating will be examined. As it will be demonstrated, a number of these variables are bridge specific, and conclusions could not be drawn for general use. Even more so, some of these bridge specific variables are also condition specific, and they could easily be altered during routine maintenance procedures.

6.1 Bridge Rating

In order to evaluate the NCDOT bridge rating software, the previously described AASHTOWare software was used, in addition to an elaborate spreadsheet developed at UNC Charlotte based on the AASHTO load rating equations discussed earlier. As

mentioned before, the limited availability of the demonstration versions of the AASHTOWare programs Virtis and Pontis, only allowed one test bridge to be evaluated using these software packages. These programs were used to analyze the RCDG bridge12-0271.

Evaluating the RCDG bridge with the software package Virtis began with entering the original NCDOT data about the bridge. This information came from the as-built bridge plans, and the current load-rating summary, which ensured that the data was entered correctly. Table 6.1 shows the comparison between the three load rating programs used.

As it can be seen in the table, the three sources generated nearly identical ratings. A 1 % difference was calculated between the NCDOT Load Rating Program and the created Excel spreadsheet, and only a 5 % difference resulted from the comparison between Virtis and the NCDOT program. In both cases, the NCDOT program was lower. These calculations were also performed with higher percent effective and different material properties for concrete, and yielded approximately the same good agreement between the three sources.

Table 6.1 Load rating comparison for bridge 12-0271

Input/Output Category	NCDOT	Virtis 4.1	UNCC
Percent Effective (%)	95	95	95
f'_c (psi)	1950	1950	1950
f_y (ksi)	30	30	30
Slab Thickness (in)	8	8	8
Inventory Rate	9.9	10.38	10
Percent Difference (%)	-	5	1
Operating Rate	16.5	17.33	16.7
Percent Difference (%)	-	5	1
SV Post	23	n/a	n/a
TTST Post	27	n/a	n/a

6.2 Distribution Factors

Current AASHTO specifications define transverse load distribution factors to longitudinal members based on girder spacing and number of lanes. Furthermore, separate transverse distribution factors are provided for interior and exterior girders. Table 6.2 summarizes the AASHTO load distribution factors relevant to the current bridge project, involving concrete deck bridges with steel and concrete girders, a timber deck bridge with steel girders, and finally a glass fiber reinforced polymer (GFRP) composite deck bridge with steel girders. As it can be seen, only the factors for bridges with two or more lanes were considered. Table 6.3 offers a direct comparison between the predictions based on the AASHTO distribution factors with the test result for each bridge investigated. For the GFRP deck bridge only one expression was provided.

Table 6.2 AASHTO ASD transverse load distribution factors

Girder Type	Girder Material	Deck Type	Girder Spacing ¹	Distribution Factor (DF)
Interior	Steel I	Concrete	$S < 14$ ft	$\frac{S}{5.5}$
		GFRP ²	-	$\frac{S}{5.0}$
		Timber	-	$\frac{S}{4.0}$
	Concrete T	Concrete	$S < 10$ ft	$\frac{S}{6.0}$
Exterior ³	-	-	$S < 6$ ft	$\frac{S}{5.5}$
	-	-	$S > 6$ ft $S < 14$ ft	$\frac{S}{4.0 + 0.25S}$

Notes: ¹For girder spacing larger than the upper limit, special analysis is required

²Deck manufacturer suggested value

³For four or more girders

Table 6.3 Comparison of distribution factors

Bridge Number	Girder - Deck	Av. Girder Spacing (ft)	Interior Girder			Exterior Girder		
			DF ¹	DF ²	Test ³	DF ¹	DF ²	Test ³
89-0022	Steel – GFRP	3.92	0.78	x	0.74	0.78	x	0.39
59-0361	Concrete – Concrete	6.67	1.11	0.65	1.33	1.18	0.59	0.71
12-0271	Concrete – Concrete	8.00	1.33	0.72	1.44	1.33	0.65	1.29
59-0038	Steel – Concrete	3.89	0.74	0.43	0.64	0.74	0.36	0.60
12-0227	Steel – Concrete	7.00	1.27	0.69	1.29	1.22	0.57	0.73
59-0841	Steel – Concrete	9.33	1.70	x	0.93	1.47	x	0.70
89-0219	Steel – Timber	2.58	0.65	0.36	0.64	0.47	0.30	0.54

Notes: ¹Calculated using AASHTO ASD equations
²Calculated using AASHTO LRFD equations
³Calculated from test data

It is clear from this comparison, that the distribution factors calculated using Equation 5.2 and the test data are surprisingly close to the design values. Except for the two RCDG bridges, the test values for the interior girders are at or slightly below (with a difference of up to 10%) the predicted values. Even for the RCDG bridges the difference is only 8 and 19%, respectively.

This is surprising to some degree, considering the fact that these predicted values do not take into account several key factors in transverse load distribution, such as, girder torsional rigidity, slab stiffness, and slab to girder connection, among others.

However, the same can not be concluded for the exterior girders. With one exception, the predicted values are far greater than the test results. Furthermore, it is not clear why the large difference (about 80%) exists between the predicted and test factors

for the interior girders of bridge 59-0841 (the new continuous steel girder bridge with spans close to 150 ft), the predicted values being far too conservative for most of the tested bridges.

6.3 Impact Factors

In order to account for dynamic, vibratory and impact effects, for design purposes, AASHTO specifies an impact factor that is used to increase the live load effects on a bridge. As it can be seen from Equation 6.1, the formula for impact factor (I) is based on the bridge span. The upper limit for this value is set for 0.30, representing a 30 % increase for the live loads applied.

$$I = \frac{50}{L + 125} \quad 6.1$$

where: I – live load impact factor; and L – bridge span length (ft).

It is clear from this equation, that this equation will yield lower impact factors for longer span bridges with possibly longer dynamic periods. This philosophy follows the classical seismic design approach based on spectral accelerations, yielding higher seismic forces for stiffer, and therefore, shorter period structures (all other aspects being equal).

Table 6.4 provides a comprehensive evaluation on the dynamic loadings. It is clear from this table, that with the exception of one or two values, the vast majority of the dynamic loadings did not result in any significant impact factors. Virtually all the dynamic readings, with the exception of the first (1st) and maybe the second (2nd) highest values, were lower than the corresponding static or slow experimental result.

By carefully reviewing all of the results it was obvious, that some of the spikes resulting in a higher dynamic reading were erroneous, and could not be confirmed with

any other readings. This could have been caused by a temporary instrument malfunction, or a sudden fluctuation in the power supplied by the portable generator – for no apparent reason, the voltage supplied to the DAQ system sometimes dropped a few volts, causing a small error in the current readings (which were especially small for the RCDG bridges).

Table 6.4 Comparison of impact factors

Bridge Number	Girder Material	Deck Type	Av. Span Length (ft)	Impact Factor			
				AASHTO	Test		
					1 st	2 nd	3 rd
89-0022	Steel	GFRP	42.00	0.30	n/a	n/a	n/a
59-0361	Concrete	Concrete	40.00	0.30	0.18	0.15	<0
12-0271	Concrete	Concrete	43.75	0.30	1.25	0.43	<0
59-0038	Steel	Concrete	36.00	0.30 ¹	<0	<0	<0
12-0227	Steel	Concrete	40.25	0.30	0.13	0.02	<0
59-0841	Steel	Concrete	144.00	0.19	na ²	na ²	na ²
89-0219	Steel	Timber	28.33	0.30 ¹	0.20 ³	0.08 ³	0.03 ³

Notes: ¹Values reduced to the maximum level of 0.30

²Dynamic loading was performed using only one truck (two trucks were used for static loading)

³Values recorded from the same dynamic path

It is obvious from Table 6.4 that none of the bridges had significant dynamic effects. Considering the shape of the approach slabs and deck joints for some of the bridges tested, this is somewhat of a surprise. However, one also has to consider the facts that the RCDG bridges for example, recorded strain values in the lower teens, approaching the lower bound of the instruments' accuracy. At this low strain level, the difference between the static and dynamic readings could be questionable.

Furthermore, the first three bridges were tested with a low sampling rate, and using only few dynamic paths. This was however, significantly improved for the last three bridges, for which, dozens of dynamic paths were scheduled, repeating each path

twice, to ensure repeatability.

6.4 Composite Action

A bridge girder's flexural capacity is significantly increased if positive connections are provided between the girder and the bridge deck. The connection in contemporary construction is realized by shear studs welded to steel girders, and poured integrally with the concrete deck. Shear studs however, have not always been used to transfer the longitudinal shear loads between girders and deck.

For these older bridges, no composite action exists – at least theoretically. In reality, out of the five steel girder bridges tested, only the timber deck bridge behaved as expected. As it was shown in the previous chapter, the neutral axes of the superstructure for the other four steel girder bridges was found to be well above the mid-height of the girders, clearly indicating a certain level of composite action in most of the cases.

Bridge 89-0022

Traditionally, composite action was accounted for by using transformed sections, where a homogeneous section was created from the two materials of the superstructure. Based on the manufacturer's recommendation, in the design of the GFRP deck replacement, for structure 89-0022, no composite action was assumed. However, the load testing clearly showed interaction between the steel girders and the GFRP deck.

To verify this result, an attempt was made to develop a transformed section. This was done by using the modular ratio of the steel and the composite material. Using the manufacturer's information for the modulus of elasticity of the deck panels, and the steel

modulus of elasticity (see Table 6.5), the modular ratio (n) was computed using Equation 6.2.

$$n = \frac{E_s}{E_c} = 11.6 \quad 6.2$$

where: E_s – modulus of elasticity of steel (psi); and E_c – modulus of elasticity of GFRP deck in the transverse direction (psi).

Table 6.5 Steel girder and composite panel information

Steel Girder	GFRP Deck
$E_s = 2.90E+07$ psi	$E_c^L = 2.50E+06$ psi
$H = 24.31$ in	$h = 7.66$ in
$T_{sf} = 0.875$ in	$T_{pf} = 0.66$ in
$I_g = 2700$ in ⁴	$W = 47$ in
$A_s = 27.7$ in ²	$A_p = 31.02$ in ²
$S_x = 222.1$ in ³	

Using this information and the girder spacing as the tributary width, the effective width of deck panel for the section was computed using Equation 6.3 to be 4.1 in.

$$b_{eff} = \frac{W}{n} \quad 6.3$$

where: b_{eff} – effective section width (in.); and W – girder spacing (in.).

Using this effective area and the dimensions of the girder, the neutral axis was computed using Equation 6.4, to be located at 14.98 in. above the bottom flange of the girder.

$$y_b = \frac{\left(A_s \times \frac{H}{2} \right) + \left[b_{eff} \times 2 \times T_{pf} \times \left(H + \frac{h}{2} \right) \right]}{A_s + (b_{eff} \times 2 \times T_{pf})} \quad 6.4$$

$$y_b = \frac{\left(27.7 \times \frac{24.31}{2} \right) + \left[4.05 \times 2 \times 0.66 \times \left(24.31 + \frac{7.66}{2} \right) \right]}{27.7 + (4.05 \times 2 \times 0.66)} = 14.98 \text{ in}$$

where: y_b – transformed section neutral axis location (in.); A_s – area of steel girder (in²); H – height of steel girder (in.); h – height of GFRP deck panel (in.); and T_{pf} – top flange thickness (in.).

Using the location of the neutral axis, the composite section properties can be found, such as the section modulus (273.03 in³), and the moment of inertia (4136.2 in⁴). As it was shown in Table 5.1, the measured neutral axis position was nearly identical with the value calculated using Equation 6.4, clearly proving that full composite action exists between the steel girders and the GFRP deck.

Bridge 59-0038

As one more example of composite calculations, the results of bridge 59-0038 will also be presented, for which, the steel girder was embedded in the concrete deck. Table 6.6 shows the calculations for the strains, the bending stresses and the deflections based on non-composite and composite sections. As it can be seen, the composite section results are much closer to the actual test data. There are some discrepancies, however, and they can be the result of higher compressive strength for the concrete deck.

This would certainly affect the modular ratio, as well as the stiffness results for the composite section. But would this automatically imply a composite action even at

higher load levels? This is questionable – and some researchers recommended calculating the horizontal shear capacity of the steel-concrete bondline to find the limiting bond stresses between the steel girder and the concrete deck.

Table 6.6 Analysis results for bridge 59-0038

Loading Path	Test Results			Non-Composite Section Properties			Composite Section Properties		
	ϵ ($\mu\epsilon$)	Δ (in.)	f (ksi)	ϵ ($\mu\epsilon$)	Δ (in.)	f (ksi)	ϵ ($\mu\epsilon$)	Δ (in.)	f (ksi)
Path 1	119	0.12	3.45	247	0.41	7.17	156	0.133	4.54
Path 4	132	0.11	3.83	247	0.41	7.17	156	0.133	4.54

6.5 Girder End Conditions

Except bridge 59-0841 (which is a continuous span structure), all the other bridges tested during this project were single or multi-span bridges, consisting of simply supported girders. Once again, the strain measurements from gages mounted close to the girder supports, and the deflection profiles along the girders suggest that, a certain degree of fixity existed at the supports for most of the bridges considered.

For some of the bridges these girder end conditions resulted in continuities with the girders from the adjacent spans. However, in most cases, the conditions of the deck joints were uncertain. When debris and asphalt runoff filled up these joints, they provided a certain degree of fixity. But again, to count on these joints to transfer load for every bridge and under any circumstance would be unconservative, to say the least.

There was one exception to this, however. As it was mentioned previously, bridge 89-0022 received a new deck system, including a semi-integral end wall for the steel girders and the GFRP deck. To estimate the upper and lower bounds of the end-

wall conditions, both fixed and pinned supports were analyzed. It is clear from Figure 6.1 that the test results for the selected girder were between the two end conditions assumed.

This fact was also confirmed by the compression strain readings at the bottom flanges near the end walls, as well as the tension strain readings at the top flanges. The uncertainties of these end conditions make it difficult to set up a reliable analytical model – as these partial fixities greatly influence the stiffness of the bridges, and lower the flexural demand of the girders around the mid-span.

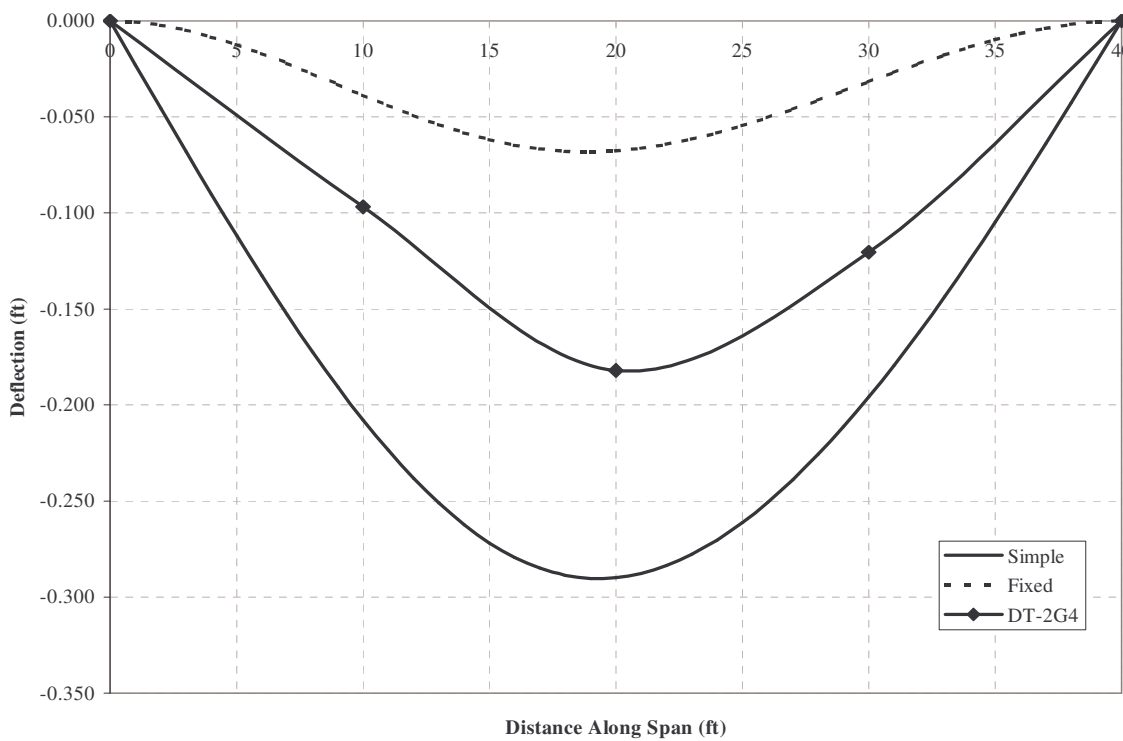


Figure 6.1 Deformation profile of bridge 89-0022

6.6 Strain Levels

In the second phase of this project, in order to estimate the expected strain levels in the bridge girders, all of the factors mentioned in this chapter were considered in different combinations. However, this created upper and lower bound strain values that were so far apart, the range became too wide to be meaningful.

The largest differences between predicted and tested strains and stresses occurred for the RCDG bridges. For these concrete girders, strains in the 200-300 $\mu\epsilon$ levels were predicted. This numbers were also confirmed with simpler finite element analyses. Nevertheless, during testing, the strain levels recorded were well below 100 $\mu\epsilon$. Even the deformations were in the few hundreds of an inch range, proving that these structures are far stiffer and stronger than anticipated.

To find the reasons for this unexpected behavior, non-destructive tests (NDT) were performed to verify the concrete compressive strength for the girders. As it was mentioned earlier, AASHTO and NCDOT guidelines clearly specify the concrete strength for older structures (for these two bridges the values were 1,950 and 2,500 psi, respectively), when the original specifications are not clear, or they are no longer available.

Schmidt hammer and Windsor probes were used in the NDT, and the results were surprisingly high. Virtually all of the measurements for the two RCDG bridges resulted in concrete strengths well above 6,000 psi. Indeed, one could argue that f'_c has little or no effect on the girder's flexural capacity – when these values were used in the NCDOT bridge rating software, the significantly higher concrete strength resulted in a difference less than 10%.

However, there could be no argument about the fact that these high concrete strengths will yield much stiffer girders, and the shear capacity is also increased for these members. Furthermore, the effect of non-structural elements is also increased. Strain gages attached to the concrete railing and curb on bridge 12-0271 indicated compressive strain levels up to $21 \mu\epsilon$ (see Figure 6.2), higher than the maximum tensile strains at the girder bottom for the same path.

These relatively large compression members can not be ignored, but they are extremely difficult to incorporate in the analysis or in preliminary calculations. Especially since insufficient details exists on the curb and the rail connection to the concrete deck. Without this information, one could only guess their contribution to the strength and stiffness of the superstructure.

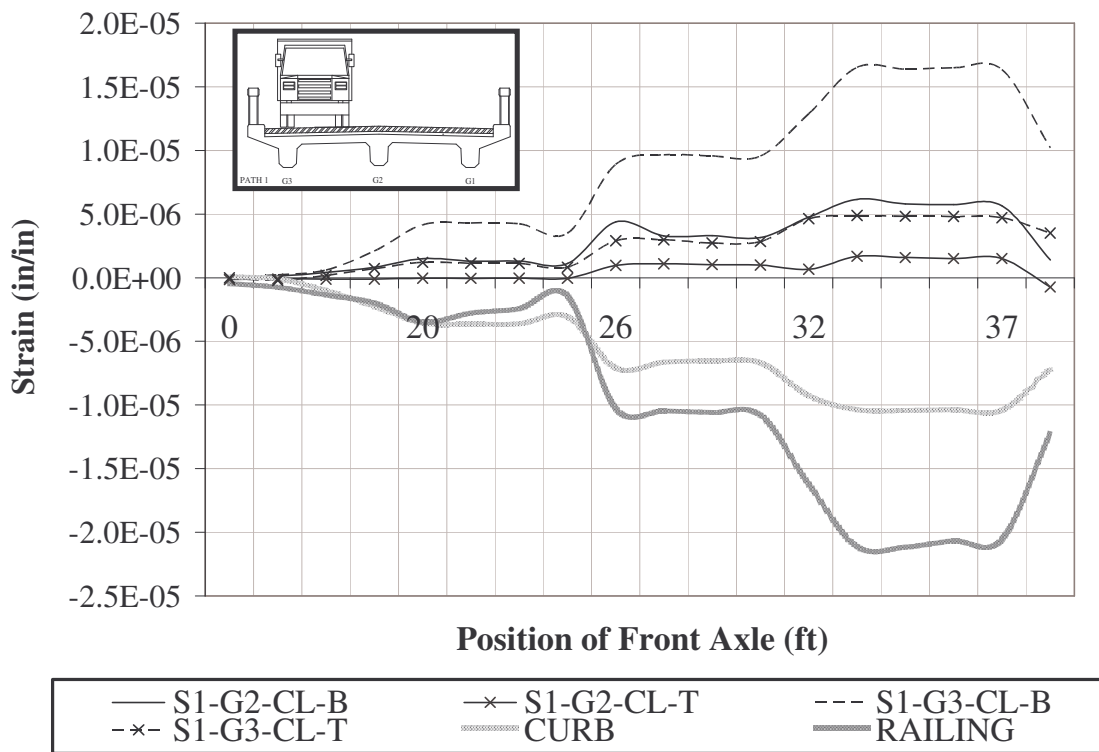


Figure 6.2 Strain readings at midspan – path 1

For the steel girder bridges, the strain values were more predictable, and the best estimates were within 40 % of the measured data. As an example, Table 6.6 shows the strain and stress comparisons between test data and analytical results for bridge 59-0038. As it can be seen, the predicted strain values for both paths 1 and 4 are reasonably close to the composite section estimates. Similar results have been found for bridge 89-0219 as well.

6.7 Crutch Bent Retrofit

As it can be seen in Figures 6.3 and 6.4, the crutch bent retrofit increased the Inventory Rating for bridge 89-0219 from HS 7.2 to HS 20.8, and the Operating Rating from HS 12.1 to HS 29.4. This is close to 200% increase, and once the second span is retrofitted, posting on the bridge could be removed entirely.

As it was presented in Section 5.7, this increase in bridge rating is also proven by experimental data. The peak steel girder strain in tension decreased from 180 $\mu\epsilon$ to 70 $\mu\epsilon$, and the maximum girder deflection decreased from 0.26 in. to 0.08 in. These values represent the same 200% change as the above-mentioned rating adjustments due to the crutch bent retrofit, clearly proving its effectiveness.

=====

NORTH CAROLINA DEPARTMENT OF TRANSPORTATION - BRIDGE MAINTENANCE
ANALYSIS SECTION

=====

RATING SUMMARY SHEET

Non-InterState Highway Bridge

STRUCTURE NUMBER: 890219 COMPILED BY: F.KHAJA DATE: 08/13/02
COUNTY: Union CHECKED BY: *[Signature]* DATE: *[Signature]*

=====

MEMBER:	floor	Int.Beam
HS inv	20.2	7.2
HS opr	27.0	12.1

SH	12.50	13.6
S3C	21.50	14.0
S3A	25.02	14.9
S4A	29.42	16.2
S5A	33.55	17.0
S6A	37.95	18.0
S7B	40.00	17.8
S7A	40.00	19.0

T4A	31.08	18.5
T5B	35.20	19.8
T6A	39.60	21.3
T7A	40.00	22.1
T7B	40.00	20.8

=====

CALCULATED POSTING: SV 14 tons - TTST 18 tons	Design Loading: unknown
CONTROLLING MEMBER: Int.Beam	INVENTORY RATING: HS 7.2
EXISTING POSTING: SV 14 tons - TTST 18 tons	OPERATING RATING: HS 12.1
RECOMMENDED POSTING: SV 14 tons - TTST 18 tons	Item 70 - Bridge Posting CODE: 0
ANALYSIS METHOD Inventory Rating: LF	Operating Rating: LF
COMMENTS: <i>Change in AWS</i>	

=====

Figure 6.3 Summary of bridge rating for 89-0219 before crutch bent retrofit

=====

NORTH CAROLINA DEPARTMENT OF TRANSPORTATION - BRIDGE MAINTENANCE
ANALYSIS SECTION

=====

RATING SUMMARY SHEET

Non-InterState Highway Bridge

STRUCTURE NUMBER: 890219 COMPILED BY: F.KHAJA DATE: 03/05/03
 COUNTY: Union CHECKED BY: DATE:

=====

MEMBER:		Int.Beam	Cap
HS inv		22.0	20.8
HS opr		36.7	29.4
SH	12.50	36.7	39.6
S3C	21.50	44.3	37.2
S3A	25.02	51.5	38.7
S4A	29.42	54.3	42.3
S5A	33.55	61.2	43.6
S6A	37.95	69.1	45.7
S7B	40.00	72.1	44.1
S7A	40.00	72.9	48.2
T4A	31.08	64.0	48.1
T5B	35.20	72.5	49.8
T6A	39.60	73.1	54.0
T7A	40.00	78.2	56.2
T7B	40.00	73.6	53.8

PROPOSAL

=====

CALCULATED POSTING: No posting required	Design Loading: unknown
CONTROLLING MEMBER:	INVENTORY RATING: HS 20.8
EXISTING POSTING: SV 14 tons - TTST 18 tons	OPERATING RATING: HS 29.4
RECOMMENDED POSTING: No posting required	Item 70 - Bridge Posting CODE: 5

=====

REASON FOR POSTING CHANGE:
THIS IS A PROPOSAL TO UPGRADE BY PROVIDING A CRUTCH BENT

=====

ANALYSIS METHOD Inventory Rating: LF Operating Rating: LF

=====

COMMENTS: NOT FOR POSTING

=====

Figure 6.4 Summary of bridge rating for 89-0219 after crutch bent retrofit

7. NCDOT BRIDGE ANALYSIS SOFTWARES

7.1 Simple Span Analysis Software

During this research project, five of the bridges tested were also analyzed using NCDOT's simple span analysis software. As it was mentioned in Chapter 3 of this report, the NCDOT analysis software directly follows the AASHTO (2000) bridge condition evaluation procedures. The only added feature in the software is the use of an effective girder cross section, a factor (smaller than one) that accounts for the loss of effective area due to corrosion or vehicular damage. This feature adds an additional safety factor to the already conservative AASHTO approach.

In addition, two other softwares have been used to verify the results of the NCDOT analysis software. One is the Virtis program developed by AASHTOWare, the other is an Excel-based spreadsheet developed by the UNC Charlotte research group. Both of these programs verified the accuracy of the NCDOT program, and once again, proved its safe and conservative approach to bridge evaluation.

In order to have a better appreciation of the accuracy of the NCDOT software, an example calculation will be presented here. This example presents the findings of the analysis and testing of bridge 59-0038.

Figures 7.1 and 7.2 are the output sheets from the NCDOT bridge analysis program using the original data for Bridge 59-0038. For the original conditions, the S3C single loading vehicle and the T4A - TTST loading vehicle govern the analysis, and result in a bridge posting of 19 tons for SV, and 25 tons for TTST.

NORTH CAROLINA DEPARTMENT OF TRANSPORTATION - BRIDGE MAINTENANCE
ANALYSIS SECTION

```

-----
BRIDGE NUMBER      590038                DATE OF RATING  1/7/01
COUNTY           meclenburg             RATED BY       RS
DATE OF INSPECTION 11/19/01                CHECKED BY
  
```

Load Factor Method
NONCOMPOSITE BEAM RATING

```

-----
Truck Weight Operating Inventory Llmoment Section Controls
HS15  15.00  15.8    9.5    257.59 Compact Serviceability
H15   15.00  19.0   11.4   214.71 Compact Serviceability
TR2   15.75  20.5   12.3   208.23 Compact Serviceability
TR3   24.94  21.1   12.6   321.02 Compact Serviceability
TR4   33.60  21.0   12.6   435.01 Compact Serviceability
TR5   36.75  26.0   15.6   383.44 Compact Serviceability
SH    12.50  19.0   11.4   178.92 Compact Serviceability
S3C   21.50  19.5   11.7   300.03 Compact Serviceability
S3A   25.02  20.4   12.2   333.31 Compact Serviceability
S4A   29.42  21.9   13.1   365.43 Compact Serviceability
S5A   33.55  22.6   13.5   402.92 Compact Serviceability
S6A   37.95  24.5   14.7   420.82 Compact Serviceability
S7B   40.00  23.8   14.3   456.42 Compact Serviceability
S7A   40.00  25.7   15.4   423.55 Compact Serviceability
T4A   31.08  25.2   15.1   334.51 Compact Serviceability
T5B   35.20  25.4   15.2   376.23 Compact Serviceability
T6A   39.60  27.8   16.7   387.01 Compact Serviceability
T7A   40.00  28.5   17.1   381.51 Compact Serviceability
T7B   40.00  28.4   17.0   382.62 Compact Serviceability
  
```

Last update 3-25-98 -----NON-INTERSTATE TRAFFIC-----Version 4.1

BEAM ASSUMED BRACED TO THE FLOOR. SPAN A

INPUT:

Rating for Maximum Moment Possible

Rolled 20" x 59.5 # I-Beam.

Section Area = 17.4; Section Depth = 20.00;

Flange Thickness = 0.647; Web Thickness = 0.375

Interior Beam Concrete Slab Clear Roadway = 24.833

Asphalt Wearing Surface = 8.00 in. Full Slab Depth = 7.00 in.

Posts & Rails = 10 lb/ft. Diaphragm = 1.00 lb/ft.

Beam Spacing = 4.083 ft. Percent Effective = 95.7 %

Span length = 34.000/ft. Yield Stress = 33000 psi

Figure 7.1 Live load calculations for loading vehicles on Bridge 59-0038

```

=====
NORTH CAROLINA DEPARTMENT OF TRANSPORTATION - BRIDGE MAINTENANCE
ANALYSIS SECTION
=====
RATING SUMMARY SHEET
Non-InterState Highway Bridge
STRUCTURE NUMBER: 590038      COMPILED BY: RS      DATE: 1/7/02
COUNTY:      meclenburg      CHECKED BY:          DATE:
=====

MEMBER:      int bm

-----
HS inv      9.5
HS opr      15.8

-----
SH      12.50      19.0
S3C     21.50      19.5
S3A     25.02      20.4
S4A     29.42      21.9
S5A     33.55      22.6
S6A     37.95      24.5
S7B     40.00      23.8
S7A     40.00      25.7

-----
T4A     31.08      25.2
T5B     35.20      25.4
T6A     39.60      27.8
TZA     40.00      28.5
3       40.00      28.4

-----
CALCULATED POSTING:      Design Loading:
SV 19 tons - TTST 25 tons      |      unknown
-----
CONTROLLING MEMBER:      INVENTORY RATING:
int bm      |      HS      9.5
-----
EXISTING POSTING:      OPERATING RATING:
SV 19 tons - TTST 25 tons      |      HS      15.8
-----
RECOMMENDED POSTING:      Item 70 - Bridge Posting
SV 19 tons - TTST 25 tons      |      CODE:      0
-----
ANALYSIS METHOD      Inventory Rating: LF      Operating Rating: LF
-----
COMMENTS:
=====

```

Figure 7.2 Summary of NCDOT bridge analysis of Bridge 59-0038

Based on the actual tandem truck loading setup (generating a maximum moment of 212.2 K-ft versus 300.0 K-ft resulted from the governing S3C), hand calculations were performed to estimate the stresses, strains, and deflections at mid-span. Figure 7.3

shows the non-composite girder (as assumed in the original analysis based on field construction and design details) calculations.

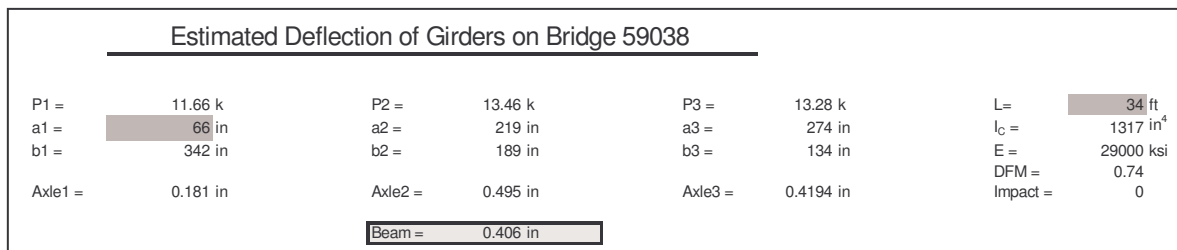
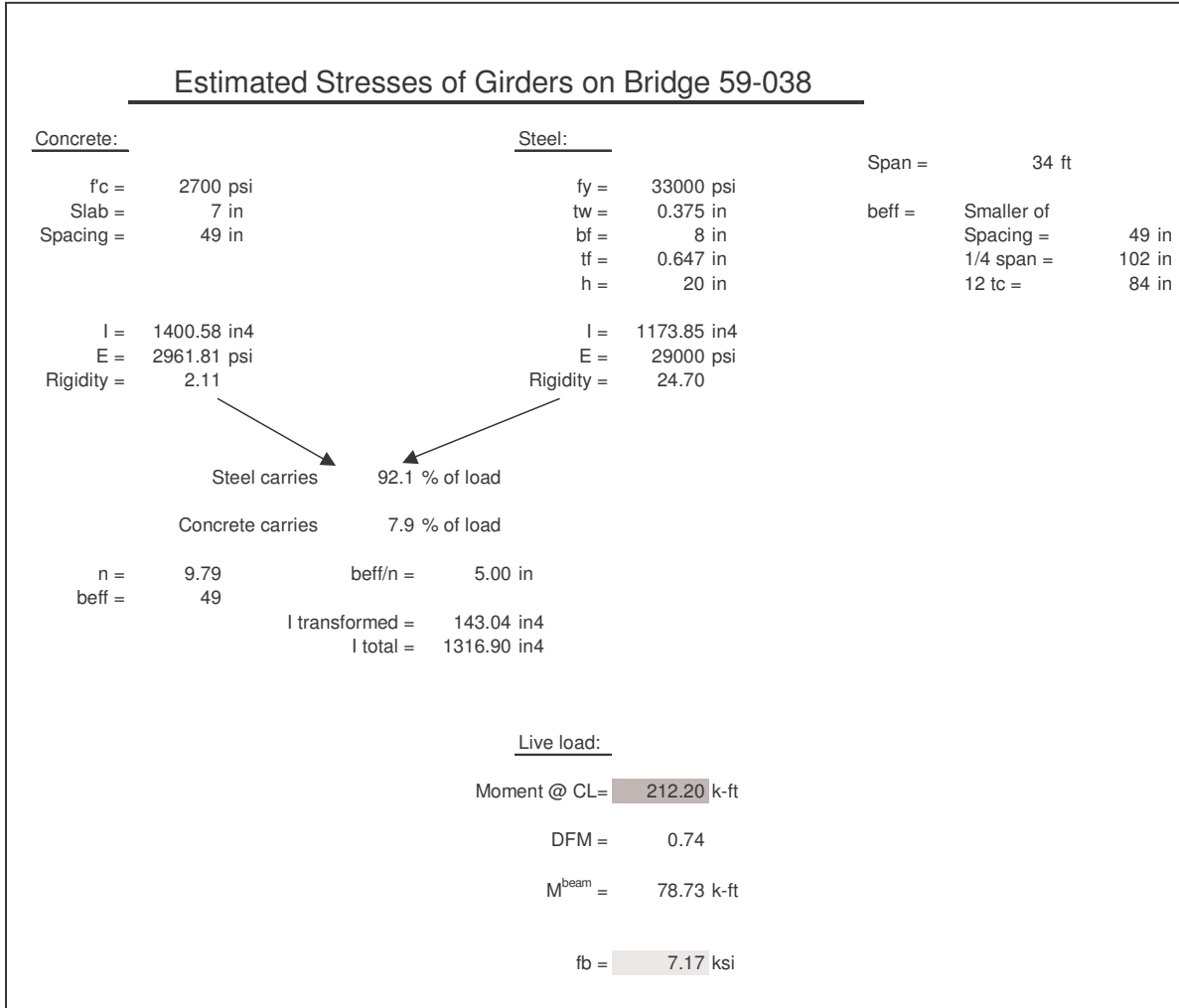


Figure 7.3 Non-composite hand calculations for Bridge 59-0038

After testing Bridge 59-0038, the results of the tests were compared to the hand calculations to determine if the structure was performing as expected. Similar to other bridges, Bridge 59-038 performed better than anticipated. Although the differences in strain and deflection values were not as large, the steel girder bridge still experienced only half the estimated strain and a quarter of the estimated deflection.

One of the reasons for these differences is a result of a possible composite action between the girders and the bridge deck. The bridge was inspected and the top flange of the girder is embedded into the concrete deck, bracing the compression flange and tying the girder firmly to the deck. This connection was strong enough to allow the bridge to act partially composite at the load level tested. Figure 7.4 shows the hand calculations performed assuming full composite action in the bridge superstructure.

Table 7.1 compares the strain and deflection values at mid-span of one of the steel girders from the loading tests, as well as the results from the non-composite and composite hand calculations. From this table, it is clear that the test strains values are slightly less than the composite values, whereas the deflections are practically identical.

However, one should remember that the horizontal shear capacity between the girders and the deck could be exceeded if a significantly larger truckload was applied to the bridge. This should need to be further investigated on a case-by-case basis.

Table 7.1 Strain and deflection values at mid-span for Bridge 59-0038

Loading Path	Test Values			Analysis Based on Non-Composite Sections			Analysis Based on Composite Sections		
	$\mu\epsilon$	Δ (in)	f (ksi)	$\mu\epsilon$	Δ (in)	f (ksi)	$\mu\epsilon$	Δ (in)	f (ksi)
1	119	0.12	3.45	247	0.41	7.17	156	0.133	4.54
4	132	0.11	3.83	247	0.41	7.17	156	0.133	4.54

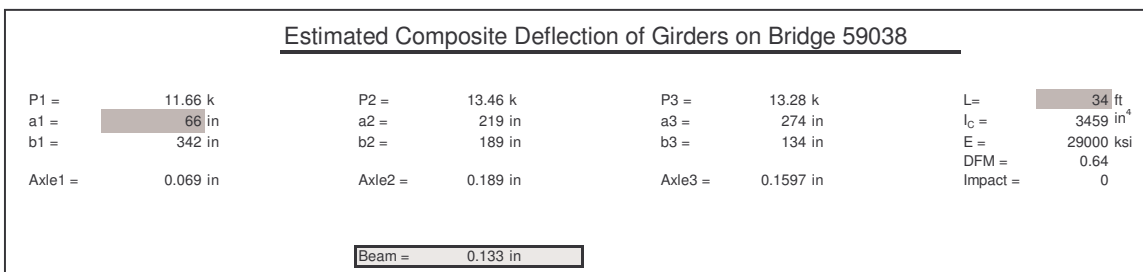
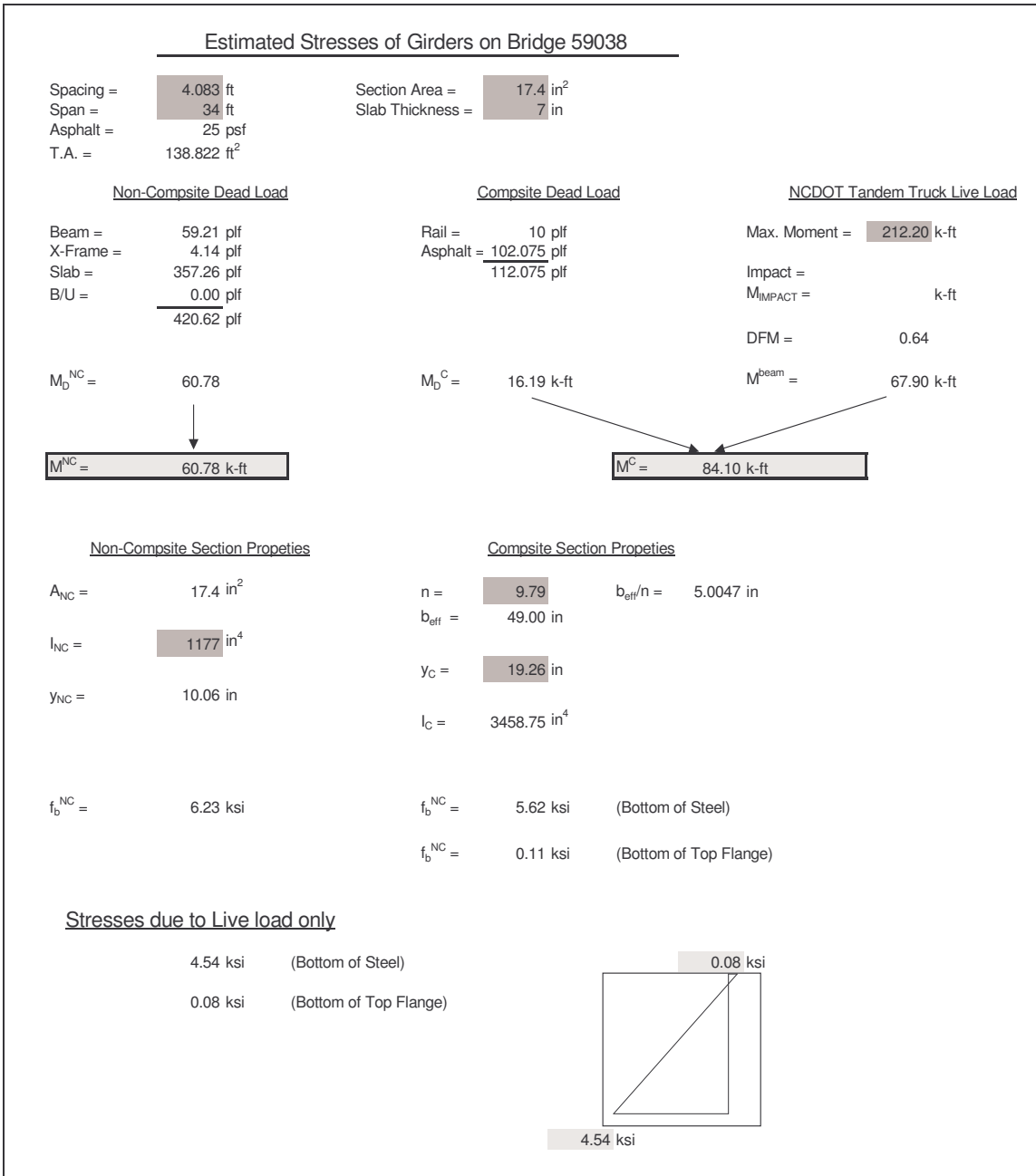


Figure 7.4 Composite hand calculations for Bridge 59-0038

So the real question is - how safe is bridge 59-0038? If one considers the fact that the moment generated by the S3C truck used in the load rating software is about 40% higher than the actual load applied, and realizing that the superstructure materials are well within their linear range, the maximum strain values in Table 7.1 would be 189 $\mu\epsilon$ for the S3C, or 5.41 ksi tensile stress at the bottom of the steel girder.

It should also be noted that an additional moment of 118.5 K-ft will result from dead load, increasing the total tensile stress in the steel girders to 7.55 ksi, well within the allowable/elastic range for a 33 ksi steel, even though, no load factors have been used in this simple evaluation.

7.2 Continuous Span Analysis Software

A similar analysis to the above described simple span example has been also performed for the continuous span software, using the information from bridge 59-0841. As mentioned before, this was a new bridge at the time of the testing, and due to the geometry and load capacity of the bridge, two testing trucks have been used in the experimental analysis.

Bridge 59-0841 was opened for traffic one week before load testing was performed, therefore, the inventory and operating ratings for this structure are extremely high and do not require the bridge to be posted. The NCDOT continuous bridge analysis program was used to determine the ratings. Figure 7.5 is a summary sheet of the latest analysis for Bridge 59-0841. The load rating is based on a maximum negative moment of -1,629 K-ft (governed by lane loading), and a positive moment of 1,940 K-ft in Span 1, and 1,931 K-ft in Span 2, respectively.

NORTH CAROLINA DEPARTMENT OF TRANSPORTATION - BRIDGE MAINTENANCE ANALYSIS SECTION		
RATING SUMMARY SHEET		
Non-InterState Highway Bridge		
STRUCTURE NUMBER: 590841	COMPILED BY: F. KHAJA	DATE: 03/02/04
COUNTY: Mecklenburg	CHECKED BY: <i>H. A. Blundell</i>	DATE: <i>3/2/04</i>
MEMBER:	floor	Cont.Bm
Span Length:		145 ft.
Beam spacing:		9.3 ft.
HS inv	17.9	40.5
HS opr	28.3	67.4
SH	12.50	111.8
S3C	21.50	113.0
S3A	25.02	115.6
S4A	29.42	116.3
S5A	33.55	116.7
S6A	37.95	119.7
S7B	40.00	118.6
S7A	40.00	120.4
T4A	31.08	121.0
T5B	35.20	120.4
T6A	39.60	121.2
T7A	40.00	122.7
T7B	40.00	123.0
CALCULATED POSTING: No posting required	Design Loading:	HS-20
CONTROLLING MEMBER:	INVENTORY RATING:	HS 40.5
EXISTING POSTING: Not Posted	OPERATING RATING:	HS 67.4
RECOMMENDED POSTING: No posting required	Item 70 - Bridge Posting CODE:	5
ANALYSIS METHOD	Inventory Rating: LF	Operating Rating: LF
COMMENTS: Bridge Revised before construction.		

Figure 7.5 Rating summary for Bridge 59-0841

These rating values are somewhat different from the actual moment levels induced by the two tandem trucks used in the tests. The actual negative moment achieved was -1,310 K-ft, and the positive moments for the two spans were 2,379 K-ft and 2,300 K-ft, respectively – an overloading accepted by the NCDOT Analysis Team. The results of the “hand calculations” are shown in Figures 7.6 and 7.7.

Estimated Stresses of Girders on Bridge 59-0841

Geometric Properties of the Concrete Deck

Deck thickness = 8.75 in
 Beff = 105 in
 B/U = 2.5 in
 f'c = 3000 psi
 Ra

Geometric Properties of the Plate Girders

Top flange width = 20 in
 Top flange thickness = 1 in
 Bottom flange width = 22 in
 Bottom flange Thickness = 1.125 in
 Web thickness = 0.5625 in
 Web height = 64 in
 Spacing = 9.33 ft

Span 1

NCDOT Tandem Truck Live Load

Span = 146.5 ft
 Beff = Smaller of
 Spacing = 112 in
 1/4 span = 440 in
 12 tc = 105 in

Max. Moment = 2379.30 k-ft
 Impact =
 M_{IMPACT} = k-ft
 DFM = 0.93
 M^{beam} = 1106.37 k-ft

Section Area = 918.75 in²
 I = 5861.81641 in⁴
 E = 3155.92425 ksi

Section Area = 80.75 in²
 I = 98726.37 in⁴
 E = 29000 ksi

Non-Composite Section Properties

Composite Section Properties

A_{NC} = 80.75 in²
 y_{NC}^t = 34.93 in
 y_{NC}^b = 31.19 in
 I_{NC} = 98726.373 in⁴

n = 9.19 b_{eff}/n deck = 11.43 in
 b_{eff}/n B/U = 2.18 in
 A_C = 186.17 in²
 I_C = 178341.2 in⁴
 y_C^t = 22.67203 in
 y_C^b = 54.70297 in

Stresses due to Live load only

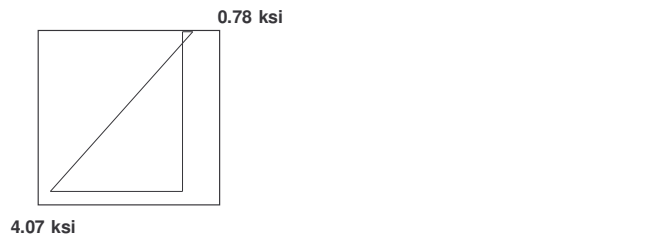


Figure 7.6 Composite hand calculations for span 1 of Bridge 59-0841

Estimated Stresses of Girders on Bridge 59-0841

Geometric Properties of the Concrete Deck

Deck thickness = 8.75 in
 B_{eff} = 105 in
 B/U = 2.5 in
 f'_c = 3000 psi
 R_a

Geometric Properties of the Plate Girders

Top flange width = 20 in
 Top flange thickness = 1 in
 Bottom flange width = 22 in
 Bottom flange Thickness = 1.125 in
 Web thickness = 0.5625 in
 Web height = 64 in
 Spacing = 9.33 ft

Span 2

Span = 144 ft
 B_{eff} = Smaller of
 Spacing = 112 in
 1/4 span = 432 in
 12 t_c = 105 in

Section Area = 918.75 in²
 I = 5861.8164 in⁴
 E = 3155.9243 ksi

NCDOT Tandem Truck Live Load

Max. Moment = 2300.00 k-ft

Impact =
 M_{IMPACT} = k-ft
 DFM = 0.93
 M^{beam} = 1069.50 k-ft

Section Area = 80.75 in²
 I = 98726.4 in⁴
 E = 29000 ksi

Non-Composite Section Properties

A_{NC} = 80.75 in²
 $y_{t_{NC}}$ = 34.93 in
 $y_{b_{NC}}$ = 31.19 in
 I_{NC} = 98726.373 in⁴

Composite Section Properties

$3n$ = 27.57 b_{eff}/n deck = 3.81 in
 n = 9.19 b_{eff}/n B/U = 0.73 in
 A_C = 115.89 in²
 I_C = 141196.38 in⁴
 y_{t_C} = 33.592272 in
 y_{b_C} = 43.782728 in

Stresses due to Live load only

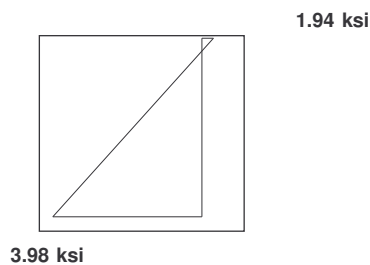


Figure 7.7 Composite hand calculations for span 2 of Bridge 59-0841

After testing Bridge 59-0841, the results of the tests were compared to the hand calculations to determine if the structure was performing as expected. Table 7.2 shows a good agreement between anticipated and test live load values (considering only truck loads). Once again, these values are far from the allowable stresses for the AASHTO M270 Grade 50W steel, even though only live loads have been considered in this example.

Table 7.2 Strain values at mid-span for Bridge 59-0841

Loading Configuration	Test Values		Hand Calculations	
	$\mu\epsilon$	$f(ksi)$	$\mu\epsilon$	$f(ksi)$
Path 1, Span 1	165	4.79	140	4.07
Path 5, Span 1	147	4.26	140	4.07
Path 1, Span 2	165	4.79	137	3.98
Path 5, Span 2	145	4.21	137	3.98

7.3 Conclusions

In conclusion, it is clear that based on the seven bridge tests and extensive analytical work, the NCDOT simple and continuous span softwares directly follow the AASHTO requirements (with one minor conservative exception) for bridge rating, and provide a safe and conservative estimate for the load capacity of existing bridges. At this point, improvement to these softwares could only be made if the bridge analysis program results are complemented by bridge tests to allow for more realistic estimates of important factors, such as transverse load distribution, impact, composite action, etc...

8. BRIDGE RATING THROUGH LOAD TESTING

It is clear from the discussions presented in the previous chapters that the true behavior of each individual bridge largely depends on the specific conditions present at the bridge being investigated. Would a full finite element analysis provide these factors with confidence? Yes, for some of them (e.g. load distribution factors, contribution of secondary elements); but even slight deviations from the design specifications, in combination with the under- or over-estimation of the true condition of structural elements (degree of corrosion and cracking), deck and girder joints, approach slabs and material properties, would provide erroneous results.

Based on the data presented in this report, it is evident that some of the factors that influence the true response of a bridge structure can be estimated with confidence. However, a good number of other factors can only be evaluated through actual load testing. The *Manual for Bridge Rating Through Load Testing* (1998) published by the NCHRP Research Results Digest provides detailed information on factors influencing bridge rating, load testing protocols, and guidelines for re-evaluating bridges based on test data.

Would it make economical and engineering sense to test every single bridge in the country? Probably not, these tests would be most feasible for posted bridges or structures with questionable strength, damaged bridges, or bridges evaluated for special permits. As sensor technology evolves in the near future, it would be beneficial to embed sensors

into several bridge components, and either monitor them continuously, or record their data as a load testing is performed in the future.

8.1 Rating Procedure

As it was mentioned earlier, for the last three bridges tested in this research project an additional portable data acquisitions system was also used to monitor the bridges' response. It was clear, that the handful of instruments used with this system provided reliable data that could be used to re-rate these bridges based on test information. These instruments allowed the more realistic evaluation of several factors, including the load distribution and impact factors, the true strain levels in primary bridge components, the presence of composite action, and the degree of fixity for simple span superstructure components.

Although it is not anticipated to occur with frequency, the bridge testing might reveal a weaker-than-expected structure. Experience shows that most bridges tested exhibit significant load reserves. No matter what is the result, load testing will provide a more realistic "picture", well worth the effort. The actual procedure should include the following steps:

1. *Bridge inspection and evaluation* – this step is already being done every other year. Should also include material tests using NDT techniques, or tests on actual samples collected from selected members.

2. *Initial bridge load rating* – based on real material properties and updated loading information, perform an initial load rating of the bridge.

3. *Design of instrumentation and loading protocol* – based on the make-up, geometry, size, ADT, and other factors, design an instrumentation plan. Select the loading truck(s) sufficiently large to perform a diagnostic testing in function of the current load rating of the bridge.

4. *Instrumentation of bridge components* – this step involves the preparation of the bridge site, and the positioning of the instruments. These instruments (up to two dozens) should include strain measuring devices, e.g. strain transducers, strain gages or LVDTs, depending on the girder and deck material. If load testing will not immediately follow the installation of the instruments, these devices must be protected against environmental effects and vandalism.

5. *Bridge load testing* – during this phase, the bridge is partially or fully closed to traffic. Then, following a predetermined loading protocol, the bridge is loaded with a slow-moving truck. The load path is designed to provide maximum effect on the girders and decks, as applicable. In order to provide a more realistic impact factor for the bridge being evaluated, data would be recorded while the loading truck moves at the legal speed limit.

6. *Experimental data analysis* – using simple hand calculations (or in-house spreadsheet programs, or commercially available software), the test data is analyzed, and compared with predicted values.

7. *Update of initial bridge load rating* – based on the experimental data, the bridge is then re-rated, to provide a more realistic performance level for the structure being analyzed. The above mentioned Manual for Bridge Rating Through Load Testing provides detailed rating procedures using actual field test data.

8.2 Personnel and Equipment Needs

Bridge rating through load testing is not new. Several commercial entities exist around the country specialized in this procedure. However, in order to provide a more economical approach, with minimal training and a reasonable initial investment in equipment, several testing crews could be established. Table 8.1 summarizes the personnel and equipment needs to perform the 7 steps outlined in the previous section.

Table 8.1 Summary of bridge testing personnel and equipment needs

Step	Task Description	Personnel Need	Personnel Training	Equipment Type	Equipment Cost	Estimated Time
1	bridge inspection	existing inspection crew	minimal for NDT	NDT (if used)	depends on NDT type	1 hour for NDT
2	initial load rating	existing bridge analysis team	no change	no change	no change	no change
3	design bridge test protocol	1-2 additions to bridge analysis	minimal to moderate	none	none	2-3 hours
4	bridge instrumentation	1 addition to inspection crew	minimal	6-12 for strain	\$3k - \$6k	2-3 hours
				4-6 for deformation	\$2k - \$3k	
5	bridge load testing	truck driver (from NCDOT yard)	minimal to moderate	data acquisition	~\$25k	1-2 hours
				loading truck traffic control	minimal	
6	test data analysis	same as Step 3	moderate	in-house or commercial software	~\$5k for commercial	2-4 hours
7	update bridge load rating	same as Step 3	moderate	same as Step 6	none	1-2 hours

As it can be seen, the majority of personnel are already in place, requiring only 1 additional inspection crew member trained to place instrumentation and conduct bridge load testing. This crew member would travel with the testing equipment to bridge test sites, and would be assisted by the local bridge maintenance and/or inspection team.

There would be a need for 1 or 2 additional bridge analysis personnel. The training for these engineers would be relatively simple, including experimental stress

analysis, basic instrumentation, and test data interpretation.

The initial equipment cost is approximately \$40k - \$50k, not including consumables such as clamps, ties, etc... This cost could be recovered within the first few bridge tests by minimizing or eliminating some of the structural repair and strengthening work otherwise required. These instruments are well documented and established within the bridge testing community. Some of these firms also developed software programs that directly import test data, and perform the necessary load rating calculations.

The actual field work (steps 4 and 5) requires 3-5 hours per bridge, depending on the complexity of the project, access to the bridge site, etc... However, the bridge would be closed for only an hour to perform the actual bridge testing. The instrumentation placement and tear-down requires no special traffic control (bridge or lane closure), for most of the bridges.

Table 8.1 only provides cost estimates for the initial equipment investment. The objective of the project did not include a detailed cost analysis of per bridge testing and analysis, however, it is safe to estimate this cost as \$10k-\$15k, depending on project specifics. The same work can be also contracted to outside firms, in which case the cost per bridge would probably be in the \$30k to \$45k range (estimated price for 2003).

Based on this information, is bridge testing worth the effort and the investment by any DOT? Not for all the bridges, but if severe postings, expensive bridge repairs or bridge replacements can be delayed or avoided, it is clear that a comprehensive bridge testing program benefits the travelers both short term and long term. This project provided only a pilot study on this topic. In order to develop a detailed test and analysis, and to field test the entire procedure, further studies are required.

9. SUMMARY AND CONCLUSIONS

This project involved the analysis and testing of seven bridges in Division 10. The list of bridges included two RCDG bridges, three steel girder bridges with concrete deck, one steel girder bridge with GFRP deck, and finally, one steel girder bridge with timber deck. The analysis included simple spreadsheet programs, NCDOT and AASHTOWare bridge rating softwares, finite element analysis, and simple calculations.

The testing phase of the project involved the instrumentation (using up to 102 instruments, and two separate DAQ systems) and the load testing of these bridges using static, slow and dynamic load cases. Two types of trucks were used in the experimental phase, a 9 cy concrete mixer, and a standard NCDOT tandem dump truck, loaded to generate stresses in the structures close to the operating rating load.

As it was mentioned earlier, only representative experimental data and analytical results are provided in this report. More detailed information can be found in the theses and project report of the co-author graduate research assistants involved in this project.

After analyzing and testing seven bridges, several conclusions can be drawn.

9.1 General Conclusions

- Considering the factors influencing the behavior of (especially older) bridges, it is difficult to estimate their behavior. These factors included girder/deck composite action, impact and distribution factors, material strength, contribution of non-structural elements, girder end conditions, etc... Based on the load tests, significant capacity reserves were

found in every bridge, well beyond the analytical predictions.

- Properly planned load testing can provide valuable information on the true capacity of a bridge for a service load test desired. However, some of the factors mentioned before, are dependent of the load level. They include: (1) the composite action based only on friction and bond; (2) the condition of the approach slabs as a contributor to the impact factors; (3) the connections between structural and non-structural elements; etc...
- Based on the last three bridges tested, it was concluded, that a relatively simple instrumentation setup can be effective in the load rating of bridges through testing. As it was mentioned earlier, a second data acquisition system was used in the second phase of this project, recording test data from six independent strain transducers. This setup was successful in capturing valuable bridge-specific conditions. These findings were also confirmed by the more elaborate DAQ and instrumentation system.
- Sixteen displacement transducers were used at each bridge; however, the data recorded by these instruments was not as useful as anticipated. At the most, they proved the existence of girder end conditions, and indicated the stiffness of the superstructure.
- The applicability and the reliability of the results from the strain transducers far exceeded the expectations. Properly mounted, these instruments were superior to the strain gages and LVDT-s considered in this project.
- After several bridge tests, it was concluded that the static loading sequences did not provide results that complimented the data from the slow moving loading trucks. Therefore, the time consuming static loadings were eliminated from the rest of the bridge tests, reducing the bridge preparation and closure time.

9.2 Concrete Girder Bridges

- Current analysis procedures significantly underestimate the strength and stiffness of reinforced concrete deck girder (RCDG) bridges.
- The concrete compressive strength in the RCDG bridges tested was much higher than the initially assumed values.
- Both the assumed transverse distribution factors and the impact factors were off, as compared to the test values.
- Concrete railings and curbs significantly contribute to the strength and stiffness of these bridges, especially to the exterior girders.
- Besides minor hairline cracks, these bridges were in relatively good shape.
- It is very difficult to predict the girder end conditions (they depend on the condition of the deck, the joint, etc...).

9.3 Steel Girder Bridges

- The predicted (AASHTO) distribution factors were surprisingly close to the test results.
- Virtually no impact factors were experienced during the dynamic loading. This was the case even for the bridge with poor approach slab and deck joint conditions.
- Composite action between steel girders and concrete deck was experienced for most of the cases. However, it is difficult to predict its effectiveness at higher loads.
- It was difficult to quantify the effects of girder bearing plate and diaphragm conditions. These certainly affected the transverse load distribution.

9.4 GFRP Deck Bridge

- Since this was a relatively new bridge system (the first in North Carolina), this bridge received a lot of the attention, both experimentally and analytically.
- The results confirmed full composite action between the steel girders and the GFRP deck.
- The recorded strain levels on the GFRP deck were significantly lower than the allowable values recommended by the manufacturer.
- The semi-integral end walls provided a certain level of end fixities for the steel girders.

9.5 Crutch Bent Repair

- Although this is a temporary safety measure, this relatively simple repair method significantly improved the capacity and stiffness of one of the spans for the steel girder timber deck bridge.
- As expected, the timber deck did not provide any composite action with the steel girders.

10. RECOMMENDATIONS AND IMPLEMENTATION

Based on the finding of this project, several recommendations are being made. Each of these recommendations is accompanied by a suggested method of implementation, and the resources required for achieving them.

- Based on the seven bridges analyzed and tested (the authors do not suggest that the number of bridges tested allows for a full statistical evaluation – the pool of bridges considered only reflects representative bridges), the following recommendations can be made on bridge analysis and rating:

- Ø Reconsider the use of PercEffective in the NCDOT bridge rating software, especially for concrete girder bridges with only minor hairline cracks in tension zone.

- Ø Consider reducing or eliminating the impact factor for existing bridges with “healthy” approach slabs and deck joints.

- Ø Consider the use of UNC Charlotte’s spreadsheet program (properly tested) to allow the analysis to include simple span girder end restraint. This could be as high as 30% for semi-integral and integral end walls.

- Ø Consider the composite action (up to a certain horizontal shear level) between steel girders and concrete decks for older bridges with certain construction details.

- Expand the bridge files to include non-destructive tests and damage extent and propagation (cracks, spallings, and corrosion signs). More accurate material properties and reinforcing steel details are needed, at least once for each bridge with unknown or unclear design and/or construction data.

Ø Implementation: Develop an NDT equipment list, equip and train the bridge inspection crew to use the basic NDT kit for concrete and steel material evaluation.

- Use bridge load testing to verify transverse load distribution, impact factor, and member strain levels. This will be particularly useful for posted bridges, or when issuing special permits for a particular structure.

Ø Implementation: Develop a detailed standard bridge loading protocol. Train and equip a bridge maintenance crew to perform relatively simple bridge tests, using only a handful of instruments strategically located and applied in a short period of time, and tested with well planned loading paths and a standard truck. The recorded test information can be then forwarded to the analysis team for evaluation.

- Enforce bridge posting more effectively.

Ø Implementation: move the posting sign (or provide additional ones) further away from the posted bridge. During this project, in several occasions, trucks with significantly larger loads than the allowed were traveling over the posted bridge. Special sensors could be embedded in the road surface to warn the driver of large loads of possible detours and bridge postings.

- As the technology becomes more available and affordable, in the future remote sensing could significantly increase the interaction between the inspection and analysis (load rating procedures). This investment may streamline operations such as evacuation, detour and construction zone management, etc...

- A revised and expanded analysis software, with an upgraded field report to include specific information on materials and details, combined with selected testing would enhance the bridge rating procedures allowing for a more accurate assessment.

11. REFERENCES

- AASHTOWare. Pontis Version 4.1 User's Manual. 2001.
- AASHTOWare. Virtis Version 4.1 User's Manual. 2001.
- Advanced Composites Technology Transfer / Bridge Infrastructure Renewal Consortium (2000). "Advanced Composites for Bridge Infrastructure Renewal – Phase II." Final Report. DARPA MDA972-94-3-0030 Volume IV Task 16 – Modular Composite Bridge. Defense Advanced Research Projects Agency.
- Aktan, A.E., Farhey, D.N., Helmicki, A.J., Brown, D.L., Hunt, V.J., Lee, K-H, and Levi, A., (1997) "Structural Identification for Condition Assessment: Experimental Arts." Journal of Structural Engineering, ASCE, 123 (12), 1674-1684.
- Aktan, A.E., Catbas, N, Turer, A., and Zhang, Z., (1998) "Structural Identification: Analytical Aspects." Journal of Structural Engineering, ASCE, 124 (7), 817-829.
- Alampalli, S. and Kunin, J. (2001). "Load Testing of An FRP Bridge Deck On A Truss Bridge." Final Report, FHWA/NY/SR-01/137.
- American Association of State Highway and Transportation Officials. LRFD Bridge Design Specifications – US Units. Washington DC. 2001.
- American Association of State Highway and Transportation Officials. Manual for Condition Evaluation of Bridges, Second Edition (revised by 1995 to 2000 Interim Revisions). Washington DC. 2000.
- American Association of State Highway and Transportation Officials. Standard Specifications for Highway Bridges, Sixteenth Edition. Washington DC. 1998.
- Bakht, B., and Jaeger, L.G. "Bridge Testing – A Surprise Every Time." Journal of Structural Engineering. Volume 116 Number 5. May 1990.
- Bridge Diagnostic, Inc. www.bridgetest.com. Feb 2003.
- Burdette, E.G., and Goodpasture, D.W. Correlation of Bridge Load Capacity Estimates with Test Data, NCHRP Report 306, National Research Council. Washington DC. June 1988.

Galambos, T.V, Hajjar, J.H., Huang, W-S, Pulver, B.E., Leon, R.T., and Rudie, B.J. (2000). “Comparison of Measured and Computed Stresses in a Steel Curved Girder Bridge.” *Journal of Bridge Engineering*, ASCE, 5(3), 191-199.

Gergely, J., Pantelides, C.P., and Reaveley, L.D., (2000) “Shear Strengthening of R/C T-joints Using CFRP Composites.” *Journal of Composites for Construction*, ASCE, 4 (2).

Moses F. and Verma D. Load Capacity Evaluation of Existing Bridges: NCHRP Report 301. National Research Council. Washington DC. December 1987.

National Bridge Inventory. www.nationalbridgeinventory.com. Jan 2003.
North Carolina Department of Transportation. Memorandum: Using Reinforcing Steel and Concrete Stress From the Plans. January 21, 2000.

National Cooperative Highway Research Program: Manual for Bridge Rating Through Load Testing. Research Results Digest number 234. November 1998.

Nowak, A. and Kim, S. (1998). “Development of a Guide for Evaluation of Existing Bridges Part I.” Michigan Department of Transportation, Project 97-0245 DIR.

Pantelides, C.P., and Gergely, J. (2002) “Carbon Fiber Reinforced Polymer Seismic Retrofit of RC Bridge Bent: Design and In Situ Validation,” *Journal of Composites for Construction*, ASCE, 6(1) – Received the 2002 BEST APPLIED RESEARCH PAPER AWARD from the *Journal of Composites for Construction*, ASCE.

Sartwell D, Heins CP, and Looney CTG. Analytical and Experimental Behavior of a Simple-Span Girder Bridge. Transportation Research Record Number 295. University of Maryland at College Park. 1976.

Schiff, S. and Philbrick Jr., T. (1999). “Load Testing for Assessment and Rating of Highway Bridges: Phase I – Review of Current and Experimental Technologies and Practices.” Final Report, SCDOT Research Project No. 588.

Stallings, JM and Yoo, CH. “Tests and Ratings of Short Span Steel Bridges.” *Journal of Structural Engineering*. ASCE Volume 119 Number 7. July 1993.

United States Department of Transportation. Recording and Coding Guide for the Structure Inventory and Appraisal of the Nation’s Bridges. Report Number FHWA-PD-96-001. 1995.

APPENDIX A

UNC CHARLOTTE BRIDGE ANALYSIS SOFTWARE

-INSTRUCTION MANUAL-

A.1 Introduction

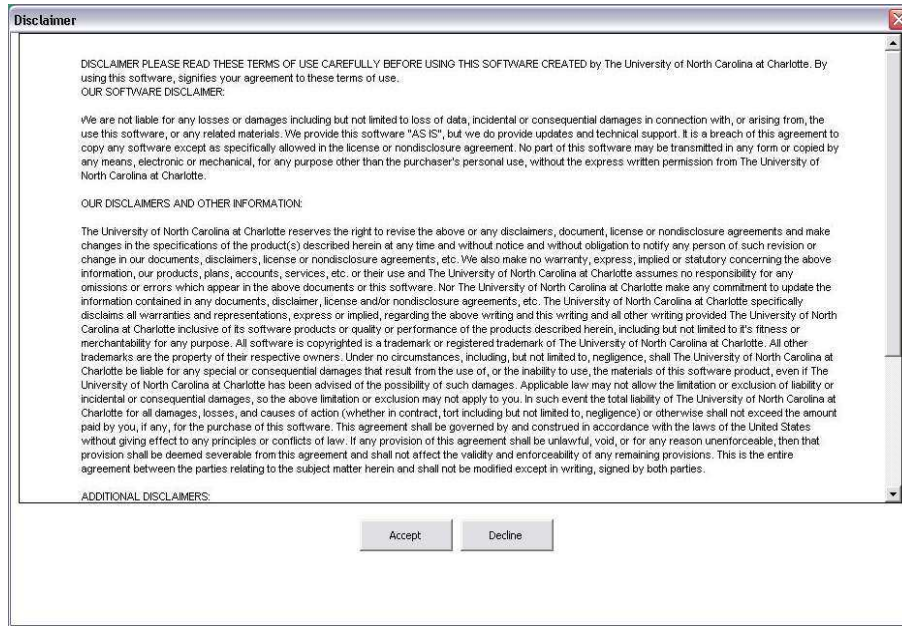
This Bridge Analysis Spreadsheet was specifically designed to analyze North Carolina Department of Transportation (NCDOT) Bridges 12-0271 and 12-0227. The spreadsheet allowed for quick evaluation of the current NCDOT Load Rating software and in-field test results. This spreadsheet was also used to compare a few NCDOT bridges with their respective NCDOT load ratings and test results. This spreadsheet is limited to the bridge types of reinforced concrete deck girder (RCDG) and steel girder with concrete deck bridges that are simply supported.

Although this spreadsheet was reviewed, tested, and verified with the current NCDOT load rating software, some errors in calculations and in software programming may have been overlooked. For this reason, this spreadsheet should not be used for load rating bridges until extensive comparative studies have been performed. It is designed to be used as a supplement to compare various factors that influence the load rating and posting of bridges.

This spreadsheet has been protected to keep inadvertent changes from being made to the spreadsheet. Please note that the screen images shown within this report may vary slightly from the actual screen image that you see in the version you are using.

A.2 Start Up

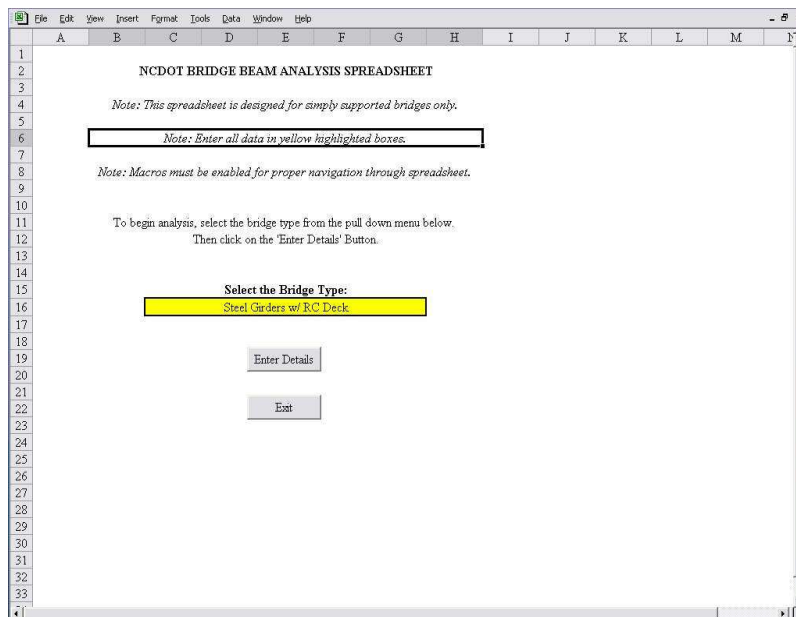
1. Locate the file “Bridge Analysis v1.4.xls” and open.
2. This spreadsheet utilizes macros that must be enabled for proper function. Therefore the macros must be enabled.
3. The spreadsheet opens up to a disclaimer that must be accepted to move on. Declining the terms of the disclaimer will lead to Excel shutting down. The ‘Disclaimer’ screen can be seen in the following figure.



4. After accepting the disclaimer terms, the 'Main Menu' screen appears.

A.3 Bridge Type Selection

1. Select the bridge type, either RCDG or Steel Girders w/ Concrete Deck, from the yellow cell which is a pull down list. The 'Main Menu' screen is seen below.



2. You will notice several key notes on this page that attention must be paid to.
 - a. "This spreadsheet is designed for simply supported bridges only." This states that the analysis of continuous beams cannot be performed by this spreadsheet at the present level of development.

b. “Enter all details in yellow highlighted boxes.”

Information can only be entered in yellow cells. This includes selections made from pull-down lists.

c. “Macros must be enabled for proper navigation through spreadsheet.”

3. After selecting the bridge type desired for analysis, hit the ‘Enter Details’ button.
4. The appropriate bridge details page opens.
5. Pushing the ‘Exit’ button will shut down Excel.

A.4 RCDG Bridge Details

1. Known information concerning the basic design of the bridge is to be entered on this page. Enter the desired information in the appropriate yellow boxes. A view of the ‘RCDG Bridge Details’ page can be seen below.

2. White boxes indicate information that is calculated for the user. This page calculates the clear span and beam section properties that include area, moment of inertia and the section modulus.
3. Several checks are also done which include depth ratios, effective length, and the term D_e for the calculation of LRFD distribution factors.
4. There is a pull-down list to choose which span to evaluate the interior girder.
5. There are also pull-down lists for entering in the ‘Design Load’, ‘Inv. Rating’, and ‘Opr. Rating’.
6. Navigation buttons located at the top of the screen allow the user to move to next desired page. These include: returning back to the ‘Main Menu’, ‘View Moments’, ‘View M_n ’, ‘View Shears’, ‘View DFs’, ‘Cracked Section Analysis’, ‘Stress & Strains’, and ‘Load Rating’. Clicking on any of these buttons will take the user to the selected page.
7. Another navigation button is located below these for entering rebar details.

A.5 Girder Rebar Details

1. Known information concerning the rebar layout of the interior girder is to be entered on this page. Enter the yield strength, f_y , of the steel.
2. Enter the desired information concerning the rebar in the yellow boxes. White boxes indicate information that is calculated for the user. This page checks the minimum area of steel required.
3. The user can either enter the area of steel, or enter the rebar details up to 6 bars in each layer and up to 6 layers. This choice can be made by selecting the appropriate choice from the pull-down list under 'Select the method to determine A_s '. A view of the 'Rebar Details' page with the 'Calculated' method chosen is shown below.

Rebar Details

Checks: min A_s 2.601, 200-oh 3.927. Note: Enter all data in yellow highlighted boxes.

Distance from bottom of beam to center of rebar: 3 in, f_y : 30 ksi

Measurement of Cover to Bottom of Rebar: 2.65 in

Number of Rebar Layers: 3 (1 thru 3). Select the method to determine A_s : Calculated (18.73 in²)

Layer	# of Rebar in Layer (top to bottom)	Spacing between rebar (in)	Are the rebars in this layer the same? (Y or N)	Area of Steel in Layer (in ²)	Dia. Of max rebar (in)	All Rebars (in ²)
Layer 1	4	3	Y	6.24204	1.41	All Rebars 8 #1
Layer 2	4	3	Y	6.24204	1.41	All Rebars 8 #1
Layer 3	4	3	Y	6.24204	1.41	All Rebars 8 #1

Calculated Total Area of Steel: 18.73 in²

Distance from bottom to NA of Steel: 6 in

Select the effective depth to be used: effective depth excluding CWS, d. effective depth, d: 33 in

4. With the 'Calculated' method chosen, the user can enter the number of rebar layers. One to six layers can be evaluated with this spreadsheet. The table below this will be altered according to the number entered.
5. Enter the distance, in inches, representing the cover from center of rebar to bottom of beam.
6. For each layer, specify how many individual rebars are located in this layer, up to 6.
7. Enter, in inches, the distance from one layer to the next.
8. Then specify, using 'Y' or 'N', whether or not the rebars in the layer are of the same type. If yes, select the rebar size from the pull-down list in the box next to 'All Rebars'. If no, then enter the appropriate rebar size in the appropriate rebar location. This is based on the number of rebars in the layer entered by user.
9. The area of steel and the distance from the bottom of the beam to the neutral axis of the steel is calculated by the spreadsheet.

File Edit View Insert Format Tools Data Window Help

1 RCDG Bridge
2 12-0271
3
4 Rebar Details

6 Checks: min As 2.601
7 200-in 3.327

8 Note: Enter all data in yellow highlighted boxes.

9
10
11 Distance from bottom of beam to center of rebar: 3 in f_y 30 ksi

12
13 Measurement of Cover to Bottom of Rebar: 2.385 in

14
15 Number of Rebar Layers: 3 (1 thru 6) Select the method to determine As: Calculated 15.73 in²

	# of Rebar in Layer (up to 6)	Spacing between next layer (in)	Are the rebars in this layer the same? (Y or N)	Area of Steel in Layer (in ²)	Dia. Or max (rebar (in))	Rebar #1 (in)	Rebar #2 (in)	Rebar #3 (in)	Rebar #4 (in)
Layer 1	4	0	N	6.242634	141	All Rebars			
Layer 2	4	0	Y	6.242634	141	All Rebars			
Layer 3	4	0	Y	6.242634	141	All Rebars			

28 Calculated Total Area of Steel: 18.72 in²

29 Distance from bottom to NA of Steel: 0 in

30
31 Select the effective depth to be used: effective depth excluding CWS, d

32
33 effective depth excluding CWS, d: 33 in effective depth, d: 33 in

10. The effective depth chosen from the pull-down list includes: 'effective depth excluding CWS', 'effective depth including CWS', and 'User Defined'.
11. A view of the 'Rebar Details' page with the 'User Defined' method chosen is shown below.

File Edit View Insert Format Tools Data Window Help

1 RCDG Bridge
2 12-0271
3
4 Rebar Details

6 Checks: min As 2.601
7 200-in 3.327

8 Note: Enter all data in yellow highlighted boxes.

9
10
11 f_y 30 ksi

12
13 Select the method to determine As: User Defined 15.97 in²

14
15 User Defined Area of Steel: 15.97 in²

28 Enter the User Defined effective depth below:

29 effective depth, d: 33 in

12. Enter the user defined area of steel in the yellow box.
13. Using the user defined area of steel requires that the user defines the effective depth. Enter the effective depth in the appropriate yellow box.
14. Whether using the 'Calculated' method or the 'User Defined' method, navigation buttons are seen at the top of the screen. These will take return you to the 'Main Menu' or 'Return to Bridge Details'.

A.6 Steel Bridge Details

1. Known information concerning the basic design of the bridge is to be entered on this page. Enter the desired information in the appropriate yellow boxes. A view of the 'Steel Bridge Details' page can be seen below.

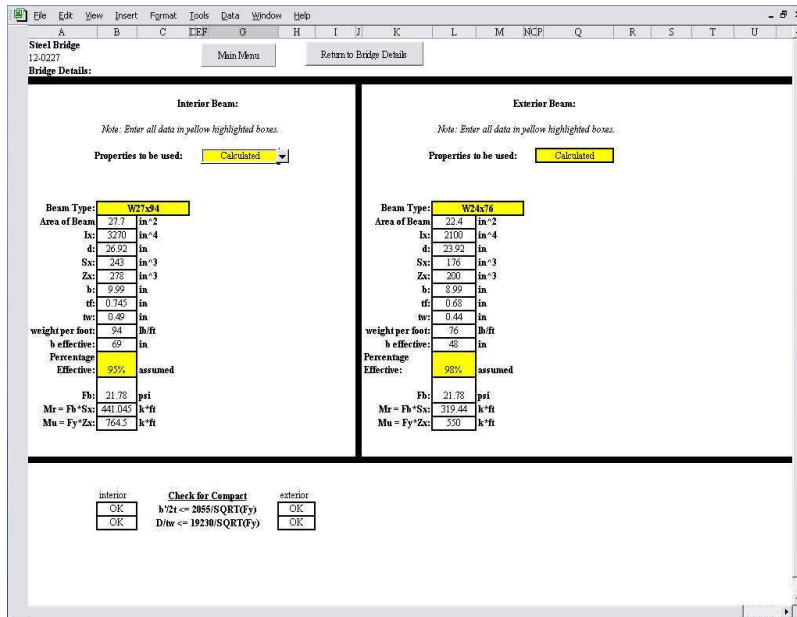
Note: Enter all data in yellow highlighted boxes.

Bridge #:	12-0227	F _y of Deck:	500	psi
Date Built:	1991	Unit weight of Concrete:	150	lb/ft ³
# of Spans:	5	Skew Angle:	0	degrees
Span Length:	40	Asphalt Wearing Surface:	0	in
Clear Span:	38.33	Concrete Wearing Surface:	0	in
# of Girders:	4	Fillets:	0	in
Beam Spacing:	7.7	Slab thickness:	5.75	in
Overhang:	0.8			
Deck (out-to-out):	22			
Between Rails:	22			
Clear roadway:	22			
# of Lanes:	2			
Lane width:	12			
Curb width:	0			
Sidewalk width:	0			
Rating Type:	Mod			
Weight of Rails:	25			
		F _y of Beam:	52	ksi
		distance from web to curb face (LRFD Sec. 4.6.2.2.2d)	0.5	ft
		Enter the value as "+" if curb is outboard of the web and "-" if inboard of the web		
Design Load:	H 18			
Inv Rating:	H5 10	Current SY Posting:	24	tons
Opr Rating:	H6 10	Current TTST Posting:	28	tons

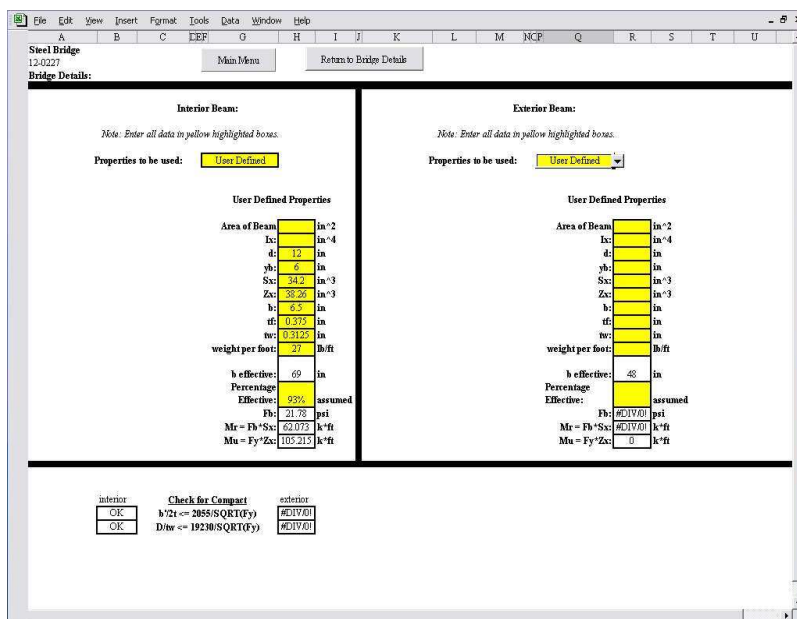
2. White boxes indicate information that is calculated for the user. This page determines the factor D_e to be used in the LRFD distribution factor calculations.
3. There is a pull-down list to choose at which span to evaluate the interior girder.
4. There are also pull-down lists for entering the: 'Design Load', 'Inv. Rating', and 'Opr. Rating'.
5. Navigation buttons located at the top of the screen allow the user to move to the next desired page. These include: returning back to the 'Main Menu', 'View Moments', 'View Shears', 'View DFs', 'Stress & Strains', and 'Load Rating'. Clicking on any of these buttons will take the user to the selected page.
6. Another navigation button is located below these for entering the steel beam properties.

A.7 Steel Beam Details

1. Known information concerning both the interior and exterior girders needs to be entered on this page.
2. Enter the desired information concerning the steel in the yellow boxes. White boxes indicate information that is calculated for the user. This page checks for beam compactness.
3. The user can either enter the steel beam properties or select the appropriate beam from the pull-down list.
4. For both the interior and exterior girders, the user can select the appropriate choice from the pull-down list under 'Properties to be used.' A view of the 'Steel Beam Details' page with the 'Calculated' method selected is shown below.



5. With the 'Calculated' method selected, the user can select the beam type from the pull-down list. This will automatically enter all other information except for the percent effective which is required to be entered by the user.
6. A view of the 'Steel Beam Details' page with the 'User Defined' method selected is shown below.
7. Enter all information in the yellow boxes.
8. Whether using the 'Calculated' method or the 'User Defined' method, navigation buttons are seen at the top of the screen. These will return the user to the 'Main Menu' or 'Return to Bridge Details'.



A.8 Moments

1. The 'Moments' page determines the dead, live, and impact moments for the selected bridge type. The desired bridge type will be shown in the upper left corner of the screen. The 'Moments' screen can be seen below.

RCDD Bridge

Loads For Simple Beams

Beam Connections: **Pinned - Pinned**

Note: Enter all data in yellow highlighted boxes.

Loading Scheme: **One Lane Loading** Controlling LL for a Clear Span of **44** ft

H Truck type: **HS** of Trailer Length of **M'**
 Live Load: **HS** Truck type: **HS** use Tandem-1 for RCDD and Tandem-2 for Steel
 NCDOT type: **-**

	Pinned - Pinned	Partial Fixity	Fixed - Fixed
H Truck Load, k/ft			
HS Truck Load, k/ft	390.692	328.181	355.891
NCDOT Truck, k/ft			
H Lane Load, k/ft			0.324
HS Lane Load, k/ft	284.680	133.856	3.132
NCDOT Lane, k/ft			

Using Design Aid: Truck: 390.700 0.000

Calculated Controlling LL: Truck: 390.692 Checks with V & M Diagram

Moment LL: 390.700 k-ft

Impact Load: Impact Formula: $I = 50/(L+125)$ **0.25** (<=30%) Use I: **0.955**

Is approach grade level enough to ignore impact? (Y or N) **N** Moment I: 18.932 k-ft

Dead Load:

	Interior	Exterior
Non-Complete DL: Slab	0.000 k/ft	0.778 k/ft
Stiffness (10% of Beam)	0.001 k/ft	0.001 k/ft
Beam	0.014 k/ft	0.014 k/ft
Filets	0.007 k/ft	0.008 k/ft
Utilities	0.000 k/ft	0.000 k/ft
Diaphragms	0.224 k/ft	0.197 k/ft
Concrete Overlay	0.200 k/ft	0.204 k/ft
Sum	2.305 k/ft	1.972 k/ft

	Interior	Exterior
Composite DL: Railings	0.133 k/ft	0.133 k/ft
Asphalt Overlay	0.140 k/ft	0.140 k/ft
Sum	0.273 k/ft	0.273 k/ft

Total DL: 2.458 k/ft 2.245 k/ft

User Defined DL: 2.43 k/ft 0.204 k/ft

Moment DL:

	Interior	Exterior
Moment DL, k-ft	588.060	588.060

Interior DL to be Used: **User Defined** 2.43 k/ft
 Exterior DL to be Used: **User Defined** 0.204 k/ft

	Interior	Exterior
Pinned - Pinned	588.060	588.060
Partial Fixity	490.050	392.040
Fixed - Fixed	392.040	95.348
Sum	79.457	83.565

Moment DL: 95.348 k-ft

Interior Moment DL: 588.060 k-ft

2. Enter the desired information in the yellow boxes. White boxes indicate information that is calculated for the user.
3. Selecting the proper 'Beam Connections', determines the type of moment calculated. This is either 'Pinned - Pinned', 'Partial Fixity', or 'Fixed - Fixed'. This selection is done from a pull-down list.
4. When the 'Partial Fixity' 'Beam Connection' is selected, the user is prompted to enter the percent of fixity assumed. Enter the percentage in the appropriate box. A view of the 'Moments' screen with 'Partial Fixity' selected can be seen below.
5. The 'Loading Scheme' is a pull-down list that allows the user to select: 'One Lane Loading', 'Two Lane, Opposite', or 'One Lane, Two Trucks'. It is recommended to leave this option as 'One Lane Loading' to ensure proper calculations throughout the spreadsheet.
6. The Live Load is determined based on the selected vehicle type. This is done from three pull-down lists. The lists coincide with the vehicle types: H, HS, and NCDOT. Only vehicle is to be selected at a time. To make a selection, choose the desired vehicle from the appropriate list. Then select the '-' from the other two lists.
7. The calculated Live Load moment is compared to moments from standard design aids for select vehicles and also compared to the maximum moment calculated on the 'V & M Diagrams' page.
8. The Impact Load is calculated based on the selected live load moment. The user can select whether or not the impact moment can be ignored due to a smother approach.

File Edit View Insert Format Tools Data Window Help

1 RCDG Bridge

2

3 Loads For Simple Beams

4

5

6 Beam Connections: **Partial Fixity** Enter % of Fixity Assumed: **50.00%**

7

8 Note: Enter all data in yellow highlighted boxes

9

10

11 Loading Scheme: **One Lane Loading** Controlling LL for a Clear Span of: **44** ft

12

13 H Truck type: **HS-20** of Trailer Length of **40** ft

14 Live Load: (Sec 3.7) **HS-20** use Tandem-1 for RCDG and Tandem-2 for Steel

15 NCDOT type: **HS-20**

16

17

18

	Pinned - Pinned	Fixity	Fixed - Fixed
H Truck Load, k/ft			
HS Truck Load, k/ft	390.692	326.161	265.691
NCDOT Truck, k/ft			
H Lane Load, k/ft			
HS Lane Load, k/ft	284.660	193.086	-3.192
NCDOT Lane, k/ft			

Using Design Aid: **0** **0.000** **0.000**

Calculated Controlling LL: **Truck 326.161**

Moment LL: **326.161 k/ft**

19

20

21

22

23

24

25

26

27

28 Impact Load: Impact Formula: $I = 50/(L+125)$ **0.258** (<=30%) Use I: **25.85%**

29 (Sec 3.8) Is approach grade level enough to ignore impact? (Y or N) **N** Moment I: **97.695 k/ft**

30

31

32

33

34 Dead Load:

35 (Sec 3.2)

	Interior	Exterior
Non Composite DL:		
Slab:	0.000 k/ft	0.150 k/ft
Stiffness (50% of Beam):	0.061 k/ft	0.091 k/ft
Beam:	0.034 k/ft	0.034 k/ft
Files:	0.077 k/ft	0.008 k/ft
Utilities:	0.000 k/ft	0.050 k/ft
Diaphragms:	0.284 k/ft	0.097 k/ft
Concrete Overlay:	0.200 k/ft	0.234 k/ft
Sum:	2.365 k/ft	1.572 k/ft

Interior DL to be Used: **User Defined 2.430 k/ft**

Exterior DL to be Used: **User Defined 0.204 k/ft**

	Interior	Exterior
Composite DL:		
Railings:	0.133 k/ft	0.133 k/ft
Asphalt Overlay:	0.140 k/ft	0.140 k/ft
Sum:	0.273 k/ft	0.273 k/ft
Total DL:	2.458 k/ft	2.245 k/ft
User Defined DL:	2.43 k/ft	0.204 k/ft

Moment DL: **Exterior 73.467 k/ft**

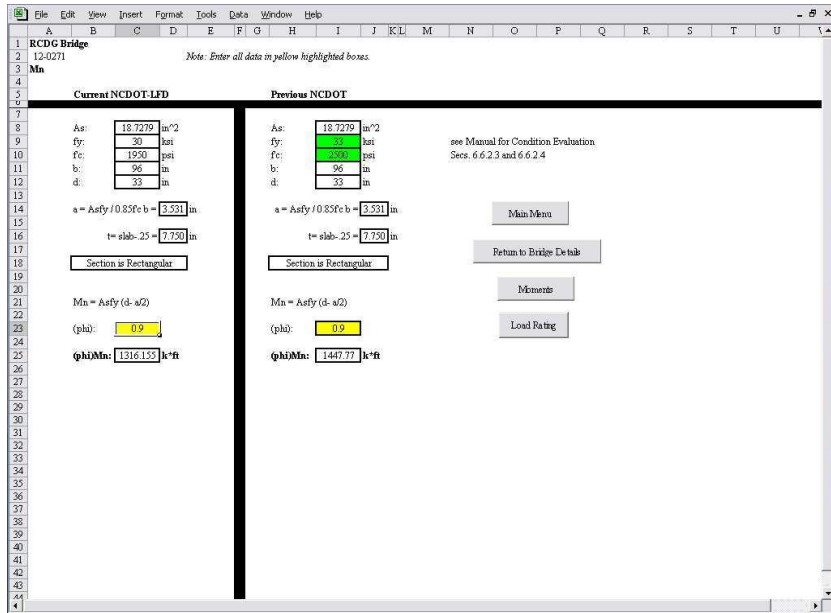
Moment DL: **Interior 490.959 k/ft**

	Interior	Exterior
Pinned - Pinned		
Partial Fixity		
Fixed - Fixed		
Moment DL, k/ft	598.060	490.050
392.040	95.348	79.457
63.565		

- The Dead Load can be either calculated or defined by the user for the interior or exterior girders. If the user defines the dead load, the uniform dead load in kips per foot is to be entered in the appropriate yellow box. If the user decides to have the spreadsheet calculate the dead loads, the user must insure that all bridge details have been properly entered at the appropriate places.
- Navigation buttons located at the top of the screen allow the user to move to next desired page. These include: returning back to the 'Main Menu', 'Return to Bridge Details', 'View Shears', 'View DFs', 'Stress & Strains', 'V & M Diagrams', and 'Load Rating'. Clicking on any of these buttons will take the user to the selected page.

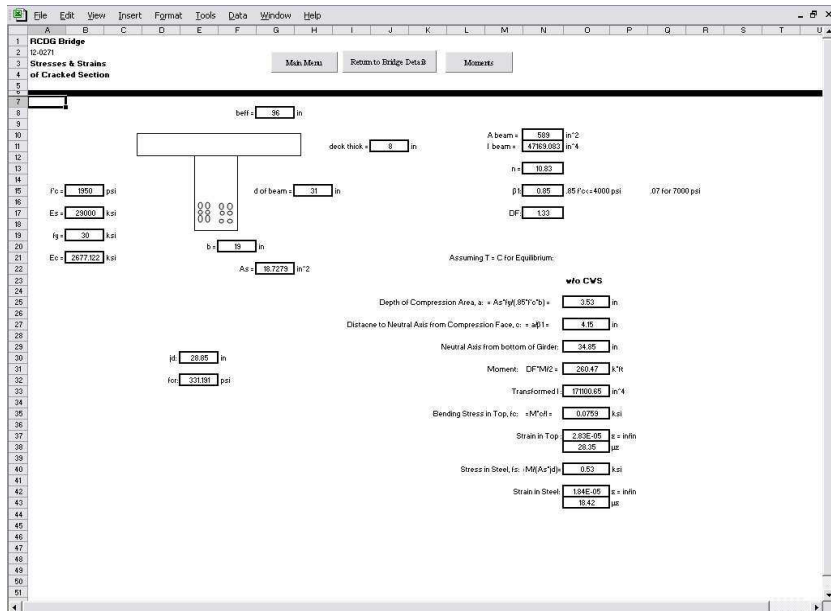
A.8 RCDG M_n

- The nominal resisting moment, ' M_n ' page, for the RCDG Bridge is based on current NCDOT M_n Load Factor Design (LFD) calculations.
- The only user information required on this page is the phi (Φ). Enter this value in the yellow box.
- If the bridge number is 12-0271, then the spreadsheet will display the 'Previous NCDOT' M_n calculation, seen on the right, using 33 ksi and 2,500 psi for f_y and f'_c , respectively.
- Navigation buttons located to the right of the screen allow the user to move to next desired page. These include: returning back to the 'Main Menu', 'Return to Bridge Details', 'Moments', and 'Load Rating'. Clicking on any of these buttons will take the user to the selected page.



A.9 RCDG Cracked Section Analysis

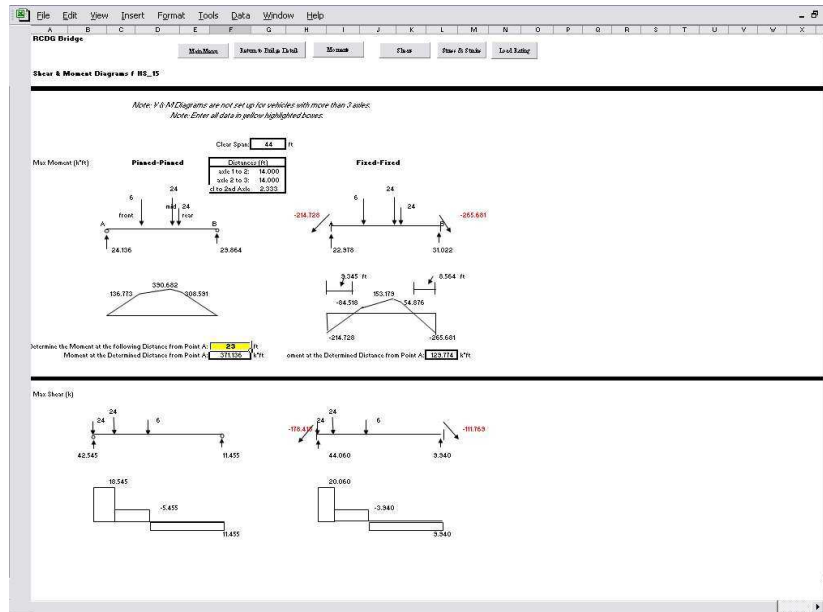
1. The 'Cracked Section Analysis' of the RCDG Bridge is a completely calculated page. No user inputs are required for this page. This page can be seen below.



2. Navigation buttons located to the right of the screen allow the user to move to next desired page. These include: returning back to the 'Main Menu', 'Return to Bridge Details', and 'Moments'. Clicking on any of these buttons will take the user to the selected page.

A.10 V & M Diagrams

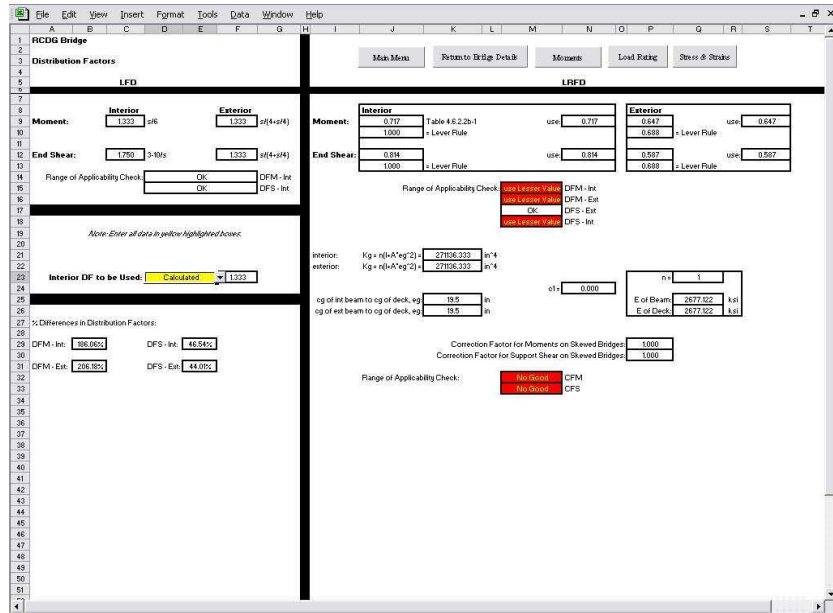
1. The 'V & M Diagrams' page represents the maximum shear and moment diagrams for both 'Pinned – Pinned' and 'Fixed – Fixed' 'Beam Connections' for the selected live load vehicle. The desired bridge type will be shown in the upper left corner of the screen. The 'V & M Diagram' screen can be seen below.



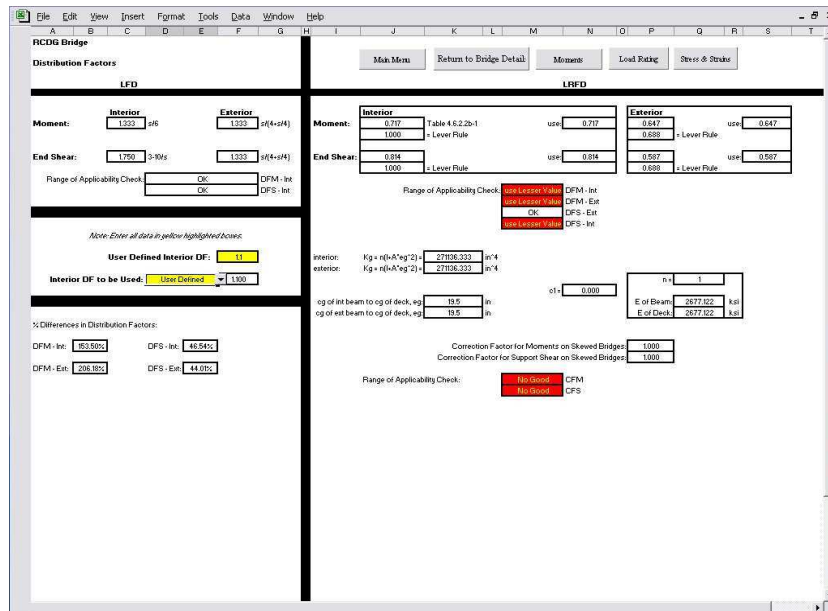
2. The shear and moment diagrams are set up to be calculated for 2 and 3 axle vehicles only.
3. The user can input a distance, in feet, from a predetermined point A, and verify the calculated maximum moment at that point.
4. Navigation buttons located to the right of the screen allow the user to move to next desired page. These include: returning back to the 'Main Menu', 'Return to Bridge Details', 'Moments', 'Shears', 'Stress & Strains', and 'Load Rating'. Clicking on any of these buttons will take the user to the selected page.

A.11 Distribution Factors

1. The 'DFs' page calculates the LFD and LRFD distribution factors for both interior and exterior girders for the selected bridge type. The desired bridge type will be shown in the upper left corner of the screen. The 'DFs' screen with the 'Calculated' interior DF to be used selected can be seen below.
2. Enter the desired information in the yellow boxes. White boxes indicate information that is calculated for the user.
3. This page calculates the distribution factors and checks the range of applicability.
4. This page only allows the user to select whether the distribution factor for the interior girder will be calculated, or user defined. This selected distribution factor will be used throughout all the calculation under the LFD heading.



5. If the user selects the 'User Defined' interior distribution factor, then the user will be prompted to enter the desired value. The 'DFs' screen with the 'User Defined' interior DF to be used selected can be seen below.



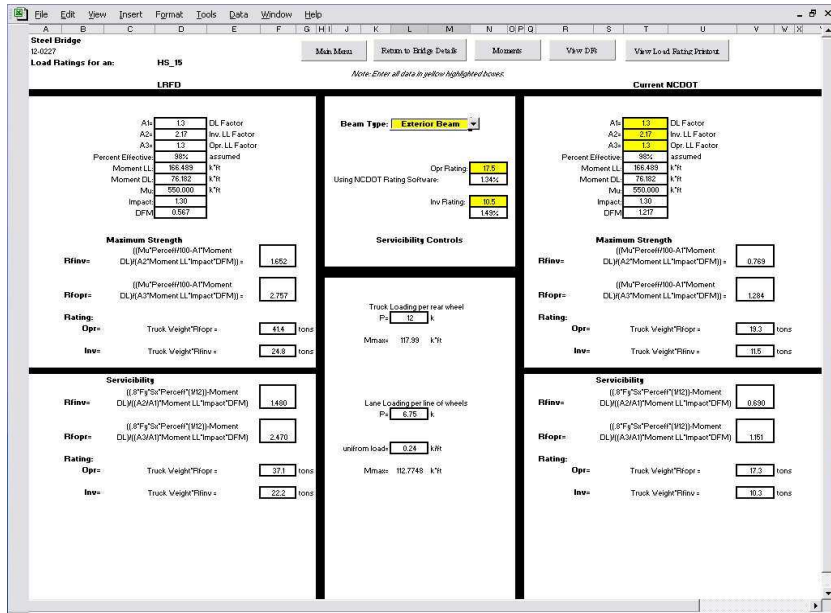
6. To ensure proper calculation of the LRFD distribution factors for the steel bridge, the user must make sure to enter details on both the interior and exterior beams.
7. Navigation buttons located to the right of the screen allow the user to move to the next desired page. These include: returning back to the 'Main Menu', 'Return to Bridge Details', 'Moments', 'Stress & Strains', and 'Load Rating'. Clicking on any of these buttons will take the user to the selected page.

A.12 Load Rating

1. The Load Rating for each type of bridges follows current NCDOT procedures.
2. The user can input Operating and Inventory Ratings that were determined using the current NCDOT software to acquire a percent difference. The user can adjust the load rating factors A1, A2, and A3 as necessary. These inputs are all in yellow boxes.
3. The Load Rating for the RCDG can be seen below. It calculates the load rating utilizing the current LFD distribution factors and the LRFD distribution factors.

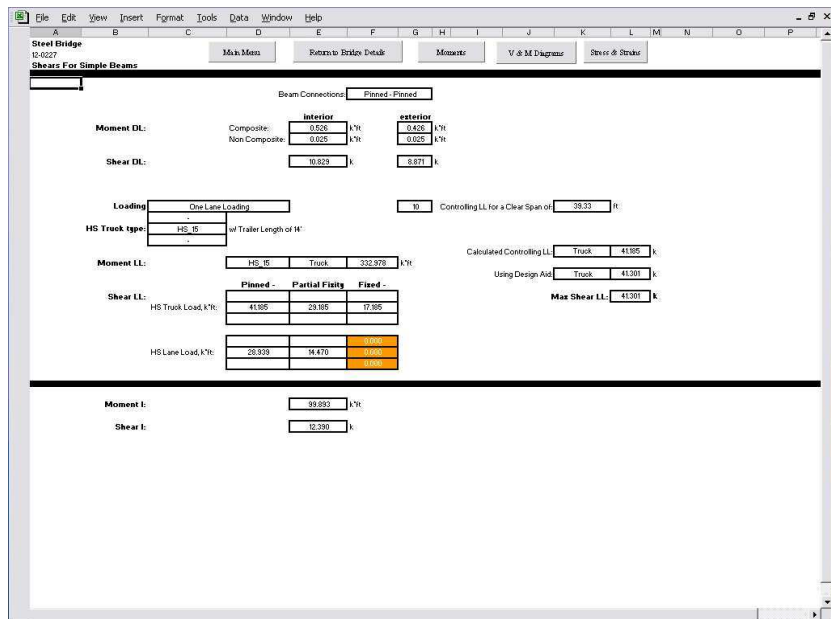
Field	LFRD	Current NCDOT	Previous NCDOT
A1	1.3	1.3	1.3
A2	2.17	2.17	2.17
A3	1.3	1.3	1.3
Percent Effective	85%	85%	85%
Moment LL	380.7 K'ft	380.7 K'ft	380.7 K'ft
Moment DL	588.060 K'ft	588.060 K'ft	588.060 K'ft
Impact	1.25	1.25	1.25
OFM-Inv	1.32	1.32	1.32
RfInv	0.084	0.084	1.12
RfOppr	1.478	1.478	1.856
Oper Rating	30.3 tons	30.3 tons	20.9 tons
Inv Rating	19.5 tons	19.5 tons	32.5 tons
Using NCDOT Rating Software	Oper Rating: 33.5 tons % Diff: -0.66%	Oper Rating: 33.5 tons % Diff: -0.66%	Oper Rating: 33.5 tons % Diff: -0.66%
	Inv Rating: 19.5 tons % Diff: -0.51%	Inv Rating: 19.5 tons % Diff: -0.51%	Inv Rating: 19.5 tons % Diff: -0.51%

4. If the bridge number is 12-0271, then the spreadsheet will display the 'Previous NCDOT' Load Rating calculation, seen on the right, using 33 ksi and 2,500 psi for f_y and f'_c , respectively.
5. Navigation buttons are located to the right of the screen allow the user to move to next desired page. These include returning back to the 'Main Menu', 'Return to Bridge Details', 'Moments', 'View RCDG M_n', 'Load Rating', and 'View Load Rating Printout'. Clicking on any of these buttons will take the user to the selected page.
6. The Load Rating screen for a Steel Bridge seen below, calculates the load rating based on maximum strength and serviceability.
7. For the Load Rating of the Steel Bridge, the user must select from a pull-down list whether the load rating will be performed on the interior or exterior 'Beam Type'.
8. Navigation buttons located to the right of the screen allow the user to move to next desired page. These include: returning back to the 'Main Menu', 'Return to Bridge Details', 'Moments', 'Load Rating', and 'View Load Rating Printout'. Clicking on any of these buttons will take the user to the selected page.



A.13 Shears

1. The 'Shears' page for the Steel Bridge is calculated by the spreadsheet entirely and does not require any user inputs. The 'Shears' page for the Steel Bridge can be seen below.
2. Navigation buttons located to the right of the screen allow the user to move to next desired page. These include returning back to the 'Main Menu', 'Return to Bridge Details', 'Moments', 'V & M Diagrams', and 'Stress & Strains'. Clicking on any of these buttons will take the user to the selected page.



- The 'Shears' page for the RCDG requires user inputs only for calculating the ultimate shear. The user is required to enter the values for phi, the area of steel resisting shear, and the spacing. The 'Shears' page for the RCDG can be seen below.
- Navigation buttons located to the right of the screen allow the user to move to next desired page. These include returning back to the 'Main Menu', 'Return to Bridge Details', 'Moments', 'View RCDG M_n', 'V & M Diagrams', and 'Stress & Strain'. Clicking on any of these buttons will take the user to the selected page.

Beam Connections: Pinned - Pinned

	interior	exterior
Moment DL: Composite	2.892 k/ft	1.972 k/ft
Non Composite	0.273 k/ft	0.273 k/ft
Shear DL:	54.882 k	43.338 k

Loading: One Line Loading, Controlling LL for a Clear Span: 44 ft

HS Truck type: HS-20 of Trailer Length of 11'

	HS-15	Truck	330,700
Moment LL:			k/ft
Calculated Controlling LL:	Truck	42,545	k
Using Design Aid:	Truck	42,500	k

	Pinned - Pinned	Partial Flaty	Fixed - Fixed
Shear LL: HS Truck Load, k/ft:	42,545	30,545	15,545
HS Lane Load, k/ft:	30,060	15,030	7,515

Moment L: 115,532 k/ft **Shear L:** 13,507 k

Ultimate Shear Stress, $v_u + V_u / bw'd$: 0.252 ksi

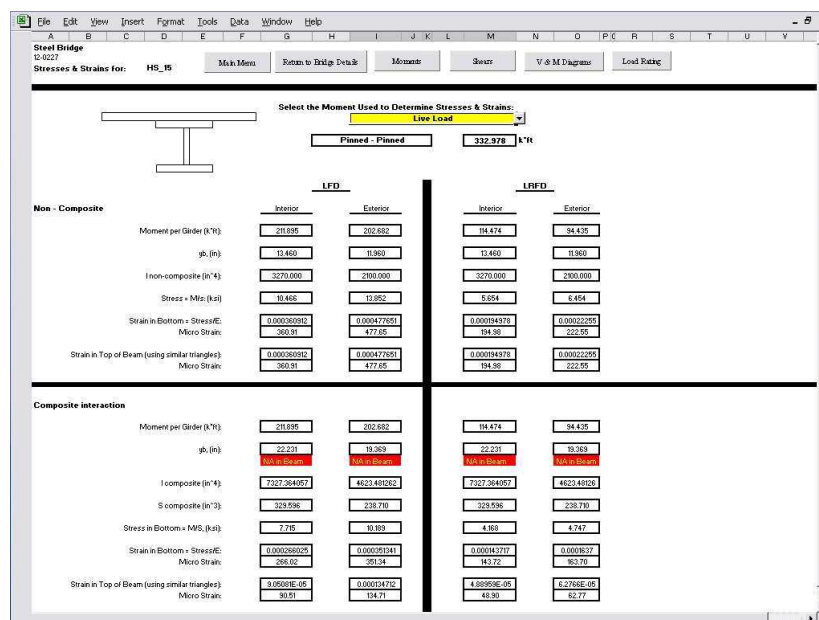
Other Calculations:
 $v_u + 2'sgn(F'_{cr})$: 0.089 ksi
 $\phi \mu f'_{cr}$: 0.254
 $v_u + (A_w / s) \phi f_y$: 0.211 ksi
 $v_u + (A_w / s) \phi f_y$: OK

Input Fields:
 ϕ : 0.85
 A_w : 0.8 in²
 f_y : 30 ksi
 s : 6 in

Note: Enter all data in yellow highlighted boxes.

A.14 Stress & Strains

1. The 'Stress & Strains' page calculates the stresses and strains based on the selected live load moment from the pull-down list in the yellow box.
2. Stresses and strains are determined for non-composite beam action only, or for composite action for the beam and deck for both the Steel Bridge and the RCDG Bridge.
3. For the RCDG Bridge, the stresses and strains due to the composite action between the beam and deck are determined twice. First, the composite action not considering the concrete wearing surface (CWS), and secondly, the composite action that includes the CWS.
4. The 'Stress & Strains' page for the Steel Bridge is shown below.



5. Navigation buttons located to the right of the screen allow the user to move to next desired page. These include returning back to the 'Main Menu', 'Return to Bridge Details', 'Moments', 'V & M Diagrams', 'Stress & Strains', and 'Load Rating'. Clicking on any of these buttons will take the user to the selected page.
6. The 'Stress & Strains' page for the RCDG Bridge is shown below.

PCDDG Bridge
 Stresses & Strains for: HS_15
 Select the Moment Used to Determine Stresses & Strains:
 Live Load
 Pinned - Pinned 330.708 k-ft

percent effective for Mo: 95%
 percent effective for I: 95%

Transformed Area of steel, (in²):
 Current NCDOT: 88.463
 LFRD: 88.463
 Previous NCDOT: 88.443

	Current NCDOT		LFRD		Previous NCDOT	
	Interior	Exterior	Interior	Exterior	Interior	Exterior
Non-Composite						
Moment per Girder (k-ft)	260.467	260.467	138.991	138.330	260.467	260.467
gb (in)	11.227	11.227	11.227	11.227	11.488	11.488
I non-composite (in ⁴)	59829.770	59829.770	59829.770	59829.770	59435.118	59435.118
Reduced I = I _c * eI (in ⁴)	56838.281	56838.281	56838.281	56838.281	56616.663	56616.663
Stress = M/S (ksi)	0.728	0.728	0.791	0.793	0.797	0.797
Strain in Bottom - Stress/E	0.0002791	0.0002791	0.0004614	0.0003881	0.0003290	0.0003246
Micro Strain	279.1	279.1	461.4	388.1	329.0	324.6
Strain in Top of Beam (using similar triangles)	0.00034485	0.00034485	0.000381	0.0003845	0.0003804	0.0003804
Micro Strain	34.87	34.87	38.1	38.45	38.04	38.04
Composite w/o FWS interaction						
Moment per Girder (k-ft)	260.467	260.467	138.991	138.330	260.467	260.467
gb (in)	24.082	24.082	24.082	24.082	24.365	24.365
I composite (in ⁴)	85467.3895	85467.3895	85467.3895	85467.3895	84951.967	84951.967
Reduced I = I _c * eI (in ⁴)	8122.871	8122.871	8122.871	8122.871	8026.368	8026.368
S composite (in ³)	6322.871	6322.871	6322.871	6322.871	6289.577	6289.577
Stress in Bottom - M/S (ksi)	0.510	0.510	0.274	0.247	0.536	0.536
Strain in Bottom - Stress/E	0.0003071	0.0003071	0.0002022	0.0001806	0.0002020	0.0002020
Micro Strain	307.1	307.1	202.2	180.6	202.0	202.0
Strain in Top of Beam (using similar triangles)	5.454E-05	5.454E-05	2.839E-05	2.520E-05	5.454E-05	5.454E-05
Micro Strain	5.45	5.45	2.839	2.52	5.454	5.454
Composite w/ FWS interaction						
Moment per Girder (k-ft)	260.467	260.467	138.991	138.330	260.467	260.467
gb (in)	26.687	26.687	26.687	26.687	26.939	26.939
I composite (in ⁴)	210780.073	210780.073	210780.073	210780.073	20264.233	20264.233
Reduced I = I _c * eI (in ⁴)	200250.563	200250.563	200250.563	200250.563	19259.521	19259.521
S composite (in ³)	7509.209	7509.209	7509.209	7509.209	7480.080	7480.080
Stress in Bottom - M/S (ksi)	0.436	0.436	0.224	0.202	0.437	0.437
Strain in Bottom - Stress/E	0.00015479	0.00015479	5.396E-05	7.540E-05	0.0001533	0.0001533
Micro Strain	154.8	154.8	53.96	75.4	153.3	153.3
Strain in Top of Beam (using similar triangles)	2.5208E-05	2.5208E-05	1.367E-05	1.239E-05	2.462E-05	2.462E-05
Micro Strain	2.52	2.52	136.7	123.9	246.2	246.2

A.15 Printout

1. The 'Printout' page allows the user to print a paper copy of the selected data for comparison with the current NCDOT load rating software. This printout shows the calculated top moments, load ratings, and recommended postings for both LFD and LFRD distribution factors. The 'Printout' page can be seen below.

Next Previous Zoom Print... Setup... Margins Page Break Preview Close Help

UNC CHARLOTTE
NCDOT BRIDGE BEAM ANALYSIS SPREADSHEET

Type of Bridge: RCDG Date: 1/24/2004
 Bridge Number: 12-0271 Number of Spans: 3 Date Built: 1933
 Clear Roadway: 20 ft Controlling Clear Span: 44 ft Analyzed Beam: Interior Beam

Beam Type: Rectangular Beam Spacing: 8 ft Effective Width: 96 in
 Depth: 31 in Icc: 47169 in⁴ Area: 589 in²
 Slab Thickness: 8 in qMx: 12.615 k/ft Scc: 3063 in³
 AWS Thickness: 5 in Steel Yield Stress: 50000 psi Percent Effective: 93.0%
 CWS Thickness: 5 in Beam Pz: 1903 psi Shear Angle: 0
 Deck Pz: 1950 psi Calculated Area of Steel: 89.73 in²
 effective depth excluding CWS, d: 33 in

One Lane Loading Scheme Only

Load Vehicle: HS_15 Moment LL: 338.18 k*ft Beam Connectors: Partial Fixity
 Design Vehicle: H_15 Impact Factor: 29.39% % of Partial Fixity Assumed: 50.0%
 User Defined Dead Load: 2630 lb/ft

Distribution Factors: LFD: 1.333 LRPD: 0.717
 Load Rating: Operating Rating: HS 25.0 Operating Rating: HS 464
 Inventory Rating: HS 15.0 Inventory Rating: HS 278

% Difference in Ratings: 186%

Vehicle	Weight (tons)	LL Moment (k-ft)	LFD Occ Rating	LRPD Occ Rating
SH	12.5	186.38	36.6	68.1
S_3C	21.5	314.02	37.4	69.6
S_3A	25.0	360.07	38.0	70.6
S_4A	29.4	406.38	39.3	73.6
S_5A	33.6	448.80	40.8	76.0
S_6A	38.0	479.00	43.3	80.5
S_7B	40.0	518.82	42.1	78.2
S_7A	40.0	494.42	44.2	82.2
T_4A	31.1	382.30	44.4	82.6
T_5B	33.2	442.27	43.4	80.9
T_6A	39.6	469.65	46.0	85.7
T_7A	40.0	464.13	47.1	87.6
T_7B	40.0	411.63	53.1	98.7

Recommended Postings: LFD: LRPD:
 SV: No Posting tons SV: No Posting tons
 TIST: No Posting tons TIST: No Posting tons

Current Postings: SV: 25.0 tons TIST: 278 tons

2. To print the 'Printout', go to File and select Print and choose the printer you wish to print from.
3. If the printout does not print correctly, the user may have to reset the print area.
4. Navigation buttons located on the top of the screen allow the user to move to next desired page. These include: 'Return to Load Rating', and 'Exit'. Clicking on the 'Exit' button will shut down Excel.

APPENDIX B

GFRP DECK BRIDGE CONSTRUCTION REPORT

B.1 Executive Summary

The 20th century brought about many innovative changes to the world of construction. While concrete and steel tend to be the materials of choice, technology has introduced a material, which may become the material of choice for future designs. This material is Fiber Reinforced Polymer (FRP). Composites being both light and strong, are being introduced to many applications, including bridge construction.

In an effort to speed construction and increase service life of a bridge, the North Carolina Department of Transportation (NCDOT) looked to composites. A deteriorating bridge in Union County presented the opportunity to test this new concept in bridge construction. Bridge #89-022 over Mill Creek on New Salem Road (SR1627) needed to be removed and rebuilt, so it was chosen to receive the first composite deck in the State of North Carolina. Martin Marietta Composites division, producer of the FRP DuraSpan™ system, was contracted to produce the panels required for the bridge replacement.

The construction of this bridge was funded in large part through a discretionary grant from the FHWA through the Innovative Bridge Research and Construction Program. Evaluation of this structure continues as a part of the NCDOT Research Project 2002-12 entitled “Evaluation of Bridge Analysis vis-à-vis Performance”. The results of this evaluation will therefore be contained in the final report for this research to be concluded in the summer of 2003.

First, the existing structure was removed, and the new steel girders were installed. Then, angles were welded to the girders to support the panel and to provide room for grout injection. After the angles were welded in place, the panels were placed in accordance with the Martin Marietta Installation Guide by NCDOT personnel, and under the supervision of Martin Marietta representatives. After the deck panels were placed, a combination of shear studs and grout were used to permanently attach the panels to the girders. Once this attachment was made, the rebar and forms for the endwalls were placed, and the concrete was poured. The asphalt overlay was then placed followed by the guardrail. The last item on the agenda was the load testing of the bridge. Once testing was completed, the bridge was opened to traffic.

B.2 General Information

The bridge over Mill Creek carrying New Salem Road through its course in Union County was first constructed in 1944. The structure spans 42 feet between masonry abutment walls. The bridge superstructure, steel plank flooring on steel girders, has seen many cars and trucks safely across Mill Creek. This structure has since seen many resurfacings and repairs in its lifetime. As with all structures, time and elements will contribute to weakening of components. County Inspectors began to notice settlement of the approach slab, rusting of the metal deck, and cracks in the concrete. As the structure became weakened, NCDOT posted the span, limiting the amount of load the structure could carry to 37 tons (see Figure B.1).



Figure B.1: Load limit sign

When the structure was recently deemed too weak, due to degradation of the beams and supports, the decision was made to replace the existing superstructure with a composite system. This system is composed of a DuraSpan™ Fiber Reinforced Polymer deck (FRP), produced by Martin Marietta, and steel girders. The replacement process began with the closure of the road on September 17, 2001 and was reopened to traffic on November 20th, 2001.

B.3 Site Preparation

Once the decision was made to remove the existing superstructure several steps were taken to bring the structure to its current rehabilitated level. The surrounding neighborhood was made aware of the impending closure of the bridge through postings along the route. The structure was closed on September 17, 2001. Once closed, the existing superstructure was removed.

The new superstructure was designed to use 7 – W24X94 in place of the 11 – W21X55 girders being replaced. In preparation for the placement of the new girders a number of modifications were required. The girder seats had to be lowered slightly due to alkali penetration of the stone and mortar used in the original abutment. A

jackhammer was used to remove approximately 3” of mortar and stone from the bridge seat at each abutment. In addition to the removal of concrete from the bridge seat, concrete was removed from the front face of each abutment as well, which was required due to longer girder length. This concrete was removed with the jackhammer at the East abutment. However, this proved to be a difficult operation and a contractor was hired to cut the concrete along the West abutment wall. This method took about the same amount of time but resulted in a cleaner and more accurate cut. To prepare a level surface for the bearing, a quick set concrete was mixed and placed at both abutments (see Figure B.2).

This concrete type was selected to allow a quick installation. Properly mixed, this concrete sets in 45 minutes and attains a compressive strength of 2000 psi in approximately two hours.



Figure B.2: Bridge seat formed and poured

B.4 Structural Steel Erection

Once the forms were removed, the surfaces were prepared for the placement of the new girders. The centerline of the road was marked at each abutment. This mark was used to lay out the location of the new bearing pads and anchor bolts. It was noticed that the centerline of the road did not fall on the middle of the abutments. The centerline of the road was actually 2” North of the centerline of the abutment (see Figure B.3). In order to center the girders on the existing abutments, the superstructure was shifted 2” below the centerline of the road. The anchor bolts were placed in 1” diameter 10” deep holes drilled into the concrete. The holes were drilled using an electric hammer drill with an elastomeric bearing pad acting as a template (see Figure B.4).

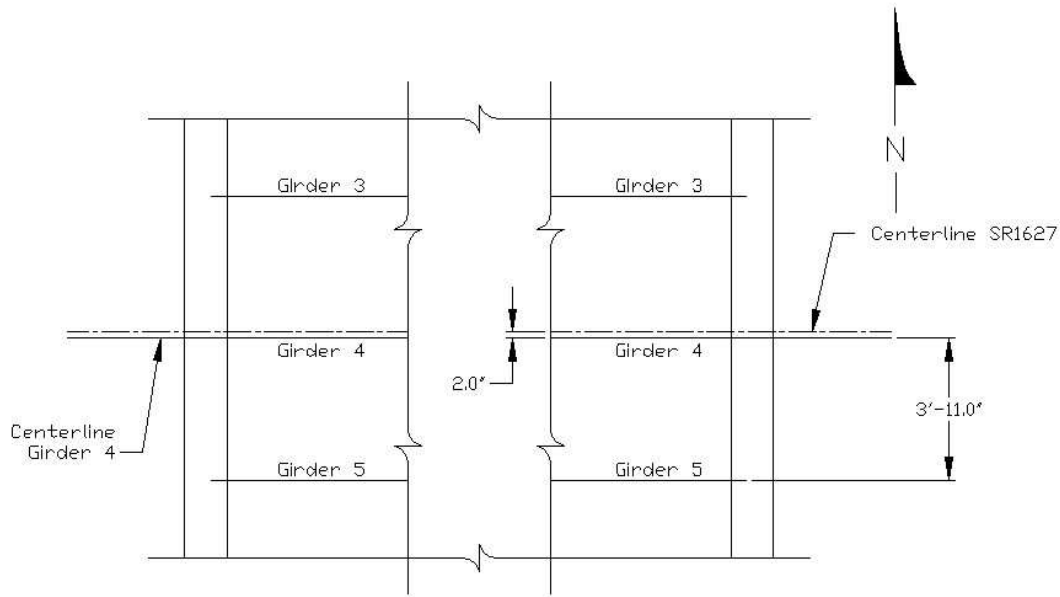


Figure B.3: Difference in road and abutment centerlines



Figure B.4: Bearing pad used as a template for drilling

Due to time constraints, work had to be halted after the holes were drilled in the first abutment. At the start of the next workday the existing holes had to be dried out with a torch due to the presence of water from a previous rainstorm that weekend. Once all the holes were drilled out and dried, an air compressor was used to blow the dust and debris out of the holes. The holes were then filled one thirds full with HIT-HY 150 epoxy/resin. The anchor bolts were placed, sometimes forcibly, into the epoxy filled holes. Care was taken not to damage the threads when more than hand pressure was required to seat the bolts to the depth of the whole (see Figure B.5).



Figure B.5: Nut being used to protect threads from damage

After the epoxy had time to cure, the W24X94 steel girders were brought to the site. Using a crane onsite, the center girder (G4) was removed from the truck and placed on blocks to the side of the trailer (see Figure B.6). Blocks were used to protect the strain gages that were previously installed on the bottom of the girder. This girder was then fitted with a “lifeline” that was used for protection when walking on the girders. This girder was lowered carefully onto the anchor bolts allowing workers to snug the nuts and washers onto the bolts. The remaining girders were then placed in the following order: G3, G5, G2, G6, G1, and finally G7.



Figure B.6: Girder placement on blocks

Once the girders were in place, plywood panels were cut to fit on top of the bottom flange of the girder. Due to the wide spacing of the new girders some intermediate support was required. This support was provided by 2X4 construction grade studs placed under the panels at the center and at the ends. The panels were attached to the supports using wood screws. Once this temporary flooring was in place, the lifeline attachment was no longer a necessity (see Figure B.7).



Figure B.7: Girders and temporary flooring in place

After the girders were secured, and the temporary flooring was in place, the diaphragms (10 – C12X20.7) were bolted into place (see Figure B.8). The diaphragms were bolted to a 3/8” thick connector plate welded to the web of the girder. For more information on the connector plate, see the Connector Plate Detail on Sheet 2 of the NCDOT Preliminary Bridge Plans supplied in Appendix A. The holes in the girder were located and placed by the fabricator of the girders. For more information on the location of the diaphragm, see the Diaphragm Detail on Sheet 1 of the bridge plans supplied in Appendix A. The connection was made using 7/8” diameter bolts. The bolts were classified as HDG Structural Screws made from A325 steel. They were 3” long and required both a nut and a washer.

After the cross members were in place, two events occurred simultaneously. First, the posts and blocks used to attach the barrier rail were installed on the exterior girders. These members were pre-assembled on the back of a boom truck and lowered into position (see Figure B.9). The same type of bolts used in the cross member connection, were used to secure the post and block to the girder.



Figure B.8: Diaphragm bolted in place

Simultaneously, the angles (L2X2) used to separate the composite deck from the girder were installed. The angles were positioned so as to be level across the bridge transversely, and angled so as to follow the camber of the bridge along the longitudinal direction. The angles were welded to the girders top flange using a 1/4" fillet weld placed every 12". The next step in the process was the installation of the suspended scaffolding. This scaffolding was attached to the bottom flanges of two girders (G2 and G6). Once in place, this scaffold allowed access to the bottom of the bridge superstructure.



Figure B.9: Post and block assembly

B.5 GFRP Panel Installation

During the next phase of the construction process, the composite deck panels were installed. The bridge deck was designed to use five DuraSpan™ FRP panels. Each panel was approximately 8' X 25'-4", creating a 40' X 25'-4" composite deck across the girders. Each panel was composed of pultruded tubes, which were bonded together. The tubes created a "honeycomb" type cross-section in the panel, with the tubes running perpendicular to the girders.

The process of placing the panels began with the installation of angles at the east end of the girders. These angles were welded in place to allow the end of the FRP panel to fit flush with the end of the steel girder (see Figure B.10).



Figure B.10: Angles at end of girders

A standard silicone caulk was used to seal any gaps between the longitudinal angles, and the girder. The same caulk was placed on the top of the longitudinal angles to act as a sealant between the FRP panel and the angle (see Figure B.11). The purpose of making the seal was to prevent grout from escaping the shear stud pockets, thus creating a void in the concrete.

The DuraSpan™ FRP panels were installed in accordance with the Martin Marietta Installation Manual. The bonding surfaces (as indicated in Figure B.12) of the panels were first cleaned with acetone to remove any oils that would affect the bond of the adhesives.



Figure B.11: Caulk being applied to angles

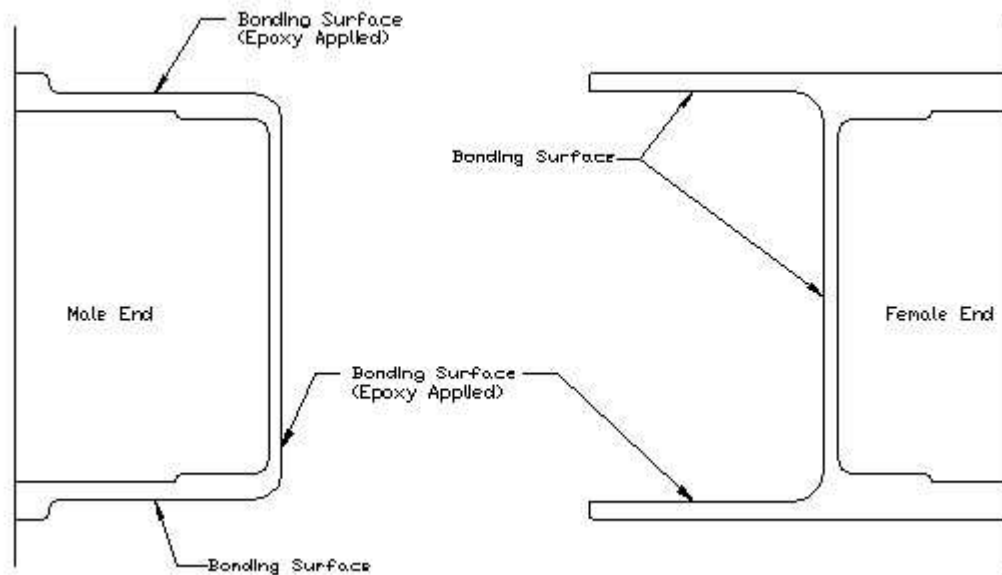


Figure B.12: Panel joint

The panels were then prepared for the epoxy application with a coat of primer applied to the bonding surfaces. Martin Marietta supplied both the primer and the epoxy, which were manufactured by Master Builder Technologies. The primer consisted of two parts, part A and part B, mixed in the proportion of two parts A to one part B per volume. The two components were poured into a bucket and mixed to an even consistency using an electric drill fitted with a mixing tool. The mixture was applied to the bonding surfaces evenly using a small paint roller (see Figure B.13). The primer was allowed to set for approximately 30 minutes before the application of the epoxy.

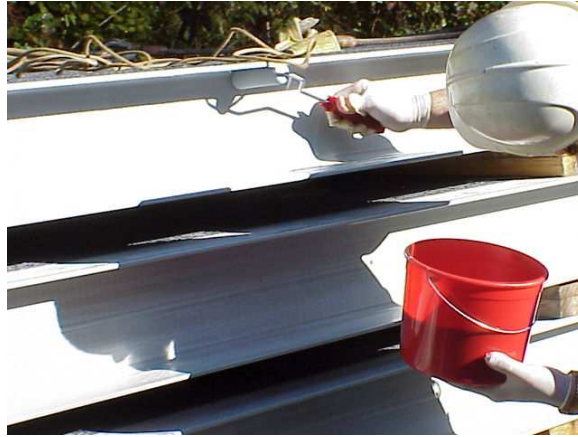


Figure B.13: Primer Application

While the primer was curing, straps were threaded through the shear stud holes in the first panel. These straps were approximately 4" wide, 10' long, flat, nylon tow straps. There was one strap placed at each corner of the panel. Once the primer had set, a crane was used to position the panels on the structure. Care was taken to align the panel between the post and block assembly. The panel was lowered on the girder and slid against the stops at the end (see Figure B.10). Once in position longitudinally, this panel was adjusted in the transverse direction as well.

After the first panel was positioned, the next panel was prepared for assembly. This preparation consisted of first attaching the lifting straps. Secondly, epoxy was mixed to create a permanent bond between the panels. The epoxy was mixed with the same ratio as the primer, and thoroughly mixed using the same electric drill. Once mixed, the epoxy was applied to the male end of the next panel to be installed, and to the female end of the panel already positioned on the girders. The epoxy for the female end was placed on the "bottom lip" of the bonding surface only. See Figure B.12 for joint details. On both panels, the epoxy was initially placed using a flat trowel, then spread using a 1/4" grooved trowel (see Figure B.14).

Once the epoxy was applied to both panels, the crane lowered the new panel into position. The panel was aligned visually in the transverse direction. After the ends were brought into contact and hand pressed together, jacks were used to press the panels together. Standard hydraulic bridge jacks were used with manual pumps. An angle was spot welded to the girder to provide a solid support for the jack. Then, the jack was positioned so the stroke of the piston would run longitudinally along the girder, pressing against a wood block placed between the head of the piston and the panel edge (see Figure B.15). Two jacks were used, one on G2, and the other on G6. The jacks were used to press the panels together and squeeze out all excess epoxy, which was then scraped off using a putty knife.



Figure B.14: Epoxy after spreading

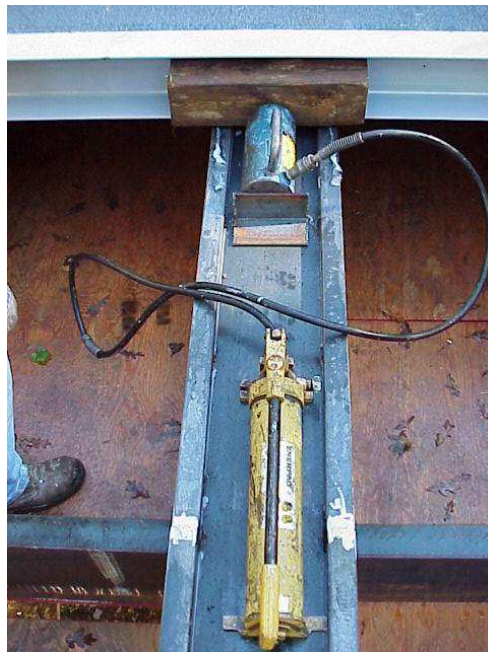


Figure B.15: Jack Placement

While the jacks were holding the pressure, a 5/8" hole was drilled through the panel joint at a point roughly centered between two girders (see Figure B.16). The holes

were drilled between girders G1 & G2, and between G6 & G7. Then, an epoxy coated composite dowel was driven into the hole to secure the two FRP panels while the adhesive cured (see Figure B.16).



Figure B.16: Dowel Placement

Once the dowels were in place, the jacks were released and the temporary angle braces removed. This process of epoxy application, panel placement, jacking, drilling and doweling was repeated for all the remaining panels. The jacking of the last panel required some modification. The last panel covered the ends of the girders, so the jack brace could not be welded to them. A brace was made from scrap wood on-site to transfer the jacking force to the approach pavement (see Figure B.17).



Figure B.17: Jack Placement at End Panel

After being allowed to set and cure overnight, the panel joints were prepared for the joint tape. This preparation consisted of grinding away any excess epoxy that expanded out of the joint during the curing process. Once this was done, acetone was used to clean the top surface of the joints of any oils that would interfere with the bonding of the tape to the deck surface.

The next step was the measurement of the fiber strips. The material for the strips was brought to the site on a large spool. The spool was unrolled across the width of the deck panel and cut, allowing for an overhang at the ends (see Figure B.18). The material itself was a triax E-glass fabric produced by Johnson Industries. The triax term comes from the direction of the fibers in the fabric. The fibers were oriented in a [90/+45/-45] pattern. This material was placed over the deck panel joint and bonded in place with a vinylester material (Atlac 580). This material was chosen due to the flexibility of the material.



Figure B.18: Joint tape rolled out

The bonding material consisted of two parts, the first part being the resin, and the second part being the catalyst. Due to the warm temperature present when the strips were being placed, only a small batch (just enough to do one strip) was mixed at a time. Approximately one gallon of resin (Promoted Hectron FR992) was mixed with 30 mL of catalyst (Cadox C50A) for each strip.

Once mixed, some of the resin was poured onto the deck joint. The material was then spread out in a thick layer over the area where the fabric would be placed (see Figure B.19). Then, the fabric was placed over the joint. A grooved steel roller was used to press the material into the underlying resin (see Figure B.19). Another layer of resin was then brushed on the top surface of the fabric. This process resulted in the material being completely soaked, and in full contact with the panels on either side of the joint.

Once the fabric was in place, any extra material at the overhang was removed. This process was repeated at each joint on the deck surface. Care was taken during the process not to have any unnecessary foot traffic on the deck surface. The strips were cured overnight before work was resumed.



Figure B.19: Resin Application

B.6 Deck-to-Girder Connection

Once the panels were completely connected to each other, the connection between the panels and the deck was established. This connection was achieved through the use of shear studs. The deck itself was manufactured with pockets along the length of the girder, which allowed the placement of shear studs. Each pocket was designed to have three $\frac{3}{4}$ " diameter shear studs (see Figure B.20).



Figure B.20: Shear stud pocket

The steel studs were installed using a specialty tool designed specifically for welding studs. The Division 10 bridge maintenance department did not have a welder of sufficient capacity to weld the large studs, so a contractor was hired to place the studs.

Once the contractor arrived to the job site, there was a minimal amount of preparation for the “stud shooting”. First, the welder was set at 1700 Amps and a stud was welded in the first pocket. This stud was then tested to check the quality of the bond. This test consisted of bending the stud a few inches in the transverse direction of the bridge, then bending it an equal amount in the opposite direction. This side-to-side movement produces a large amount of stress on the weld, and it is believed that if the weld can withstand this large movement, then it is fully attached to the girder.

With the amperage set, the studs were positioned in place to allow the welder to move quickly from one pocket to the next. Insulators, which are used to keep the heat produced from the weld localized to the stud, were placed in the pocket at each location a stud was desired. The studs were set besides each opening (see Figure B.21) resulting in an efficient installation procedure.



Figure B.21: Studs arranged for welding

There were only two complications encountered, both of which were related to a shortage of material. The welding crew was short by approximately a dozen studs, which meant that there were several pockets that only received two studs. The second problem was a shortage of insulators. The welding crew had some leftover from a previous job, and used those to finish the work. Once all the welding was completed, there was some discussion as to whether the insulators around the shear studs would interfere with the bond between the studs and the grout scheduled to be pumped into the opening. It was decided to break the insulators away from the studs, to allow the grout to completely cover the area around the base of the stud.

Once the studs were in place, the next step in the connection was the placement of the grout in the stud pockets. The grout pump was primed with Slick Willy to promote a better flow of the grout. The grout itself was mixed in a gasoline powered rotary mixer at a ratio of 50 lbs of grout to ½ gallon of water. The materials were allowed to mix for approximately 10 minutes before being placed in the hopper of the pump. The NCDOT personnel placed several batches of the mix into the pump before starting the process to ensure an adequate supply. After checking the slump of the mixture, which was approximately 11”, the process was started at the girder line farthest from the pump. Each pocket was filled to deck level before moving to the next pocket in the girder line (see Figure B.22). The crew noticed that as they worked down the line, previous pockets had settled down below deck level. These pockets were back filled manually, using a bucket of grout and a trowel (see Figure B.22). According to the manufacturer, the grout had a setting time of three hours, and a curing time of one day.



Figure B.22: Grout placement and finishing

B.7 Semi-Integral Endwall Construction

The next step in the construction of the bridge was the construction of the concrete end wall. The end wall was designed to be semi-integral with the deck slab, i.e. the deck would be tied to the concrete abutment. This tie was made through the use of rebars passed through holes pre-cored in the deck (see Figure B.23). The reinforcement was then tied into the cage placed around the girders and bearing pad.

Once the reinforcement was in place, forms for the concrete were cut and nailed into position. The formwork consisted of a plywood interior surface being braced by 2” lumber. After fully bracing the formwork against possible outward movement, the concrete was ordered.



Figure B.23: Endwall Connection

Metromont Materials supplied the concrete. Two trucks were required, one at each abutment. The first truck arrived at the West abutment with 5 yards of class AA concrete. The concrete was poured directly from the truck into the forms. A mechanical vibrator was used to remove any trapped air from the mixture as it was placed (see Figure B.24). The surface was hand finished using a trowel. The same process was repeated on the East abutment. In order to test the 28-day strength of the mix, three cylinders were collected from each truck. The samples were taken in accordance with ASTM C31-91.



Figure B.24: Concrete Poured at Endwall

B.8 Roadway Construction

Once the superstructure was finished, the next step in the construction process was to prepare the approaches to the bridge. The area surrounding the end walls had been excavated to allow access to the abutment. Therefore, the soil had to be replaced and compacted in those areas. Once the soil was in place, the structure was ready for the asphalt pavement. The I-2 asphalt was placed in 2" layers (or lifts). Three layers of binder were placed in the approaches to raise them to the desired level. After placing three layers of binder in both approaches with a layer on the deck of the bridge, crews began to place the asphalt. Each lift of binder and asphalt was compacted by a vibratory drum roller before the next layer was applied (see Figure B.25).



Figure B.25: Vibratory Drum Roller

With the raised level of the approach, some grading was required to bring the shoulder of the road up as well. In order to set the new shoulder height, the existing barrier rail had to be removed. Soil was placed along the side of the road and leveled out with a motor grader (see Figure B.26).

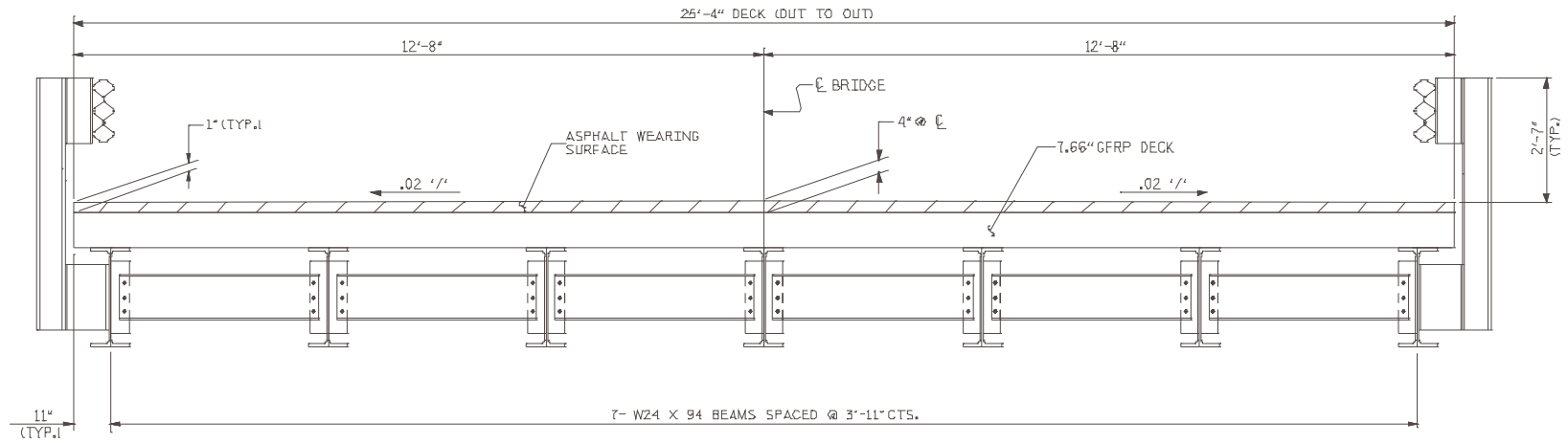
Upon completion of the grading, the road surface was brushed off with a combination of brooms and a mechanical brush.



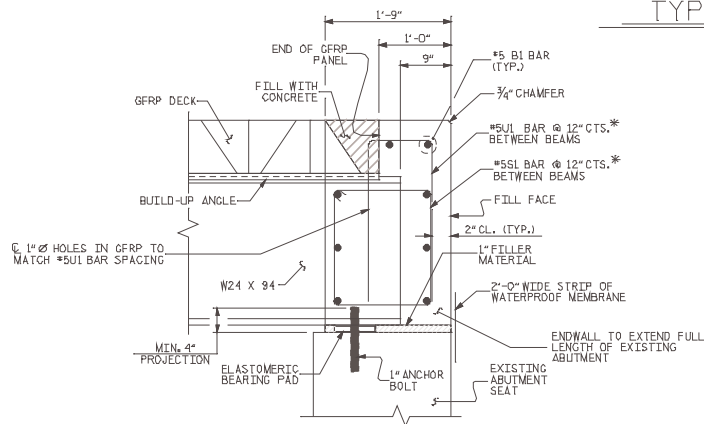
Figure B.26: Motor Grader Finishing the Shoulder

The next phase was the installation of the guardrail. NCDOT personnel attached the guardrail to the posts along the side of the bridge, and hired a contractor to install the posts leading up to the bridge from both sides. The contractor used a hydraulic ram to drive the posts into the soil, and attached the rail using an air impact wrench. Once the guardrail was in place, crews were able to apply the pavement markings, and the bridge was ready to be opened to traffic. In the period of a few months, the Mill Creek crossing was upgraded through the use of a composite deck.

B.9 NCDOT Bridge Plans



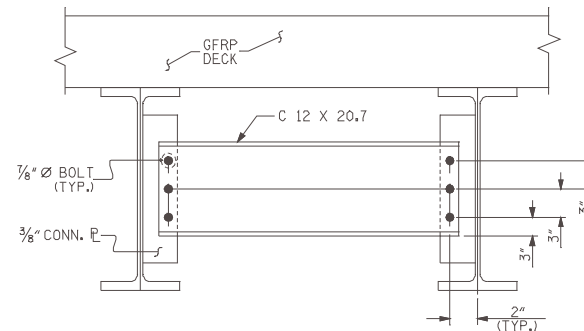
TYPICAL SECTION



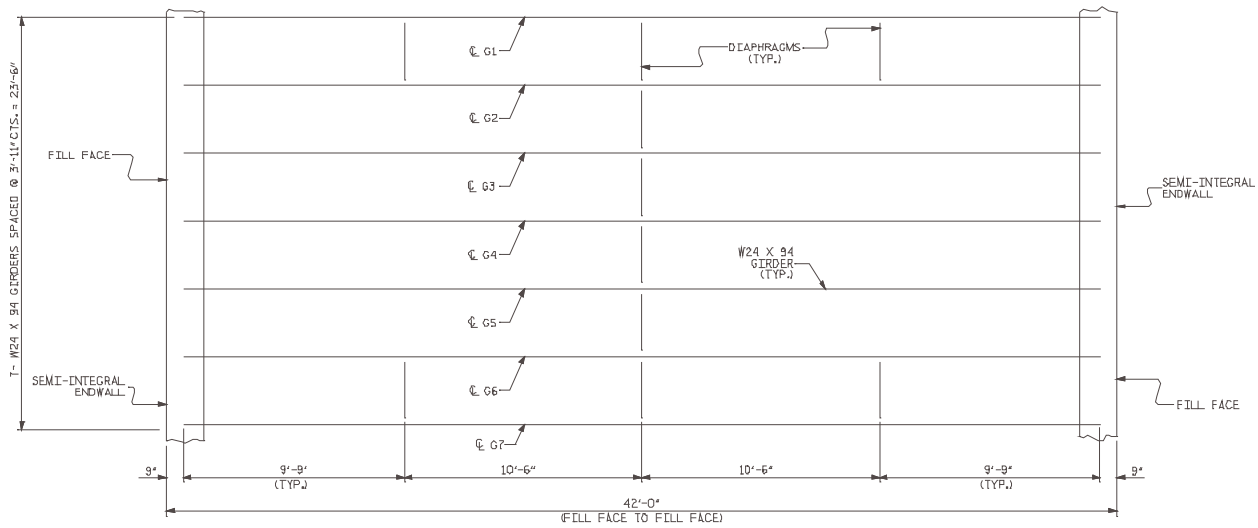
SEMI INTEGRAL ENDWALL DETAIL

* PLACE TWO ADDITIONAL #1" AND #5" BARS IN END WALL OUTSIDE EXTERIOR GIRDERS

PRIOR TO DRILLING HOLES FOR ANCHOR BOLTS, VERIFY DISTANCE OF 39'-6" BETWEEN CENTERLINE OF BEARINGS.

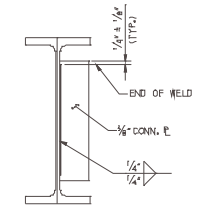


DIAPHRAGM DETAIL

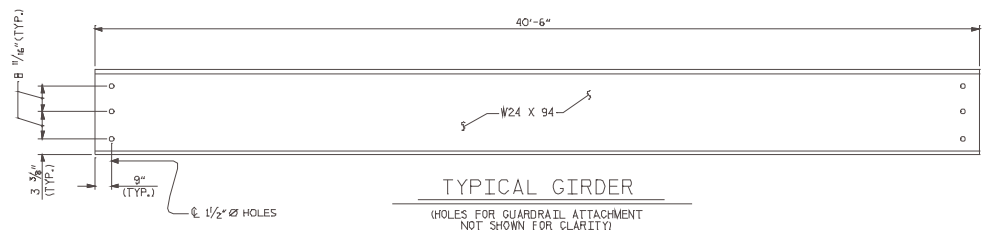


FRAMING PLAN

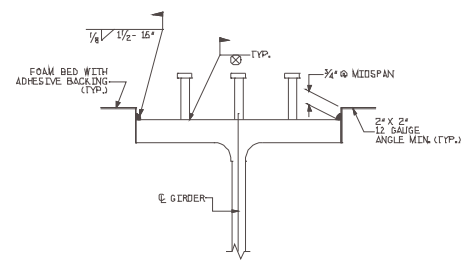
NOTES:
 TURN MILL CAMBER UP.
 3/4" X 5" STUDS TO BE FIELD
 WELDED IN GRP DECK PANEL
 BLOCKOUTS AFTER PANELS ARE
 IN PLACE



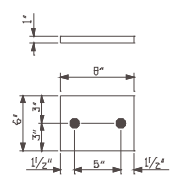
CONNECTOR P DETAIL



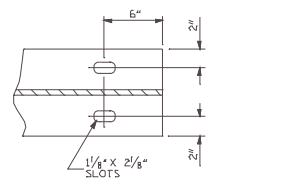
TYPICAL GIRDER
 (HOLES FOR GUARDRAIL ATTACHMENT
 NOT SHOWN FOR CLARITY)



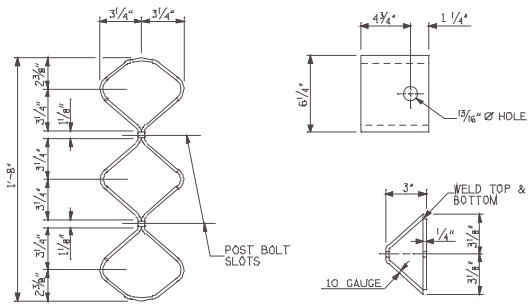
FLANGE DETAIL



ELASTOMERIC BEARING PAD
 (4 REQUIRED)
 (50 DIAMETER)



END OF GIRDER
 BOTTOM FLANGE DETAIL



TUBULAR THRIE BEAM & SPACER DETAILS

NOTES:

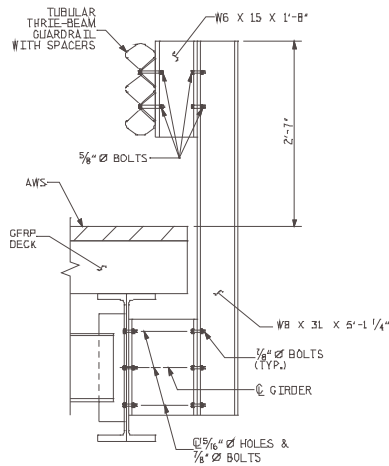
FABRICATOR TO PUNCH HOLES IN EXTERIOR GIRDERS FOR ATTACHMENT OF W12 X 26 OFFSET BLOCKS.

STRUCTURAL STEEL TO BE AASHTO M270 GRADE 50W.

ALL BOLTS TO BE ASTM A325, AND GALVANIZED.

GUARDRAIL SHALL CONFORM TO THE NCDOT STANDARD SPECIFICATIONS EXCEPT AS NOTED ON THE PLANS.

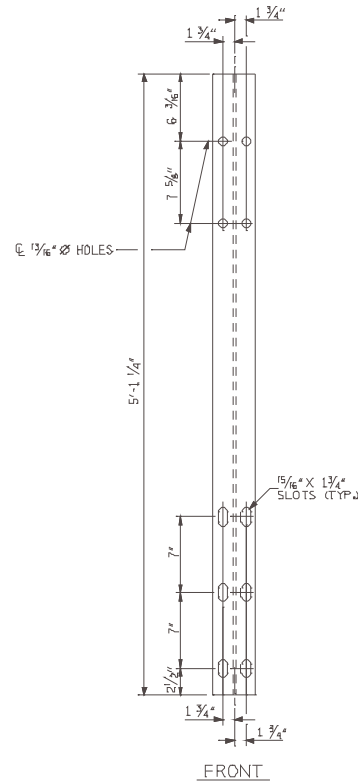
DIRECT TENSION INDICATORS SHALL BE USED WITH ALL 3/8" Ø H.S. BOLTS



RAIL DETAIL

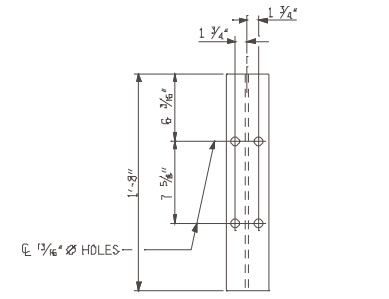
RAIL POSTS AND OFFSET BLOCKS TO BE GALVANIZED.

BOLTS FOR RAIL TO BE MECHANICALLY GALVANIZED.



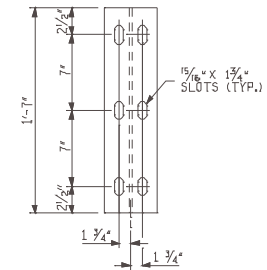
FRONT

W8 X 31 RAIL POST



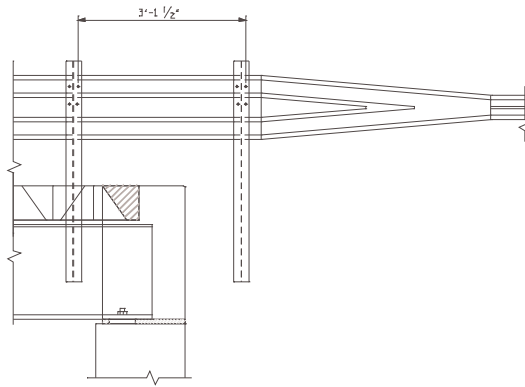
W6 X 15 OFFSET BLOCK

(HOLES IN BOTH FLANGES)

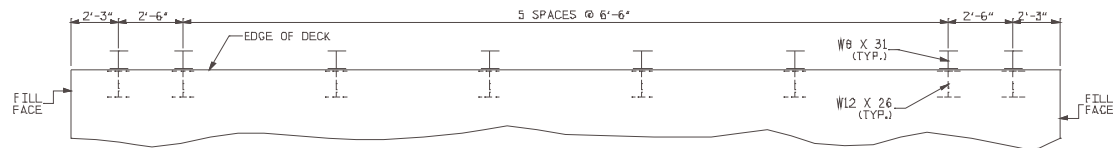


W12 X 26 OFFSET BLOCK

(SLOTS IN BOTH FLANGES)



RAIL ELEVATION



RAIL POST SPACING PLAN

(TYPICAL EACH SIDE)

B.10 Martin Marietta Installation Guide

DeckSpan™ FRP Deck
Installation Guide



Installation Procedures

Shown below is a brief pictorial illustrating the major tasks for installation of the *DeckSpan™* deck panels.

1. Unloading, storage of panels

Site handling and erection shall be performed with acceptable equipment and methods, and by qualified personnel and in accordance with the manufacturer's recommendations.

The panels shall be lifted and supported during stockpiling and erection operations only at the lifting or supporting points, as shown on the shop drawings, and with approved lifting devices. The panels shall be kept flat and true to prevent warping or twisting of the panels during lifting and storing. The panels shall not be turned or placed on their sides or with the top surface down. Lifting of the panels from one edge will not be permitted. All panels shall be stowed off of the ground and protected with covers that are impervious to sunlight and weather in order to provide protection from ultra-violet light and keep the panels clean and dry. Stacked panels shall be supported on unyielding supports and shall be separated by battens across the full width of each panel. Panels will arrive on truck as requested by the contractor.



2. Preparations prior to installation of deck panels

Steel flanges on stringers and floorbeams shall be prepared in accordance with DOT specifications, including grinding at stud locations if necessary. Light gauge stay-in-place steel angles are the preferred method of forming the haunches. These are the same angles that are used for the stay-in-place forms for concrete decks and shall be designed to support the weight of foot traffic, deck, and construction loads. Typically elevations are shot at 1/10th points along the beams and the height of the haunch is determined by subtracting this elevation from the finished grade elevation minus the deck and overlay depths. On framing systems that have a transverse floorbeam/longitudinal stringer configuration as shown, the angles will be typically be installed on the stringers only but the haunch will be continued over the floorbeams as shown. On the job shown, this was accomplished with screws and tape.



3. Installation of first panel

Proper placement of the first panel is very important. The panel needs to be placed with the proper alignment and secured (bolted) so there is no movement when other panels are jacked against it. Suggest surveying to make sure the first panel is aligned properly as well as surveying the centerline of structure. The panels will have the centerline marked on them, and at various times during installation, the alignment of the panel centerline may be checked with the surveyed centerline of structure.



4. Application of epoxy adhesive (liquid primer and paste coat)

Prior to application of the adhesive, both surfaces of the bondlines shall be cleaned with acetone. A liquid primer will be rolled on to both mating surfaces (100% coverage) and allowed to tack up. Upon sufficient set of the primer coat, the paste coat will be applied on the vertical web and flanges (100% coverage on one side of the joint only) using 3/16" notched trowels. MMC will supply the adhesive (probably 3-4 gallon buckets) and the contractor will apply it. MMC will keep track of temperature and time to ensure proper working time is not exceeded. Working time will vary depending on temperature, but in general a minimum one hour working time can be achieved.



5. Lifting/placing panels

Type 1 - Thru-truss or long span structures.

For thru-truss or longer span structures where cranes do not have sufficient reach to install the panels, panels may be lifted and placed with the lightest weight equipment (typically forklifts) possible. For this type of installation, the specific piece of equipment shall be approved by the manufacturer. In order to help spread the tire load over the wet bondlines, timber/steel planking running the full length of the tire contact area will be required as shown in the following pictures. A steel plate (or other acceptable means) shall also be placed at the beginning of the bridge to protect the unsupported edge of deck during installation.



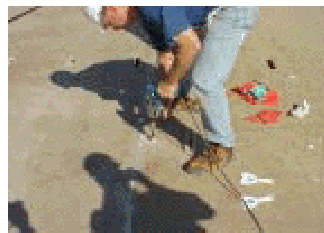
Type 2 - Short to medium span structures.

For short to medium span structures, a crane with sufficient reach to place all panels without sitting on the bridge is the preferred option and should be used whenever possible. This method not only protects the integrity of the bondline while it cures but also allows for smaller angles and welds to be used for the haunches.



6. Jacking the panels

The panel field joints overlap 4" (tongue-in-groove type joint), so the panels will need to be slid 4"-6", depending on how close they are lowered into place. Panels are jacked into place by means determined by the contractor. In the past, jacks welded to a steel plate were clamped to the top flange or the angle supports. There are several other options which MMC can share with the contractor, but ultimately the method for the placing of the panels is the responsibility of the contractor. MMC will work with the contractor with his proposed method. For most bridges, two jacking locations each side of the centerline will be sufficient. MMC will provide timbers that will fit the shape of the deck to jack against. The panels should be jacked completely together so that the lip of the female end seats flush against the top deck surface on the male end. While the jacking pressure is still being applied, permanent FRP dowel bars are installed in the lips of the field joints prior to releasing jack pressure to protect the integrity of the bondline while it cures. MMC will provide the FRP dowel bars. After the dowel bars are in place and the jacking pressure has been released, all excess adhesive that has been squeezed out of the bondline shall be struck off flush with the top surface of the deck with a scraper before the adhesive cures.



7. FRP splice strips on panel field joints

After all the panels are in place and the field bondlines have sufficiently cured (usually overnight), FRP splice strips are installed over the bondlines. These strips will be 32oz triaxial fabric and will be delivered to the site pre-cut to 7" wide and to the proper length (will wrap over vertical edge of deck). Steps for the installation of these strips are as follows:

1. The bonding surface will be prepared in the shop but will need to be sanded (40-60 grit sandpaper) or ground lightly in the field to remove all contaminants and ensure a good bonding surface (sand the section until all of the gloss is eliminated and the surface is thoroughly roughened).
2. After sanding/grinding, the surface will need to be blown as clean as possible with an air compressor and wiped with acetone wipe prior to application of the strips. Allow acetone to completely dry.
3. A vinyl ester resin and steel rollers will be used to wet out the fabric. Catalysts and mix the resin in one gallon containers. The pot life of the resin mix is temperature dependent. Therefore, the amount of catalyst must be modified according to air temperature and desired working time. The following charts depict the proper catalyst and promoter amounts and are based on specifications for Reichhold 580-05 resin systems:

Temp (F)	Gel Time (minutes)	Pound of Resin	
		MEKP (9%)	CoNaph (6%)
		%	%
40	30-40	2.4	0.7
50	30-40	1.8	0.6
60	20-30	2.4	0.6
	30-40	1.8	0.6
75	15-25	1.8	0.6
	40-50	1.2	0.4
90	15-25	1.8	0.4
	20-30	1.2	0.4
	30-40	1.2	0.3
	15-25	1.2	0.2
	30-40	0.9	0.2

Resin density 8.5 lbs/gal

Gallons of resin @ 75 F (gal)	Lbs of resin @ 75 F (lbs)	MEKP (9%) %	MEKP (9%) cc or ml	CoNaph (6%) %	CoNaph (6%) cc or ml
1	8.5	12%	45.31	0.4%	15.44
2	17	12%	92.62	0.4%	30.87
3	25.5	12%	138.92	0.4%	46.31
4	34	12%	185.23	0.4%	61.74
5	42.5	12%	231.54	0.4%	77.16
6	51	12%	277.85	0.4%	92.62
7	59.5	12%	324.16	0.4%	108.05
8	68	12%	370.46	0.4%	123.49
9	76.5	12%	416.77	0.4%	138.92
10	85	12%	463.08	0.4%	154.35

Notes:

- * Add the required promoter and catalyst to the desired amount of resin. Catalyze only one gallon at a time.
 - * Mix resin/catalyst for not less than one minute. A drill and a high shear mixer should be utilized.
 - * Never mix C-0Naph with DMEKP in the same container.
4. After the entire splice surface is coated with resin, lay the 32 oz. fabric (chop side down) and roll out with the steel rollers.
 5. Roll the mat in the direction of the joint then roll the mat perpendicular to the joint. This will force out the air. Resin will soak up through the fabric. If dry spots appear, apply additional resin on the top of the fabric as necessary if there are still dry spots and roll out until fabric is totally wet out.
 6. If there is excess resin on the top or sides, soak up the excess resin with a paintbrush.

MMC will provide all materials and technical oversight for the installation of these strips and the contractor will be responsible for the labor and equipment. These strips will need to sufficiently cure (usually overnight) before workers are allowed to walk on them. Prior to installing the overlay, light sanding with 40-60 grit sandpaper is recommended for proper adhesion.



8. Installation of shear studs (deck-to-girder connections)

After the splice strips have cured, the conventional headed shear studs may then be welded to the beams. After all of the studs are in place and have been tested in accordance with DOT specifications, the non-shrink grout may be placed.



9. Installation of non-shrink grout pockets and haunches

After the shear studs have been installed, the stud pockets and haunches may then be grouted. The grouting operation shall meet the following specification. SilcaGrout 212 has been tested and used in the past, but alternate grouts meeting the specification are acceptable. The grout will flow through the stud pockets to fill in the variable depth haunch between the bottom of the deck and the top of the beam. Grout will flow underneath deck to adjacent hole, then fill grout pockets. It is very important to get the haunches and cavities completely filled without any voids. A mobile mixer located off the end of the bridge and a pump to get the grout out on the bridge is highly recommended. Care should also be taken to prevent spillage onto deck surface (plastic was used on previous jobs).



NONSHRINK GROUT FOR HAUNCHES AND SHEAR STUD POCKETS

1.0 Materials and Mixing.

The nonshrink grout shall be a flowable nonmetallic grout meeting the requirements of ASTM C 1107 Grade C.

The mixture shall have a flow of 125% to 145% when tested in accordance with ASTM C 109M. The grout shall have a maximum allowable expansion of 0.1% at 3, 14, and 28 days when tested in accordance with ASTM C 1090. The expansion at 3 and 14 days shall not be greater than the expansion at 28 days.

The grout shall have a compressive strength of not less than 34 MPa at the age of 7 days and 40 MPa at the age of 14 days when tested using the applicable portions of ASTM C 109M. The compressive strength specimens shall be produced from a mixture of the dry grout and sufficient water to produce a flowable mixture. The initial set shall not be less than 60 minutes when tested in accordance with ASTM C 403M.

The resistance of the grout to freeze thaw shall be such that it maintains a relative dynamic modulus of elasticity of not less than 80% after 300 cycles when tested in accordance with AASHTO T 161, Procedure B.

The grout product will be accepted provided that certified test data is submitted that reflects conformance with the requirements stated herein.

Mixing shall be done with rotating paddle-type mixing machines and shall be continued until all ingredients are thoroughly mixed. Once mixed, grout shall not be retempered by the addition of water and shall be placed within 1 hour.

2.0 Forming and Placing.

The forms shall be constructed of wood, metal or other material approved by the Engineer. The forms shall be constructed to retain the grout without leakage. An adhesive-backed foam bed shall be placed on the tops of the forms in contact with the deck panels in order to seal the interface. The forms shall be designed to remain true to shape and rigidly support the weight of the FRP panels and all materials, equipment and personnel necessary for placement of the grout. Forms shall be set and maintained to the lines and grades specified on the plans and in a manner approved by the Engineer until their removal.

All tie rods, bolts, anchorages and other forming hardware which is incorporated into the haunches shall be galvanized. Tie rods, bolts and anchorages, within the forms shall be constructed so as to permit their removal to a depth of at least 40 mm from the face without injury to the concrete. Wire ties, when used, shall be cut back at least 15 mm from the face of concrete upon removal of the forms. All fittings for metal ties shall be of such design that, upon their removal, the cavities which are left will be of the smallest practical size.

If stay-in-place forms are not used, the forms should be lined or coated with a bond-breaker approved by the Engineer. The forms shall not be removed until the grout has hardened sufficiently that it will not be damaged and until the Engineer has approved such removal.

The grout shall be placed in a manner and sequence such that all voids are completely filled. Vent holes or tubes in the formwork shall be sized and located as necessary to prevent air entrapment. If the Contractor's methods of placement do not achieve full coverage of the grout, as determined by the Engineer, pumping of the grout will be required.

The grout shall be placed continuously. Delivery, mixing and placement shall proceed such that there will not be an interruption of more than 15 minutes duration in the placing of the grout over a single girder.

3.0 Finishing and Curing.

The exposed top surface of the grout shall be struck off flush with the top of the deck and finished with a float. The surface shall be given a final finish by brushing with a bristle brush. The brush shall be drawn across the grout at right angles to the centerline of the roadway.

The exposed surfaces of the grout shall be wet cure for a minimum of 3 days or as directed by the Manufacturer to achieve the required design strength. The method of wet curing shall be in accordance with the DOT specifications.

Immediately after removal of forms, the exposed surfaces shall be finished in accordance with the DOT specifications except that grout cleaning and a rubbed finish is not required.

4.0 Application of Loads.

Vehicles, equipment and materials will not be permitted on the bridge until the grout has achieved a minimum compressive strength of 40 MPa.

10. Final pour for integral/semi-integral backwalls (if applicable)

If integral or semi-integral backwalls are used, the final pour will typically be done after the deck panels are in place and the grout for the connections and haunches have cured.

11. Installation of barrier rails/curbs and expansion joints (if applicable)

After the grout has achieved a minimum compressive strength of 40 MPa, the barrier rail/curbs and expansion joints can be installed.

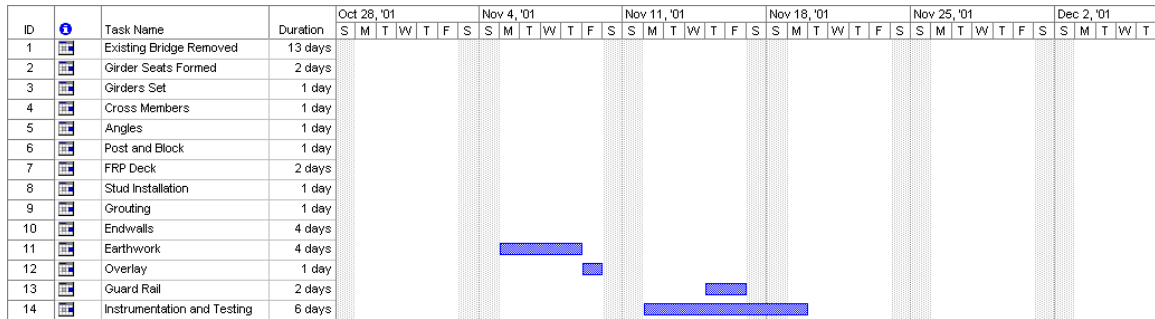
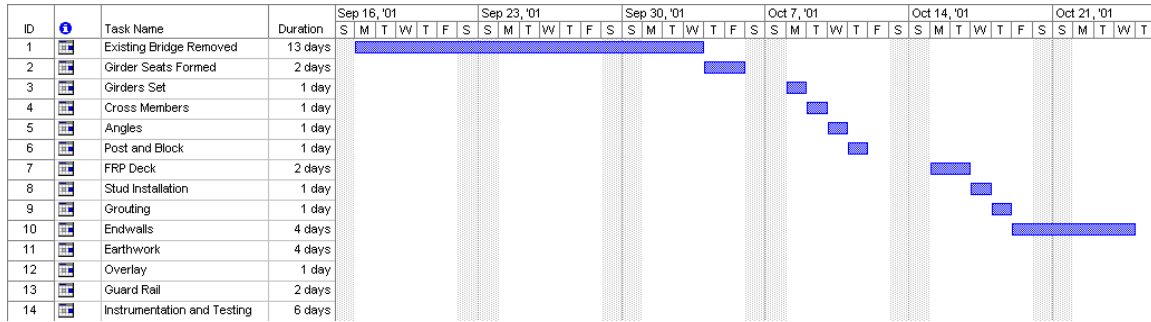
12. Installation of overlay (asphalt assumed)

The deck will be shipped to the site with an epoxy non-slip surface. Prior to applying the tack coat and overlay, a high pressure water blast (preferably using a degreaser) will be required by the contractor in the field prior to the application of the wearing surface to remove any contaminants. Allow to completely dry before applying tack coat and asphalt.

The type of overlay is the owner's choice. If another type of overlay is desired, such as polymer concrete or micro silica modified concrete, the epoxy grit will be eliminated and the surface will be heavily sanded prior to being shipped to the job site. A light sand blast will then be required at the site after the deck is in place, and after cleaning the surface, a primer will be applied to the deck surface prior to the overlay installation. For overlays other than asphalt, a scribed application is highly recommended.

B.11 Timeline

The following charts provide schedule details for the demolition of the old superstructure, and for the construction of the new GFRP deck system. As it can be seen, the actual deck installation required only a few days to complete.



APPENDIX C

INSTRUMENTATION AND LOAD TESTING

C.1 Instrument Description

In order to monitor the behavior of the bridges, several types of instruments were used. The two basic categories of instruments were displacement and strain instruments. *Displacement transducers* and *linear variable differential transformers (LVDT)* were used to record vertical deformations of bridge girders and decks. *Strain transducers*, *strain gages*, and LVDTs were used to record strain readings on the elements of the bridge superstructure.

The Celesco displacement transducers used in this project utilize a voltage source to record displacement by measuring the change in resistance of the potentiometer. The displacement transducers were calibrated by UNC-Charlotte Cameron Research Facility's Metrology Lab to an accuracy of ± 0.01 in. Each instrument had a maximum stroke of 20 in. Figure C.1 shows several views of displacement transducers mounted in position. Since the instruments required a stable base, especially on uneven ground, a concrete masonry unit with an attached plywood-mounting strip was used.



Figure C.1 Mounted 20 in. displacement transducers

A second type of displacement transducer was used to measure the position of the load vehicle during the tests. This 140 ft – stroke device was calibrated to an accuracy of ± 2.0 in., and it was mounted on a bracket that allowed it to be placed in a 2 in. truck receiver. The other end of the string was attached to the loading truck's rear or front bumper, depending on the loading position.

The BDI strain transducers were the primary strain measuring devices. These instruments developed specifically for bridge tests have an accuracy of 2 % with a strain

range of $\pm 4,000$ microstrains ($\mu\epsilon$). There were two mounting possibilities for these instruments. The preferred method was using two mounting tabs attached to the surface of the bridge member at the predetermined location (see Figure C.2). These tabs required that the surface be free of soil, debris, rust, and paint. Therefore, each location was grinded down to ensure a smooth, clean surface to adhere the tabs. The tabs were adhered using either a two-part epoxy, or Loctite's 410 Adhesive and 7452 Accelerator.



Figure C.2 Strain transducer

However, the performance of these adhesives was dependent on the current atmospheric conditions. Cold and rainy days made the curing process extremely difficult to control. Therefore, in cases where it was necessary and possible, c-clamps were used to secure the instruments to the bottom flanges of steel girders.

Towards the end of the project, up to twenty strain transducers were used at each bridge site. In order to maximize the test data recorded during the last two bridge tests, Zapata Engineering, a local engineering firm, generously donated the usage of six additional strain transducers that were used with an additional data acquisition system.

Strain gages were the only non-reusable instruments used during the test. These devices work by measuring the change of resistance over the gage length with an applied constant voltage. The strain gages used for the tests were an open face design with an overall length of $\frac{1}{4}$ in., and with a limit of 5 % total elongation.

Strain gages are inexpensive instruments. However, these devices were very dependent on the quality of application. Usually, errors in the application process are the main cause for inaccuracy in the readings. Hence, only qualified personnel were allowed to attach these instruments to bridge members. The application process and the size of these gages limited their use to steel girders. In addition, they require a lot of preparation, and are easily damaged. Figure C.3 shows a $\frac{1}{4}$ in. strain gage mounted to a steel girder.

Initially, LVDTs were also used to measure the strain level on concrete members. An LVDT is a delicate instrument, requiring frequent recalibration in the lab. The ones available to UNC-Charlotte researchers generated a fair amount of electrical noise compared to other instruments. Also, the accuracy of these instruments was within the

actual strain measurements. For these reasons, at the beginning, the use of the LVDTs was limited, and eventually discontinued.

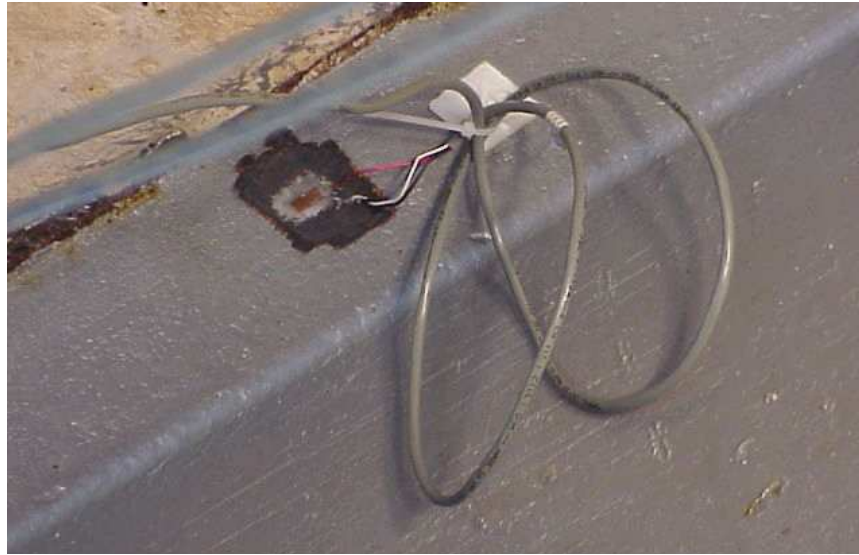


Figure C.3 Strain gage attached to girder

Each of the previously described instruments was connected to a numbered data cable that ran to the data acquisition (DAQ) system. The DAQ was a system consisting of an HP mainframe and digital multimeter, a dual processor Gateway server (see Figure C.4), and power supplies. Each numbered cable (ranging in length between 80 ft and 180 ft) was then plugged into a designated channel, which read the gathered information into a data acquisition computer program. At maximum, 112 instruments were used at one of the bridges

Over the course of the seven bridge tests, revisions were made to the original data acquisition program to improve speed. Also, new programs were written satisfy different test needs, such as higher sampling rate for dynamic tests. Each bridge required a different test program to be created. This was due to the variation in instruments for each bridge, as well as the different strain gage factors. The number of instruments for the rest of the bridges averaged at about 60 instruments.



Figure C.4 Data acquisition system

As it was mentioned earlier, for two of the bridges, and additional portable DAQ system was used to record data from six strain transducers. This portable DAQ consisted of a Dell laptop computer with power supplies, and an Agilent multimeter.

C.2 Instrument Plans

Bridge 89-022 had instruments on the steel girders, and the GFRP deck panels. In the instrumentation plan the goal was to determine the strain in both materials under a variety of loading conditions; to prove the existence of composite action between the girders and the deck panels; to establish the distribution of the load across the structure; as well as to determine the amount of fixity at the abutments resulting from the use of semi-integral back walls.

All seven girders were fitted with ¼ in. strain gages on the bottom and top flanges at the quarter and middle points. For this bridge, instrument locations are indicated by type of instrument, position number, girder number, and location number (see Figures C.5 and C.6).

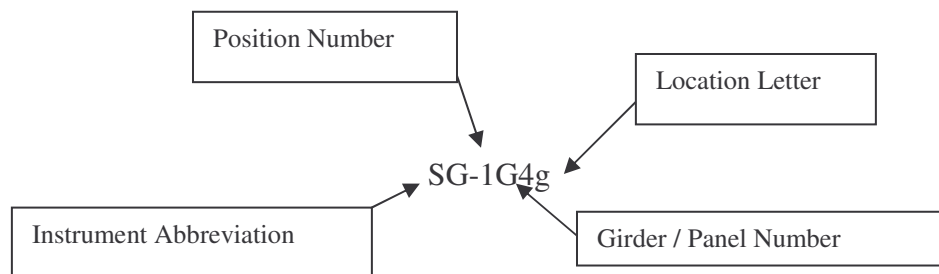


Figure C.5 Instrument identification for Bridge 89-0022

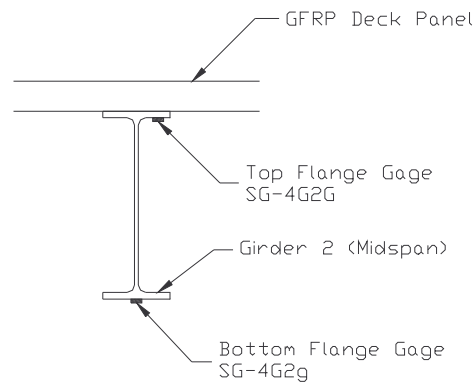


Figure C.6 Placement and nomenclature of strain gage on steel girders

In addition to measuring the deflection of the girders, there was also an interest in the net deflection of the GFRP panels. In order to measure this panel deflection, the displacement transducers were mounted to a board, which was then clamped to the bottom flanges of two adjacent girders (see Figure C.7). There were three displacement transducers used in to measure the deck deflection. They were placed in bay 3, bay 4, and bay 5.

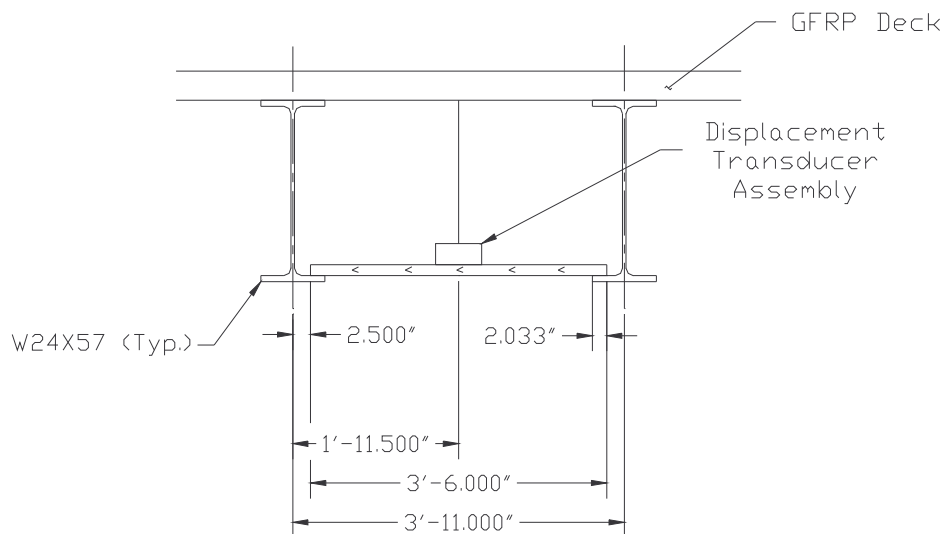


Figure C.7 Displacement transducer for panel deflections

The instrumentation of the remaining six bridges followed a similar plan. The goals of these tests were to verify continuity, composite action, strain and deformation levels, and transverse distribution of loads. These plans are provided in detail in the individual theses of Brad Stiller, Chad Ritter, Tim Lawrence, and in the project report of Claudia Prado.

C.3 Load Testing Procedures

The objective of any bridge load testing is to quantify the capacity of the structure, which in many cases, well exceeds the theoretical values predicted by traditional analysis tools. Furthermore, during the analysis of the test data, it is important to identify the inherent strength and stiffness reserves in a bridge, provided by unexpected composite action or continuity/end restraints, by superior material properties, or by contributions from secondary elements, such as guard rails, parapets, curbs, etc...

The *Manual for Bridge Rating through Load Testing* (TRB, 1998) introduces two types of nondestructive load tests, diagnostic and proof load tests. During a *diagnostic load test*, a selected load is placed at predetermined locations on the bridge. The load applied during a diagnostic test represents the rating load level. The structure's response is monitored through instrumentation attached to the bridge. Finally, this response is compared to analytical predictions.

During a *proof load test* however, the bridge is incrementally loaded until it reaches its elastic limit, or it develops visible signs of distress. As such, the proof load is significantly higher than the diagnostic load, and can be used to verify the capacity of a bridge. Since the proof load results in stresses close to the elastic limit, this must be done incrementally, and by experienced personnel.

During this project, all seven bridges were tested up to their rating level. More specifically, whenever it was possible, the goal was to find the truck load closer to the operating level. Therefore, diagnostic load tests were performed on these structures. This was also evidenced by the low (sometimes very low) stress and deformation levels reached in these tests. Furthermore, none of the bridges exhibited even the slightest sign of distress, such as additional cracking, excessive deformation, concrete spalling, etc...

Due to the load levels required in this project, it was decided to use trucks to perform the diagnostic load tests. In design and load rating H or HS type vehicles are being considered. However, these are fictitious trucks, with similarities to real vehicles. Therefore, an attempt was made in each bridge test to find the vehicle that will generate a similar moment and shear diagram, in shape and magnitude, to the operating rating load.

This was not a simple task, considering the large variations in the seven bridges, some posted at 14 tons SV, others spanning close to 300 ft with an intermediate support. Finally, two types of trucks were used in this project. The first truck was a concrete truck (its use donated by Concrete Supply Co. of Charlotte, NC) loaded with wet aggregate. Figure C.8 shows a diagram with the axle spacing and weights for the loaded concrete truck. Obviously, this weight distribution changed slightly for bridge 59-0361, the only other bridge loaded with a similar truck.

This 9 yd³ truck had a similar effect to an HS-25 truck for spans in the 40 ft range. As it can be seen in Figure C.9, the bending moment generated by the concrete truck is close to the one calculated with an HS-25, with 14 ft axle spacing. A comparable similarity existed between the actual and theoretical shear forces as well.

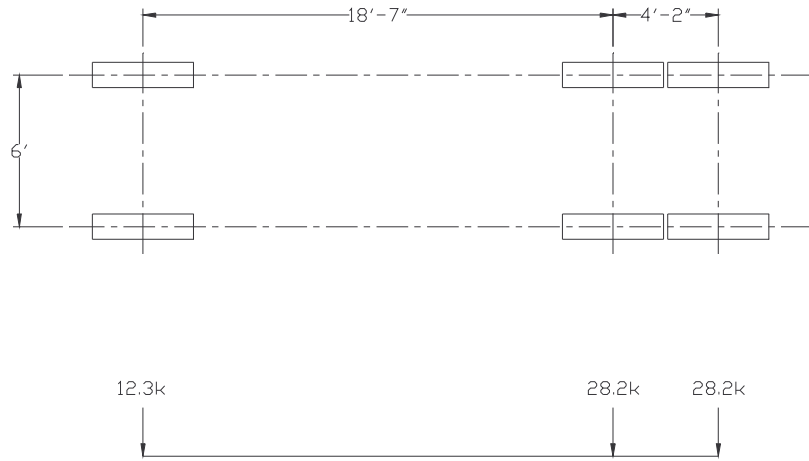


Figure C.8 Concrete truck axle loads and spacing – bridge 89-0022

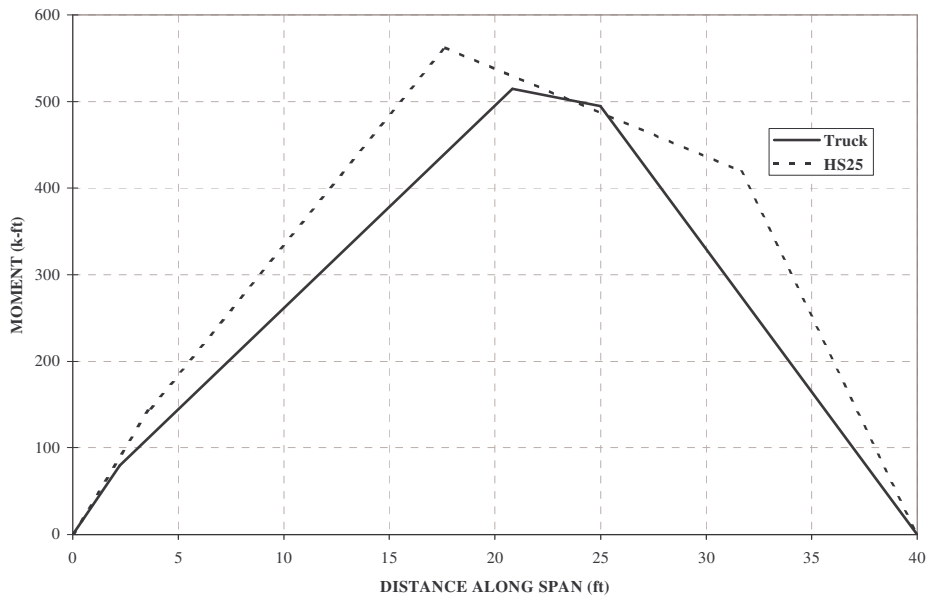


Figure C.9 Bending moment comparisons – bridge 89-0022

The second truck type was a NCDOT tandem truck loaded with aggregate at different levels (see Figure C.10). This loading system resulted in gross weights between 18 to 25 tons, close to most of the posting levels of the bridges considered. For bridge 59-0841 two of these trucks were used to simulate the effects of the governing lane load (for all of the other bridges truck loads governed the design and analysis).

Whenever it was possible, the trucks were weighed, axle by axle, by the Division of Motor Vehicles in the morning of the tests. Also, the axle spacing was verified in each case – this was necessary because there was a few feet difference in the tandem trucks available on a particular test date.



Figure C.10 Tandem truck loading bridge 89-0219

As it was mentioned earlier, a diagnostic load test requires the positioning of a loading vehicle at predetermined locations, while reading the bridge's structural response. Based on this requirement, it makes sense to position the loading vehicle to locations on the bridge that would generate the largest shear and bending forces, and vertical deformations. In this project, four different loading protocols were followed: static, dynamic, and slow movements, and finally, ambient traffic loading.

The static load followed the above-mentioned recommendations for diagnostic testing. The trucks were positioned at dozens of locations throughout the bridges, loading all the lanes, one at the time, from both traffic directions. In order to confirm test repeatability, the most important locations were loaded twice, then the result compared.

For one of the early bridges, these same static "spots" were loaded again, but with a slow moving truck. The position of the truck along the bridge was recorded using the 146 ft displacement transducer. By comparing the result of the static and the slow loading procedures, no real differences were observed. Therefore, it was decided for the

rest of the bridge tests to eliminate the static loading. By doing this, the bridge testing time was significantly reduced, allowing the bridge to be reopened much sooner, without losing important experimental data.

The dynamic load was induced by the loading truck traveling along the bridge at the speed limit. This test method provided valuable information on the measured impact factors for each of the bridges tested. And finally, for most of the bridges, the instruments were recording ambient traffic data for at least 30 minutes after the controlled loadings had been completed, and the bridges reopened for traffic.

C.4 Load Paths

For each of the seven bridges, load paths were specified for both static/slow and dynamic test procedures. These load paths were designed to maximize the effect on certain girders and deck segments. Once again, this section only provides the load paths for one bridge, the rest of them are in Attachment D. Furthermore, a detailed description and explanation for each of these paths are included in the previously mentioned theses and report.

Bridge 89-0022 was tested using five load paths. Each path was chosen to subject various components of the structure to the worst case of shear and moment/deflection. The paths selected were (see Figure C.11):

- Path 1: Truck traveling West to East with right wheels on G6.
- Path 2: Truck traveling West to East with right wheel between G5 and G6.
- Path 5: Truck traveling West to East centered on bridge.
- Path 3: Truck traveling West to East with right wheels on G2.
- Path 4: Truck traveling East to West with right wheels between G2 and G3.

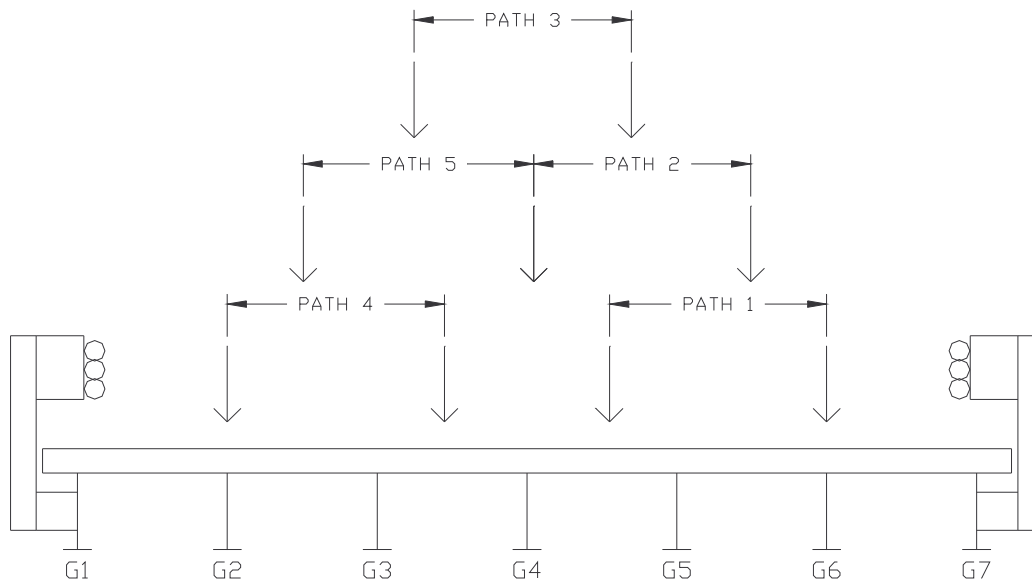


Figure C.11 Static load paths – bridge 89-0022

The stopping points used in the static testing varied depending on the path. These stopping points are also summarized in Table C.1, and are shown in Figure C.12.

The eight stopping points for this bridge were:

- a) Back wheels located to produce maximum moment in span.
- b) Back wheels located to produce maximum shear in span.
- c) Back wheels centered in GFRP panel 1.
- d) Back wheels centered in GFRP panel 2.
- e) Back wheels centered in GFRP panel 3
- f) Back wheels centered in GFRP panel 4.
- g) Back wheels centered in GFRP panel 5
- h) Back wheels positioned over joint between panel 2 and panel 3.

The slow testing was performed along the same paths as the static testing. The location of the load path was measured and marked on the pavement with a chalk line. During the testing, there was a spotter just in front of the load truck guiding the driver along the proper path. The load was applied slowly across the span in order to avoid any dynamic effects.

Table C.1 Stopping points for testing

Path Number	Static							
	a	b	c	d	e	f	g	h
1	X	X						
2	X	X	X	X	X			X
3	X	X						
4	X	X						
5	X	X			X	X	X	X

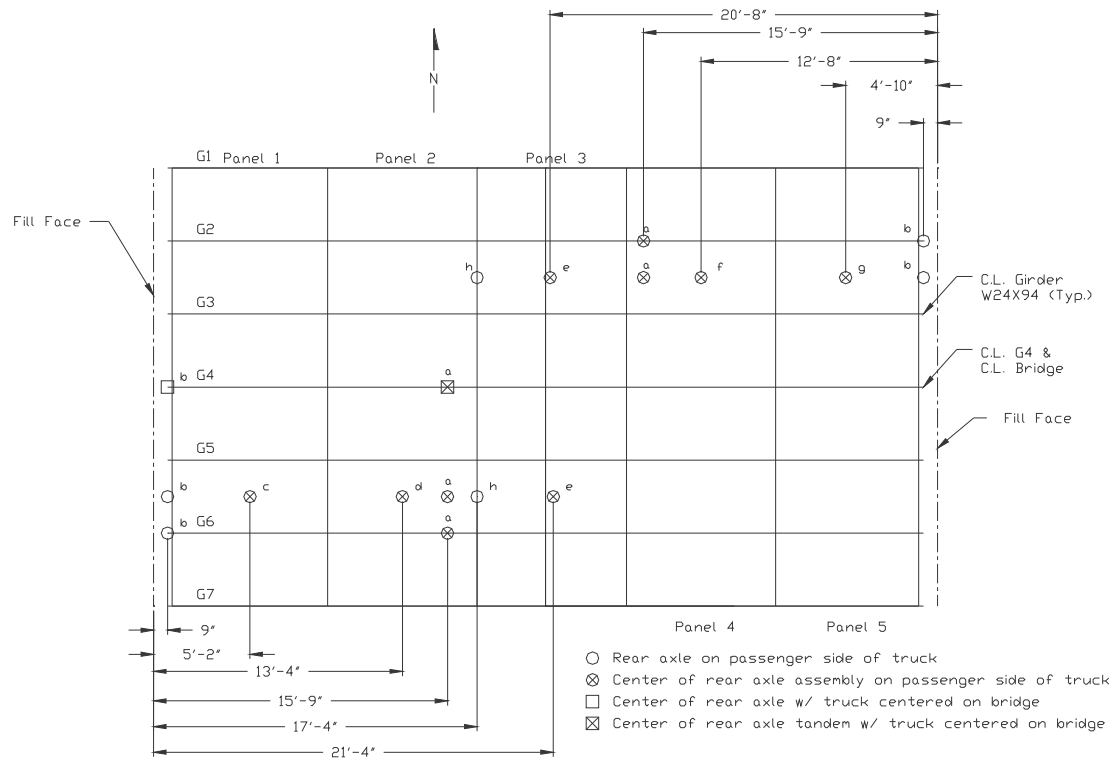


Figure C.12 Stopping points for static loading – bridge 89-0022

C.5 Bridge 89-022

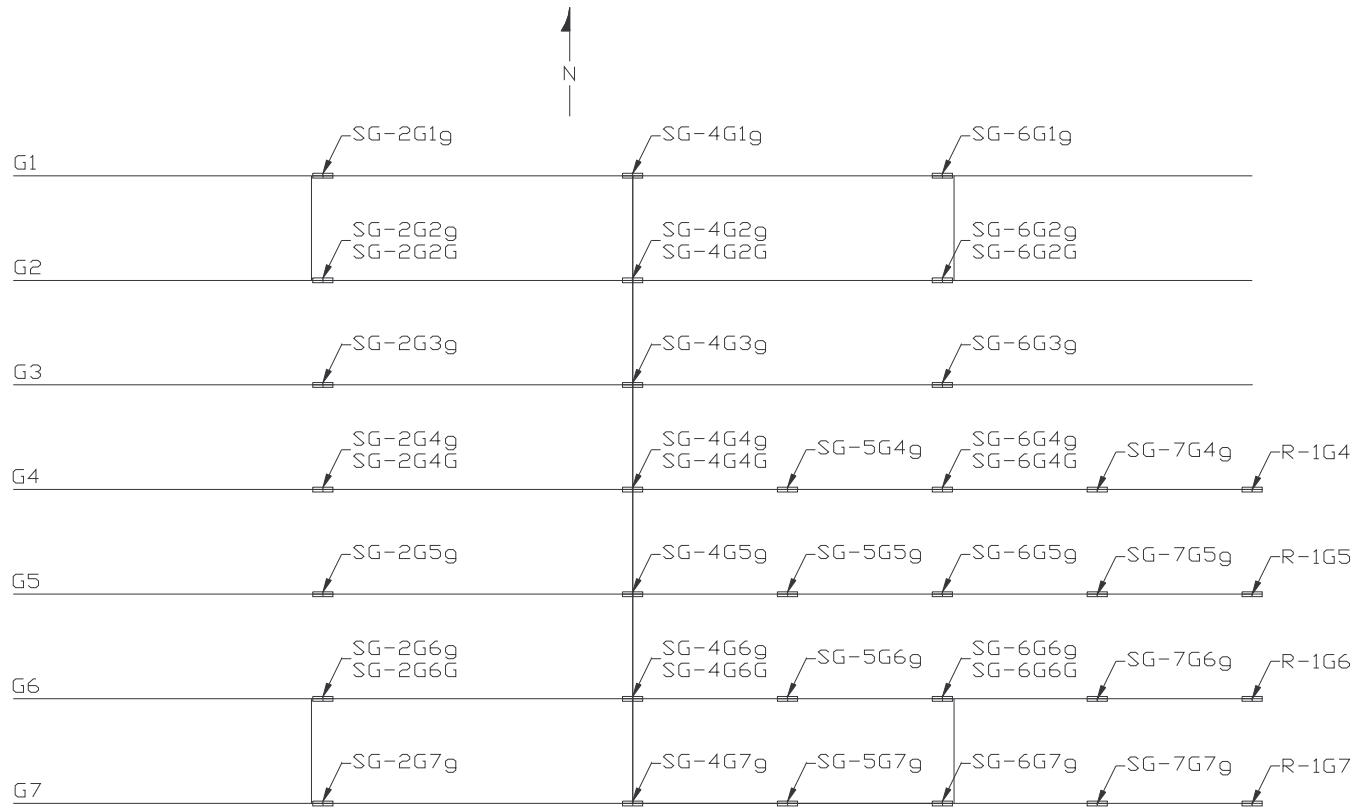


Figure C.13 Strain gage location on girders

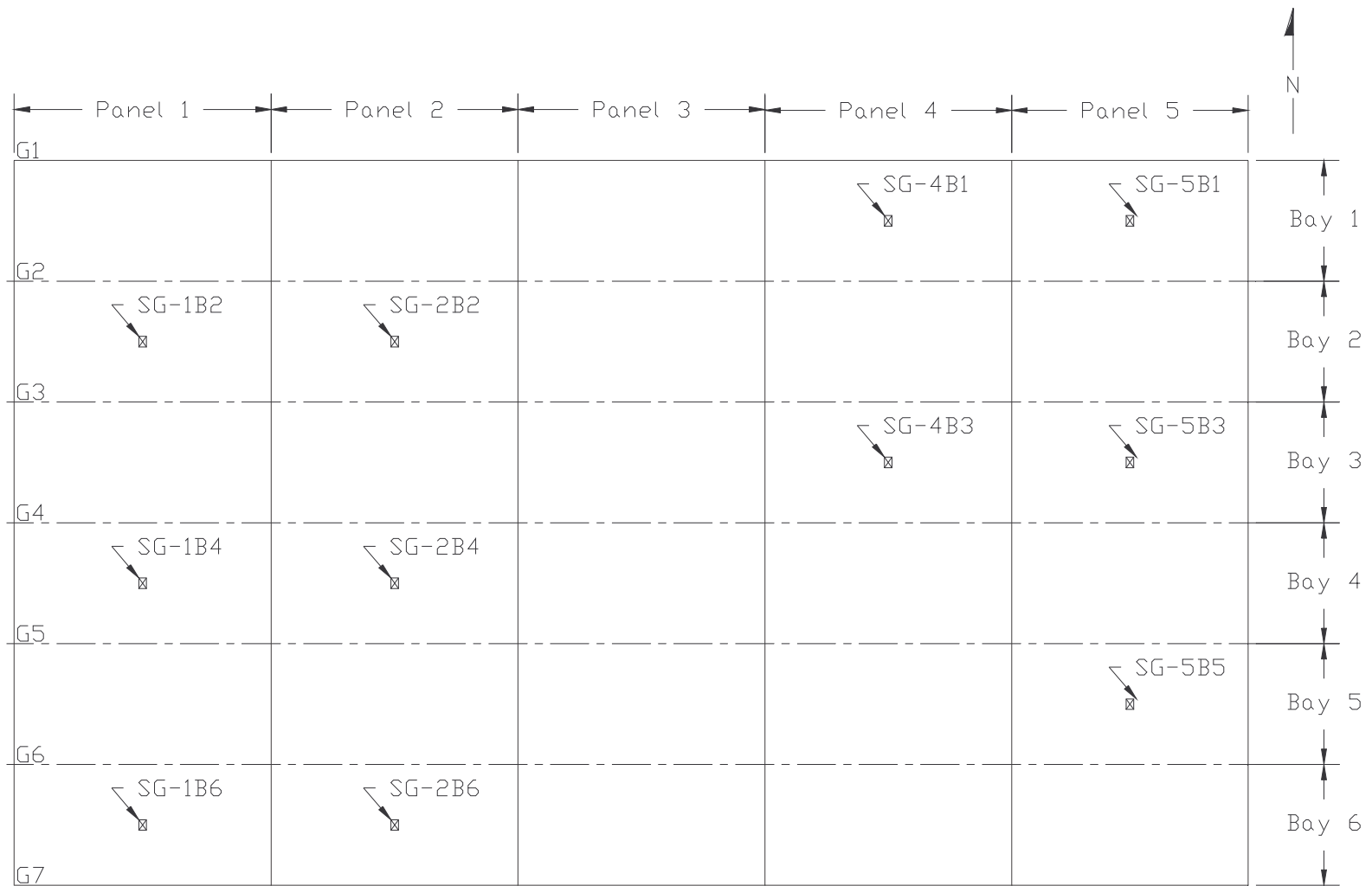


Figure C.14 Strain gage location on GFRP deck

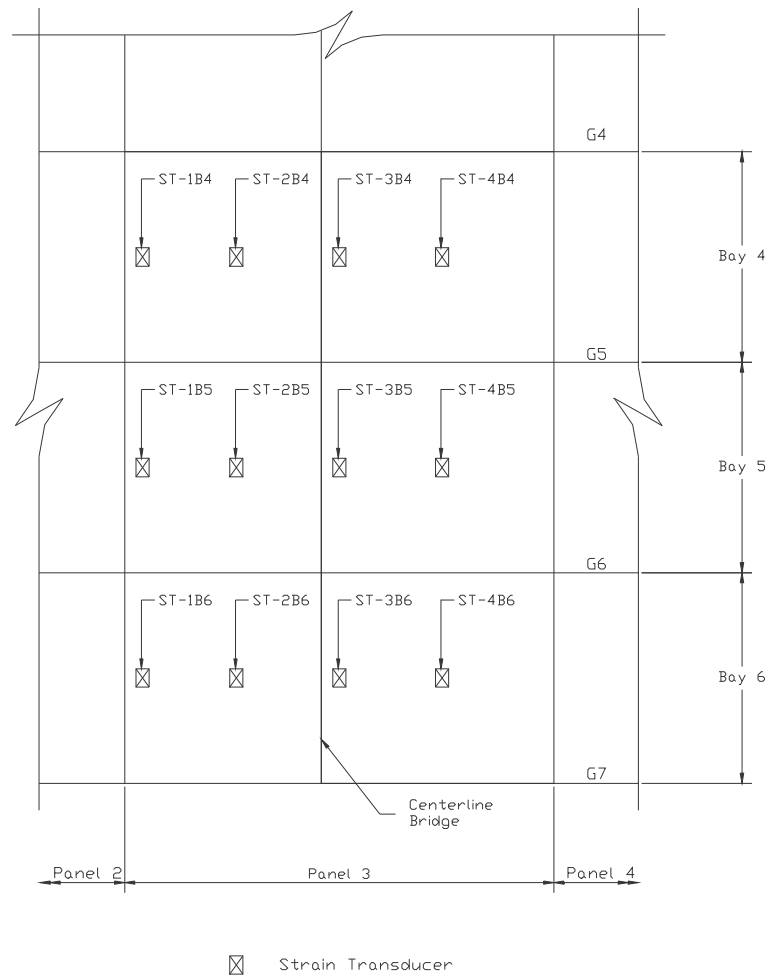


Figure C.15 Strain transducer location on GFRP deck

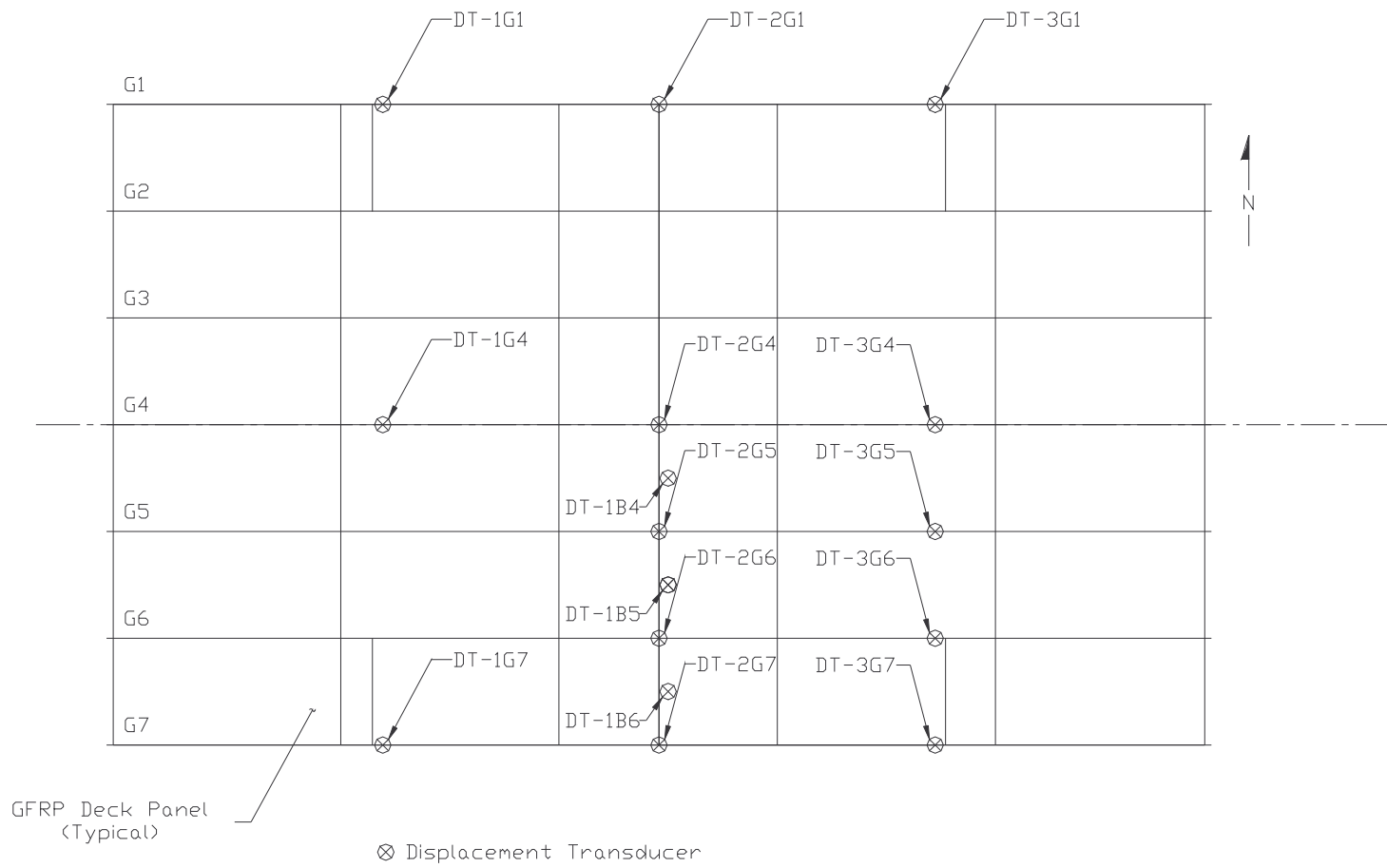


Figure C.16 Location of displacement transducers

C.6 Bridge 59-0361



Figure C.17 Instrumentation on Span 1



Figure C.18 Instrumentation on Span 2

C.7 Bridge 12-0271

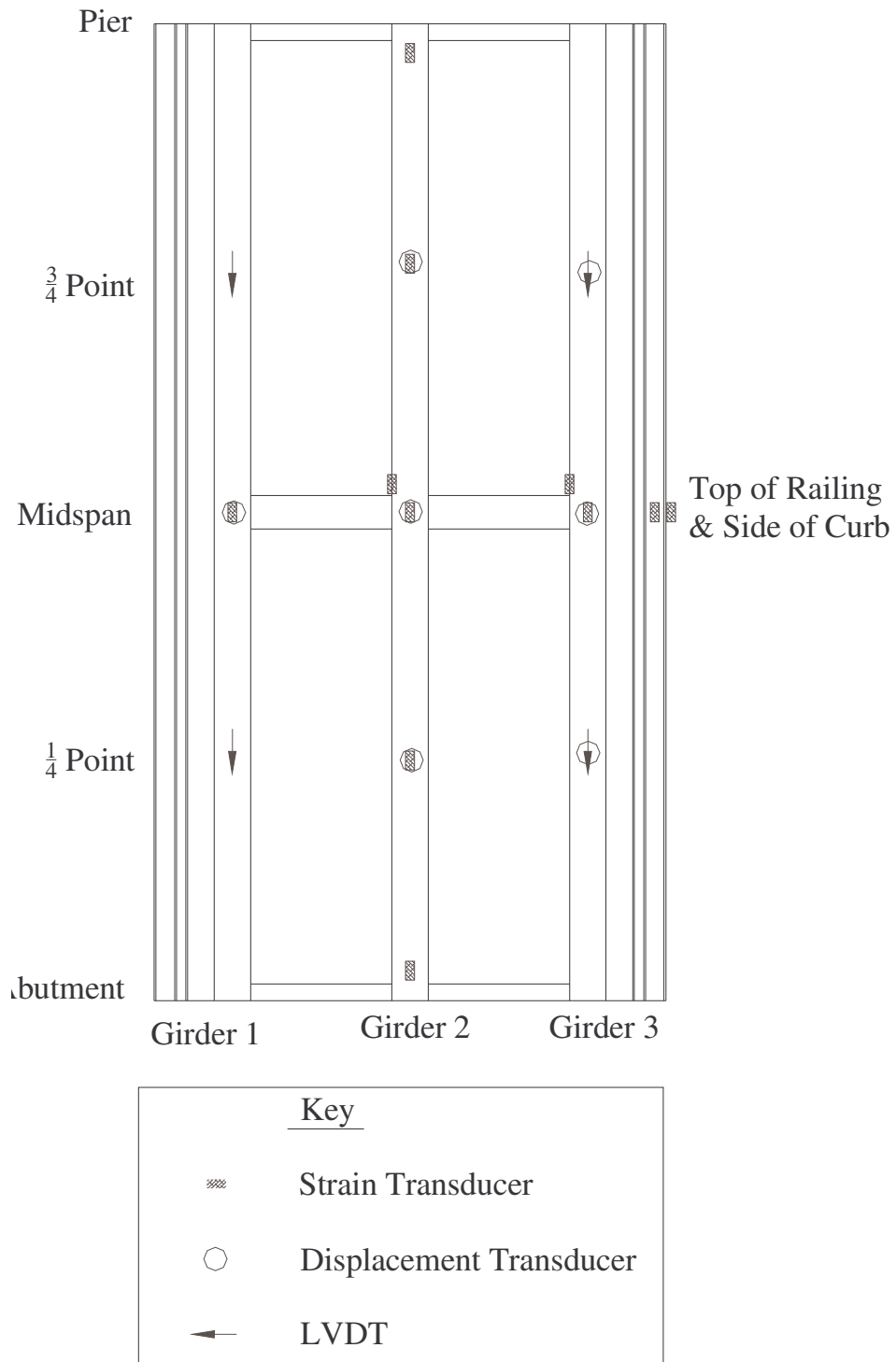


Figure C.19 Instrumentation for Span 1

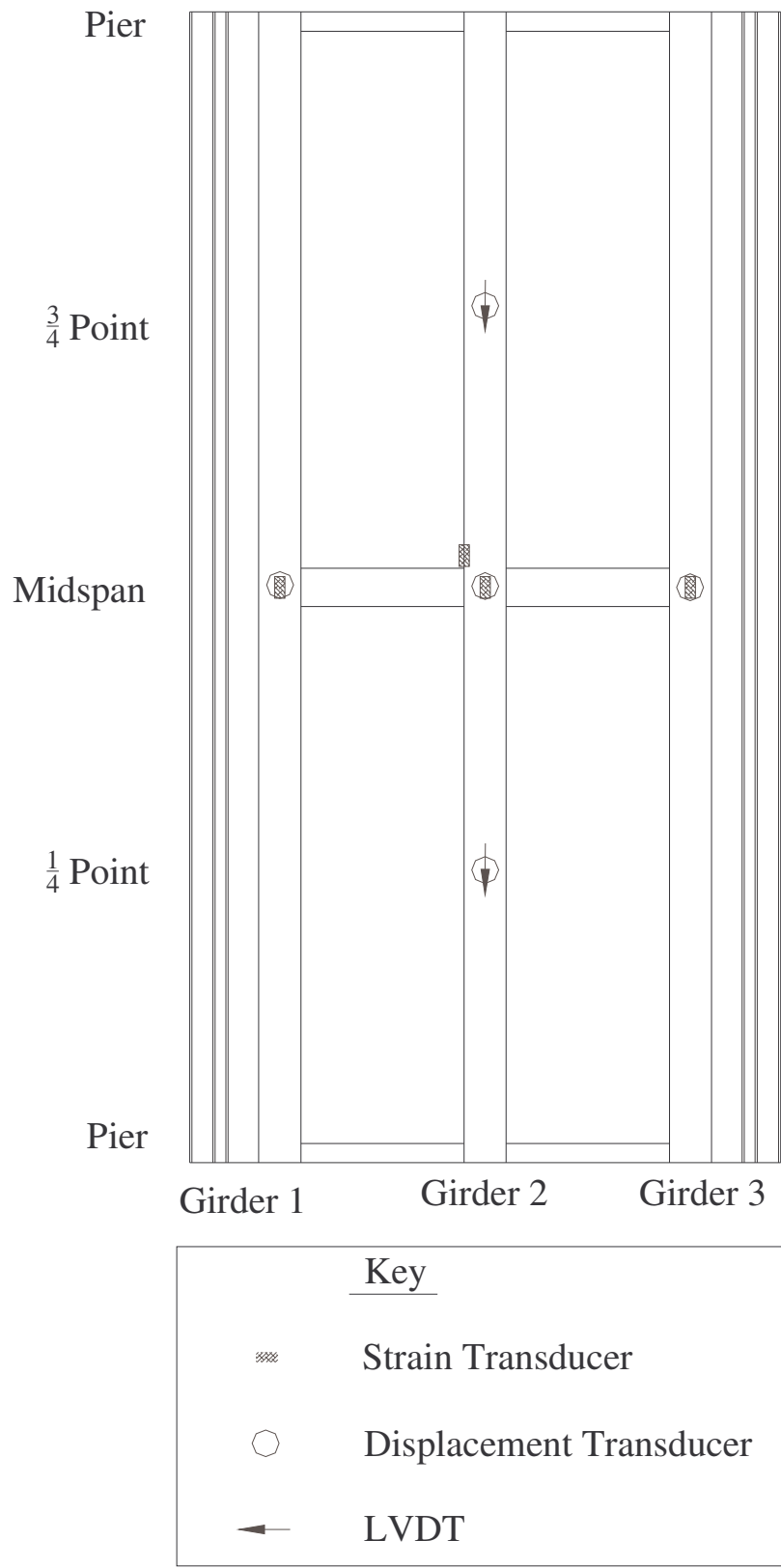
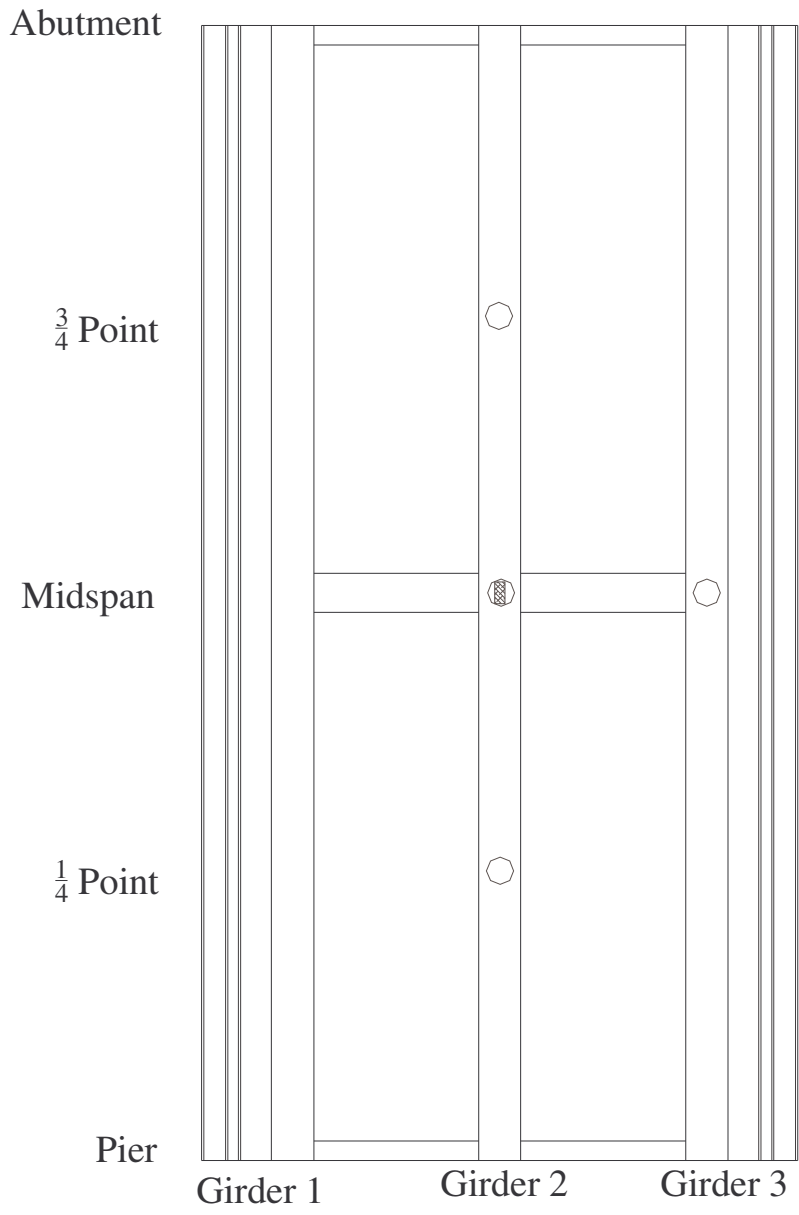


Figure C.20 Instrumentation for Span 2



Key	
▨	Strain Transducer
○	Displacement Transducer
←	LVDT

Figure C.21 Instrumentation for Span 3

C.9 Bridge 59-0038

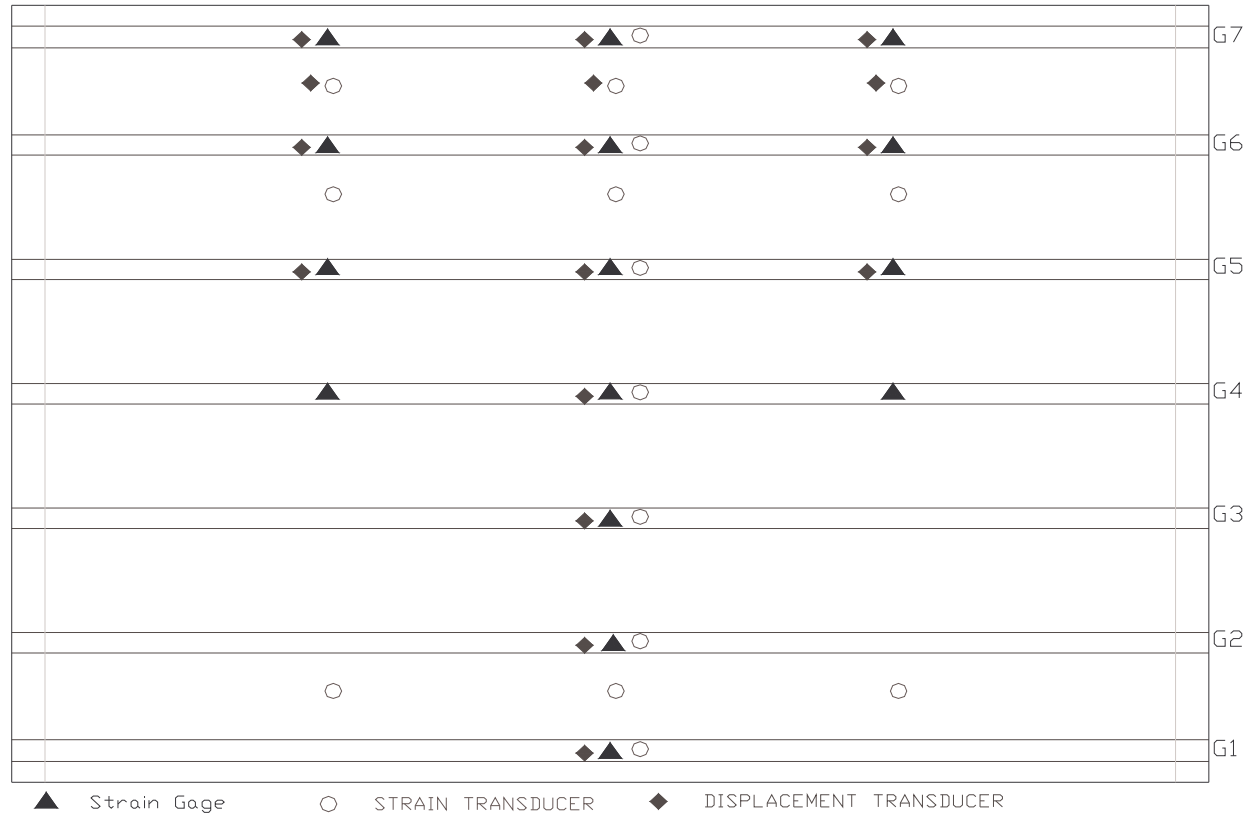
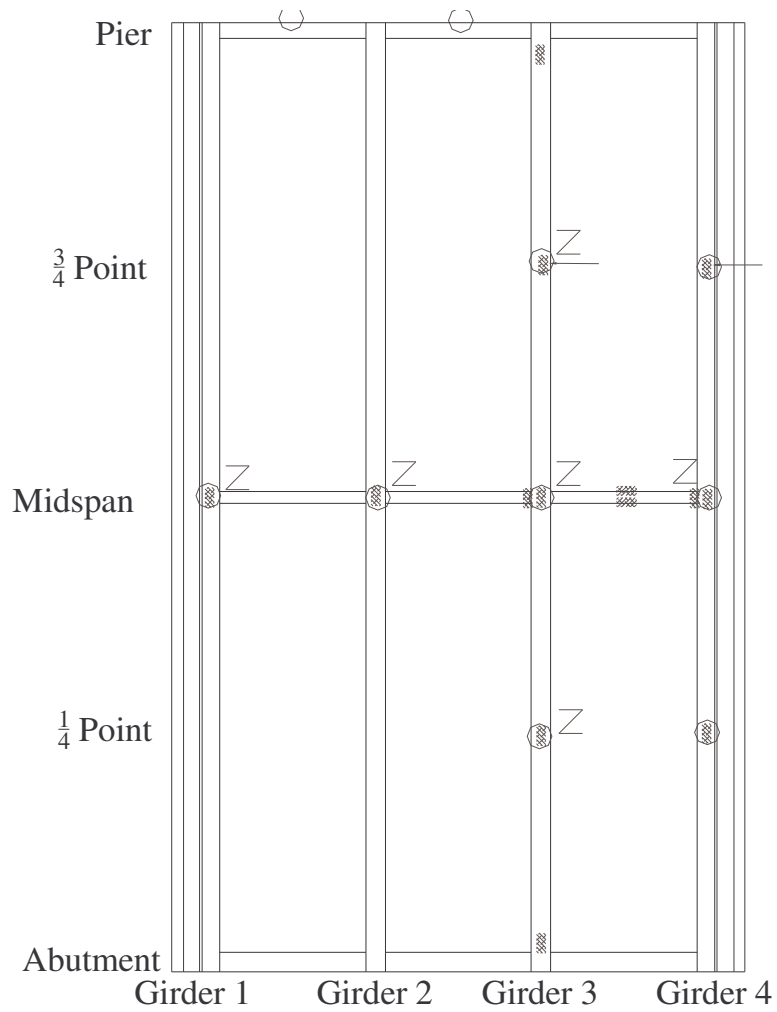


Figure C.22 Instrument plan for static testing

C.10 Bridge 12-0227



Key	
▨	Strain Transducer
○	Displacement Transducer
—	LVDT
×	Strain Gages
Z	Zapata Strain Trans.

Figure C.23 Instrument plan for Span 1

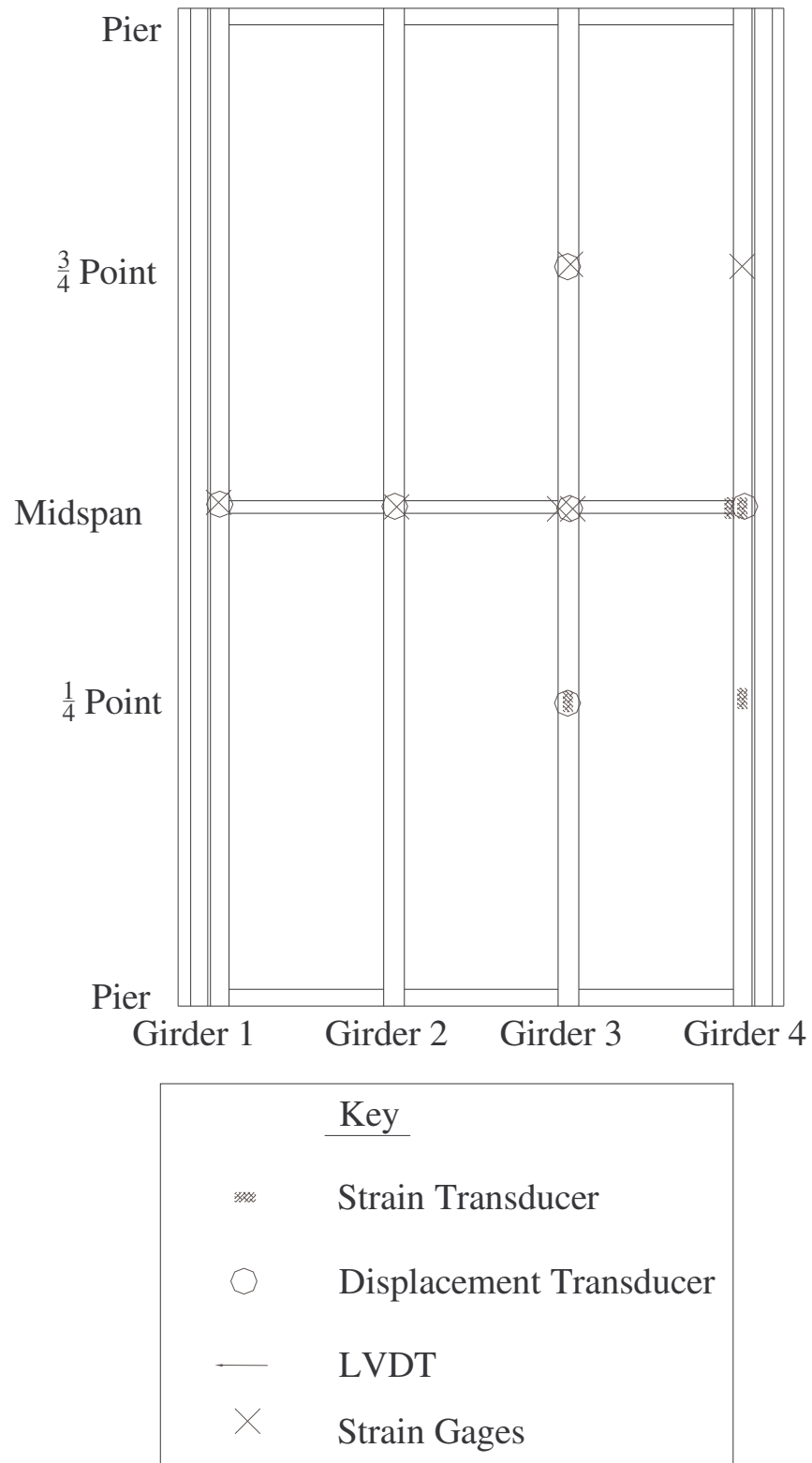


Figure C.24 Instrument plan for Span 2

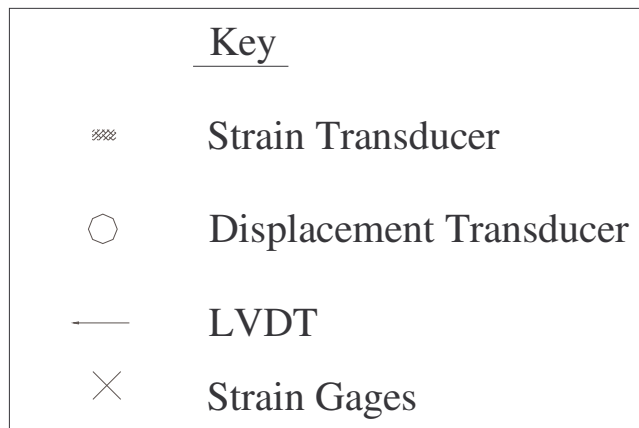
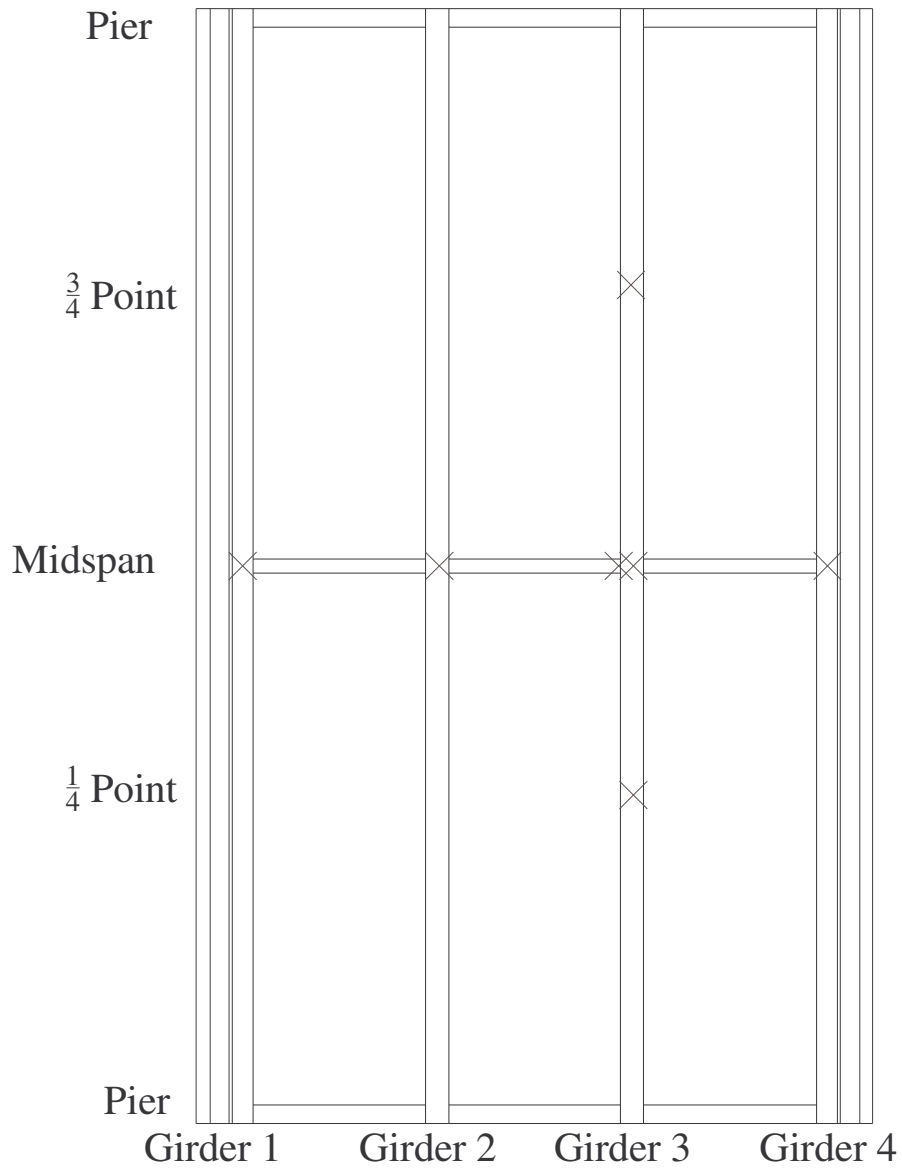


Figure C.25 Instrument plan for Span 3

C.11 Bridge 59-0841

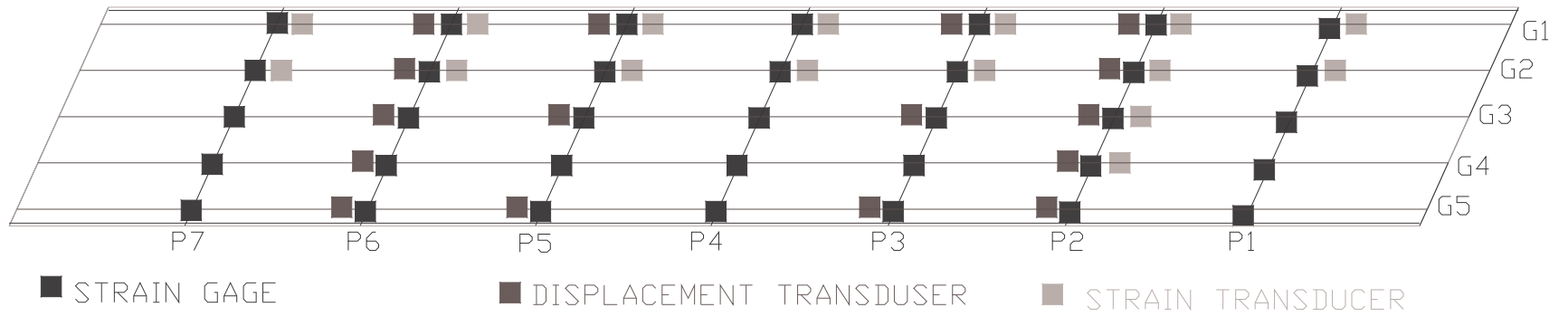


Figure C.26 Instrument plan for static loading

C.12 Bridge 89-0219

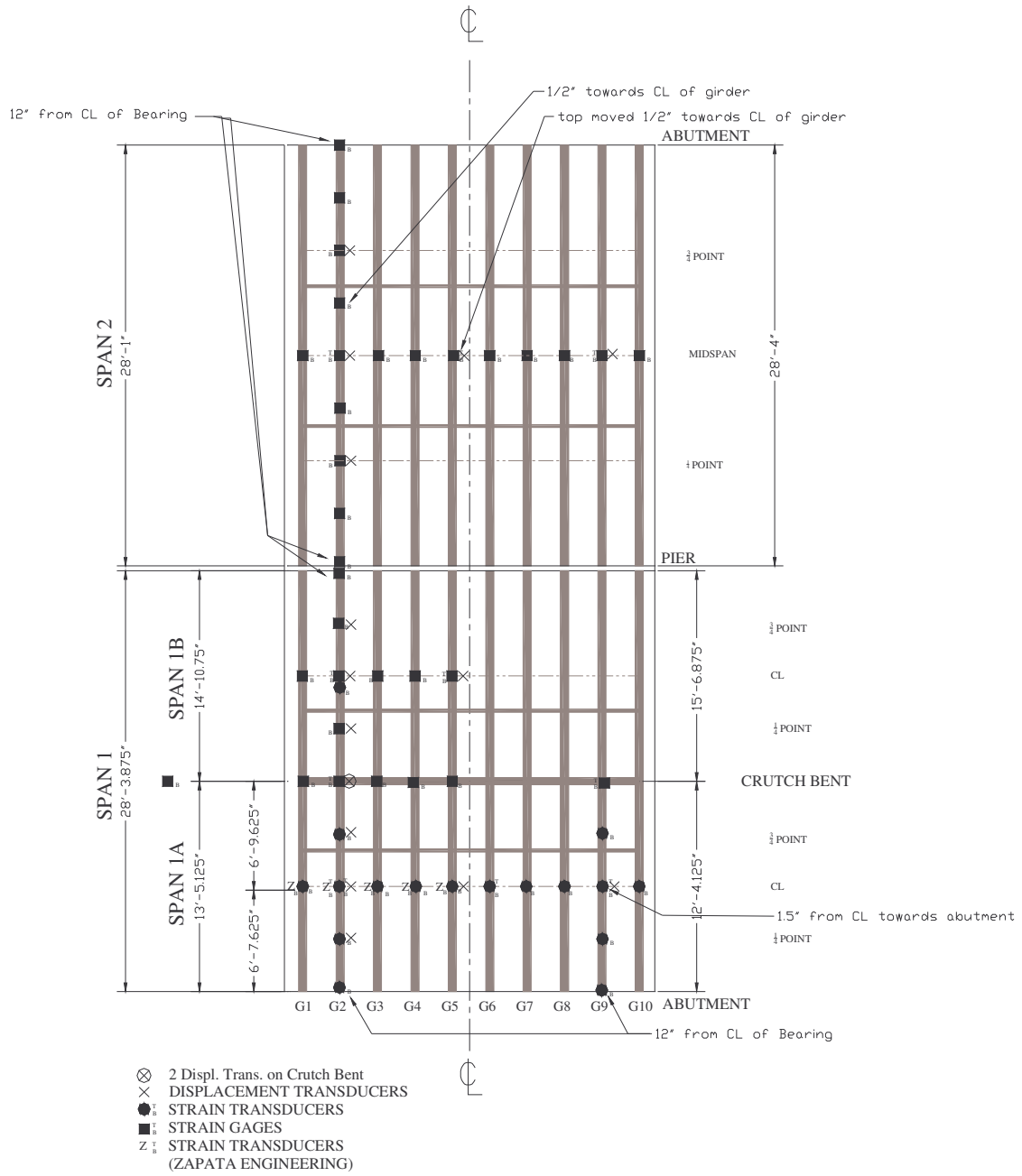


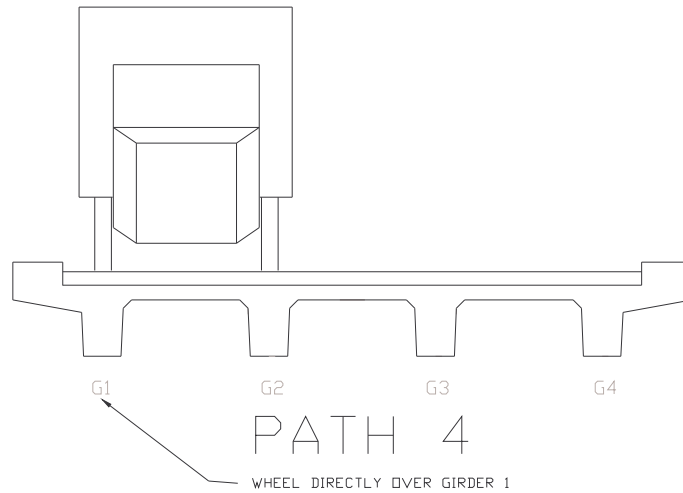
Figure C.27 Instrumentation plan for Bridge 89-0219

APPENDIX D

LOAD PATHS

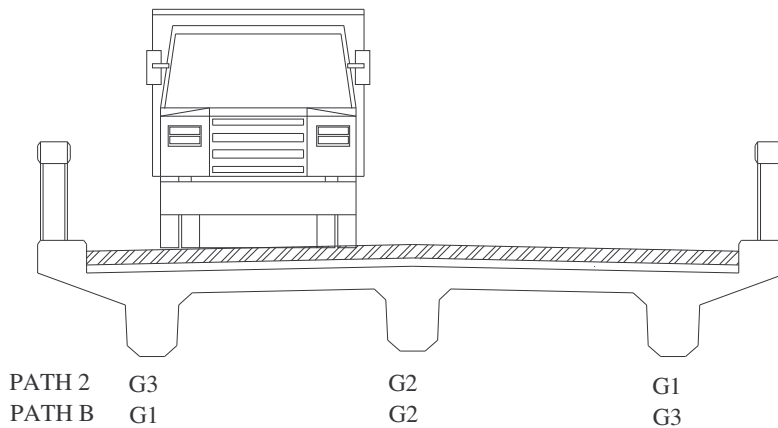
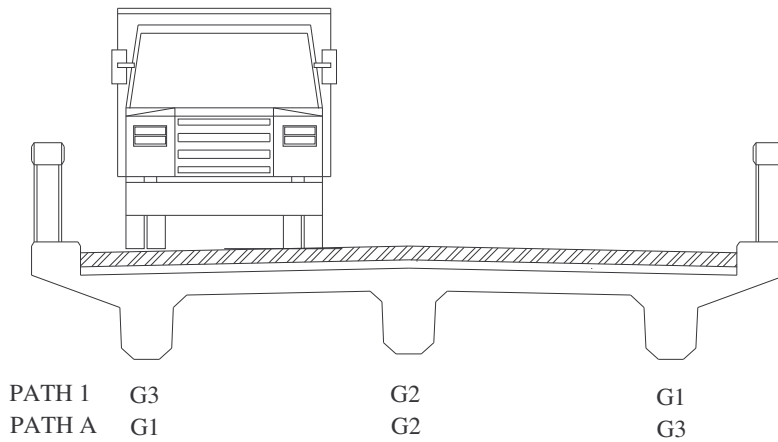
D.1 Bridge 59-0361

Path No.	Description of path	Static								Slow	Dynamic
		a	b	c	d	e	f	g	h		
1	Right wheel line over girder 4	x	x	x	x	x	x	x	x	x	
2	Truck centered in southbound lane	x	x							x	x
3	Right wheel line between girders 3 and 4	x	x	x	x	x	x	x	x	x	
4	Right wheel line over girder 1	x	x							x	x
5	Truck center of yellow line on bridge	x	x							x	
6	Truck centered in northbound lane	x	x							x	x
7	Right wheel line between girders 1 and 2	x	x							x	



D.2 Bridge 12-0271

Path #	Description
1	Right wheel line over girder 3
2	Load vehicle in center of lane
3	Right wheel between girders 2 & 3
4	Load vehicle in center of bridge
5	Load vehicle in center of opposite lane
A	Right wheel line over girder 1
B	Load vehicle in center of lane
C	Right wheel between girders 1 & 2
D	Load vehicle in center of bridge
E	Load vehicle in center of opposite lane



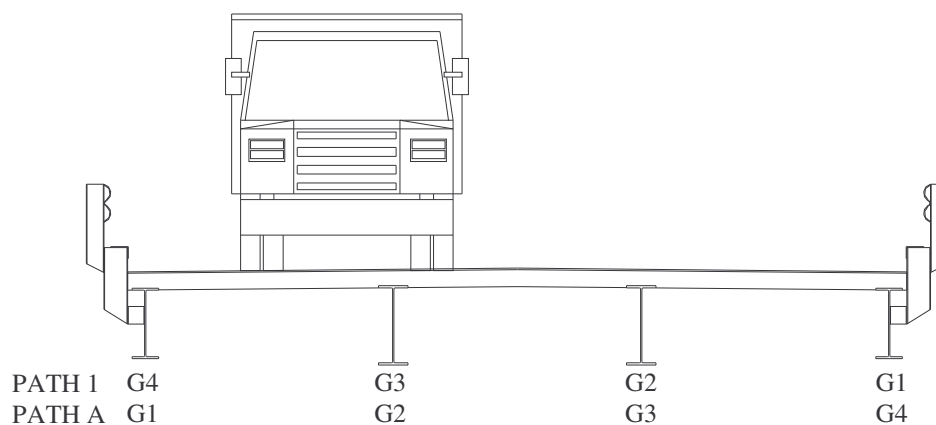
D.3 Bridge 59-0038

Path No.	Description of path	Static					Dynamic
		a	b	c	d	e	
1	Right wheel line between G6 and G7 (also middle of northbound lane)	x	x	x	x	x	x
2	Right wheel line over G6	x	x	x	x	x	
3	Center line of truck over center line of bridge	x	x				x
4	Right wheel line between G1 and G2 (also middle of southbound lane)	x	x				x
5	Right wheel line over G2	x	x				

D.4 Bridge 12-0227

Path #	Description
1	Load vehicle in center of lane
2	Load vehicle straddling girder 3
3	Load vehicle in center of bridge
4	Load vehicle straddling girder 2 in opposite lane
5	Load vehicle in center of opposite lane
6	Load vehicle between girders 3 & 4
7	Load vehicle between girders 1 & 2
8	Right wheel on girder 3
9	Right wheel on girder 2

Path #	Description
A	Load vehicle in center of lane
B	Load vehicle straddling girder 2
C	Load vehicle in center of bridge
D	Load vehicle straddling girder 3
E	Load vehicle in center of opposite lane
F	Load vehicle between girders 1 & 2
G	Load vehicle between girders 3 & 4
H	Right wheel on girder 2
I	Right wheel on girder 3



D.5 Bridge 59-0841

Path #	Description (two trucks for static, one for dynamic tests)
1	Right wheel line over girder 1
2	Right wheel line between girders 1 and 2
3	Trucks centered in eastbound lane
4	Trucks centered on bridge center line
5	Right wheel line over girder 5
6	Right wheel line between girders 4 and 5
7	Trucks centered on westbound lane

D.6 Bridge 89-0219

Path No.	Description of path	Slow	Dynamic
1	Truck centered in lane, traveling towards Waxhaw	x	x
2	Truck centered on bridge center line, traveling towards Waxhaw	x	x
3	Truck centered in lane, traveling towards Waxhaw	x	x
A	Truck centered in lane, traveling from Waxhaw	x	x
B	Truck centered on bridge center line, traveling from Waxhaw	x	x
C	Truck centered in lane, traveling from Waxhaw	x	x

